INVESTIGATION OF CHEMICAL VAPOR DEPOSITED ALUMINUM AS A REPLACEMENT FOR CADMIUM

SERDP Project WP-1405

FINAL REPORT

Draft - Revision 0

9 February, 2008

Prepared by

Dr. Elizabeth S. Berman - Co-Principal Investigator

Dr. Eric W. Brooman - Co-Principal Investigator

Air Force Research Laboratory

Acquisition Systems Support Branch

Materials & Manufacturing Directorate

WPAFB, OH

Approved for public release; distribution is unlimited.

Table of Contents

List of Figures vii
List of Tables xii
List of Acronyms xv
Acknowledgments xviii
Executive Summary xix
1.0 Objective and Approach 1
1.1 Objective 1
1.2 Technical Approach 3
2.0 Background to Alternative Coating and Process Selection 7
2.1 Problem Addressed by this Technology 7
2.2 Prior Work on Cadmium Replacement 8
2.3 Best Cadmium Alternative Candidates 9
2.4 Selection of Aluminum for Study 10
2.5 Selection of Chemical Vapor Deposition as the Deposition Method 10
2.6 Selection of Atmospheric Pressure CVD as Preferred Deposition Method 13
3.0 Materials, Coating Deposition, and Test Methods 14
3.1 Materials 14
3.1.1 Substrates 14
3.1.1.1 Low Carbon, Mild and High-strength Steels 14
3.1.1.2 Other High-strength Aerospace Alloys 15
3.1.1.3 Coupon, Panel, and Test Specimen Designs 15
3.1.2 Cleaning Chemicals 19
3.1.3 Precursor Chemicals 19
3.1.3.1 Tri-ethyl Aluminum 19
3.1.3.2 Tri-isobutyl Aluminum 19
3.1.3.3 Proprietary Blend 1 19
3.1.3.4 Proprietary Blend 2 19
3.1.4 Carrier Gases 19
3.1.5 Post-treatment Chemicals 20
3.1.6 Reference Materials 20
3.1.6.1 Aluminum Metal 20
3.1.6.2 IVD Aluminum 20
3.1.6.3 Electroplated Aluminum 20
3.2 Coating Deposition Methods 21
3.2.1 Deposition in Tubular Reactor 22
3.2.2 Deposition in Rotating Barrel Reactor 24
3.2.3 Deposition in Commercial Barrel Reactor 26

Table of Contents (continued)

3.3 Testing Methods 26
3.3.1 Coating Structure 28
3.3.1.2 X-ray Diffraction 28
3.3.2 Thickness and Surface Roughness 28
3.3.3 Throwing Power and Conformal Coverage 28
3.3.4 Density and Porosity 28
3.3.4.1 Optical Microscopy 29
3.3.4.2 Electrochemical Impedance Spectroscopy 29
3.3.5 Chemical Composition 29
3.3.5.1 Energy Dispersive Analysis with X-rays 29
3.3.5.2 Auger Electron Spectroscopy 29
3.3.5.3 Nuclear Reaction Analysis 29
3.3.5.4 X-ray Photoelectron Spectroscopy 30
3.3.5.5 Glow Discharge Optical Emission Spectroscopy 30
3.3.5.6 Electron Probe Microanalysis 30
3.3.6 Electrochemical and Corrosion Properties 30
3.3.6.1 Open Circuit (Galvanic) Potential and Polarization Behavior 30
3.3.6.2 Salt Fog Exposure Corrosion Resistance 31
3.3.6.3 Alternating Immersion Corrosion Resistance 32
3.3.6.4 Exposure to Aircraft Maintenance Fluids 33
3.3.6.5 Stress-Corrosion Cracking Resistance 34
3.3.7 Mechanical Properties 35
3.3.7.1 Adhesion 35
3.3.7.2 Hardness 36
3.3.7.3 Young's Modulus 36
3.3.7.4 Coefficient of Friction 37
3.3.7.5 Tensile and Notch Fracture Strength 37
3.3.7.6 Hydrogen Embrittlement and Re-embrittlement Resistance 38
3.3.7.7 Fatigue Resistance 39
3.3.8 Electrical Properties 39
3.3.8.1 Contact Resistance 40
3.3.8.2 Electrical Resistivity 40
4.0 Test Results and Accomplishments 42
4.1 Test Results 42
4.1.1 Coating Structure 42
4.1.1.1 Optical Microscopy and Metallography 42
4.1.1.2 X-ray Diffraction 44
4.1.2 Thickness and Surface Roughness 47
4.1.3 Throwing Power and Conformal Coverage 48
4.1.4 Density and Porosity 52

Table of Contents (continued)

4.1.4.1 Optical Microscopy *53*
4.1.4.2 Electrochemical Impedance Spectroscopy *54*
4.1.5 Chemical Composition 55
4.1.5.1 Energy Dispersive Analysis with X-rays *55*
4.1.5.2 Auger Electron Spectroscopy *56*
4.1.5.3 Nuclear Reaction Analysis *62*
4.1.5.4 X-ray Photoelectron Spectroscopy *64*
4.1.5.5 Glow Discharge Optical Emission Spectroscopy *67*
4.1.5.6 Electron Probe Microanalysis *67*
4.1.6 Electrochemical and Corrosion Properties 68
4.1.6.1 Open Circuit (Galvanic) Potential and Polarization Behavior *68*
4.1.6.2 Salt Fog Exposure Corrosion Resistance *77*
4.1.6.3 Alternating Immersion Corrosion Resistance *81*
4.1.6.4 Exposure to Aircraft Maintenance Fluids *83*
4.1.6.5 Stress-Corrosion Resistance *87*
4.1.7 Mechanical Properties 88
4.1.7.1 Adhesion *88*
4.1.7.2 Hardness *89*
4.1.7.3 Young's Modulus *89*
4.1.7.4 Coefficient of Friction *89*
4.1.7.5 Tensile and Notch Fracture Strength *92*
4.1.7.6 Hydrogen Embrittlement and Re-embrittlement Resistance *95*
4.1.7.7 Fatigue Resistance *100*
4.1.8 Electrical Properties 104
4.1.8.1 Contact Resistance *104*
4.1.8.2 Electrical Resistivity *104*
4.2 Accomplishments 105
4.2.1 APCVD Process for Depositing Aluminum Coatings 105
4.2.2 Properties of APCVD Aluminum Coatings Deposited at 275-300ºC 106
4.2.3 Performance of APCVD Aluminum Coatings Deposited at 275-300ºC 108
4.2.4 Properties of APCVD Aluminum Coatings Deposited at 230-245ºC 109
4.2.5 Performance of APCVD Aluminum Coatings Deposited at 230-245ºC 120
5.0 Technology Transfer 126
5.1 Suitable Substrate Materials and Applications 126
5.2 Status of APCVD Process Commercialization 131
6.0 Conclusions and Recommendations 133
6.1 Conclusions 133
6.2 Recommendations for Future Work 135
7.0 Appendices 137

Table of Contents (continued)

7.1 Effect of Temperature on High-strength Alloy Substrate Properties 137
7.1.1 AISI 4130 Steel 138
7.1.2 AISI 4340 Steel 139
7.1.3 300 M Steel 141
7.1.4 H11 Modified Steel 143
7.1.5 AF1410 Steel 145
7.1.6 AerMet 100 Alloy 145
7.1.7 AerMet 310 Alloy 147
7.1.8 Best Substrate Choices for Using APCVD Aluminum Coatings 150
7.2 Comparison of APCVD Al with Other Candidate Replacement Coatings 150
7.2.1 IVD Aluminum 152
7.2.2 Sputtered Aluminum 155
7.2.3 Electroplated Aluminum 156
8.0 Technical Publications 159
8.1 Technical Papers and Articles 159
8.2 Technical Reports 159
8.3 Conference/Symposium Presentations and Proceedings 159
8.4 Published Technical Abstracts 160
8.5 Text Books and Book Chapters 160

List of Figures

Figure 1-1 SERDP Project WP-1405 Project Outline 3
Figure 2-1 Schematic Diagram of a Typical CVD Process 12
Figure 3-1 Schematic of a Standard Charpy CV2 Specimen 17
Figure 3-2 C-ring Specimens Used for Accelerated Corrosion and HE Testing 17
Figure 3-3 Drawing for the Smooth Round Bar Used for Fatigue Testing 18
Figure 3-4 Drawing for the Notched Round Bars Used for HE/HRE Testing 18
Figure 3-5 Basic Design of a Tubular APCVD Reactor 22
Figure 3-6 Laboratory Tubular Reactor and Ancillary Equipment 22
Figure 3-7 AkzoNobel Overall APCVD Aluminum Processing Scheme 24
Figure 3-8 Bench Scale Rotary APCVD Reactor and Ancillary Equipment 25
Figure 3-9 AkzoNobel Commercial APCVD Unit Set Up for Preproduction Testing 26
Figure 3-10 Electrochemical Cell used for EIS Measurements Showing Specimen that is to be Immersed in a Salt Solution 31
Figure 3-11 Corrosion Chamber Used for GM 9540P Corrosion Testing 32
Figure 3-12 Samples Immersed in a Jar Containing Hydraulic Fluid and Internal Sample Support Structure 33
Figure 3-13 Hot Water Bath with Monitoring Thermometers and Bath Interior Showing Arrangement of Jars Containing Samples in Different Fluids 34
Figure 3-14. Fixture Used for Stress-corrosion Cracking Testing 34
Figure 3-15 Adhesion (Pull) Test Equipment 35
Figure 3-16 Apparatus for Determining Hardness and Young's Modulus 36
Figure 3-17 Pin-on-Disc Test Apparatus for Determining Coefficients of Friction 37
Figure 3-18 Tensile (Hydrogen Embrittleemnt) Testing Machine 38
Figure 3-19 Specimen Mounted in Fixture for HE Testing 38
Figure 3-20 Electrical Resistivity Test Apparatus 40
Figure 4-1 Photomicrographs of Cross-sections of APCVD Al-Coated Steel Fasteners 42
Figure 4-2 Photomicrographs of Cross-sections of APCVD Al-Coated Bolts 43
Figure 4-3 Photomicrographs of the Surfaces of APCVD Al-Coated Substrates 43
Figure 4-4 FE-SEM Image of Cross-section of Middle of an APCVD Al-coated Small Diameter, Steel Tube 44
Figure 4-5 XRD Pattern of APCVD Al Coating Compared to that of an Al Powder Reference Material 44
Figure 4-6 XRD Patterns for APCVD Al Coatings Deposited at Different Temperatures 45
Figure 4-7 XRD Patterns of APCVD Al and IVD Al Coatings with Post-treatments 46
Figure 4-8 AFM Derived Topography of the Surface of an APCVD Al Coating 47

List of Figures (continued)

Figure 4-9 SEM Images of the Surface of APCVD Al and IVD Al Coatings 48

Figure 4-10 Diagram Showing Cross-sectioning of APCVD Aluminum on Tubes 49

Figure 4-11 Ratio of Inside to Outside Aluminum Coating Thickness along Tube Length 51

Figure 4-12 Schematic Diagram Showing Coating Thickness Measurement Points on Hollow Rivet Sleeve for Step Coverage Measurement 51

Figure 4-13 FE-SEM Images Showing Measurement Points and Excellent Step Coverage 52

Figure 4-14 Cross-sections of APCVD Al Coatings Showing Areas of Damage, Poor Coverage and Closed Porosity 1

Figure 4-15 Low Frequency Impedance of APCVD Al and IVD Al Coatings on AISI 4130 Steel Obtained from EIS as a Function of Immersion Time 54

Figure 4-16 SEM Images of APCVD Al and IVD Al Coatings after EIS Measurements 55

Figure 4-17 SEM Images of the Al Coating (a) on Top of Nut with (b) EDAX Analysis and (c) on Top of Bolt with (d) EDAX Analysis 55

Figure 4-18 FE-SEM Images of Cross-sections of APCVD Al-Coated Bolt (a) and Coupon (b) and Corresponding EDAX Images 56

Figure 4-19 AES Spectrum of the Al-coated Steel (a) before and (b) after Eight Minutes Sputter Etching 56

Figure 4-20 AES Composition Depth Profile of APCVD Al Coating on Steel 58

Figure 4-21 AES Depth Profiles of APCVD Aluminum Coatings Produced with Different Deposition Conditions 59

Figure 4-22 AES Depth Profile of Carbon Impurity Present in the Al Coatings Produced with Different Deposition Conditions 61

Figure 4-23 AES Depth Profile of Oxygen Impurity Present in the Al Coatings Produced with Different Deposition Conditions 61

Figure 4-24 NRA Depth Profile of Hydrogen Present in the Aluminum Coatings 63

Figure 4-25 XPS Spectrum of the APCVD Al Surface Showing Aluminum, Oxygen, and Carbon Peaks Present in the Coatings 64

Figure 4-26 XPS Al 2p, O 1s, and C 1s Spectra as a Function of Sputter Time for the APCVD Al Coatings 66

Figure 4-27 GD-OES Depth Profiles of APCVD Al Coatings Deposited at (a) 275°C and (b) 300°C Using Precursor PB1 67

Figure 4-28 Corrosion Potentials of APCVD and IVD Al Coatings on AISI 4130 Steel as a Function of Immersion Time 68

Figure 4-29 Photomicrographs of APCVD Al Coatings Demonstrating Sacrificial Protection of the Steel Substrates 69

Figure 4-30 Corrosion Potentials of APCVD Al Coatings on AISI 4340 Steel as a Function of Immersion Time 70

List of Figures (continued)

Figure 4-31 Nyquist Plots for Bare AISI 4340 Steel Bars in 3.5 wt% NaCl Solution During 12 Hours Immersion 71

Figure 4-32 Predicted and Actual Impedance Data for Bare AISI 4340 Steel Bars in 3.5 wt% NaCl Solution During 12 Hours Immersion 72

Figure 4-33 Equivalent Circuit Model and Element Values for Bare AISI 4340 Steel Bars in 3.5 wt% NaCl Solution During 12 Hours Immersion 72

Figure 4-34 Nyquist Plots for APCVD Al-Coated Steel Bars in 3.5 wt% NaCl Solution During 12 Hours Immersion 74

Figure 4-35 Predicted and Actual Impedance Data for APCVD Al-Coated AISI 4340 Steel Bars in 3.5 wt% NaCl Solution During 12 Hours Immersion 75

Figure 4-36 Equivalent Circuit Model and Element Values for APCVD Al-Coated AISI 4340 Steel Bars in 3.5 wt% NaCl Solution During 12 Hours Immersion 75

Figure 4-37 Polarization Resistance of Bare and APCVD Al-Coated Bars as a Function of Immersion Time in a 3.5% Salt Solution 76

Figure 4-38 Visual Appearance of EIS Specimens after 12 Hours Exposure to Salt Solution ... 77

Figure 4-39 APCVD Al Coatings on Steel Panels after 24 hr Salt Fog Exposure 78

Figure 4-40 APCVD Al Coatings on Steel Panels after 96 hr Salt Fog Exposure 79

Figure 4-41 APCVD Al-coated Coupons after 17 Days in ASTM B 117 Salt Fog Test 79

Figure 4-42 Painted APCVD Al-coated Coupons after 17 Days in ASTM B 117 Salt Fog Test 80

Figure 4-43 Painted APCVD Al Coatings after Paint Adhesion Testing 80

Figure 4-44 As Received APCVD Al-Coated Panels With and Without a Commercial Trivalent Chromium Treatment 81

Figure 4-45 APCVD Al-Coated Panels after 2 Cycles in GM 9540P Test 82

Figure 4-46 APCVD Al-Coated Panels after 10 Cycles in GM 9540P Test 82

Figure 4-47 APCVD Al-Coated Panels after 60 Cycles in GM 9540P Test 83

Figure 4-48 APCVD Al-Coated Panels after 165 Cycles in GM 9540P Test 83

Figure 4-49 Appearance of Post-treated Samples after Immersion 86

Figure 4-50 Appearance of Non-post-treated Samples after Immersion 86

Figure 4-51 Whisker (Crystal) Formation on Samples Exposed to CEM483 87

Figure 4-52 Photograph of an APCVD Al Coating on Steel after Bending around a Mandrel ... 89

Figure 4-53 Results of the Coefficient of Friction of Cadmium and APCVD Al-Coated Steel Samples as a Function of Wear Track Distance 90

Figure 4-54 Mean Coefficient of Friction of Cadmium and APCVD Al-Coated Steel Substrates as a Function of B 117 Exposure Time 90

Figure 4-55 Samples Tested for 75 Hours in an ASTM B 117 Salt Fog Chamber 92

Figure 4-56 Photomicrographs of the Fracture Surface of the Specimen D9 99

List of Figures (continued)

Figure 4-57 Photomicrographs of the Fracture Surface of the Specimen D11 99

Figure 4-58 Photomicrographs of the Fracture Surface of the Specimen D4 99

Figure 4-59 SEM Image of Part of the Fracture Surface of an APCVD Al-Coated Specimen after HE Testing 100

Figure 4-60 Cadmium and APCVD Al-Coated AerMet 100 Specimens after Fatigue Testing. 102

Figure 4-61 Fatigue Curves for Cadmium-Plated, APCVD Al-Coated, and Uncoated AerMet 100 Specimens 102

Figure 4-62 SEM Image of an APCVD Al Coating Deposited on a Si_3N_4-Coated Steel Substrate 105

Figure 4-63 Diagram of Hollow Rivet Sleeve Showing Dimensions 110

Figure 4-64 XRD Patterns of APCVD Al Coatings Deposited at 230°C and 246°C 110

Figure 4-65 Surface SEM Image of 18µm Thick APCVD Al Coating Deposited at 230°C 113

Figure 4-66 Surface SEM Images of APCVD Al Coatings of Different Thickness Deposited at 246°C (Coating thickness of (a) 13 µm and (b) 32 µm) 113

Figure 4-67 SEM Images of APCVD Al Coating Deposited on Hollow Rivet Sleeve at 230°C 114

Figure 4-68 SEM Images of APCVD Al Coating Deposited on Hollow Rivet Sleeve at 246°C 115

Figure 4-69 SEM Image of APCVD Al Coating at 246°C Used to Calculate the Step Coverage Ratio 115

Figure 4-70 GD-OES Depth Profiles of APCVD Al Coatings Deposited at (a) 230°C and (b) 246°C using Precursor PB2 116

Figure 4-71 GD-OES Depth Profiles of Carbon and Oxygen Present in APCVD Al Coatings Deposited at 230°C and 246°C 118

Figure 4-72 Corrosion Potential of APCVD Al Coatings Deposited at 246°C as a Function of Immersion Time in a Salt Solution saturated with Oxygen 120

Figure 4-73 Polarization Resistance of APCVD Al Coatings Deposited at 246°C as a Function of Immersion Time in a Salt Solution Saturated with Oxygen 122

Figure 4-74 Examples of Glass Bead Burnished APCVD Al CoatingsDeposited at 246°C onAerMet 100 and AISI 4340 Specimens 103

Figure 5-1 SEM Photomicrograph of an Aluminum Coating Deposited in the INTA MOCVD Process Pilot Plant 129

Figure 5-2 MOCVD Pilot Plant with a Fixed, Vertical Reactor for Depositing Al-based Coatings 129

Figure 7-1 Ultimate Tensile Strengths and Yield Tensile Strengths vs. Tempering Temperatures of High-strength Steels 150

Figure 7-2 Typical Surface Morphology of an IVD Aluminum Coating 152

Figure 7-3 Composition of an IVD Aluminum Coating Compared to a Reference Material 154

Figure 7-4 Cross-sections of an IVD Aluminum Coating Showing Porosity 154

List of Figures (continued)

Figure 7-5 Cross-section of a Magnetron Sputtered Al Coating 155

Figure 7-6 Magnetron Sputtered Al Coating with Conversion Coating 156

Figure 7-7 AlumiPlate Al Coating on C-ring Specimens after 29 Cycles in GM 9540P Test - Outside Diameter 157

Figure 7-8 AlumiPlate Al Coating on C-ring Specimens after 29 Cycles in GM 9540P Test - Inside Diameter 157

Figure 7-9 AlumiPlate Al Coating on a Grade 8 Bolt after 3,420 Hour Salt Fog Exposure 158

List of Tables

Table 1-1 Modified SERDP Approved Project Plan for Project WP-1405 5
Table 3-1 Specimen Types, Sizes and Materials Used for Testing 16
Table 3-2 Overview of the Tests Conducted and the Corresponding Pass-Fail Criteria 27
Table 3-3 GM 9540P Cyclic Corrosion Test Sequence 32
Table 4-1 Full Width at Half Maximum of All Peaks Measured from XRD Analysis 45
Table 4-2 Full Width at Half Maximum of All Peaks Measured from XRD Analysis on APCVD Al Coatings with Different Precursors and at Different Temperatures 46
Table 4-3 Full Width at Half Maximum of All Peaks Measured from XRD Analysis on IVD and APCVD Al Coatings 47
Table 4-4 Coating Thickness on Outside and Inside of Tube with 3.0 mm Inner Diameter: Pure TIBAL Precursor 49
Table 4-5 Coating Thickness on Outside and Inside of Tube with 3.0 mm Inner Diameter: PB1 Precursor 49
Table 4-6 Coating Thickness on Outside and Inside of Tube with 6.0 mm Inner Diameter: Pure TIBAL Precursor 50
Table 4-7 Coating Thickness on Outside and Inside of Tube with 6.0 mm Inner Diameter: PB1 Precursor 50
Table 4-8 Coating Thickness on Outside and Inside of Coated Hollow Rivet Sleeve 52
Table 4-9. Summary of NRA Analysis of Hydrogen in APCVD Aluminum Coatings 55
Table 4-10 Mass Changes for APCVD Al-Coated Specimens Exposed to Maintenance Fluids 85
Table 4-11 Corrosion Ratings of APCVD Al-Coated Specimens Exposed to Maintenance Fluids 85
Table 4-12 Results of Stress-corrosion Cracking Testing 88
Table 4-13 Notch Fracture Strength of Uncoated AISI 4340 Steel Bars 92
Table 4-14 Results of Tensile Testing of APCVD Al-coated Notched Round Bars before Hydrogen Relief Baking 94
Table 4-15 Results of Tensile Testing of APCVD Al-coated Notched Round Bars after Hydrogen Relief Baking 94
Table 4-16 Results of Tensile Testing of Notched Round Bars as a Function of Temperature and Time 95
Table 4-17 Results of Tensile Testing of Notched Round Bars Cleaned with HCl 95
Table 4-18 Results of Preliminary Hydrogen Embrittlement Testing for Cd Controls and APCVD Al-Coated AISI 4340 Steel Specimens 97
Table 4-19 Results of Additional Hydrogen Embrittlement Testing for Heat Treated APCVD Al-Coated AISI 4340 Steel Specimens 97
Table 4-20 Results of Preliminary Hydrogen Embrittlement Testing for APCVD Al-Coated AerMet 100 Specimens 98

List of Tables (continued)

Table 4-21 Electrical Contact Resistance of APCVD Al Coatings 104

Table 4-22 Typical APCVD Aluminum Deposition Rates and Times 106

Table 4-23 Summary of the Composition of APCVD Aluminum Coatings Deposited at 275ºC and 300ºC 107

Table 4-24 APCVD Al Lower Temperature Deposition Coating Matrix 110

Table 4-25 XRD Results for Coatings Deposited at 230°C and 246°C 112

Table 4-26 Surface Roughness of APCVD Al Coatings Deposited at 230°C and 246°C 112

Table 4-27 Effect of Lower Deposition Temperature, Burnishing and Cr(VI) CCC Post-Treatment on Notch Fracture Strength of AISI 4340 Steel 123

Table 4-28 Effect of Lower Deposition Temperature and Burnishing Post-Treatment on Notch Fracture Strength of AerMet 100 123

Table 4-29 Results of Additional Hydrogen Embrittlement Testingfor APCVD Al-Coated AISI 4340 Specimens 101

Table 4-30 Results of Additional Hydrogen Embrittlement Testingfor APCVD Al-Coated AerMet 100 Specimens 101

Table 5-1 Allowable Temperatures for Some High-strength Aerospace Alloys 127

Table 5-2 Allowable Temperatures for Some Shot Peened Aerospace Alloys 127

Table 5-3 Approximate Loss in Design Allowable Tensile Strength at 246°C and 300°C for Selected Materials 128

Table 6-1 Summary of the Ability of APCVD Al Coatings to meet Property and Performance Requirements for High-strength Steel Substrates 113

Table 7-1 Compositions of the Medium-carbon, Low-alloy, Ultra-high-strength Steels 137

Table 7-2 Compositions of the Ultra-high-strength Steels 138

Table 7-3 Typical Mechanical Properties and Tempering Temperatures for AISI 4130 139

Table 7-4 Mechanical Properties and Tempering Temperature for AISI 4130 Steel Water Quenched at 855°C 139

Table 7-5 Typical Mechanical Properties and Tempering Temperatures for AISI 4340 140

Table 7-6 Mechanical Properties and Tempering Temperatures for AISI 4340 Steel 140

Table 7-7 Typical Mechanical Properties and Tempering Temperatures for 300M Steel 141

Table 7-8 Typical Longitudinal Mechanical Properties of H11 Mod Steel 144

Table 7-9 Longitudinal Room Temperature Tensile Properties of H11 Mod Steel after Exposure at Elevated Temperatures for 10 or 100 Hours 144

Table 7-10 Typical Mechanical Properties of AerMet 100 Alloy 147

Table 7-11 Typical Mechanical Properties of AerMet 310 Alloy 149

Table 7-12 Typical Longitudinal Mechanical Properties at Room Temperature and Elevated Temperatures of AerMet 310 Alloy 149

List of Tables (continued)

Table 7-13 Comparison of Properties for Aluminum Coatings Deposited by Different Methods 153

List of Acronyms

AES	Auger electron spectroscopy
AFRL	Air Force Research Laboratory
AISI	American Iron and Steel Institute
Al	Aluminum
AMS	Aerospace Materials Specification
APCVD	Atmospheric pressure chemical vapor deposition
ARL	Army Research Laboratory
ASTM	American Society for Testing and Materials
at.%	Atomic percentage
C	Carbon
CCC	Chemical conversion coating
Cd	Cadmium
cm	Centimeter(s)
Co	Cobalt
COF	Coefficient of friction
CPE	Constant phase element
Cr	Chromium
Cr(III)	Trivalent chromium
Cr(VI)	Hexavalent chromium
Cu	Copper
CVD	Chemical vapor deposition
dc	Direct current
DIBAL	Di-isobutyl-aluminum
DoD	Department of Defense
EAC	Environment assisted cracking
EC	Equivalent circuit
ECR	Electrical contact resistance
E_{Corr}	Corrosion potential
EDAX	Energy dispersive analysis with x-rays
EIS	Electrochemical impedance spectroscopy
EPMA	Electron probe microanalysis
ESOH	Environmental safety and occupational health
ESTCP	Environmental Security Testing and Certification Program
eV	Electron volt(s)
°F	Degree(s) Fahrenheit
FE-SEM	Field emission scanning electron microscopy
FWHM	Full width at half maximum (of peak)
ft	Foot/feet
GD-OES	Glow discharge optical emission spectroscopy
GPa	Giga-Pascal(s)
H_2	Hydrogen
HB	Brinnell hardness number
HCl	Hydrochloric acid
HE	Hydrogen embrittlement
hr	Hour(s)
HRC	Rockwell C hardness number
HRE	Hydrogen re-embrittlement
HSS	High-strength steel

List of Acronyms (continued)

HV	Vickers hardness number
id	Inside diameter
in	Inch(es)
IVD	Ion vapor deposited/deposition
JCAT	Joint Cadmium Alternatives Team
JG-PP	Joint Group for Pollution Prevention
JTP	Joint Test Protocol
kg	Kilogram(s)
kHz	Kilo-Hertz
K_{ISCC}	Plane-strain stress-intensity threshold (below which SCC does not occur)
ksi	1,000 pounds per square inch
LG	Landing gear
LHE	Low hydrogen embrittlement
µm	Micrometer(s)
mHz	Milli-Hertz
MHz	Mega-Hertz
MMPDS	Metallic Materials Properties Development and Standardization
Mn	Manganese
Mo	Molybdenum
MOCVD	Metallo-organic chemical vapor deposition
MPa	MegaPascal(s)
MRO	Maintenance, repair, and overhaul
nA	Nano-Ampere(s)
N	Nitrogen, nitride
N_2	Nitrogen gas
NaCl	Sodium chloride (“salt”)
NAVAIR	Naval Air Systems Command
NCAP	Non-chrome Aluminum Pretreatment
NFS	Notch fracture strength
Ni	Nickel
NIST	National Institute for Standards and Technology
NJIT	New Jersey Institute of Technology
NRA	Nuclear reaction analysis
Ω	Ohm(s)
od	Outside diameter
O_2	Oxygen gas
OCP	Open circuit potential
OEM	Original equipment manufacturer
OSHA	Occupational Health and Safety Agency
P	Phosphorus
PB1	Proprietary (TIBAL) Blend 1
PB2	Proprietary (TIBAL) Blend 2
PECVD	Plasma-enhanced chemical vapor deposition
PEL	Permissible exposure limit
Pt	Platinum
PVD	Physical vapor deposition
QPD	Quantitative depth profiling
R_a	Average surface roughness
Ref.	Reference

List of Acronyms (continued)

RF	Radio frequency
rms	Root mean squared
RSL	Rising step load
SCC	Stress-corrosion cracking
SCE	Saturated calomel electrode
SEM	Scanning electron microscopy
SERDP	Strategic Environmental Research and Development Program
Si	Silicon
SiC	Silicon carbide
SiO_2	Silicon dioxide
Sn	Tin
TACOM	Army Tank Automotive Command (now TACOM Life Cycle Management Command)
TCP	Trivalent chromium pretreatment
TEAL	Tri-ethyl-aluminum
Ti	Titanium
TIBAL	Tri-isobutyl-aluminum
TiN	Titanium nitride
UTS	Ultimate tensile strength
UV	Ultra-violet
V	Vanadium
wt.%	Weight percentage
W	Tungsten
WC	Tungsten carbide
WDS	Wavelength-dispersive spectrometry
XPS	X-ray photoelectron spectroscopy
XRD	X-ray diffraction
XRR	X-ray reflectivity
Zn	Zinc

Acknowledgments

The overall objective of this program was to investigate the use of atmospheric pressure, chemical vapor deposition to produce high quality, aluminum coatings for the corrosion protection of high strength steels, so that the use of cadmium coatings can be eliminated. To achieve this objective the U.S. Air Force assembled a team from the Department of Defense, academe, and industry as follows:

* **Air Force Research Laboratory (WPAFB, OH)**
  DoD requirements, project administration, testing, and technical support
  Dr. Elizabeth S. Berman, Dr. Eric W. Brooman, and Mr. John Kleek
* **Army Research Laboratory (Aberdeen Proving Ground, MD)**
  DoD requirements, testing of coatings
  Dr. John H. Beatty and Mr. Brian E. Placzankis
* **Naval Air Systems Command (Patuxent River, MD)**
  DoD requirements, testing of coatings (years 1 and 2 efforts only)
  Mr. Andrew Schwartz, Mr. Bill Nickerson, and Mr. Steven Brown
* **New Jersey Institute of Technology (Newark, NJ)**
  Process, coating characterization, testing, and equipment development
  Prof. Roland A. Levy, Dr. Sungmin Maeng, and Mr. Sipeng Gu
* **AkzoNobel (Deer Park, TX and Chicago, IL)**
  Coating deposition, commercial process and equipment development
  Dr. Alexander Borovik, Dr. Dennis Deavenport, Dr. Fernando Gómez, and Mr. Sam Newberg
* **The Boeing Company (St. Louis, MO)**
  Aircraft industry liaison and technology insertion assistance
  Mr. Stephen P. Gaydos.

The contributions of these Team Members, supporting the Co-Principal Investigators at the Air Force Research Laboratory, cannot be underestimated. Without their continuous involvement, thoughtful suggestions, cogent technical contributions, and the use of their facilities, this Project would not have been possible.

Others have contributed to the accomplishments described in this Final Report. We would like to thank Mr. J. Kane of Acton Materials, Inc. (now Wells Corporation) for assistance with the deposition of coatings using tri-ethyl aluminum as the precursor; Dr. J. Thorton and Mr. R. Helton for their assistance with sample preparation at AkzoNobel; Mr. R. Moore for performing AES and XPS analyses, Dr. B. Lanford for conducting NRA analysis, and Dr. Y. Suh for performing adhesion tests at the New Jersey Institute of Technology. Also, the contributions are recognized of Mr. J Bushi of Twin Analytical, Ltd. for conducting the GD-OES chemical composition analyses, and Mr. N. Jacobs and Dr. D. Hansen of the University of Dayton Research Institute, who performed much of the hydrogen embrittlement and fatigue testing, and electrochemical testing, respectively. Finally, recognition is made of the helpful comments and suggestions regarding the interpretation of the data, especially with respect to technology insertion, from Mr. B. Sartwell of the Strategic Environmental R&D Program Office, and Dr. Keith Legg, of the Rowan Technology Group.

Executive Summary

The overall objective of this SERDP-funded study (Project WP-1405) was to evaluate the use of atmospheric pressure, chemical vapor deposition (APCVD) to produce uniform and conformal aluminum (Al) coatings with desirable properties, primarily on high-strength steel substrates. This process offers an environmentally benign alternative to cadmium (Cd) plated coatings, as well as promises to provide high production through-put, low cost, and coatings with the performance necessary to meet a wide range of end user requirements.

Cadmium is a carcinogen, teratogen, and toxic chemical. It is easily released or leached during routine maintenance operations, such as paint removal and the wash down of aircraft, causing particulate emissions and the contamination of ground water and the food chain, respectively. Spills and leaks from the plating process, and unauthorized dumping directly to rivers and streams, or surges into waste water treatment facilities, have a much greater effect. These environmental and health related concerns are further aggravated by the use of sodium cyanide (a toxic and reactive chemical) in the Cd plating baths, and the use of a hexavalent chromium (Cr) toxic and carcinogenic chemical in the post deposition treatment for some applications to increase the corrosion resistance of the electroplated Cd coating.

APCVD Al deposition focused on using tri-isobutyl-aluminum (TIBAL) as a precursor to deposit coatings at different deposition temperatures, originally in the range of 275° to 300°C, and to explore the effects of other processing parameters. The test results, feedback from the SERDP Office, and a review of published design allowables for high-strength steels used for aircraft critical components, indicated that the maximum deposition temperature should not exceed 246°C. Consequently, during the last two quarters of this project, the focus shifted to depositing coatings at temperatures in the range of 230° to 250°C. In addition, some efforts were directed at using blended mixtures of TIBAL and other Al alkyl compounds to improve coating quality and facilitate process control.

The APCVD deposition process equipment was scaled up from using a bench top tubular reactor to a small, prototype rotating barrel pilot plant. In a parallel effort, the latter was scaled up to the first commercial unit for depositing Al coatings on small discrete parts - such as fasteners - for use in the automotive and other industries.

The principal accomplishments during the first phases of this project (deposition at temperatures in the range 275°-300°C) may be summarized as follows:

1. It was established that the APCVD process could be used to **successfully deposit aluminum coatings** on substrate materials of interest by using the right combination of equipment design, precursor chemicals and carrier gases, substrate preparation, and operating parameters, such as temperature and deposition time.
2. **Deposition rates** depended on processing temperature and other process variables, but typical values for the required 8.5 to 25 μm (0.3 to 1.0 mil) thick coatings were 1.1 to 2.0 μm/min. Typical deposition times at temperature were from 7 to 22 minutes, depending on the precursor used and the deposition temperature.
3. It was demonstrated that the **process could be scaled up** from using a laboratory, bench top reactor, to a small, pilot plant reactor, to a full size commercial unit for applying Al coatings to discrete, small parts, such as fasteners.

4. Using experience gained from other commercial uses of the process chemicals, especially the precursors, **worker** and **equipment safety** and **environmental issues have been addressed** satisfactorily.
5. Coatings with **high aluminum content** (average ~96.9 at.%; ~98.3 wt.%) were obtained with pure TIBAL. The actual concentration in each coating varied according to the deposition temperature and the methods used for analysis. With optimization of the processing parameters, it was possible to obtain Al concentrations greater than 99 wt.%.
6. Small amounts of **oxygen, carbon,** and **hydrogen were incorporated in the coatings** during deposition, but only in the surface regions (≤25 nm). Of these, the presence of hydrogen is the greatest concern with high-strength steels, but it can be removed by the conventional heat treatment (low temperature "bake") that is applied to Cd coatings to prevent hydrogen embrittlement.
7. The **throwing power and conformal coverage** of the APCVD Al coatings was excellent, and in the required thickness range the coverage was uniform and the surfaces were relatively smooth (≤1,000 nm, rms).
8. The **crystalline structure** of the APCVD Al coatings was equi-axed, which is desirable for providing good properties and satisfactory performance in service. The coatings exhibited a face-centered cubic crystalline structure with an (111) preferred orientation, comparable to that obtained for pure, bulk Al metal. This structure was found to be independent of the deposition conditions for the ranges of pretreatment, deposition, and post-treatments parameters used.
9. The overall APCVD Al **coating integrity** was very good. As deposited coatings were denser and exhibited fewer defects than the benchmark IVD Al coating. In a few instances, small pits were detected in some of the electrochemical and corrosion tests; however, pits also were found in IVD Al coatings. The **density** measured for the APCVD Al coatings (~2.6 ±0.04 gm/cm^3) was similar to that reported for the benchmark electroplated Al coating (note that a typical value in the literature for bulk Al metal is 2.70 gm/cm^3).
10. No problems with coating **adhesion** were observed in either the pull off test or the mandrel bend adhesion test. Cracking or spalling of the coatings did not occur.
11. **Hardness** was measured, although it is not considered to be a critical parameter for USAF and most other applications. Nano-hardness measurements yielded an average value of ~550 MPa for the APCVD Al coatings, compared to an average of about 835 MPa for an Al single crystal used as a reference material. The calculated **Young's Modulus** was between 21.4 and 51.2 GPa, compared to 70 GPa for bulk Al metal and IVD Al coatings.
12. APCVD Al coatings, as deposited at 275º to 300ºC, easily passed the **contact resistance** requirement of 10 milli-ohms per square inch, even after being exposed to a salt fog environment for 168 hours.
13. The **electrical resistivity** of an APCVD Al coating of the required thickness was found to be 3.5 ±0.1 μohm.cm, which is similar to, but a little higher than that for bulk Al metal.
14. It was demonstrated that APCVD Al coatings can provide the required **galvanic (i.e., sacrificial) protection** to high-strength steel. As an example, the **corrosion potential** (E_{corr}) of the coatings was about 200mV more anodic than that observed for AISI 4130 steel, and remained constant (and similar to that measured for IVD Al coatings) even after 10 days exposure to salt fog. The E_{corr} difference was found to be 300-400 mV for AISI 4340 steel. At the sites of any pits present in the APCVD Al coatings, SEM analysis showed that the exposed substrate material remained free of corrosion products (red rust) and the adjacent Al coating had dissolved to provide protection.

15. In the ASTM B 117 test, the APCVD Al coatings, as deposited or painted, provided **corrosion protection** that met the criterion set for pass or failure. However, coating optimization will be necessary to demonstrate that this type of Al coating can perform well in a salt fog environment for at least 1,000 hours, as has been demonstrated for electroplated Al coatings. Also, during the corrosion reaction that occurs, aluminum hydroxide is formed and some hydrogen is generated that can lead to hydrogen re-embrittlement in service. This obstacle must be overcome before technology insertion can occur.
16. In the GM 9540P **accelerated corrosion** tests, the APCVD Al coatings, as deposited at 300ºC, provided corrosion protection that also met the "pass" criterion. Coatings that had received a commercial, trivalent chromium (TCP) chemical **conversion coating** performed better than the as deposited coatings with no post-treatment.
17. In the ASTM F 1624 test, the APCVD Al coatings, as deposited at 300ºC, demonstrated that they had no adverse effect on **stress-corrosion cracking**, provided that they had received a standard hydrogen relief bake.
18. **Fluid compatibility** tests were conducted with five liquids commonly used in aircraft maintenance, repair, and overhaul (MRO) operations. In general, the results were similar to those for the corrosion tests mentioned above; namely, the samples that had received the standard hydrogen relief bake fared much better than those that had not, and those with the commercial, TCP conversion coating performed better than the as deposited coatings with none. The one exception was with a hydrogen peroxide-based paint stripper, where corrosion attack of the Al was significant, and whisker like crystals had grown all over the exposed surfaces. However, peroxide-based strippers are not used much in DoD MRO operations, so this does not constitute a major barrier to implementing the APCVD process.
19. The deposition temperatures (275º to 300ºC) used in the first part of this project had a negative impact on the high-strength steel substrate materials, reducing their notch **tensile strength** in some cases to unacceptable levels (>10%) that would not meet design allowables for strength. This loss in strength, in turn, resulted in an unacceptable fatigue debit. The standard hydrogen relief bake applied to the APCVD Al-coated notched test bars had a positive effect, in so far as there was less loss in tensile strength of the substrate material, but it was not sufficient to alleviate the problem. Consequently, during the last two quarters of developmental work the focus shifted to obtaining satisfactory coatings at lower deposition temperatures in the range of 230º to 245ºC.
20. In the constant amplitude, axial **fatigue** tests the Cd-plated AerMet 100 specimens exhibited some flaking of the coatings whereas the APCVD Al-coated specimens did not. The latter failed at just less than 69,000 cycles, but the former failed after only 20,500 cycles. In other fatigue tests with cadmium plated, APCVD Al-coated, and bare AerMet 100 specimens, S/N curves (with Kt = 1, R = -1, and f = 5Hz) were generated over 5,000,000 cycles. The fatigue debit was about three times greater for the APCVD Al-coated specimens than for the Al plated specimens, which was unacceptable.
21. The **hydrogen embrittlement** test results with both the coated AISI 4340 steel and AerMet 100 alloy substrates were mixed. Specimens receiving the standard hydrogen relief bake treatment passed the test criterion for the experiments done in air, but failed when the tests were done in deionized water or a 3.5% salt solution. In contrast, the Cd-plated AISI 4340 steel control specimens passed when tested in air and the salt solution, but the Cd-plated AerMet 100 control specimens failed when tested in both deionized water and the salt solution. Thus, to some degree, the APCVD Al-coated specimens performed as well as the Cd-plated control specimens. Further investigation is needed to explain the results that were obtained.

The accomplishments made during the last phase of this project, which focused on depositing coatings at lower temperatures, may be summarized as follows:

22. APCVD Al coatings **can be deposited at 230º to 250ºC** using a proprietary TIBAL blend as a precursor and adjusting the residence time at temperature in the reactor. The coating **structure** remains fcc crystalline.
23. **Deposition rates** depended on processing temperature and other process variables, but typical values for the required 8.5 to 25 µm (0.3 to 1.0 mil) thick coatings were 0.3 to 0.65 µm/min. Typical deposition times at temperature were 20 to 75 minutes, depending on the precursor used and the deposition temperature.
24. The **composition** of the coatings was similar to that obtained at the higher deposition temperatures. Small amounts of **oxygen, carbon,** and **hydrogen were incorporated in the coatings** during deposition, but only in the surface regions.
25. The **throwing power and conformal coverage** of the APCVD Al coatings was similar to that observed with the coatings deposited at the higher temperatures.
26. The coating **structure** remains fcc crystalline, and is not columnar.
27. The overall APCVD Al **coating integrity** for these no-optimized coatings was good, but more nodular, especially for the thicker coatings (~30 µm).
28. No problems with coating **adhesion** were observed.
29. The standard hydrogen relief bake had a positive effect on **notch fracture strength**, and the limited data obtained indicated that, for coatings deposited at 230º to 246ºC on AISI 4340 steel specimens, the loss in strength could fall in the acceptable range; this would result in a much **smaller fatigue debit**, which might meet the test requirements criterion.
30. The **hydrogen embrittlement** test results with both the coated AISI 4340 steel and AerMet 100 alloy substrates were also mixed, and similar to those obtained for the coatings deposited at the higher temperatures. Coatings deposited at 246ºC passed when tested in air, with or without being glass bead burnished and receiving a Cr(VI) based CCC; whereas, coatings deposited at 230ºC did not pass. On AerMet 100 substrates, coatings deposited at 246ºC and glass bead burnished passed the HE test in air, but failed when tested in the salt solution.

In summary, the results obtained with the coatings deposited at the lower temperatures are promising, in so far as better performance was observed, but it is obvious that, to meet all the specified test criteria, further optimization of the precursor and other deposition parameters is needed to determine the optimum deposition temperatures and post-treatments for each high-strength alloy of interest. For lower strength steels and other substrate materials, where loss in strength as a result of the time at temperature during deposition is not an issue, technology insertion is possible and one commercial production facility has been commissioned to apply aluminum coating to small discrete steel parts.

1.0 Objective and Approach

In this section, the rationale leading to the objective of this project is briefly described, followed by an outline of the approach for meeting this objective.

1.1 Objective

Cadmium plating has been used to protect steel parts used in a wide range of weapon systems from corrosion in service. However, cadmium is known to be a carcinogen, teratogen, and toxic chemical. It is easily leached from routine maintenance operations, such as the wash down of aircraft, causing contamination of ground water and the food chain. Spills and leaks from the plating process, and unauthorized dumping directly to rivers and streams, or surges into waste water treatment facilities, will have a much greater effect. These environmental and health related concerns are further aggravated by the use of sodium cyanide (a toxic and reactive chemical) in the cadmium plating baths, and the use of a chromium(VI) toxic and carcinogenic chemical in the post plating (conversion) treatment for some applications to increase the resistance of the cadmium coating to corrosion.

In summary, there is a wide range of environmental, safety and occupational health issues associated with cadmium plating. Consequently, the use of cadmium is heavily regulated at the federal, state, and local level. In addition, two Executive Orders (13480 and 14323) have been promulgated with a mandate to reduce the use of cadmium at government facilities, including those owned and/or operated by the Department of Defense (DoD). For the latter, it is a time consuming and costly endeavor to keep these facilities in compliance with the relevant laws and regulations, and to maintain a healthy and safe environment for its workers. Non-compliance also has a negative effect on readiness and sustainability.

With the above brief explanation of the general environmental problem in mind, and the fact that the Strategic Environmental Research and Development Program (SERDP) has posted numerous Statements of Need relating to pollution prevention associated with weapon systems, the **overall objective of this project** may be stated as follows:

> *Investigate the feasibility of using atmospheric pressure, chemical vapor deposition (APCVD) to deposit high quality, aluminum coatings for the corrosion protection of high-strength steels, so that the use of cadmium coatings for this purpose can be eliminated during weapon systems manufacture and maintenance, repair, and overhaul operations at DoD facilities.*

The **technical objective of this project** may be stated as follows:

> *Develop a high throughput and low cost APCVD process to produce aluminum coatings on high-strength steel parts and components that:*
>
> - ✓ *Can replace electroplated cadmium coatings and meet environmental/compliance, health, and safety goals*
> - ✓ *Provide conformal surface coverage to desired thickness (8.5-25.4 μm, 0.0003-0.0010 in)*
> - ✓ *Have desirable physical, chemical, and mechanical properties that meet specified performance requirements*
> - ✓ *Can be tailored for high-strength steel components and parts used in military (and commercial) aircraft*

- ✓ *Is robust and easily scalable for both commercial and military applications*
- ✓ *Reduces life cycle costs while meeting DoD mission (and industry) requirements.*

1.2 Technical Approach

A tiered, iterative (continuous improvement) approach was used - as outlined in Figure 1-1 below and indicated by the list of major tasks, subtasks, and activities in Table 1-1 - to evaluate the APCVD process, which included: selecting deposition parameters; optimizing the deposition process for small, discrete parts (such as steel fasteners); measuring the properties of the coatings; determining the performance of the coatings against baseline data; beginning process scale up; and investigating opportunities for applying the aluminum (Al) coatings to larger parts. Two "Go/No Go" decision points were incorporated into the project plan - as shown in Figure 1-1 - and subsequent activities were not commenced until it had been mutually agreed that the progress made justified continuing the evaluation of the process and the coatings it produced.

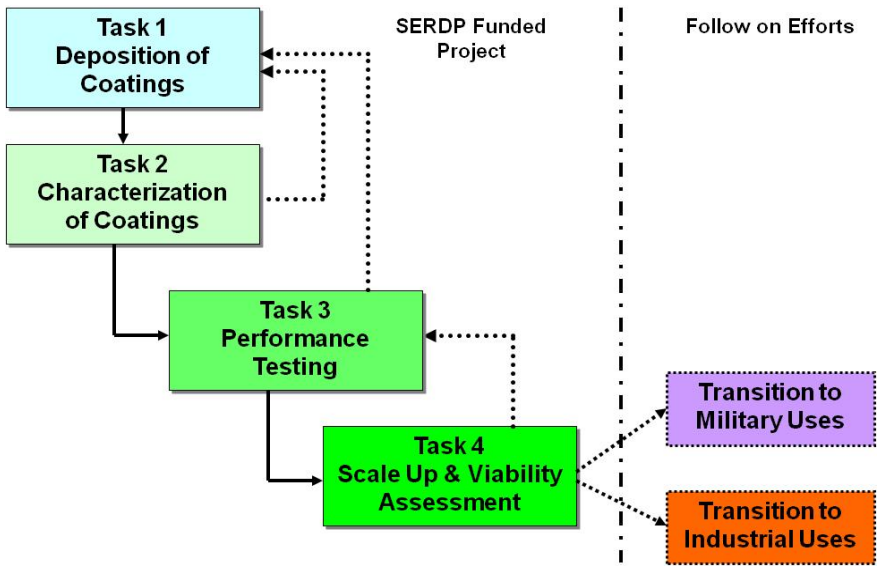

Figure 1-1. SERDP Project WP-1405 Project Outline

KEY:

Task 1: Deposition of Coatings

- ✓ Establish coating requirements, controls, and criteria for success
- ✓ Set up and calibrate equipment
- ✓ Investigate effect of processing parameters and deposit Al coatings

Task 2: Characterization of Coatings

- ✓ Determine composition and structure
- ✓ Perform selected screening tests
- ✓ Provide feedback on optimal process parameters ..... **GO/NO GO DECISION**

Task 3: Performance Testing of Coatings

- ✓ Appearance/quality/thickness uniformity, etc. measurements
- ✓ Corrosion and chemical resistance, etc. testing
- ✓ Fatigue debit, reparability, etc. testing ..... **GO/NO GO DECISION**

Task 4: Scale Up and Viability Assessment

- ✓ Deposit Al coatings on selected part(s)
- ✓ Evaluate if there is a need for post-treatment(s)
- ✓ Perform a preliminary cost benefit analysis ..... **RECOMMENDATIONS**

Table 1-1. Modified SERDP Approved Project Plan for Project WP-1405

Task No.	Subtask No.	Description of Activity	Comments	Cross-reference to Section in Final Report
1.0	- -	**Deposition of APCVD Aluminum Coatings**		
	1.1	Set up APCVD bench-top reactor	Initially at NJIT; later small pilot plant at AkzoNobel	3.1.3, 3.1.4, 3.2.1, 3.2.2
	1.2	Calibrate reactor and ancillary equipment	Initially at NJIT; later small pilot plant at AkzoNobel	3.1.6, 3.2.2
	1.3	Deposit Al coatings on high-strength steel substrates	Other substrates also coated	3.1.3, 3.1.4, 3.2.1, 3.2.2; 4.1
	1.4	Measure growth rate as function of processing parameters	Time in reactor and temperature for high-strength steels	3.3; 4.2.1
	1.5	Determine nature of (coating) growth mechanism	To assist in optimization efforts	3.3
	1.6	Optimize growth conditions from feedback data	Continuous effort to improve process, provide test specimens	4.0
	1.7	Investigate new precursor for lower temperature deposition	Added in 2008	4.2.1, 4.2.4, 4.2.5
2.0	- -	**Characterization of APCVD Aluminum Coatings**		
	2.1	Perform compositional analysis of coatings	Using AES, NRA, XPS, GD-OES, etc.	3.3.5
	2.2	Carry out structural, morphological, mechanical and electrical characterization of coatings	Using Metallography, XRD, SEM, AFM, etc.	3.3.1, 3.3.2, 3.3.3, 3.3.4, 3.3.7, 3.3.8
	2.3	Interpret characterization data, summarize findings and provide feedback for optimizing coatings	Down select best conditions for additional coating deposition trials	4.1.1, 4.1.2, 4.1.3, 4.1.4, 4.1.5, 4.1.6, 4.1.7, 4.1.8
	2.4	Perform characterization (property) testing on coatings deposited at lower temperatures	Added in 2008	4.2.1, 4.2.4, 4.2.5
3.0	- -	**Performance Testing of APCVD Aluminum Coatings**		
	3.1	Evaluate adhesion of coating to substrate, paint to coating	In service OEM, MRO requirement	3.3.6, 3.3.7; 4.1.6, 4.1.7
	3.2	Evaluate compatibility of coating with substrate materials	Establish that coating has no adverse effect on substrate properties	3.3.7; 4.1.7
	3.3	Evaluate sacrificial corrosion protection capability	Critical, in service requirement	3.3.6; 4.1.6
	3.4	Measure fluid compatibility/corrosion resistance	In service MRO requirement	3.3.6; 4.1.6
	3.5	Investigate general (coating) properties and performance	Such as throwing power, uniformity, reparability, contact resistance, etc.	3.3.3, 3.3.7, 3.3.8; 4.1.2, 4.1.3, 4.1.4, 4.1.6, 4.1.7, 4.1.8
	3.6	Evaluate lubricity of coating	OEM, MRO requirement for fasteners	3.3.7; 4.1.7
	3.7	Evaluate (coating) susceptibility to H_2 embrittlement and SCC	Critical, in service requirement	3.3.6, 3.3.7; 4.1.6, 4.1.7
	3.8	Evaluate effect of coating on substrate fatigue resistance	Critical, in service requirement	3.3.7; 4.1.7
	3.9	Perform performance testing on coatings deposited at lower temperatures	Added in 2008	4.2.4, 4.2.5, 5.1
4.0	- -	**Scale-up and Viability Assessment**		
	4.1	Set up commercial APCVD reactor, ancillary equipment	Subject to successful completion of Tasks 1 - 3	3.2.3; 5.2;
	4.2	Fit prototype reactor with optimized APCVD Al process	For a selected application	5.2
	4.3	Deposit APCVD Al on selected high-strength steel parts	For a selected application, if possible	5.2
	4.4	Evaluate properties and performance of coated parts	For selected application, if possible	4.24; 5.1, 5.2
	4.5	Fine tune process in prototype, commercial reactor	For selected application, if possible	5.2
	4.6	Assess need for coating post-treatments to improve performance	Such as corrosion resistance and primer, paint adhesion	3.3.6, 3.3.7; 4.1.6, 4.1.7, 4.2.4; 5.1; 7.2
	4.7	Carry out preliminary cost benefit analysis; assess potential for technology transfer, commercial viability	Subject to successful completion of Tasks 1 - 3	4.2.1; 5.1; 7.1, 7.2
5.0	- -	**Annual Briefings and Reports; Final Report**	As required by contract	1.2; 8.2, 8.3, 8.4

The entries shown in red in Table 1-1 were Subtasks added at the end of the original planned activities to explore the feasibility of depositing coatings at a lower processing temperature, using a proprietary precursor developed during the third year by AkzoNobel. Because some activities were conducted iteratively and/or concurrently, a cross-reference is made in Table 1-1 between the numbered Subtasks and where the corresponding activities are described or discussed in this Final Report.

Finally, as the APCVD process is a “dual use” technology, both defense and industrial applications were considered. These applications included those in the defense industrial base, the automotive industry, and the commercial aircraft industry. Consequently, to accomplish the project objectives, the Project Team (listed in the Acknowledgments section) was structured to include representatives from the Tri-services, commercial aircraft manufacturing, academe, and industrial chemical vendors, including one that had initiated its own efforts to commercialize APCVD technology. As a result, the probability of meeting the objectives and subsequent technology insertion was maximized. This final deliverable, the Final Report, documents how well the technical objectives were met by the Project Team.

2.0 Background to Alternative Coating and Process Selection

In this section the focus not only is on environmental issues, mentioned in Section 1.0, but also on occupational health and safety issues. The latter include past and present evaluations of possible alternatives to Cd coatings. Finally, the rationale is given behind choosing Al as the coating material, and APCVD as the preferred deposition technology.

2.1 Problem Addressed by this Technology

Cadmium plating is used to protect high strength steel parts (e.g., landing gear, rotor shafts, pneumatic/hydraulic actuator rods and cylinders, aircraft engine attach points, thrust pins, torsion links, locks, fasteners, etc.) from corrosion in a wide range of DoD weapon systems. It is used also as a sacrificial (protective) metal coating under painted surfaces on weapon systems. Unfortunately, Cd is easily removed during aircraft wash downs, depainting, and surface preparation during maintenance, repair, and overhaul (MRO) operations resulting in costly disposal of large volumes of liquid and solid wastes. In addition, there are concerns with Cd airborne dust generation (as is the case with mechanical removal) and the Occupational Safety and Health Administration (OSHA) has imposed a relatively low permissible exposure limit (PEL) for cadmium dust[1], leading to increased compliance costs. Therefore, despite cadmium's excellent properties (adhesion, corrosion resistance, and lubricity), its ease of application, low processing cost, and versatility, the environmental, health, and safety issues associated with its use are significant, and many regulations have been imposed on its use and disposal.

Cadmium is known to be a carcinogen, teratogen, and toxic metal. In addition, if disposed of in landfills, it easily can be leached out causing contamination of the ground water supply and food chain. These environmental and health related concerns are further aggravated by the common use of sodium cyanide in Cd plating baths, and the use of hexavalent chromium-based post-treatments, both of which pose serious worker health and safety concerns.

The U.S. Air Force is promoting a policy to minimize and eventually eliminate the use of Cd coatings on aircraft as well as ground support systems. This directive affects the original equipment manufacturers (OEMs) and their suppliers. Additionally, the more stringent world-wide environmental standards and regulations also affect commercial aircraft. Thus, this is a significant driver to find one or more satisfactory alternatives. Any proposed replacements for Cd, therefore, must not only match or surpass its current performance, production throughput, maintainability, reparability, and cost, but also guarantee elimination of the current cadmium-related waste streams without generating another regulated hazardous waste stream. Any alternative coating must exhibit the following properties:

- ✓ Compatibility with substrate materials and working fluids used during manufacturing, and MRO operations
- ✓ Acceptable galvanic (sacrificial) protection and corrosion resistance
- ✓ No adverse effect on hydrogen embrittlement and re-embrittlement
- ✓ No adverse effect on other environmentally assisted cracking
- ✓ Low electrical contact resistance
- ✓ Acceptable lubricity and torque/tension values for fasteners
- ✓ Ability to be subsequently painted.

[1] The OSHA PEL established for cadmium dust is five micrograms per cubic meter of air (5 $\mu g/m^3$) calculated as an eight-hour, time-weighted, average exposure.

To address the need for a replacement, several technologies for applying alternative coatings to high strength steels have been, or are being evaluated[2], such as the use of electroplated zinc-nickel (Zn-Ni) and tin-zinc (Sn-Zn) alloys from aqueous plating baths[3, 4], electroplated Al from an organic plating bath[5], and ion vapor deposited (IVD) Al[6, 7]. These and some of the other candidates are discussed below. However, no candidate has emerged yet as the ***single*** best alternative to Cd for all end uses.

2.2 Prior Work on Cadmium Replacement

Numerous processes and materials have been evaluated as an electroplated Cd alternative over the last few decades, as discussed in Footnote [2]. Besides the candidates mentioned above, metal-filled polymeric coatings have been evaluated, especially for fasteners[8], and replacing the substrate material with one that does not corrode[9] to avoid the need for any coating.

The Zn-Ni and Sn-Zn alternatives involve alloy plating, which are more complex and less robust processes than the deposition of elemental cadmium because the alloy composition, which determines the final coating performance, depends on many bath processing parameters (e.g., current density, solution chemistry, and temperature) that are difficult to control. Furthermore, because steel parts are exposed to aqueous solutions during plating, hydrogen generated and entering the part during plating must be removed by either: (1) a post plating baking protocol, typically 24 hours at 191°C (375°F) or (2) mitigated by pre-coatings - such as a nickel strike - that provide a barrier to the migration of hydrogen into the substrate during plating. A near neutral or alkaline, "low hydrogen embrittlement" (LHE) Zn-Ni process appears to be the best "drop in" plating technology, and this alkaline technology is being developed by Boeing as a possible alternative to Cd plating for the C-17 Program Office of the U.S. Air Force[10]. However, even this requires a nickel strike as a barrier to hydrogen ingress, otherwise the Zn-Ni coating cannot pass the hydrogen embrittlement tests.

Another alternative technology to Cd plating consists of using polymers filled with metal flakes (i.e., Zn or Al). These coatings are deposited by the dip-spin method, in which fastener parts to be coated are loaded in a basket that is dipped into the polymer resin composite, then lifted out and spun at high speed to remove the excess material. The parts are subsequently baked to set the resin. This technology has been tested by the U.S. Army TACOM and found to be as

---

[2] G. C. Wright, E. W. Brooman, et alii, "*Evaluation of Alloy Coatings Being Developed as Alternatives to Cadmium Coatings*", Proc. SUR/FIN '03, Session P, Milwaukee, WI, The American Electroplaters & Surface Finishers Society (June, 2003).

[3] K. O. Legg, "*Overview of Chromium and Cadmium Alternative Technologies*", Proc. of the 15th International Conf. on Surface Modification Technologies, ASM International, Materials Park, OH, pp. 235-244 (2002).

[4] G. F. Hsu and R. C. Colonel, "*Zinc-Nickel Electroplated Article and Method for Producing the Same*", U.S. Patent No. 4,765,871 (1988).

[5] J. Fischer, B. Fuhr, "*Aluminum Plating Replaces Cadmium*", Advanced Materials & Processes, **155** (4), pp. 27-29 (1999).

[6] D. E. Muehlberger, "*Ion Vapor Deposition of Aluminum: More than Just a Cadmium Substitute*", Plating & Surface Finishing, **25** (11), p. 65 (1983).

[7] A. Malazgirt, J. W. Evans, "*Production of Aluminum and Aluminum Coatings by Thermal Decomposition of Aluminum Alkyls*", Metallurgical Transactions B, **11** (2), pp. 225-232 (1980).

[8] G. Shaw, "*The Nuts and Bolts of Cadmium Plating Alternatives: a Study of Long Term Performance Characteristics by the U.S. Army*", Automotive Finishing Magazine On-line.

[9] C. J. Kuehmann, "*Computational Design of Corrosion-Resistant Steels for Structural Applications in Aircraft*", Final Report, Project PP-1149, Strategic Environmental R&D Program (2001).

[10] S. P. Gaydos, "*Cadmium Alternative Studies for C-17 Pollution Prevention Projects*", Joint Cadmium Alternatives Team Meeting (March 16, 2005).

good as Cd plating in the case of fasteners. Although highly cost-effective (~$0.70 per kg or $0.30 per pound of parts) control of the process is crucial in insuring the proper resin viscosity in order to avoid excessive coating thickness that clogs fastener threads. Coatings typically require an elevated temperature cure that makes their use impractical for heat sensitive substrates (such as tempered Al alloys or high-strength steels) or for the *in situ* repair of sacrificial coatings.

The environmental issues associated with cadmium-coated steels can be totally eliminated by using specially designed stainless steel alloys. One example is the proprietary Ferrium® S53 alloy developed under the SERDP Project PP-1149 referenced in Footnote [9]. Aircraft manufacturers have successfully implemented this elimination approach in engines (e.g., F-119 used in the F-22), aircraft actuators, and landing gears. Although such an approach works well for the afore-mentioned applications, stainless steels are generally more costly and in some cases (e.g., 15-5PH precipitation hardened steels) are inferior in strength to Cd-plated, high strength steel. Furthermore, stainless steels still cannot be used without a sacrificial coating in situations where painting is required or galvanic corrosion may develop, such as on airframes where the steel would be in contact with the aluminum skin of the aircraft.

2.3 Best Cadmium Alternative Candidates

The Air Force Research Laboratory (AFRL) tasked Concurrent Technologies Corporation, in cooperation with The Boeing Company, to develop a Joint Test Protocol (JTP) for identifying and evaluating Cd alternatives for use on high-strength steels (with the understanding that they also would be suitable for use on other steels). The purpose of the JTP was to design and outline a single suite of performance requirements and test methods that can be used to qualify alternative Cd coating processes in accordance with DoD-wide requirements and acceptance criteria. To support the JTP development and ensure accuracy and completeness, the Joint Services (U.S. Air Force, Army, and Navy) and the OEMs were asked to participate to determine the necessary tests to meet common and Service-specific needs; provide a means of confirming vendor performance claims; allow for Joint Service analyses; and outline the requirements for coating developers to qualify new materials and processes to replace cadmium.

In addition to the JTP, the AFRL and Concurrent Technologies Corporation developed for the Environmental Security Technology Certification Program (ESTCP) the "High Strength Steel Cadmium Alternative Test Plan". This test plan organized the required testing into sequential phases, and described the logistics, roles, and responsibilities involved with the execution of the JTP. Phase I activities under the supervision of the Naval Air Systems Command (NAVAIR) have been completed for the testing of both primary and repair coatings identified as potential replacements for Cd. The Phase I testing consisted of hydrogen embrittlement (HE), re-embrittlement (HRE), and stress-corrosion cracking (SCC) analysis of the selected coatings to ensure that potential replacement processes had no detrimental effect on the steel substrates. In addition, bend adhesion testing was performed for each process to determine whether the deposited coating was capable of adequately adhering to the substrate materials.

Data generated during Phase I testing[11] were reviewed with the Joint Cadmium Alternatives Team (JCAT), who down-selected the coatings and processes for testing and evaluation in

[11] E. N. Beck, "*Joint Test Report for Execution of Phase I of High Strength Steel Joint Test Protocol for Validation of Alternatives to Low Hydrogen Embrittlement Cadmium for High Strength Steel Landing Gear and Component Application - of July 2003*", Naval Air Warfare Center Aircraft Division Technical Report NAWCADPAX/TR-2006/164 (10 January, 2007).

Phase II. An electroplated Al coating outperformed all other primary coatings, including Cd, in Phase I evaluations, while the Sn-Zn coating and an acidic Zn-Ni coating were dropped from the study due to poor performance. Results for the repair coatings were mixed, with brush plated Sn-Zn performing the best, though there was considerable interest in the other repair coatings.

While significant testing remains to be completed, some candidate coatings selected for Phase II evaluation under the JTP show potential as replacements for Cd based on current results[12]. Specifically, the electroplated Al and sputtered Al coatings have exhibited the strongest performance in tests completed up to this point. Significant concerns exist with the LHE Zn-Ni coating after failing portions of the strippability, bend adhesion, and paint adhesion tests. Currently, all the brush plated, repair coatings are showing promise, although only a limited number of tests have been completed to this point. Once the complete set of tests has been finished and results are available for all coatings, the JCAT will meet to select the most promising coating(s) for the next step towards DoD technology insertion.

2.4 Selection of Aluminum for Study

The simplest approach to finding a Cd coating replacement appears to be to use an Al-based coating. Aluminum is environmentally friendly, non-toxic, and safe to handle and use by workers. These qualities eliminate some life cycle costs, such as waste collection, storage, and disposal in association with the processing of hazardous materials. Acid salt fog, neutral salt fog, and outdoor exposure tests have demonstrated unequivocally that Al coatings provide equal or superior corrosion protection to Cd-plated steel parts. They offer additional advantages; e.g., they can be subjected to temperatures as high as ~500°C (925°F), while Cd is limited to ~230°C (450°F). Also, they may be exposed to fuels with no adverse effects and can be used in space applications (Cd sublimates in a vacuum environment and plates out on neighboring surfaces).

2.5 Selection of Chemical Vapor Deposition as the Deposition Method

Currently, Al coatings have been applied to high-strength steel parts by either electroplating or IVD and, for a very few landing gear applications, by inverted cylindrical magnetron sputtering. Currently, the IVD Al process is the only DoD *qualified* replacement for Cd for certain applications.

The electrodeposition process, known as AlumiPlate®, requires the use of a toluene-based plating solution. Deposition takes place in an enclosed, oxygen-and water-free environment where the parts to be coated are introduced through a load-lock vacuum system. No hydrogen is generated and, therefore, no post baking is required to mitigate hydrogen embrittlement. Although the coatings produced by this process appear to have excellent corrosion resistance properties, several shortcomings are evident, namely: (1) the process uses toxic chemicals and is unlikely to be implemented at DoD depots, logistics centers, or at OEM facilities; (2) the technology is proprietary and currently is controlled by a small business with only one processing site; and (3) the part geometries and sizes that can be coated are limited by the plating bath size.

IVD is a type of physical vapor deposition (PVD) process that takes place in a vacuum chamber where Al is evaporated onto a substrate being simultaneously subjected to bombardment by

[12] E. S. Berman, et alii, "*Testing Some Cadmium Coating Alternatives for High-Strength Steels - An Update*", Proc. SUR/FIN, Airline/Aerospace Symposium, National Association for Surface Finishers, Indianapolis, IN (June, 2008).

plasma-ionized argon gas. Because the Al deposition takes place in vacuum and no hydrogen is generated, a hydrogen embrittlement relief bake is not necessary. Despite this advantage; however, the IVD Al process exhibits several limitations:

- The IVD growth mechanism results in the formation of columnar grains[13] that leads to porosity and pathways, which in turn allow oxygen and corrosive agents to readily diffuse through the grain boundaries and attack the underlying substrate. Although this problem may be minimized by increasing the coating thickness and peening, it can be eliminated by forming, if possible, a dense, randomly oriented grain structure.
- The fact that an evacuated chamber is required to produce the coatings severely limits the throughput and results in a higher cost per coated part as compared to continuously operated atmospheric processes.
- Furthermore, the IVD process, being essentially a line-of-sight limited deposition technique, often requires more than one coating cycle to achieve acceptable coating thickness uniformity on parts with complex shapes[14]. After the application of the first coating, the chamber is vented, the parts manually rotated, and the deposition process re-started. Thus, the need for a vacuum atmosphere, restraints on chamber size, and long processing times limit the utility of IVD technology.

IVD Al, as well as other currently used sacrificial coatings, relies on hexavalent chromium [Cr(VI)] containing post-treatments for the purpose of providing optimum corrosion protection and paint adhesion. Therefore, although Cd is eliminated from the coating system life cycle, hexavalent chromium is still present.

Chemical vapor deposition (CVD) offers promising solutions to the problems associated with the IVD process for producing coatings. CVD is a well-established technique that is widely used for a wide range of coating applications. A large variety of materials can be deposited by CVD. These include metals, mixtures of metals, insulators and dielectrics, elemental and compound semiconductors, electrical conductors, and superconductors[15]. In addition to this unique versatility, this material synthesis/vapor phase growth method can operate at relatively low temperatures - in the case of Al less than 205°C (400°F) - causing the substrate to experience minimal induced crystallographic changes or damage, and little if any contamination by diffusion of impurities[16].

CVD is defined as a process whereby constituents of the gas or vapor react chemically on a substrate surface to form a solid product (see Figure 2-1). This product can be in the form of a thin film, a thick coating, or even, if allowed to grow further, a massive (bulk) deposit.

[13] D. P. Monaghan, et alii, "*An Improved Method for the Deposition of Corrosion-Resistant Aluminum Coatings for Aerospace Applications*", J. Surf. Coat. Tech., **60**, p. 592 (1993).

[14] Typical IVD "throwing power" (or conformal coverage) allows for functional aluminum coatings to be deposited inside a cylinder to a depth equivalent to its diameter. In view of the fact that a large percentage of parts requiring corrosion protection have inside diameters, blind holes, and complex geometric surfaces, there is a need to resolve this coating conformability limitation.

[15] K. L. Choy, "*Chemical Vapor Deposition of Coatings*", Progress in Mater. Sci., **48**, p. 57 (2003).

[16] R. A. Levy (Ed.), Microelectronic Materials and Processes, Kluwer Academic Publishers, Boston, MA (1989).

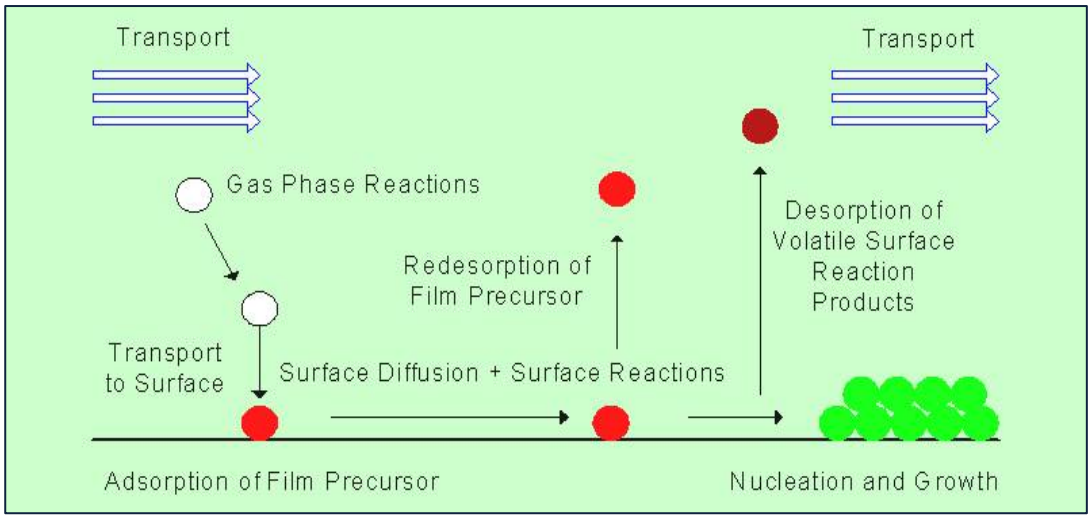

Figure 2-1. Schematic Diagram of a Typical CVD Process

Depending on the growth conditions, the product can have a single crystal, polycrystalline, or amorphous structure. Typical CVD processes are surface-catalyzed reactions (i.e., they are heterogeneous as compared to homogeneous, where the reactions nucleate in the gas phase). The occurrence of a chemical reaction distinguishes CVD from physical vapor deposition processes, such as sputtering, and IVD. Chemical reactions that can take place include pyrolysis (thermal decomposition), oxidation, reduction, hydrolysis, synthesis, nitride and carbide formation, disproportionation, and chemical transport. Deposition variables such as temperature, pressure, input concentrations, gas flow rates, and reactor geometry determine the deposition rate and the deposit properties.

CVD processes are classified according to the type of energy supplied to initiate and sustain the deposition reaction, as follows:

(1) Thermally activated reactions in various pressure ranges, where heat is applied by resistance heating, RF induction heating, or infrared heating
(2) Plasma promoted reactions, where an RF (or dc) induced glow discharge is the source for most of the energy that initiates and enhances the rate of reaction
(3) Photon-induced reactions, where radiation of a given wavelength triggers and sustains the reaction by direct photolysis, or by an energy transfer agent (UV-activated mercury for example).

Some chemicals used in the CVD process are reactive, metallo-organic compounds; as a consequence, sometimes this technology is referred to as metallo-organic CVD (MOCVD) and useful aluminum coatings have been obtained in the laboratory and with pilot plants[17] by this deposition process.

Optimization of the CVD process has proven to yield coatings that are adherent, highly dense, chemically pure, and uniform in thickness as well as in composition. Also, optimized process parameters have resulted in CVD coatings that exhibit low intrinsic stress, desirable micro-structures (i.e., randomly oriented versus columnar grains), and a good surface finish.

[17] A. Agüero, et alii, "*Low Temperature MOCVD Process for Fast Aluminum Deposition on Metallic Substrates*", Materials and Corrosion, **56**, pp. 937-941 (2005).

However, the key property that distinguishes CVD from PVD is the superior surface conformability (throwing power or surface coverage). The large values of the mean-free path (resulting from the use of high vacuum conditions) and the high sticking coefficient of the atoms dictate that PVD processes are largely "line-of-sight" limited. In CVD, the mean-free path of the molecules and their sticking coefficients are often reduced. This means that the "precursor" undergoes a large number of collisions upon entering the reactor before it collides with a surface. As a result of these collisions, the lower sticking coefficients of the molecules (compared to the atoms produced in PVD), and the enhanced surface diffusion caused by the heated substrate, yield conformal surface coverage. In the microelectronics industry, CVD metal coatings (e.g., TiN, W, Cu, Al, etc.) are routinely used to conformally cover submicron-sized vias (< 0.12 µm or 0.0005 in) with severe aspect ratios (hole depth/diameter ratio ~20:1)[18]. For high strength steel tubing or parts with blind holes having typical diameters of 6.35 mm (0.25 in), this means achieving conformal surface coverage down to depths of ≥125 mm (5 in).

The CVD technique also allows for the introduction of novel alloying elements that may impart improved characteristics to the Al coating, such as lubricity, which is one criterion for an acceptable alternative to Cd coatings. The abrasive nature of aluminum corrosion products and the inherent galling/seizing properties of pure and IVD Al make them unacceptable as a direct replacement for Cd coatings, especially on fasteners.

2.6 Selection of Atmospheric Pressure CVD as Preferred Deposition Method

The simplest CVD process is that done at atmospheric pressure (i.e., APCVD). One or more reactant gases are introduced in the reaction chamber at normal atmospheric pressure. Energy is supplied by heating the substrate to the temperature required to initiate and maintain the chemical reaction. The three principal variables that determine the rate of coating deposition are deposition temperature, reactant flow rate, and the gas composition. The advantages of APCVD include: (i) the simplicity of the technique, and (ii) no vacuum pumps and associated vacuum monitoring apparatus are required, as is the case with PVD, which reduces equipment costs. The disadvantage is that, with the available precursors, there is the need to minimize any uptake of the hydrogen gas produced as a byproduct during deposition.

Information about the APCVD equipment, materials, and processes used in this project is given in sections 3.1 and 3.2. In the early stages of the development work, coatings were deposited using a tubular reactor at NJIT, and by Acton Materials, Incorporated. Later, coatings were deposited using a prototype rotating barrel reactor for discrete parts that had been built by one of the industry team members, AkzoNobel. This commercial partner recently is currently implementing a commercial reactor for discrete small parts, and this is described in Section 3.2.3, and in the section on technology transfer.

[18] N. Ramanuja, R. A. Levy, et alii, "*Synthesis and Characterization of Low Pressure Chemically Vapor Deposited Titanium Nitride Films Using $TiCl_4$ and NH_3*", Material Letters, **57**, p. 261 (2002); and similar references provided in the Second Annual Report for Project WP-1405, SERDP (December, 2006).

3.0 Materials, Coating Deposition, and Test Methods

This section contains a brief description of the materials and deposition processes used to produce coated coupons, panels, test specimens, and small parts for evaluating the APCVD Al coatings against mutually agreed criteria. The testing methods employed also are described. Any exceptions to these materials, processes, and/or testing methods are identified in the appropriate results sections of this report.

3.1 Materials

The materials used to deposit and evaluate the properties and performance of the APCVD Al coatings on representative substrates used for aircraft parts and components are listed below. Further information about some of the substrate materials is given in Section 7.1.

3.1.1 Substrates

The main focus of this project was to identify a coating suitable for non-line-of-sight applications requiring high-strength substrates or specialty alloys. If such a coating could be identified, evaluated, demonstrated, and then qualified for these applications, it also might be suitable for use on other substrate materials, such as lower strength steels and non-ferrous alloys.

3.1.1.1 Low Carbon, Mild and High-strength Steels

AISI 1030 is a relatively high carbon (0.30%) manganese steel in the low carbon steel alloy family. It provides greater strength than the lower carbon grades while still retaining reasonable ductility. AISI 1030 steel is generally used in the quenched and tempered condition for strength; thus, applications include machinery parts where strength and hardness are requisites. It was used on this project solely as a convenient substrate upon which the Al coatings were deposited under different conditions to determine their morphology and composition.

Mild steel was used for the cadmium-coated, control panels, with electroplated Cd applied in accordance with the specifications of SAE AMS QQ-P-416, Class II, Type II.

AISI 4130 is a heat-treatable low-alloy steel with relatively low hardenability; however, it is one of the most popular alloy steels because of its good formability and weldability, along with an excellent combination of mechanical properties. It is recommended for use at temperatures up to 357°C (700°F) because its strength decreases markedly with increasing temperatures above this value. In some of the early testing - using the tubular reactor described in Section 3.2.1, and later the rotating barrel reactor (Section 3.2.2) - AISI 4130 coupons and fasteners (hollow rivet sleeves, nuts and bolts) were used to evaluate throwing power and conformal coverage. Small diameter tubes ~51 mm (2.0 in) long and with a wall thickness of about 0.9 mm (0.035 in) with different inner diameters (ids) of 3.0 and 6.0 mm (0.125 and 0.25 in) also were used to validate that non-line-of sight surfaces could be coated. Flat coupons were used for fabricating corrosion and electrochemical test panels, and to evaluate the effect of using chemical conversion coatings on salt fog corrosion resistance. In addition, this steel was used as a substrate on which a thin film of an insulator (silicon nitride) was deposited using a plasma-enhanced CVD process[19] prior to depositing Al coatings for measuring their electrical properties.

[19] Conditions were: substrate temperature = 300°C (572°F); RF power = 50 W; flow rates of SiH_4 = 280 sccm and NH_3 = 4 sccm; and process pressure = 900 mTorr.

AISI 4340 is often considered the standard to which other ultrahigh-strength steels are compared. It is especially immune to temper embrittlement, and does not soften readily at elevated temperatures. Hydrogen embrittlement is a problem for AISI 4340 steel heat treated to tensile strengths greater than about 1,400 MPa (200 ksi). Parts exposed to hydrogen, such as during pickling and electroplating, should be subsequently hydrogen relief baked. This steel also exhibits extremely poor resistance to stress-corrosion cracking when tempered to tensile strengths of 1,500 to 1,950 MPa (220 to 280 ksi). For some of the tensile and hydrogen embrittlement tests conducted under this project, this steel was heat treated to a Rockwell C hardness (HRC) of 52. Also, this steel was used to fabricate the disks (25.4 mm (1 in) diameter, and 6.35 mm (0.25 in) thick) used in determining the coefficient of friction of the APCVD Al coatings, and the smooth round bar test specimens for fatigue testing.

3.1.1.2 Other High-strength Aerospace Alloys

AerMet 100 alloy is a higher strength derivative of AF1410, and this Ni-Co-Fe alloy can be heat treated to a tensile strength of >1,950 MPa (280-310 ksi) while exhibiting excellent fracture toughness and high resistance to stress-corrosion cracking. AerMet 100 has good weldability and does not require preheating prior to welding. It may be considered for use up to about 427°C (800°F). The applications of AerMet 100 alloy include armor, fasteners, landing gear, actuators, jet engine shafts, ballistic tolerant components, and structural tubing. For the ASTM F 519 hydrogen embrittlement tests conducted under this project, this alloy was heat treated to a hardness of HRC 55 (approximately 300 ksi tensile strength). For fatigue testing, AerMet 100 was used to fabricate the smooth round bar test specimens.

3.1.1.3 Coupon, Panel, and Test Specimen Designs

Table 3-1 provides a summary of the various types of substrate and specimen configurations upon which the APCVD Al coatings were deposited in order to obtain processing, property, and performance data to use as inputs in the continuous improvement and coating optimization efforts that were performed.

Coupons and Panels

Substrate materials were used in standard coupon and panels sizes and ordered from a commercial supplier or cut from sheet stock. Typical shapes and sizes are given in Table 3-1 along with the corresponding test in which the specimens were used.

Standard Test Specimens

Other test specimens were machined from bar stock. Examples of the types of “standard” test specimens are given below.

To determine the effects of the coatings on the stress-corrosion cracking threshold ($K1_{scc}$), Charpy CV2 samples were tested using the rising step load (RSL) method. These specimens were fabricated from 4340 steel heat treated to 52 HRC, and precracked according to ASTM E 399 Sec 7.3 and A2, using a $K1_c$ value of 54. Of the Charpy specimens tested, one half was APCVD Al-coated following the machining and precracking. Figure 3-1 is a drawing showing the shape of a Charpy CV2 test specimen used, with the specified dimensions tabulated.

Table 3-1. Specimen Types, Sizes and Materials Used for Testing

Substrate	Coating	Specimen Type	Size, mm (in)	Tests
AISI 1010 low C steel	APCVD Al	Flat Coupon	25.4x102x2.28 (1x4x0.090)	Adhesion (ductility)
AISI 1030 low C steel	APCVD Al	Flat Coupon	25.4x25.4x0.86 (1x1x0.034)	Compositional analysis, morphology as function of deposition temperature
AISI 1030 low C steel	APCVD Al	Flat Coupon; with and without peening and Cr(VI) CCC	25.4x25.4; 25.4x102 (1x1; 1x4)	Electrical contact resistance as function of post-treatments, deposition temperature, and corrosion
AISI 4130 alloy steel	APCVD Al	Flat Coupon; with peening and Cr(VI) CCC	25.4x102x1.02 (1x4x0.04)	Morphology, corrosion (electrochemical)
AISI 4130 alloy steel	IVD Al (benchmark coating)	Flat Coupon; with peening and Cr(VI) CCC	101.6x152x0.025 (4x6x0.001)	Morphology, corrosion (electrochemical)
AISI 4130 alloy steel	APCVD Al	Tube (rivet stem)	12.7x7.9 (0.5x5/16 od)	Density (He pycnometry)
AISI 4130 alloy steel	AlumiPlate Al (benchmark coating)	C-ring; with and without peening and Cr(VI) CCC	N/A	Cyclic corrosion
AISI 4130 alloy steel	APCVD Al	C-ring; with and without Cr(III) CCC	N/A	Cyclic corrosion
AISI 4130 alloy steel	APCVD Al; H_2 relief bake	ASTM F 519 Type 1a.1	50.8 x 9.5 od (2.0 x 0.38 od) notched center section	Ultimate (notched) tensile strength debit
AISI 4130 alloy steel	APCVD Al; H_2 relief bake	ASTM F 519 Type 1a.1	50.8 x 9.5 od (2.0 x 0.38 od) notched center section	Hydrogen embrittlement
AISI 4340 alloy steel	APCVD Al; H_2 relief bake	ASTM F 519 Type 1a.1, sectioned after coating	~203 x ~12.7 od (~8 x ~0.5 od) "dog bone" center section	Substrate hardness profile, fatigue testing
AISI 4340 alloy steel	APCVD Al; H_2 relief bake	ASTM F 519 Type 1a.1	50.8 x 9.5 od (2.0 x 0.38 od) notched center section	Hydrogen embrittlement, corrosion (OCP, EIS), coating surface composition, porosity
AISI 4340 alloy steel	APCVD Al; H_2 relief bake	Charpy notched bar	10 x 10 x 55 (0.39 x 0.39 x 2.17)	Stress-corrosion cracking
AerMet 100	APCVD Al; H_2 relief bake	ASTM E 466 round bar	88.9 x 12.7 od (3.5 x 0.5 od) "dog bone" center section	Fatigue debit
AerMet 100	APCVD Al; H_2 relief bake	ASTM F 519 Type 1a.1	50.8 x 9.5 od (2.0 x 0.38 od) notched center section	Hydrogen embrittlement, corrosion (OCP, EIS), coating surface composition, porosity

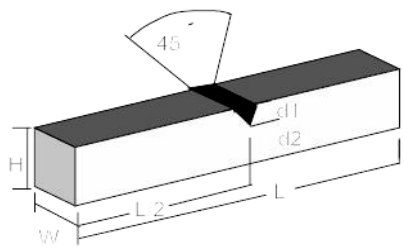

Figure 3-1. Schematic of a Standard Charpy CV2 Specimen

Height (H)	10 mm, ±0.03 mm, with adjacent sides square within 90° ±9 min
Width (W)	10 mm, ±0.03 mm,
Length (L)	55 mm, +0.00 mm, −0.3 mm
Notch position L/2	27.5 mm ±0.2 mm, perpendicular to the longitudinal axis of specimen within 90° ±9min
Notch radius	0.25 mm, ±0.025 mm, with radius tangent to the notch angle
Notch depth (d1)	2 mm, ±0.025 mm
Notch angle,	45° ±1°
Ligament depth (d2)	8.0 mm, ±0.025 mm
Surface finish	1.6 µm on notched surface and opposite face; 3.2 µm on other surfaces

In addition to the HE tests based on ASTM F 519, the propensity of the APCVD Al coatings to cause hydrogen assisted stress-corrosion cracking (SCC) was investigated using C-ring samples, the basic design of which is shown in Figure 3-2 (a). A modified design of a C-ring specimen with a notch was used for the accelerated corrosion testing (GM 9540P method). Figure 3-2 (b) shows an example of such a specimen made from tubular stock. The stress is imparted by tightening the bolt, which is threaded through the two holes in the specimen.

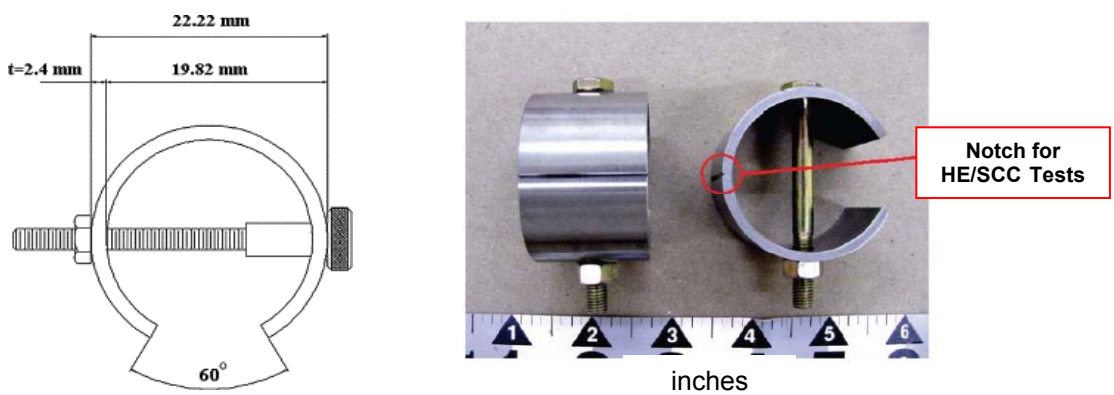

(a) (b)

Figure 3-2. C-ring Specimens Used for Accelerated Corrosion and HE Testing

Smooth round bars were used to perform the ASTM E 466 constant amplitude, axial fatigue test. Figure 3-3 is an example of a drawing of the design of a standard round bar, machined from round stock according to the appropriate specifications. The specimen configuration used was

a standard "dog bone" design; however, the grip features were reduced in size to allow them to fit in the APCVD rotating barrel reactor.

Standard notched, round bars were used for the ASTM F 519 hydrogen embrittlement test. Figure 3-4 is an example of an engineering drawing that specifies how these test specimens are made. The type of thread machined in each end is given in a call out in Figure 3.4, but not shown in the sketch in the upper left corner. The notched round bars used in this test were Type 1a.1 (per ASTM F 519) made from AISI 4340 steel per MIL-S-5000E. The bars were 65.6mm (2.54 inches) long and had a notched diameter of 4.45mm (0.175 inch). They were quenched and tempered per AMS-H-6875A to a hardness of 51-53 HRC.

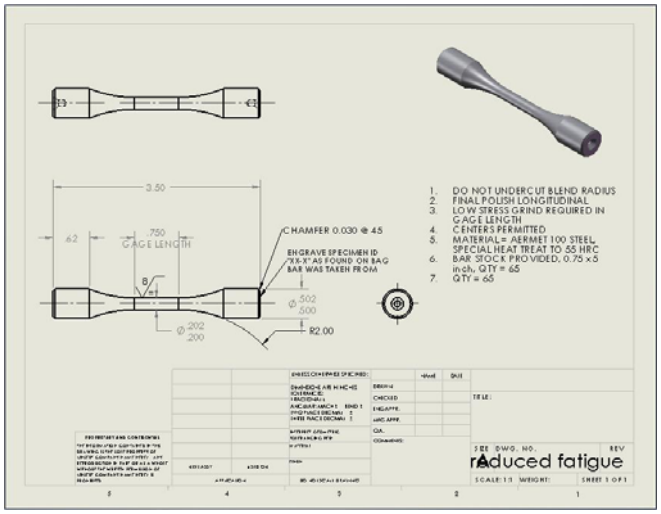

Figure 3-3. Drawing for the Smooth Round Bar Used for Fatigue Testing

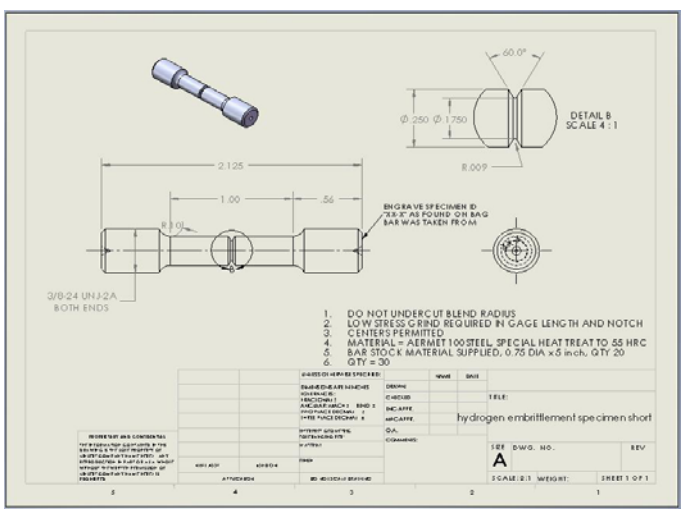

Figure 3-4. Drawing for the Notched Round Bars Used for HE/HRE Testing

3.1.2 Cleaning Chemicals

In general, prior to aluminum deposition, all the substrates were ultrasonically cleaned in heptane and acetone, followed by acid etching, alkaline neutralization, and drying in an inert atmosphere. This procedure was used to obtain clean, oxide-free surfaces with uniform texture. Different procedures and chemicals were used for cleaning test specimens only when called for in the protocols listed in standard test methods or specifications. These chemicals are listed under each test described in Section 3.3.

3.1.3 Precursor Chemicals

A number of metallo-organic compounds have been used to deposit aluminum coatings; however aluminum alkyls were the choice as precursors for this project.

3.1.3.1 Tri-ethyl Aluminum

An aluminum alkyl compound; namely, tri-ethyl-aluminum (TEAL - $(C_2H_5)_3Al$) was first used as a precursor for APCVD Al deposition. The TEAL was dissolved in octane to give a non-toxic, non-pyrophoric, and non-explosive feedstock. After loading the substrates (e.g., nuts and bolts) in the rotating barrel reactor, Al was deposited under atmospheric pressure at two temperatures of 300° and 325°C (572° and 617°F).

3.1.3.2 Tri-isobutyl Aluminum

Tri-isobutyl-aluminum [$(i\text{-}C_4H_9)_3Al$) or TIBAL] was used as the preferred precursor for APCVD Al deposition on this project. TIBAL is a colorless liquid with a vapor pressure of approximately 1.5 Torr at 45°C (113°F). For aluminum deposition the reactions with TIBAL are:

(i) $[CH_3)_2CH\text{-}CH_2]_3Al \leftrightarrow [(CH_3)_2CH\text{-}CH_2]_2AlH$ (DIBAL-H) + $(CH_3)_2C{=}CH_2$ (isobutylene)

(ii) $[(CH_3)_2CH\text{-}CH_2]_2AlH \rightarrow Al + 3/2H_2 + 2(CH_3)_2{=}CH_2$

Overall: $[CH_3)_2CH\text{-}CH_2]_3Al \rightarrow Al + 3/2H_2 + 3(CH_3)_2{=}CH_2$.

3.1.3.3 Proprietary Blend 1

Proprietary Blend 1 (PB1) was formulated based on TIBAL. This blend provided smoother surfaces, higher quality layers, and permits better process control. The goal was to be able to deposit coatings with improved mechanical properties at lower temperatures on high-strength steel substrates. The deposition procedures used for the blend were similar to those used for the pure TIBAL precursor.

3.1.3.4 Proprietary Blend 2

Proprietary Blend 2 (PB2) was formulated to allow for aluminum deposition in the range of 230° to 250°C (446° to 482°F) while maintaining the coating properties obtained with the PB1. The deposition procedures used for this blend also were similar to those used for the pure TIBAL precursor.

3.1.4 Carrier Gases

Nitrogen gas was used as a carrier gas in the deposition reactors used on this project.

3.1.5 Post-treatment Chemicals

It was hoped that if adherent, dense APCVD Al coatings were obtained there would be no need for treatments after deposition to improve corrosion resistance or paint adhesion. However, as discussed in Section 1.2, the Project Plan included an activity in Task 4 to evaluate the need for any post-treatments. Consequently, the chemical conversion coating process preferred by NAVAIR was selected for use in some of the corrosion tests that were performed. This was a Cr(III)-based chemistry - originally referred to as a “trivalent chromium pretreatment” or “TCP” - commercially available from a licensee of NAVAIR.

Also, in accordance with MIL-DTL-81706A, the APCVD Al-coated samples evaluated in this electrical contact resistance test included those as deposited, and those post-treated by glass bead burnishing followed by a Cr(VI) commercial chemical conversion coating (i.e., Iridite™ 14-2).

3.1.6 Reference Materials

A number of materials were used as *reference materials* or *benchmarks* for comparison with the APCVD Al coatings. These are described briefly below. The Cd-coated ***control*** specimens are described in Section 3.1.1.1.

3.1.6.1 Aluminum Metal

Commercial Al foil (99.999% purity) was used as a reference material in some of the electro-chemical and corrosion testing, as well as for some of the electrical contact resistance measurements. An Al powder reference material was used to help interpret the XRD results to determine the structure of the APCVD Al coatings.

3.1.6.2 IVD Aluminum

APCVD Al coatings must exhibit equal or better performance than the only currently approved general replacement for Cd coatings. Boeing-St. Louis arranged for test panels to be coated with ~25μm (1 mil) of IVD Al. Because these coatings traditionally receive a glass bead peening (or burnishing) after deposition to close surface pores and pin-holes, and a Cr(VI)-containing chemical conversion coating (CCC) to provide better corrosion resistance and paint adhesion, the specimens provided by Boeing also were subjected to these post-treatments.

3.1.6.3 Electroplated Aluminum

Similarly, a few specimens were coated with electroplated Al and tested at the Army Research Laboratory (ARL) facilities to determine how their performance compared to coatings deposited by the APCVD process. A CCC post-treatment also was used on some coated specimens. It should be pointed out that AlumiPlate™ electroplated Al has now been included as an acceptable alternative to Cd in the specification (MIL-DTL-38999K) for electrical connectors. For some applications (e.g., certain small discrete parts, including fasteners) the AlumiPlate Al process should be considered as a competitor to the APCVD Al process (despite the drawbacks mentioned earlier in Section 2.5).

3.2 Coating Deposition Methods

This section contains details about the different types of equipment that were used to obtain coated coupons, panels, specific test specimens, and small components for coating characterization and performance evaluation. The specific testing methods and procedures used are described in sufficient detail such that others may reproduce them if they wish to validate the test results that were obtained and summarized in Section 4.1.

3.2.1 Deposition in Tubular Reactor

Early deposition trials at NJIT were accomplished using a small, laboratory scale, horizontal, tubular reactor, the basic design is shown schematically in Figure 3-5, and as set up in the laboratory in Figure 3-6. The temperature, precursor and carrier gas flow rates were calibrated, as reported in Reference 1 in Section 8.3. During deposition, the pressure in the reactor is controlled to be slightly above atmospheric by the restriction of gas flow at the exit part of the system. If pressure control is necessary to improve, for example coating uniformity, the exhaust opening size can be changed.

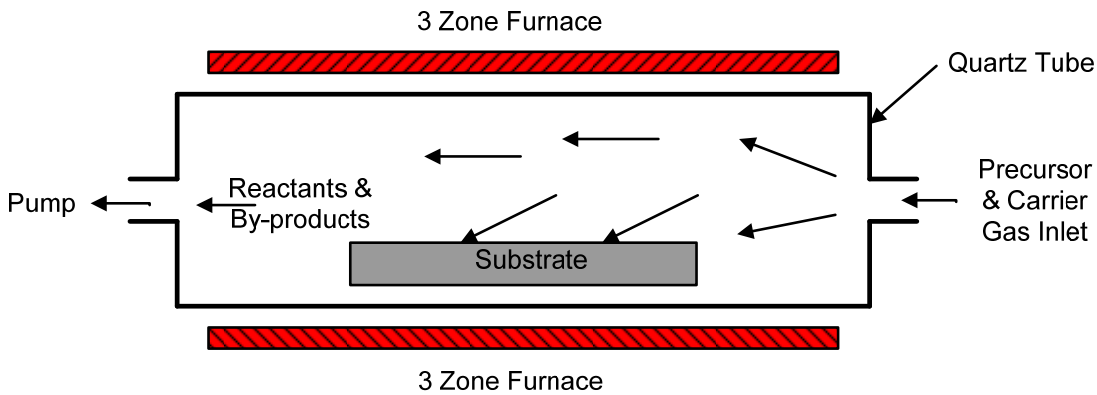

Figure 3-5. Basic Design of a Tubular APCVD Reactor

Figure 3-6. Laboratory Tubular Reactor and Ancillary Equipment

TEAL was used first as a precursor for Al deposition in this reactor. After loading the substrates (e.g., a batch of small nuts and bolts) in the reactor, Al was deposited under atmospheric

pressure at temperatures of 300°C and 325°C (572°F and 617°F). Nitrogen was used as a carrier gas. The coatings obtained with TEAL in this reactor by NJIT were not satisfactory.

3.2.2 Deposition in Rotating Barrel Reactor

An overall processing scheme[20] has been developed by AkzoNobel for use with their prototype, rotating barrel (rotary) reactor, as shown schematically in Figure 3-7 below. The pretreatment step and post-treatment are tailored to the substrate material and end use application. The process depicted has been used by AkzoNobel with numerous aluminum alkyls as precursors.

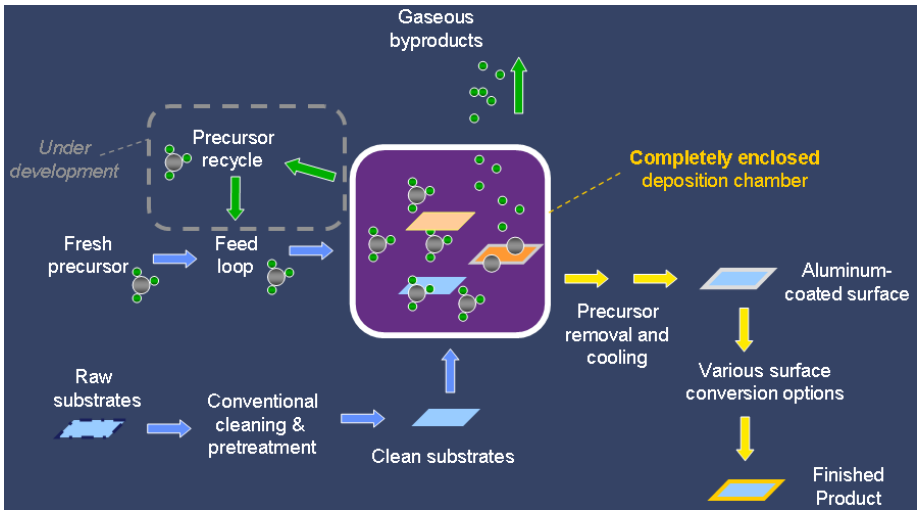

Figure 3-7. AkzoNobel Overall APCVD Aluminum Processing Scheme

Figure 3-8 shows the AkzoNobel bench scale prototype unit used to deposit the majority of the aluminum coatings for this project.

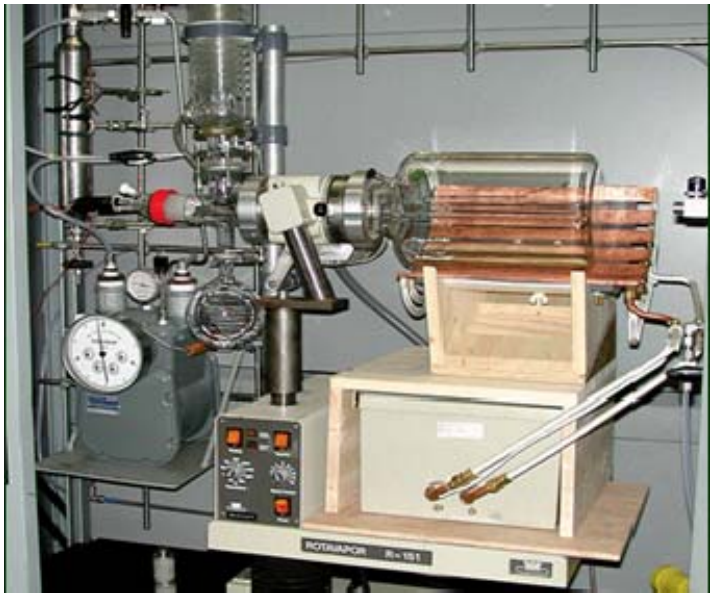

[20] The commercial, patented technology is called "FUZEBOX®, which is a Registered Trade Mark of AkzoNobel, and is covered by U.S. Patent No. 7,387,815.

Figure 3-8. Bench Scale Rotary APCVD Reactor and Ancillary Equipment

After loading the substrates (test specimens) into the glass barrel, it was rotated to tumble them to expose all surfaces during deposition at substrate temperatures between 230° and 310°C (446° and 590°F) under atmospheric pressure. A 20 kW induction system was used to heat the substrates. Vapor phase and substrate temperatures were monitored using thermocouples. A residence time of typically less than 60 minutes was used to deposit coatings with a thickness in the range of 10 to 35 μm (0.0004 to 0.0015 in). The coating thickness was determined by the type of specimen and the tests to be carried out. A refrigerated condenser and demister were used to treat vented gases. After Al deposition, the coated parts were cooled in an inert atmosphere and rinsed to remove any excess reactant chemicals.

3.2.3 Deposition in Commercial Barrel Reactor

Figure 3-9 shows the AkzoNobel commercial unit in the final stages of assembly prior to pre-production testing and delivery to the customer. The operating scheme shown in Figure 3-7 applies, with the primary differences with the bench scale unit being the scale up in size (work load), and the automation of the operation. The commercial barrel reactor shown below, as well as the bench scale rotary reactor shown in Figure 3-8, are examples of the infrastructure available for the practice of AkzoNobel's patented metal deposition technology.

Figure 3-9. AkzoNobel Commercial APCVD Unit Set Up for Preproduction Testing

3.3 Testing Methods

Table 3-2 lists the tests that were conducted on the APCVD Al coatings along with the pass-fail criteria used for each, and the Project Team Member responsible for performing the test. Details of these tests are provided in the following paragraphs in this section of the report.

Table 3-2. Overview of the Tests Conducted and the Corresponding Pass-Fail Criteria

Engineering Requirement	Test	Acceptance Criteria: Measurements	Reference	Facility
Composition	XRF composition uniformity; others as needed	Composition is within the process specification requirements; or values obtained for information only	ASTM B 568 ASTM E 1621	NJIT ARL
Thickness	Optical/SEM Microscopy	Meets specified or required value; plating thickness remains in class for Cd when making comparisons	SAE AMS QQ-P-416F	NJIT
Surface Coverage, Throwing Power	Optical/SEM Microscopy	Uniform thickness on all coated surfaces; remains within class for Cd when making comparisons	SAE AMS QQ-P-416F	NJIT
Surface Roughness	Atomic Force Microscopy	Information only requirement	- -	NJIT
Hardness	Nano-indentation	Information only requirement	- -	NJIT
Adhesion	Pull-off adhesion	Adhesion values > 3,500 psi* ; steel panels > 1/8" must be used	ASTM D 4541	ARL
Adhesion	Tape adhesion	Ratings of 4 or 5 (X-cut and cross-cut methods)	ASTM D 3359	ARL
Adhesion	Mandrel bend	No cracking or delamination	ASTM B 571	ARL
Compatibility with Substrate	Metallographic examination	No degradation of substrate properties as a result of deposition	- -	NJIT ARL
Electrical Conductivity	Contact resistance	ECR <5,000 micro-ohms as coated: ECR < 0,000 micro-ohms after salt fog exposure	MIL-DTL-81706 ASTM B 117	NJIT
Lubricity (as deposited)	Pin on Disk Coefficient of Friction	Coefficient of friction (COF) compared with Cd-plated controls	ASTM G 99	ARL
Lubricity (after corrosion)	Pin on Disk COF after salt fog exposure or accelerated corrosion testing	COF measured and compared with Cd-plated controls after several successive specimen exposures (accelerated corrosion methods)	ASTM G 99 ASTM B 117 GM 9540P	ARL
Corrosion Resistance	Fluid corrosion resistance	No coating degradation greater than that of Cd-plated control specimens	MIL-PRF-5624 ASTM F 483 ASTM F 1110	ARL
Sacrificial Protection	Unscribed salt fog exposure	3,000 hours minimum with no red rust	ASTM B 117; MIL-DTL-83488	ARL AFRL
Sacrificial Protection	Scribed salt fog exposure	1,000 hours minimum with no red rust	ASTM B 117 MIL-DTL-83488	ARL AFRL
Sacrificial Protection	Unscribed cyclic exposure	80 cycles with no red rust.	GM 9540P	ARL
Sacrificial Protection	Scribed cyclic exposure	40 cycles with no red rust	GM 9540P	ARL
Sacrificial Protection	Immersion (E_{corr} vs. time) and EIS	Coating degradation ≤ to that of cadmium control	ARL T.O.	ARL
Resistance to H_2 Embrittlement	Rising Step Load	No degradation vs. Cd-plated controls on precracked CV2 (Charpy) specimens	ASTM F 1624	ARL
Resistance to H_2 Embrittlement	Tensile with and without NaCl	No degradation vs. Cd-plated, precracked 1.a.1 notched bars	ASTM F 519	AFRL NAVAIR
Resistance to HE and/or SCC	C-ring	No degradation vs. Cd-plated controls	ASTM E 399 ASTM F 1624	ARL
Fatigue Resistance	High cycle fatigue Constant amplitude	No degradation vs. Cd-plated controls	MIL-STD-1312 ASTM E 466	AFRL

* Failure of the adhesive, typically 3,300-4,000 psi.

3.3.1 Coating Structure

The thickness, coverage, structural, and compositional, properties of the deposited APCVD Al coatings were evaluated using a variety of characterization methods to assess their quality, before conducting any performance testing. Prior to characterization, all the coated samples were ultrasonically cleaned in methanol followed by acetone, mounted, then cross-sectioned and polished. Etching solutions were used as necessary to reveal coating structure.

Care is needed in the preparation of coating cross-sections because the Al coating is so much softer than the steel substrate materials. At worst, coatings can be polished too much, causing smearing and making the detection of grain boundaries, defects, and porosity difficult.

3.3.1.2 X-ray Diffraction

X-ray diffraction (XRD) was performed using a Philips X'Pert MRD X-ray diffractometer (Bragg-Brentano θ:θ) with Cu Kα radiation operated at 45 kV and 40 mA. This instrument was used to investigate the crystallographic structure of the APCVD Al coatings deposited at two different temperatures (275 and 300°C). The XRD patterns of the Al coatings were compared to those of an Al powder reference spectrum.

3.3.2 Thickness and Surface Roughness

After mounting a specimen, producing a cross-section, and polishing it by conventional metallographic methods, coating thickness and uniformity was determined. Energy dispersive X-ray spectroscopy (EDAX, Oxford INCA Energy 400) was one method used to determine approximate coating thickness; a more accurate method was the use of a scanning electron microscope with an appropriate reticule. Coating surface macro-roughness was measured with a commercial DekTak Profilometer. Substrate micro-roughness was measured using a Digital Instruments atomic force microscope (AFM), model Nanoscope IIIA, multimode scanning probe microscope in the "contact" mode.

3.3.3 Throwing Power and Conformal Coverage

The surface morphology and conformal coverage of the aluminum coatings on small specimens was investigated using a field emission scanning electron microscope (FE-SEM, LEO 1530 VP).

3.3.4 Density and Porosity

The density of APCVD Al coatings has been obtained using He pycnometry. This method uses a gas (He) displacement technique to determine the volume of sample under test with high accuracy. The weight (W_{s+c}) and volume (V_{s+c}) of the Al-coated substrate are measured using a balance and a He pycnometer (AccuPyc 1330), respectively. After compete removal of the Al coating from the substrate using a 5% sodium hydroxide solution, the weight (W_s) and volume (V_s) of the substrate are measured. Based on these measured values, coating density ρ_c is calculated from the following equation:

$$\rho_c = \left[\frac{W_{s+c} - W_s}{V_{s+c} - V_s} \right].$$

3.3.4.1 Optical Microscopy

Metallurgical optical microscopes and scanning electron microscopes (SEMs) were used to examine the bulk structure of the coatings and the substrates - including identifying any defects such as porosity, cracking and delamination and changes in morphology - after mounting a specimen, producing a cross-section, and mechanically polishing it using silicon carbide (SiC) with grit sizes decreasing to 1,200, followed by a polycrystalline diamond suspension paste with particle sizes down to 0.05 µm.

The fractured surfaces of the specimens after HE testing were examined using a field emission scanning electron microscope (LEO 1530 VP) with backscattered electron detector.

3.3.4.2 Electrochemical Impedance Spectroscopy

Electrochemical impedance spectroscopy (EIS) with a Gamry Reference 600 instrument was used to evaluate coating properties and performance as a function of immersion time (up to 10 days) in a 3.5 wt.% NaCl solution saturated with oxygen at room temperature. An electro-chemical flat cell (Princeton Applied Research) was used in these measurements, with a saturated calomel reference electrode (SCE) and a platinum gauze auxiliary electrode. All electrochemical tests were carried out with an exposed coating area of 10 mm^2. Al foils and AISI 4130 steel coupons were used as references for comparative purposes.

3.3.5 Chemical Composition

The correlation between processing parameters and resulting coating compositions has been evaluated using a variety of diagnostic techniques, including Auger electron spectroscopy (AES), X-ray photoelectron spectroscopy (XPS), nuclear reaction Analysis (NRA), and glow discharge, optical emission spectroscopy (GD-OES).

3.3.5.1 Energy Dispersive Analysis with X-rays

Energy dispersive X-ray spectroscopy (EDAX, Oxford INCA Energy 400) was one technique used for the elemental analysis of the coatings.

3.3.5.2 Auger Electron Spectroscopy

For the AES, a Perkin-Elmer Physical Electronic Model 660 Scanning Auger Microprobe was used, operating under a base pressure of $<1.0\times10^{-9}$ Torr, with a primary beam energy and current of 10 keV and 1.0 µA, respectively. AES was used to profile composition with depth of the coatings. During the AES measurement, Ar ion etching was simultaneously conducted (at an etching rate of 20 nm (SiO_2)/min over a 2×2 mm area) in order to determine the depth profile.

3.3.5.3 Nuclear Reaction Analysis

The $^{1}H(^{15}N, \alpha\gamma)^{12}C$ resonance nuclear reaction (NRA) method was employed to determine hydrogen incorporation in the Al coatings. Each sample was loaded in the analysis chamber at room temperature and bombarded with ~20 nA of ^{15}N ion. The ion beam energies used for the depth profiles were 7.0 MeV (0.38µm), 7.3 MeV (0.57µm), 7.6 MeV (0.76µm), and 7.9 MeV (0.95µm), then the measurement at 7.0 MeV was repeated to check the stability of the hydrogen content in the samples. The hydrogen concentration values corresponding to each ion beam energy/depth were averaged.

3.3.5.4 X-ray Photoelectron Spectroscopy

To evaluate the composition of the coatings, XPS (ThermoElectron VG Scientific ThetaProbe with X-ray source of monochromatic Al Kα (1,486.6 eV) operating at 15 kV and 100 W) was used over an analytical area of 400×400 μm^2. Survey and profile pass energies were 300 and 100 eV, respectively. For the depth profile during XPS measurement, Ar ion etching (etching rate of 4 nm (SiO_2)/min) was performed over a rastered area of 3×3 mm^2.

3.3.5.5 Glow Discharge Optical Emission Spectroscopy

In the third year of this project, the compositional depth profile analysis on APCVD Al coatings was conducted by glow discharge-optical emission spectroscopy (GD-OES). The samples were cleaned with spectroscopically clean heptane prior to the analysis, and analyzed using a LECO GDS750A instrument with Quantitative Depth Profiling (QDP). Certified analytical check standards were run prior to QDP analysis in accordance with ISO 17025. The method used in this analysis was validated with NIST standards prior to running any Al coating samples.

3.3.5.6 Electron Probe Microanalysis

Additionally, the bulk concentration information of the Al coatings was obtained using an electron probe micro-analysis (EPMA) technique with a JEOL JXA-8900 microprobe analyzer operating at 15 kV accelerating voltage and 100 nA beam current (25 μm beam size) along with five wavelength-dispersive spectrometers (WDS). The sampling depth was about 3 μm, and the points for analysis on the sample were randomly selected.

3.3.6 Electrochemical and Corrosion Properties

Corrosion in the context of this report covers responses to exposures to a wide range of environments, some of which result from weapon system deployment and missions, and others from routine cleaning, maintenance, repair, and overhaul operations. There are several tests that try to simulate these environments, ranging from simple immersion, to alternate immersion, to salt spray with and without added sulfur dioxide (as found on aircraft carriers). In addition, some corrosion is the result of the conjoint action of water, chemicals and stresses and strains. Corrosion fatigue and hydrogen embrittlement can lead to catastrophic failure, with loss of weapon systems and lives.

3.3.6.1 Open Circuit (Galvanic) Potential and Polarization Behavior

The open circuit potential corrosion potential and current, and anodic polarization behavior of APCVD Al coatings were investigated using potentiodynamic polarization experiments in a 3.5 wt.% NaCl solution with and without oxygen (O_2) saturation at room temperature using a Gamry Reference 600™ Potentiostat. A flat cell (Princeton Applied Research) was used with a three-electrode configuration consisting of a test specimen, a saturated calomel reference electrode (SCE), and a platinum gauze auxiliary electrode. The specimen area exposed was 1 cm^2. Polarization was measured one hour after immersion with a scan rate of 10 mV/min from –0.2 to +1.5 V *versus* the open circuit potential (OCP). Al foils and AISI 4130 steel coupons were used as references for comparative purposes.

Electrochemical impedance spectroscopy (EIS) measurements also were made to investigate open circuit potential corrosion potential and anodic polarization behavior of APCVD Al coatings, as well as the nature of the surface reactions on the bare AISI 4340 steel and coatings that

affect corrosion behavior. Figure 3-10 shows the laboratory apparatus (Princeton Applied Research Model K0235) used for these measurements. Bare and coated notched round test bars (see Figure 3.4) were tested in a 3.5 wt.% NaCl solution. A platinum mesh was used as the counter electrode, and a saturated calomel electrode (SCE) was used as the reference electrode. The steel, notched round bar specimen comprises the "working" electrode, and the threaded ends were coated with a black, jeweler's wax so that only the desired surfaces were exposed to the corrosive test solution.

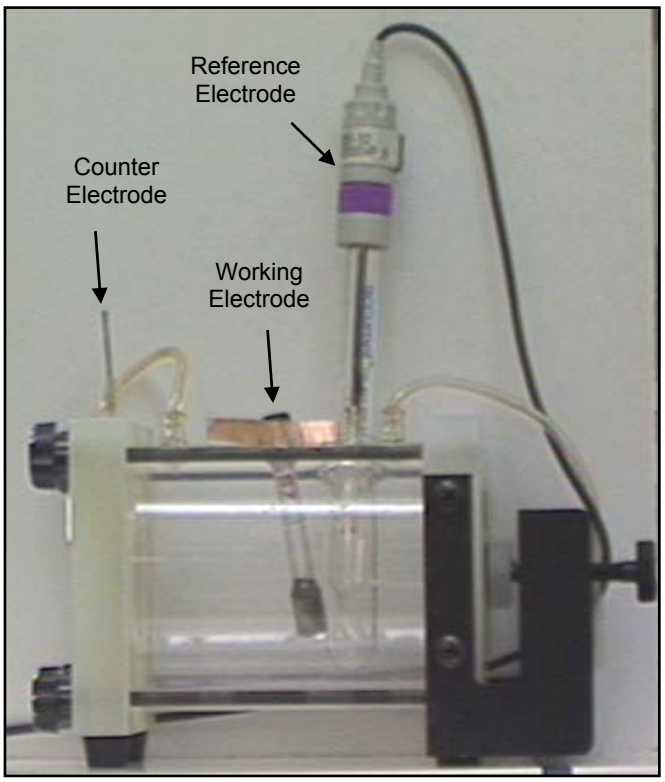

Figure 3-10. Electrochemical Cell used for EIS Measurements Showing Specimen that is to be Immersed in a Salt Solution

Open circuit measurements were taken over a period of eight hours. The EIS measurements were made at one hour intervals during the 12-hour open circuit potential measurement period. The amplitude of the applied ac was 10 mV, and the frequency range was 100 kHz to 10 MHz. After these tests were concluded, the test specimens were inspected and their condition documented and photographed.

3.3.6.2 Salt Fog Exposure Corrosion Resistance

Corrosion tests based on the ASTM B 117 Salt Fog testing method are carried out on bare and painted Al coatings (~20 μm thickness) to evaluate their general corrosion resistance and ability to provide sacrificial (galvanic) protection to the steel substrate materials. Bare Al-coated specimens consisted of unscribed and scribed coupons, post-treated both with and without a trivalent chromium conversion coating (TCP) or other post-treatment. Painted Al coatings were comprised of a MIL-PRF-23377C primer and a MIL-PRF-85285 topcoat. A paint adhesion test based on ASTM D 3359 Method A can be conducted before and after corrosion testing.

The ASTM B 117 test method can be used to identify uniform/general corrosion attack, as well as localized corrosion attack (such as blistering, delamination, pitting, and filiform corrosion).

3.3.6.3 Alternating Immersion Corrosion Resistance

Corrosion resistance, more representative of in service conditions, was measured at the Army Research Laboratory facilities using the GM 9540P Method B 18-stage testing protocol[21] (Table 3-3. Figure 3-11 shows the Atotech Model CCT-NC-20 chamber used to perform the testing.

Table 3-3. GM 9540P Cyclic Corrosion Test Sequence

Stage	Description	Time, min	Temp., ±3°C
1	Ramp to salt fog test conditions	15	25
2	Salt fog cycle	1	25
3	Dry cycle	15	30
4	Ramp to salt fog test conditions	70	25
5	Salt fog cycle	1	25
6	Dry cycle	15	30
7	Ramp to salt fog test conditions	70	25
8	Salt fog cycle	1	25
9	Dry cycle	15	30
10	Ramp to salt fog test conditions	70	25
11	Salt fog cycle	1	25
12	Dry cycle	15	30
13	Ramp to relative humidity test conditions	15	49
14	Humidity cycle	480	49
15	Ramp to drying test conditions	15	60
16	Dry cycle	480	60
17	Ramp to ambient temperature test conditions	15	25
18	Ambient temperature cycle	480	25

Figure 3-11. Corrosion Chamber Used for GM 9540P Corrosion Testing

[21] "*Accelerated Corrosion Test; GM 9540P*", General Motors Corporation, Engineering Standards (1997).

The AISI 4130 steel panels were 25mm wide by 35mm long (scribed) or 50mm long (unscribed) and about 1mm thick. These were coated with APCVD Al, and some received a commercial, Cr(III) CCC post-treatment. The C-ring specimens were coated with AlumiPlate Al, and some of these received a commercial, Cr(VI) CCC post-treatment. Standard steel mass loss specimens were used to calibrate this chamber. The test solution was 0.9% NaCl + 0.1% $CaCl_2$ + 0.25% $NaHCO_3$. The arbitrary acceptance criterion was 80 cycles with no visible red rust for unscribed specimens and 40 cycles for scribed specimens.

3.3.6.4 Exposure to Aircraft Maintenance Fluids

A selection of fluids was made from a list of acceptable fluids provided by the Joint Test Protocol (JTP) for the Joint Cadmium Alternatives Team (JCAT). Five fluids were chosen from a list of fourteen for this initial testing for SERDP. The MRO fluids selected were: reagent water conforming to ASTM D 1193; synthetic sea water conforming to ASTM D 1141; Turco 6813E, a solvent-based paint remover conforming to TT-R-2918 Type I; CEM 483WW32, a peroxide-based paint remover; and a water saturated, hydraulic fluid conforming to MIL-PRF-5606.

The samples provided were cleaned in de-ionized water, followed by methyl ethyl ketone, then allowed to dry. After the initial drying, they were placed in a desiccant cabinet. Following a 16 hour period of desiccation stipulated in the JTP, each sample was removed from the cabinet and weighed. Each sample was immersed after weighing in the order it was weighed so as to remove any confusion as to which samples were which since labeling of the samples was not possible. Samples were then tested in accordance with ASTM F 483, "*Total Immersion Corrosion Test for Aircraft Maintenance Chemicals"* with a few minor changes. A wide-mouth sealable glass jar was the vessel chosen to house the samples and fluids (Figure 3-12, left) with another smaller glass jar inside filled with fluid used as a support structure to allow for the maximum surface area of each sample to be exposed to its respective fluid (Figure 3-12, right).

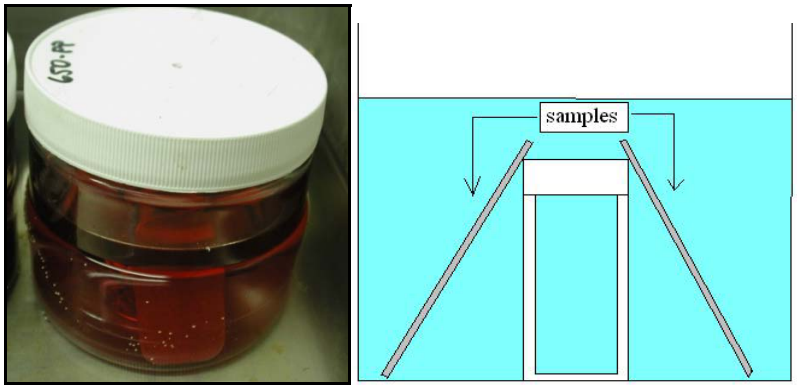

Figure 3-12. Samples Immersed in a Jar Containing Hydraulic Fluid and Internal Sample Support Structure

Each jar was carefully placed into a hot water bath with a maintained temperature of 38ºC (100ºF) as shown in Figure 3-13. Thermometers were used to monitor and ensure a consistent temperature was maintained in each of the glass jars. The duration of the test was amended to 168 hours from the 24 hour period of immersion prescribed by ASTM F 483. Upon removal, the samples were washed first in hot tap water, followed by a rinsing in deionized water, and finally with a stream of acetone. After rinsing, the panels were placed back into the desiccant cabinet for another 16 hour period to fully dry.

Figure 3-13. Hot Water Bath with Monitoring Thermometers and Bath Interior Showing Arrangement of Jars Containing Samples in Different Fluids
(From left to right: reagent water, sea water, Turco 6813E, CEM483, hydraulic fluid)

After drying, the samples were reweighed to establish to what extent any corrosion had occurred. The test fluids were also investigated for evidence of any metal that had dissolved during the immersion period. Finally, the appearance of each sample was evaluated in accordance with the criteria established in ASTM F 1110.

3.3.6.5 Stress-Corrosion Cracking Resistance

In addition to the HE tests based on ASTM F 519, the propensity of the CVD Al coating to cause hydrogen assisted stress-corrosion cracking (SCC) was investigated. This was done by using Rising Step Load (RSL) samples and C-ring samples. To determine the effects of the coatings on the threshold of $K1_{scc}$, Charpy CV2 samples were tested using the ASTM F 1624 RSL method and the fixture shown in Figure 3-14.

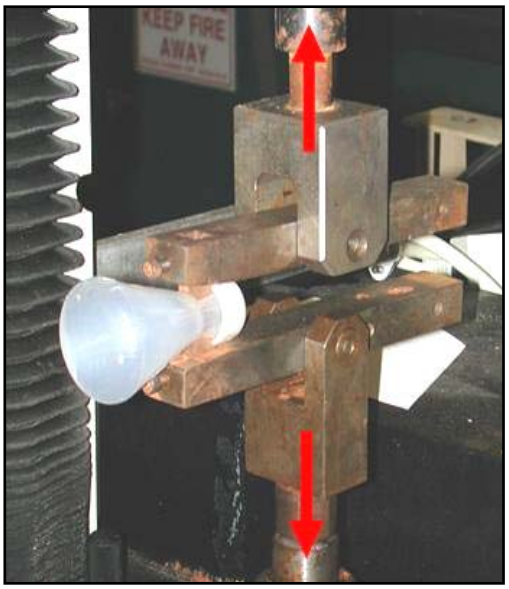

Figure 3-14. Fixture Used for Stress-corrosion Cracking Testing

These specimens were fabricated from 4340 steel heat treated to 52 HRC, and precracked according to ASTM E 399 Sec 7.3 and A2, using a $K1_c$ value of 54. Of the Charpy specimens tested, one half was APCVD Al-coated following the machining and precracking.

3.3.7 Mechanical Properties

Mechanical testing in this Final Report includes adhesion, hardness, coefficient of friction, wear resistance, tensile strength, hydrogen embrittlement, and fatigue resistance measurements.

3.3.7.1 Adhesion

Qualitative adhesion of the coatings to the various substrates was determined using the knife or mandrel bend test protocols. A quantitative measure of the adhesion of the Al coatings to the substrate materials was obtained by performing the pull test, also described below.

Knife Adhesion Test

Adhesion was determined by using a sharp knife to cut an "X" through the coating, to the substrate. Each line of the "X" had a minimum length of 38.1 mm (1.5 in) and intersected at a 30-45° angle. Any coating removed during the cutting process was disregarded. The tip of the knife was used in an attempt to lift the coating, starting at the vertex of the angle. The quantity of removal can be rated on a 0-10 scale per ASTM D 6677, if necessary.

Mandrel Bend Adhesion Test

During this test, a coated panel with a uniform coating thickness was bent over a mandrel at a steady rate. The Al coating was examined for any cracking or defects, and the results were determined as PASS or FAIL. The adhesion testing was performed on 1 x 4 x 0.090 in panels, in accordance with ASTM B 571, "*Standard Test Methods for Adhesion of Metallic Coatings*".

Pull Test

This test was done to evaluate the adhesive bond strength between an Al coating and steel substrate. It was conducted using a SEBASTIAN FIVE-A instrument (Figure 3-15) with a maximum load of 1,755 kg/cm^2 and accuracy of 1% at 20 ±4°C.

Figure 3-15. Adhesion (Pull) Test Equipment

Prior to the test, the coated sample was mounted on the test stud coated with standard, high-strength epoxy adhesive, and then cured on a hot plate at 150°C for one hour, followed by cooling to room temperature. For comparison, this test was performed with the thermal oxide film on silicon, which exhibits a relatively high adhesive strength (498.3 kg/cm^2). The location of the failures for the APCVD Al coatings was confirmed by examining the exposed surfaces with a FE-SEM/EDAX instrument.

3.3.7.2 Hardness

The mechanical characterization of the Al coatings included measurements of hardness, Young's Modulus, and adhesion. A nano-indentation test using a Hysitron Nanoindenter with a triangular (Berkovich) pyramid-shaped diamond tip (Figure 3-16) was performed to determine both hardness and the Young's Modulus of the coatings. A quartz reference specimen was used to calibrate the apparatus prior to making any measurements.

Figure 3-16. Apparatus for Determining Hardness and Young's Modulus

3.3.7.3 Young's Modulus

Young's Modulus is calculated based on the reduced modulus (E_r) measured from the nano-indentation, as calculated from the following equation:

$$\frac{1}{E_r} = \left(\frac{(1-\nu^2)}{E}\right)_{\text{Specimen}} + \left(\frac{(1-\nu^2)}{E}\right)_{\text{Indenter}}$$

where E and ν are the Young's Modulus and Poisson's Ratio of the specimen and indenter (1,140 GPa and 0.07 respectively) and the Poisson's Ratio for polycrystalline, bulk Al is 0.345. Prior to the measurement on the Al coatings a calibration was conducted by using fused quartz with a reduced modulus of 70.7 GPa and a hardness 10.0 GPa. Afterward, two Al single crystals with (100) orientation were used as reference samples, giving an average hardness of 958.5 ± 58.7 MPa, and average Young's Modulus of 41.7 ± 4.5 GPa. In this nano-indentation test, seven points were selected on each of the two Al-coated steel coupons. The values of hardness and Young's Modulus were averaged by excluding minimum and maximum values.

3.3.7.4 Coefficient of Friction

The relative sliding friction of each coating was measured using the Pin-on-Disc technique. The system consisted of an Implant Sciences Corp ISC-200 tribometer and a computer interface data acquisition unit (PC-strip chart computer-based chart recorder used to display and store data in real time). The samples were mounted on the top of a rotating platform of the tribometer (Figure 3-17). A 12.27mm (0.5 in) diameter stainless steel ball (pin) was attached to a precision balanced lever arm, which was used to both apply vertical loads to the disc and to read the friction force on the pin. The ball was placed in contact with the surface of the sample and a load applied. To measure the friction coefficient of the sample the applied load used was 10 gm (0.35 oz). The sample was then rotated and the total distance for the steel ball travel on the sample was set (200 revolutions; i.e., approximately 8 m or 25 ft). All the friction measurements were conducted dry (without lubrication). Finally, the mean (kinetic) friction coefficient measurements obtained at a distance of 6 m (~20 ft) were plotted as a function of ASTM B 117 exposure time for each sample and compared.

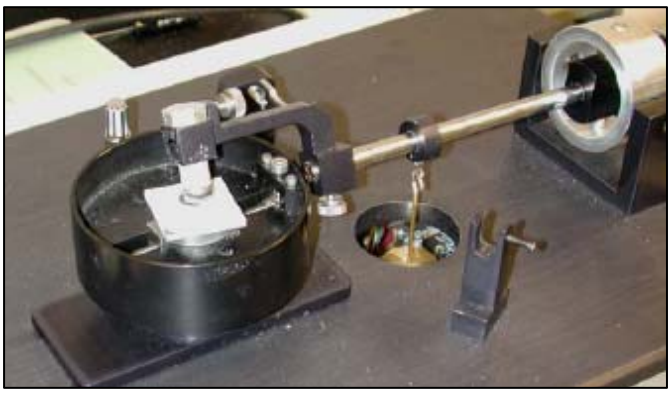

Figure 3-17. Pin-on-Disc Test Apparatus for Determining Coefficients of Friction

The samples were subjected to the salt fog for a total duration of 75 hours. The samples were removed from the chamber for observations and for friction measurements at intervals of 3, 51, and 75 hours. After each removal from the chamber, the samples were rinsed in deionized water and allowed to dry in ambient conditions for at least two hours before testing. Different wear tracks were used for each test.

3.3.7.5 Tensile and Notch Fracture Strength

According to the specification provided by an independent source (Dirats Laboratories, Westfield, MA) the notch fracture strength (NFS) of the notched round bars used for HE testing was 400.7 ksi (mean value of 10 bars) with a minimum of 395.1 and a maximum of 405.2 ksi.

Prior to the HE testing, tensile tests were carried out by applying a load to the bars at a constant rate of 454 kg (1,000 lb) per minute until fracture occurred. Figure 3-18 shows the load frame that was used for these tests. As per Table 3-2, in the ASTM F 519 test method the Notch Fracture Strength (NFS) of the specimens under evaluation should exhibit a difference within ±10 ksi of the average value measured for the bare bars.

Figure 3-18. Tensile (Hydrogen Embrittlement) Testing Machine

3.3.7.6 Hydrogen Embrittlement and Re-embrittlement Resistance

Hydrogen embrittlement (HE) testing was performed at the AFRL in accordance with ASTM F 519, "*Standard Test Method for Mechanical Hydrogen Embrittlement Evaluation of Plating Processes and Service Environment*". The notched round bars used in this test were Type 1a.1 (per ASTM F 519) made from AISI 4340 steel and AerMet 100 per MIL-S-5000E. The bars were 65.6 mm (2.54 inches) long and had a notched diameter of 4.45 mm (0.175 inch) and mounted as shown in Figure 3-19. They were quenched and tempered per AMS-H-6875A to a hardness of 53-55 HRC to attain the strength typically required for aircraft landing gear (LG) applications.

Figure 3-19. Specimen Mounted in Fixture for HE Testing

HE testing was performed on a “Satec” dead-weight mechanical loading frame, using standard threaded couplers. For the tests in deionized water or a 3.5% NaCl solution, the couplers were modified to accommodate a small plastic cup, which was potted in place. These cups were sealed to ensure that the test fluids were in constant contact with the notched areas on the bars.

The HE test consists of applying a load (75% of the notch fracture strength (NFS) of the notched round bar specimens tested in air; 45% for the specimens tested in deionized water or a 3.5% salt solution) to the coated specimens under evaluation and sustaining the load for 200 hours. Subsequently, the sustained load was stepped up 5% every hour until the specimens fractured. In order for a process to pass HE testing, it must withstand the 200-hour test period without showing any signs of fracture. In the preliminary HE tests on APCVD Al coatings, the test was performed in air to evaluate if Al-coated bars experienced hydrogen embrittlement by being sensitized during the deposition process.

3.3.7.7 Fatigue Resistance

Fatigue testing was performed on a 25-kip MTS servo-hydraulic fatigue testing machine with specially designed fatigue specimens coated with APCVD Al, as well as on baseline Cd-plated specimens. The specimen configuration was a standard "dog bone" design conforming to ASTM E 466 guidelines; however, the grip features were reduced in size to reduce weight and allow them to fit in the APCVD reactor (see Figure 3-3). The substrate material for all fatigue specimens was AerMet 100 high strength steel, heat treated to 55 HRC (approximately 300 ksi tensile strength). All specimens were final ground in the longitudinal direction and hand polished in the gage sections. A number of bare (uncoated) AerMet 100 specimens were fatigue tested at the same stress conditions to allow comparison of the relative fatigue debit (if any) due to the APCVD coating processes, as well as allow direct comparison of fatigue performance between each coating.

The constant amplitude fatigue testing was done in accordance with ASTM E 466 procedures at a number of stress levels designed to generate a stress-life (S/N) curve for each specimen condition. A single stress ratio of R = -1 was selected, based on prior work, for all tests to ensure the most rigorous tension-compression loading condition. The load cycle frequency was 5 Hz. All tests were performed at room temperature in a laboratory air environment. Coating behavior (e.g., spalling or peeling) was monitored and recorded using a custom designed, computer-controlled camera.

The AISI 4340 steel samples for the Rising Step Load fatigue testing were coated with APCVD Al at the AkzoNobel facility. These samples were prepared in two conditions: (a) one set was fatigue pre-cracked before the coating was applied; and (b) the other set was not pre-cracked. The former had a coating thickness of 17.4 μm, and the latter had a coating thickness of 17.5 μm. The same deposition processing conditions were used for both sets, and both received a post treatment hydrogen relief bake at 191°C for 23 hours. The specimens were placed on test at the Army Research Laboratory facilities and testing continues.

3.3.8 Electrical Properties

Electrical and electronic equipment often require a low electrical resistance on their finished surfaces for uninterrupted contact, grounding, and electromagnetic field shielding purposes. A number of standard test methods are used to obtain relevant property data.

3.3.8.1 Contact Resistance

The test method given in MIL-DTL-81706A evaluates a coating system's ability to provide initial electrical contact resistance after application of post-treatment - such as a chromate/dichromate chemical conversion coating, and after exposure to a corrosive environment.

In accordance with MIL-DTL-81706A, the samples evaluated in this test included APCVD Al coatings as deposited and post-treated with glass bead burnishing followed by a Cr(VI) conversion coating (Iridite™ 14-2). Electrical contact resistance (ECR) measurements were conducted before and after continuous exposure to a neutral salt fog for 168 hours. Operation of the fog chamber for this test was done in accordance with ASTM B 117, "*Standard Practice for Operating Salt Spray (Fog) Apparatus"*. The samples were placed into a fog chamber at a 6-degree angle. The coupons were not allowed to contact other surfaces in the chamber, and condensate from a coupon did not contact any other coupons. The salt solution and the fog chamber were prepared as specified in the Test Methodology of the Non-chrome Aluminum Pretreatment (NCAP) Project Joint Test Protocol (JTP). The nozzles were adjusted in the fog chamber so that sprayed salt solution did not directly impinge on the coupon surfaces. After exposure, the coupons were carefully removed and cleaned with running water at a temperature less than 38°C (100°F). The coupons were then air-dried at ambient conditions, and visually examined for corrosion.

3.3.8.2 Electrical Resistivity

Electrical sheet resistance measurements on Al coatings were conducted using a four-point resistance probe (Veeco FPP-5000 or Magne-Tron 800 – Figure 3-20) for comparison with data on Al deposited by other techniques.

Figure 3-20. Electrical Resistivity Test Apparatus

Measurement on an Al coating deposited on a steel substrate is not possible because the interface between the Al coating and the steel substrate provides an electrical (grounding) contact. Therefore, samples prepared for electrical resistivity measurements consist of AISI 4130 steel coupons on top of which an insulating silicon nitride layer (1µm thick) is synthesized by plasma enhanced, chemical vapor deposition (PECVD). Optimal conditions for this PECVD process were established to be a deposition temperature of 350°C, RF power of 50 W, flow rates of SiH_4 at 280 sccm and NH_3 at 4 sccm, and a process pressure of 900 mTorr. APCVD Al coatings are deposited on top of these insulating layers at 300°C without shielding the substrate.

4.0 Test Results and Accomplishments

4.1 Test Results

The results in this section are presented, for the most part, in the chronological order in which the tests were performed - first with TEAL as the precursor (in the tubular reactor at NJIT), then with pure TIBAL and PB1 as the precursors in AkzoNobel's bench scale rotary reactor). Because the better performing coatings were obtained with the latter, the experiments and tests associated with these Al coatings constitute the bulk of the characterization, property, and performance data obtained. The additional work with the new, proprietary precursor PB2 (for lower temperature deposition) is discussed in the "Accomplishments" section (see Section 4.2).

4.1.1 Coating Structure

The ideal coating should exhibit uniform coverage, uniformity of composition, an equi-axed or nano-scale grain structure, with no columnar grains, porosity, delamination, or other defects that could impair its performance in service.

4.1.1.1 Optical Microscopy and Metallography

Figures 4-1(a) through (c) are photomicrographs of cross-sections of APCVD Al coatings on steel fasteners obtained by using a TEAL precursor at 325 and 300°C, respectively, in the NJIT tubular reactor. The thicker Al coating was deposited at the higher deposition temperature, and the coatings at the apex of the screw and bolt specimens were thicker than those on the sides and in the troughs of the threads. All of these coatings are unsatisfactory, because their appearance was very irregular, with discontinuities in some locations, and they had a very nodular structure.

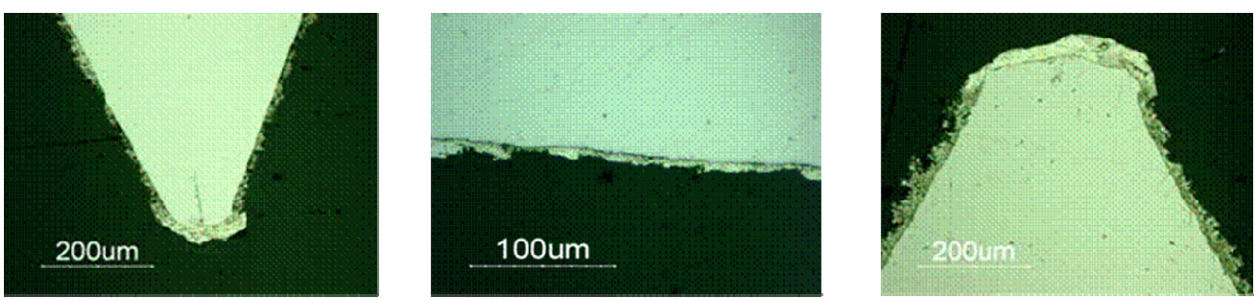

(a) Screw: TEAL at 325°C (b) Nut: TEAL at 300°C (c) Bolt: TEAL at 300°C

Figure 4-1. Photomicrographs of Cross-sections of APCVD Al-Coated Steel Fasteners

Figure 4-2 is a montage of cross-sections of similar coatings deposited on fasteners using a TIBAL precursor in the same temperature range in the rotating barrel reactor using AkzoNobel's technology.

These TIBAL-based Al coatings - obtained early in this project - are more satisfactory. Notice the good throwing power that provided a conformal coating of uniform thickness inside a surface defect.

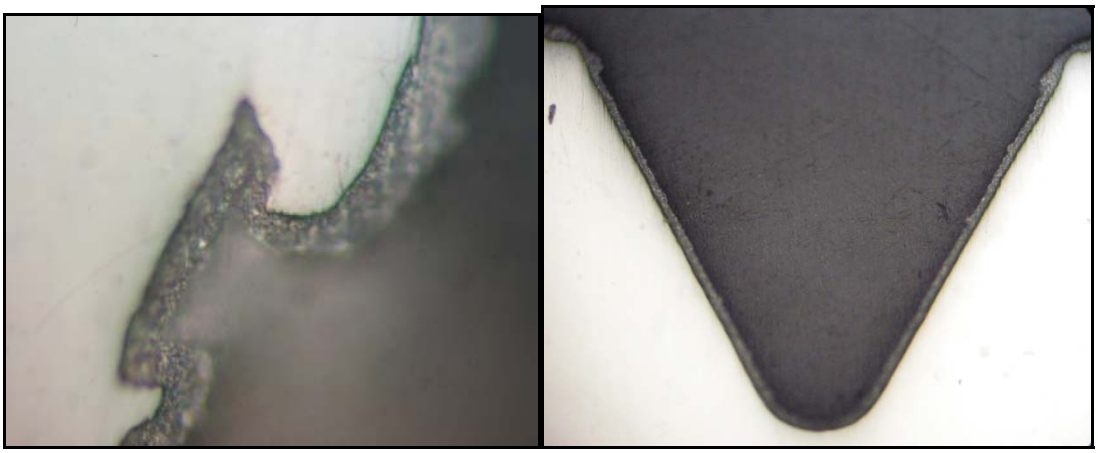

(a) (b)

Figure 4-2. Photomicrographs of Cross-sections of APCVD Al-Coated Bolts

Figure 4-3 shows the equi-axed, nodular/granular structure of the surfaces of TIBAL-based Al coatings such as those shown in Figure 4-2.

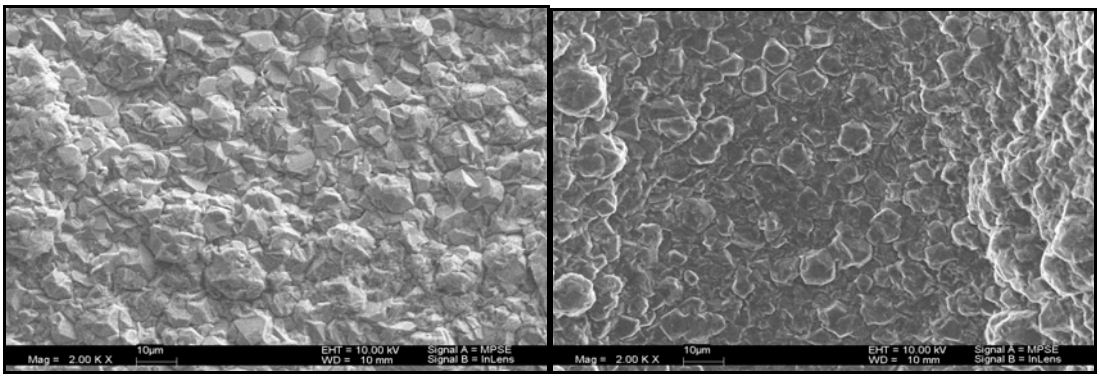

(a) Steel Coupon (b) Steel Bolt

Figure 4-3. Photomicrographs of the Surfaces of APCVD Al-Coated Substrates

A dense, thick, uniform coating on the outside and inside surfaces of a small diameter, tubular specimen is shown in Figure 4-4. This photomicrograph of a cross-section demonstrates that acceptable coatings, with the ability to fill surface defects and provide some leveling power, can be obtained with both pure TIBAL and with blended precursor PB1 in small, bench scale reactors.

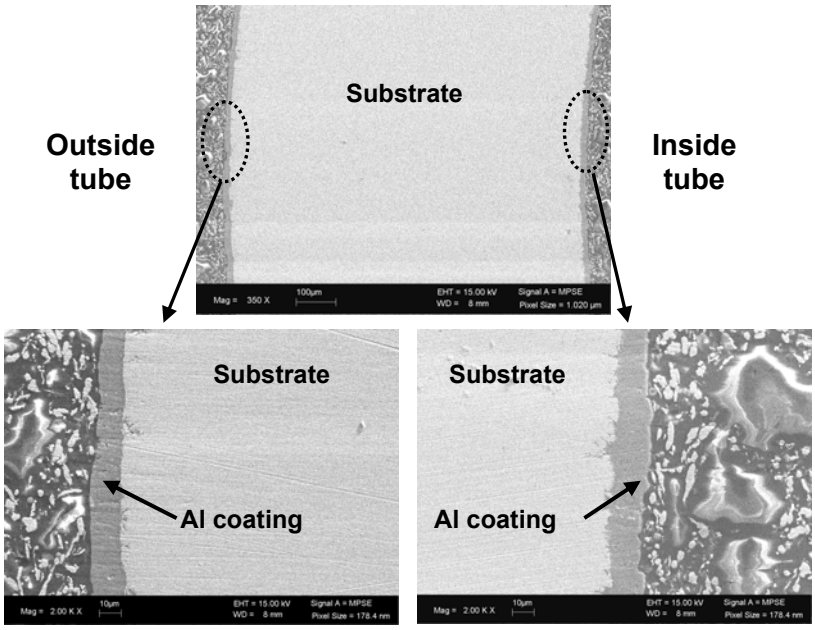

Figure 4-4. FE-SEM Image of Cross-section of Middle of an APCVD Al-coated Small Diameter, Steel Tube

4.1.1.2 X-ray Diffraction

APCVD Al coatings deposited on steel at 300°C using a TIBAL precursor were polycrystalline (face-centered cubic (fcc) structure) with an (111) preferred orientation, as demonstrated by their x-ray diffraction patterns when compared to the Al powder reference material (Figure 4-5).

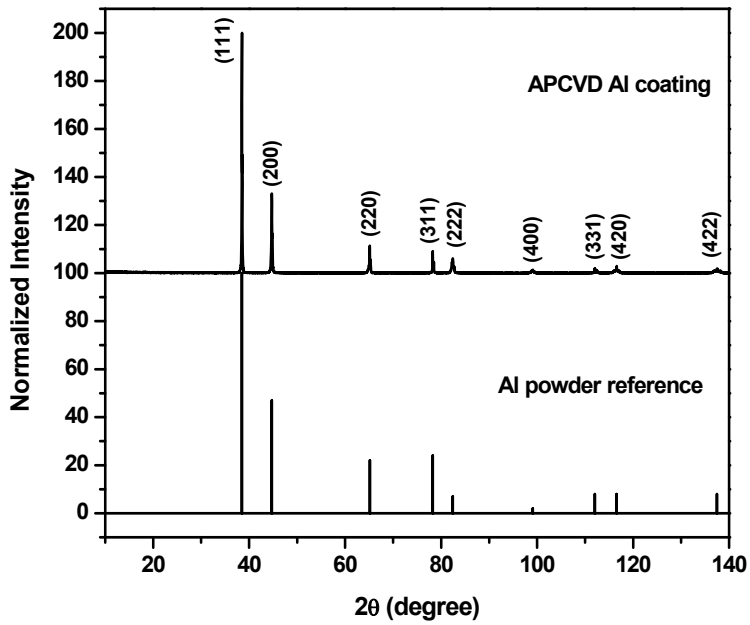

Figure 4-5. XRD Pattern of APCVD Al Coating Compared to that of an Al Powder Reference Material

The full width at half maximum (FWHM) of each peak , shown in Table 4-1, together with that of an Al foil reference material, indicates that the APCVD Al coatings had a higher degree of crystallinity.

Table 4-1. Full Width at Half Maximum of All Peaks Measured from XRD Analysis

2θ (deg)	38.47	44.74	65.14	78.23	82.44	99.08	112.05	116.57	137.46
Miller Indices (hkl)	(111)	(200)	(220)	(311)	(222)	(400)	(331)	(420)	(422)
FWHM APCVD Al	0.059	0.079	0.096	0.096	0.144	0.960	0.192	0.288	0.576
FWHM Al Foil*	0.103	0.141	0.127	0.104	- -	- -	- -	- -	- -

XRD analysis also was carried out on Al coatings deposited at 275° and 300°C using a pure TIBAL (Figure 4-6) and at 300°C using PB1 to investigate any effects of deposition temperature and precursor on coating structure. The coatings again were found to be polycrystalline (with a fcc structure and a (111) preferred orientation) regardless of deposition conditions.

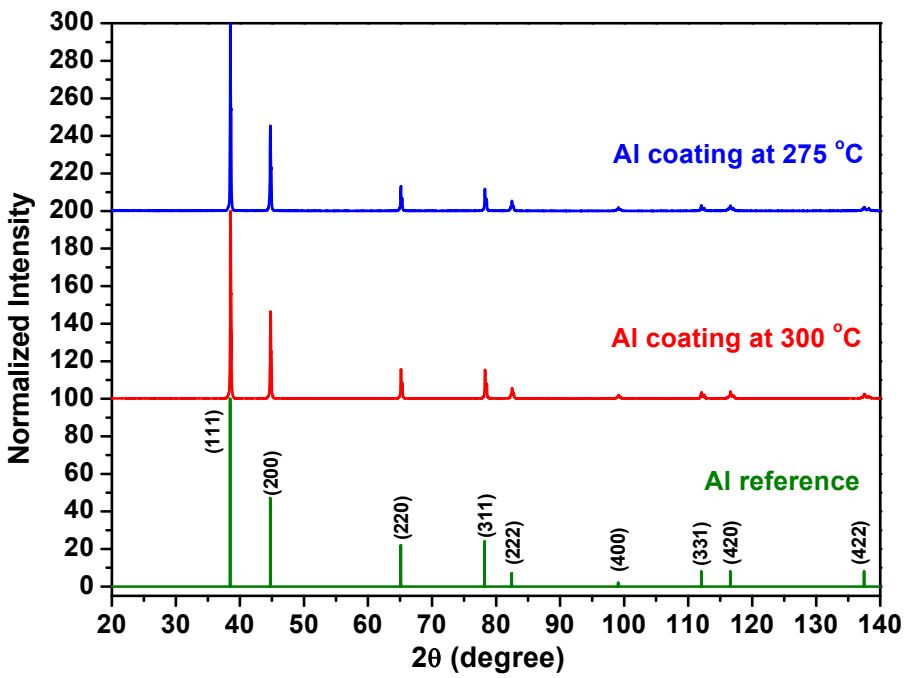

Figure 4-6. XRD Patterns for APCVD Al Coatings Deposited at Different Temperatures

The APCVD Al coating deposited with a pure TIBAL precursor showed a higher degree of crystallinity than the coating obtained with PB1, as indicated by the smaller "full width at half maximum" (FWHM) values shown in Table 4-2.

Table 4-2. Full Width at Half Maximum of All Peaks Measured from XRD Analysis on APCVD Al Coatings with Different Precursors and at Different Temperatures

2θ (deg)	Miller Indices (hkl)	FWHM (deg)		
		Pure TIBAL (275°C)	Pure TIBAL (300°C)	PB1 (300°C)
38.47	(111)	0.0960	0.1968	0.2165
44.74	(200)	0.1200	0.1574	0.1680
65.14	(220)	0.1200	0.1378	0.4320
78.23	(311)	0.1200	0.1920	0.3360
82.44	(222)	0.0960	0.1440	0.4320
99.08	(400)	0.1920	0.3840	0.5760
112.05	(331)	0.2400	0.1680	0.3360
116.57	(420)	0.1440	0.1920	0.2880
137.46	(422)	0.2880	0.2400	0.4800

XRD analysis also was carried out on Al coatings deposited at 300°C, and IVD Al coatings as a benchmark, both with post-treatments comprised of glass bead burnishing followed by a Cr(VI)-containing chemical conversion coating. The results are shown in Figure 4-7, and indicate that the post-treatments have no effect on coating structure. However, the APCVD Al coating showed a higher degree of crystallinity than the IVD Al coatings, as indicated by the smaller "full width at half maximum" (FWHM) values in Table 4-3.

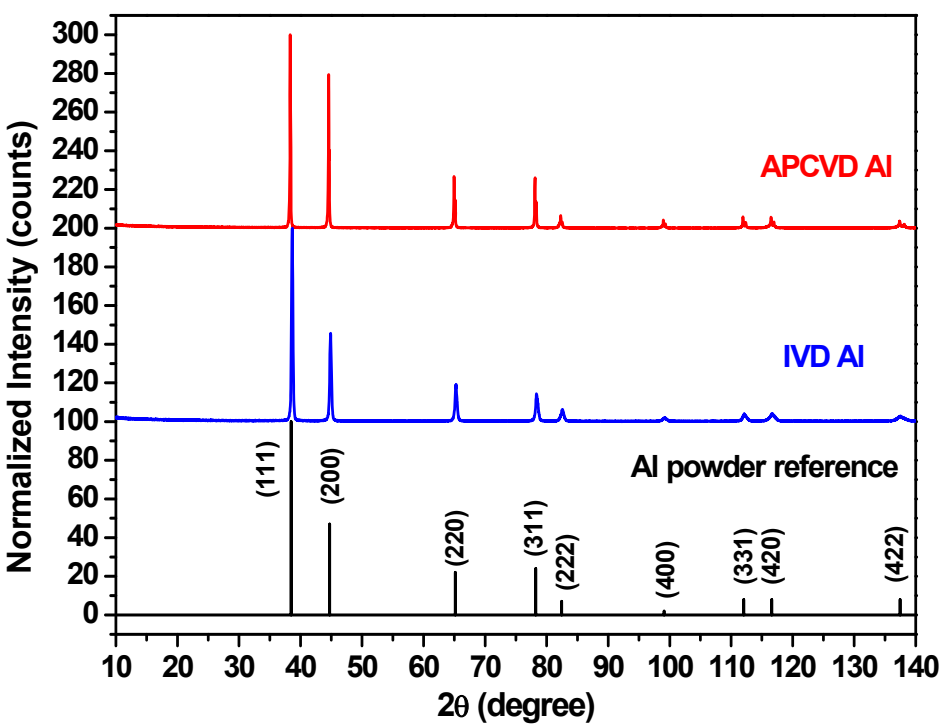

Figure 4-7. XRD Patterns of APCVD Al and IVD Al Coatings with Post-treatments

Table 4-3. Full Width at Half Maximum of All Peaks Measured from XRD Analysis on IVD and APCVD Al Coatings

2θ (deg)	Miller Indices (hkl)	FWHM (deg)		
		Al Foil*	IVD Al	APCVD Al
38.47	(111)	0.1030	0.2952	0.0720
44.74	(200)	0.1410	0.2558	0.0720
65.14	(220)	0.1270	0.1181	0.0960
78.23	(311)	0.1040	0.1574	0.0960
82.44	(222)	- -	0.2362	0.0960
99.08	(400)	- -	0.4723	0.0960
112.05	(331)	- -	0.4723	0.1200
116.57	(420)	- -	0.3936	0.1200
137.46	(422)	- -	0.7680	0.1680

* Foil was 100 mm thick.

4.1.2 Thickness and Surface Roughness

Figures 4-3 (a) and (b) illustrate the overall morphology of the surface of an APCVD Al-coated steel coupon and bolt (thread), respectively. Figure 4-8 illustrates the topography of an APCVD Al coating, such as that shown in Figure 4-3(a). On a ***nanoscale*** (R_{rms}=917 nm) the APCVD Al coatings are relatively rough, and are rougher than the underlying steel substrate surface (R_{rms}= 160 nm). However, the nano-roughness may help promote good pretreatment and primer adhesion for applications requiring the part or component to be painted after the sacrificial APCVD Al coating is applied.

SEM photomicrographs of the surfaces of an APCVD Al coating and an IVD Al benchmark coating are shown in Figure 4-9. Both of these coatings had been glass bead peened (burnished), which is often done to densify IVD Al coatings and improve their corrosion resistance.

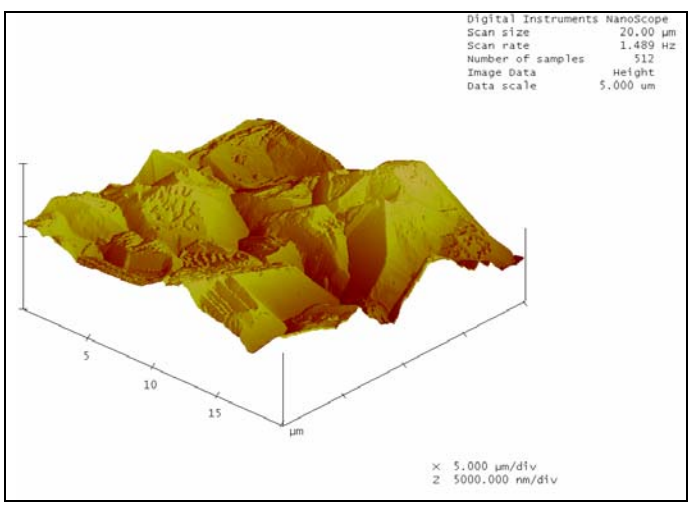

Figure 4-8. AFM Derived Topography of the Surface of an APCVD Al Coating

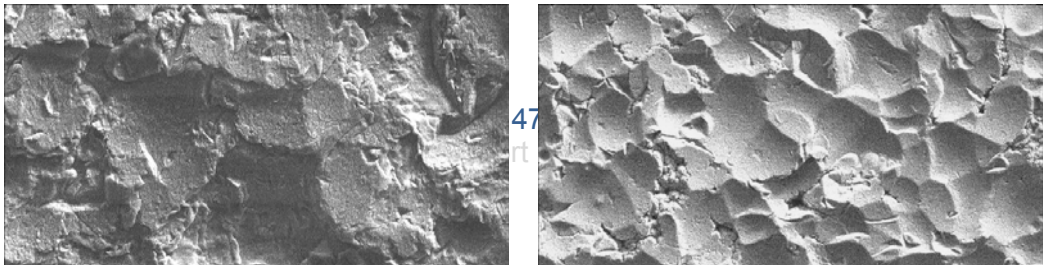

(a) APCVD Al (b) IVD Al

Figure 4-9. SEM Images of the Surface of APCVD Al and IVD Al Coatings
(Arrows indicate the presence of pin-holes in these coatings)

It can be deduced from Figure 4-9(a) that the APCVD Al coating is slightly harder than the IVD Al coating (b) because there are fewer small "dimples" left by the glass beads. However, the average surface roughness (R_a) of the peened IVD Al coating was 1.98 $\pm$ 0.18μm, and that of the peened APCVD Al coating was 3.68 ±0.75μm, indicating that the APCVD Al coating may be softer than the IVD Al coating. The hardness of these coatings was not determined in order to resolve these differences.

4.1.3 Throwing Power and Conformal Coverage

Throwing power tests were performed on APCVD Al coatings deposited at 300°C using both a pure TIBAL and PB1 precursors on cylindrical tubes with different inner diameters of 3.0 and 6.0 mm. Figure 4-4 is a photomicrograph of a representative SEM image of a cross-sectioned APCVD Al-coated tube with a 6.0 mm ID that indicates the excellent throwing power of the APCVD process.

Figure 4-10 is a diagram showing how the small diameter tubes were cross-sectioned longitudinally and radially for the thickness measurements. This diagram includes the various measurement reference points indicated by the lines used to compile Tables 4-4 through 4-7, where the letter identifier P refers to a longitudinal, and R to a radial cross-section.

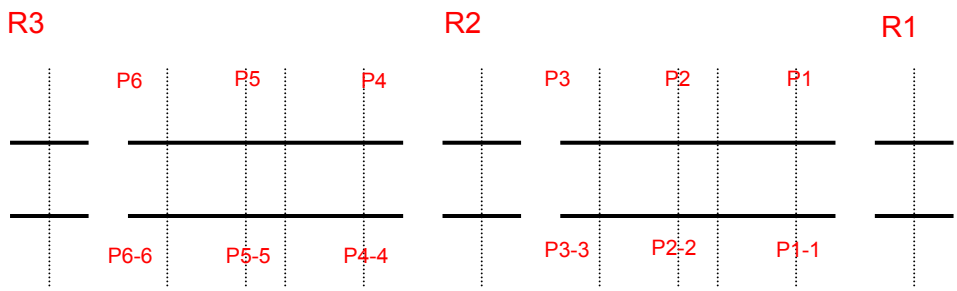

Figure 4-10. Diagram Showing Cross-sectioning of APCVD Aluminum on Tubes

Tables 4-4 through 4-7 summarize the average the coating thicknesses measured at each point shown in Figure 4-10 on the outside and inside surfaces of the tubes. The ratio of inside to outside average coating thickness represents the throwing power of Al coatings. The throwing power of Al coatings deposited on 6.0 mm ID tubes was 0.93 ±0.07 for PB1 and 1.00 ±0.13 for pure TIBAL-based coatings. There was no significant difference in throwing power between processes using pure TIBAL and PB1 precursors. However, in the case of the 3.0 mm ID tubes, the throwing power (0.73 ±0.09) for PB1 was found to be greater than that of pure TIBAL (0.56 ±0.19). In both of the 3.0 and 6.0 mm tubes, the Al coatings deposited using PB1 showed less variation in throwing power along the tube length than those using pure TIBAL (Figure 4-10).

Table 4-4. Coating Thickness on Outside and Inside of Tube with 3.0 mm Inner Diameter: Pure TIBAL Precursor

APCVD Al Deposition Using Pure TIBAL									
Points	**R1**	**P1&1-1**	**P2&2-2**	**P3&3-3**	**R2**	**P4&4-4**	**P5&5-5**	**P6&6-6**	**R3**
Outside	12.97 ± 2.26	10.65 ± 3.03	16.15 ± 0.72	16.77 ± 0.34	15.17 ± 2.67	19.27 ± 4.96	16.06 ± 1.01	13.35 ± 1.14	13.18 ± 2.89
Inside	10.02 ± 0.82	8.36 ± 1.22	6.01 ± 0.17	6.45 ± 1.39	6.63 ± 0.51	8.14 ± 1.01	6.99 ± 1.13	8.00 ± 0.61	10.37 ± 1.49
Ratio*	0.79	0.80	0.37	0.38	0.46	0.44	0.44	0.60	0.80

* Ratio of inside to outside coating thickness: thickness unit = μm.

The average thickness of the Al coating on the outside and inside surfaces of a tube was 14.84 μm and 7.89 μm, respectively. The throwing power ratio was 0.56 ±0.19.

Table 4-5. Coating Thickness on Outside and Inside of Tube with 3.0 mm Inner Diameter: PB1 Precursor

APCVD Al Deposition Using PB1									
Points	**R1**	**P1&1-1**	**P2&2-2**	**P3&3-3**	**R2**	**P4&4-4**	**P5&5-5**	**P6&6-6**	**R3**
Outside	15.11± 4.85	11.21 ± 1.06	14.00 ± 1.81	14.36 ± 0.55	12.15 ± 1.51	15.47 ± 2.94	13.06 ± 2.98	14.90 ± 0.29	13.30 ± 0.99
Inside	10.91 ± 0.80	9.52 ± 0.67	9.28 ± 0.08	9.58 ± 0.84	9.35 ± 0.38	8.86 ± 0.25	8 .89 ± 0.63	9.64 ± 1.26	11.36 ± 1.09
Ratio	0.77	0.86	0.67	0.67	0.78	0.59	0.71	0.65	0.86

* Ratio of inside to outside coating thickness: thickness unit = μm.

The average thickness of the Al coating on the outside and inside surfaces of a tube was 13.73 μm and 9.71 μm, respectively. The throwing power ratio was 0.73 ±0.09.

Table 4-6. Coating thickness on outside and inside of tube with 6.0 mm inner diameter: Pure TIBAL Precursor

APCVD Al Deposition Using Pure TIBAL									
Points	**R1**	**P1&1-1**	**P2&2-2**	**P3&3-3**	**R2**	**P4&4-4**	**P5&5-5**	**P6&6-6**	**R3**
Outside	12.29 ± 1.02	16.30 ± 0.59	11.69 ± 2.73	17.55 ± 1.00	14.81 ± 3.69	13.8 ± 1.68	15.29 ± 2.35	15.56 ± 1.47	13.81 ± 2.51
Inside	15.07 ± 2.23	14.63 ± 3.03	12.64 ± 0.29	14.84 ± 1.14	13.46 ± 2.80	14.22 ± 0.59	14.01 ± 1.64	14.45 ± 1.18	14.36 ± 1.76
Ratio*	1.25	0.90	1.11	0.85	0.93	1.04	0.92	0.93	1.07

* Ratio of inside to outside coating thickness: thickness unit = μm.

The average thickness of the Al coating on the outside and inside surfaces of a tube was 14.57 μm and 14.19 μm, respectively. The throwing power ratio was 1.00 ±0.13.

Table 4-7. Coating Thickness on Outside and Inside of Tube with 6.0 mm Inner Diameter: PB1 Precursor

APCVD Al Deposition Using PB1									
Points	**R1**	**P1&1-1**	**P2&2-2**	**P3&3-3**	**R2**	**P4&4-4**	**P5&5-5**	**P6&6-6**	**R3**
Outside	12.83 ± 0.75	12.58 ± 0.80	17.16 ± 1.30	14.16 ± 0.42	13.59 ± 0.66	17.91 ± 0.25	15.47 ± 6.06	15.58 ± 1.51	14.60 ± 1.12
Inside	13.39 ± 0.73	12.49 ± 0.51	14.46 ± 0.00	12.88 ± 0.54	13.61 ± 0.66	15.14 ± 1.14	14.57 ± 2.19	14.31 ± 1.56	12.64 ± 0.53
Ratio*	1.04	1.00	0.84	0.91	1.00	0.85	0.94	0.92	0.87

* Ratio of inside to outside coating thickness: thickness unit = μm.

The average thickness of the Al coating on the outside and inside surfaces of a tube was 14.88 μm and 13.72 μm, respectively. The throwing power ratio was 0.93 ±0.07.

The throwing power of Al coatings deposited on 6.0 mm ID tubes was 0.93 ±0.07 for PB1 and 1.00 ±0.13 for pure TIBAL, indicating that there was no significant difference in throwing power between the two precursors. However, in the case of tubes with 3.0 mm ID, the throwing power (0.73 ±0.09) for PB1 was found to be greater than that of pure TIBAL (0.56 ±0.19). In both of the 3.0 and 6.0 mm tubes, the Al coatings deposited using PB1 as precursor showed less variation in throwing power along the tube length than those using pure TIBAL (Figure 4-11).

The conformal coverage of the APCVD Al coatings was investigated by using a hollow, steel rivet sleeve with a step present on the inside surface - caused by a difference in internal diameter - as shown in Figure 4-12. The dimensions of the hollow rivet sleeve are given later in Figure 4-63.

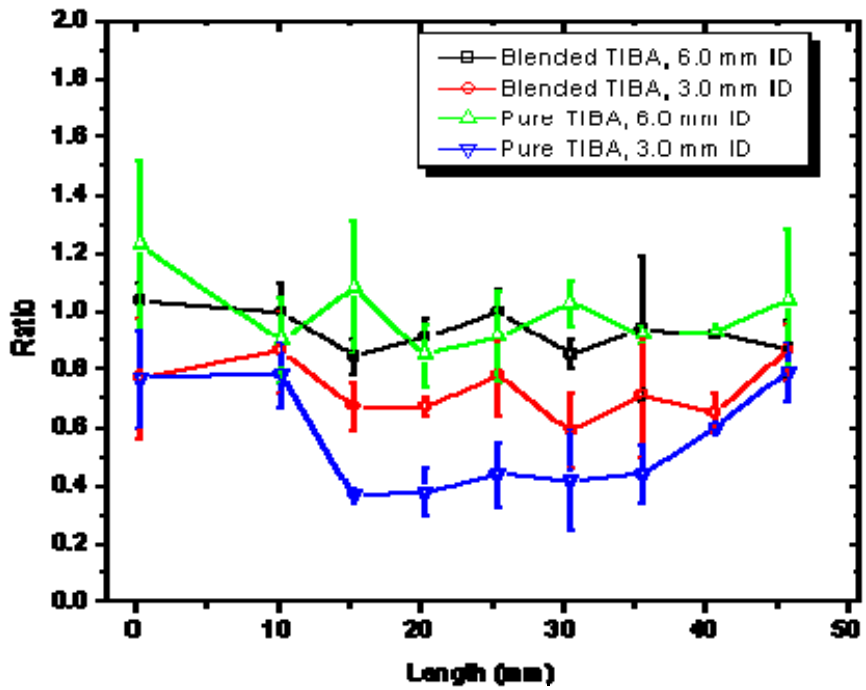

Figure 4-11. Ratio of Inside to Outside Aluminum Coating Thickness along Tube Length

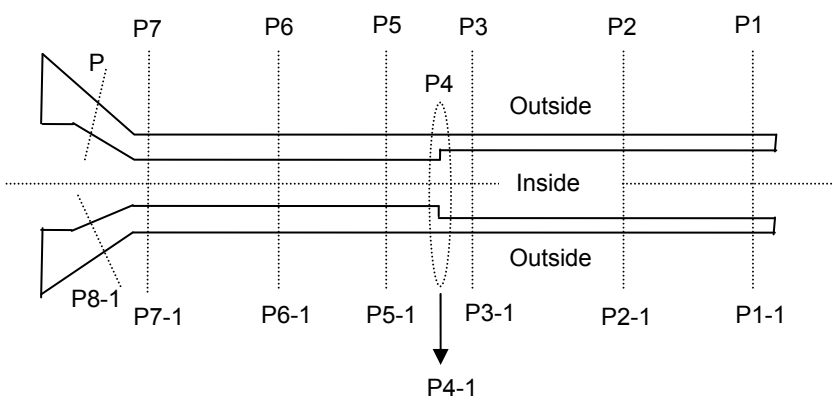

Figure 4-12. Schematic Diagram Showing Coating Thickness Measurement Points on Hollow Rivet Sleeve for Step Coverage Measurement

The specimen was cross-sectioned lengthwise and the coating thickness at each point shown in Figure 4-12 on the outside and inside surfaces of the rivet sleeve was measured. The P4 and P4-1 identifiers represent the points on the inside substrate where step coverage was measured on the step itself (d_2) and on the inside diameter surface (d_1).

Figure 4-13 shows FE-SEM images of an Al coating cross-sectioned to show the steps. The step coverage ratio (0.96 - 0.99) was found to be close to unity, indicating that the APCVD Al deposition process provides excellent conformal step coverage.

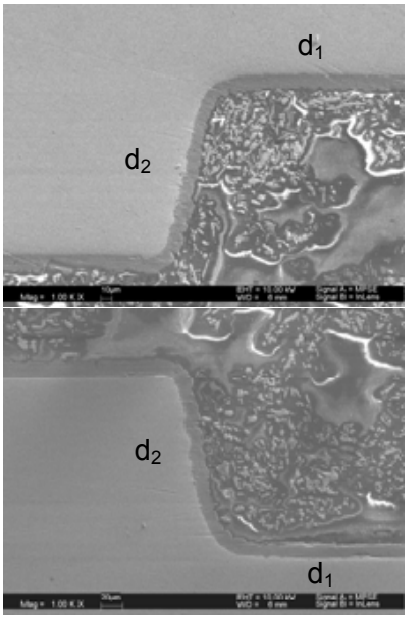

$$r = \frac{d_2}{d_1} = \frac{13.24\ \mu m}{13.41\ \mu m} = 0.99$$

$$r = \frac{d_2}{d_1} = \frac{13.56\ \mu m}{14.12\ \mu m} = 0.96$$

Figure 4-13. FE-SEM Images Showing Measurement Points and Excellent Step Coverage

In addition to the step coverage, the uniformity of the coating thickness was examined on the outside and inside surfaces of the hollow rivet sleeve along its length (Table 4-8). The average thicknesses on the inside and outside surfaces were 15.10 ±1.44 and 15.29 ±1.90 μm, respectively, and hence the ratio is ~0.99.

Table 4-8. Coating Thickness on Outside and Inside of Coated Hollow Rivet Sleeve

Points	P1	P2	P3	P4*	P5	P6	P7	P8
Outside	17.21	16.49	17.95	NA	16.20	14.48	13.79	14.37
Inside	16.08	15.87	13.41	13.24	15.23	15.05	17.18	14.48
Ratio**	0.93	0.96	0.75	NA	0.94	1.04	1.25	1.01
Points	**P1-1**	**P2-1**	**P3-1**	**P4-1***	**P5-1**	**P6-1**	**P7-1**	**P8-1**
Outside	18.25	12.41	14.18	NA	16.61	15.21	12.16	14.76
Inside	18.49	15.11	14.12	13.56	14.53	14.74	13.76	13.30
Ratio*	1.01	1.22	1.00	NA	0.87	0.97	1.13	0.90

* Coating thickness (μm) at P4 is for step coverage calculations.
** Ratio of inside to outside coating thickness.

4.1.4 Density and Porosity

At first, x-ray reflectivity (XRR) was used on very thin APCVD Al coatings (~1 μm thick, pure TIBAL precursor, 300°C). However, this method did not produce useful results because of the poor data fitting caused by the relatively rough surface profile (R_a = ~400 nm). Consequently He pycnometry was used. An Al-coated steel tube specimen was used for the first density measurements. The density of this sample was found to be 3.14 ±0.45 g/cm^3, which compares reasonably well to the reported density value of bulk Al (2.70 g/cm^3) and for the Al 1100 alloy

(2.71 g/cm^3) used for PVD/IVD process coating deposition. The density of the IVD Al coating was not measured; however, a typical value found in the published literature is also 2.71g/cm^3. For comparison, a typical value for electroplated Al coatings is 2.64 g/cm^3, which is closer to that measured for the APCVD Al coatings[22].

In the second set of measurements, APCVD Al-coated rivet stems with a coating thickness of 10.1 μm were used. For better accuracy, eight samples were tested in a single run. Based on these measured values, the average density of the Al coating was found to be 2.60 ±0.04 g/cm^3. This value is closer - but a little lower - to that for bulk Al, and may indicate some closed pores were present in the coating.

4.1.4.1 Optical Microscopy

The high magnification photomicrographs in Figure 4-9 were chosen specifically to show how a few pin-holes and some localized damage may be found in both APCVD Al coatings. In an effort to find an explanation for the poor results obtained in the hydrogen embrittlement testing (discussed later in Section 4.1.7.6), cross-sections of the APCVD Al coatings deposited at 300°C on notched round bars were prepared and mounted for metallographic inspection. Examples of the photomicrographs obtained are shown in Figure 4-14, and some closed ("micro") porosity is apparent, as well as an area where the majority of the coating thickness has been compromised by part impingement in the rotating barrel reactor.

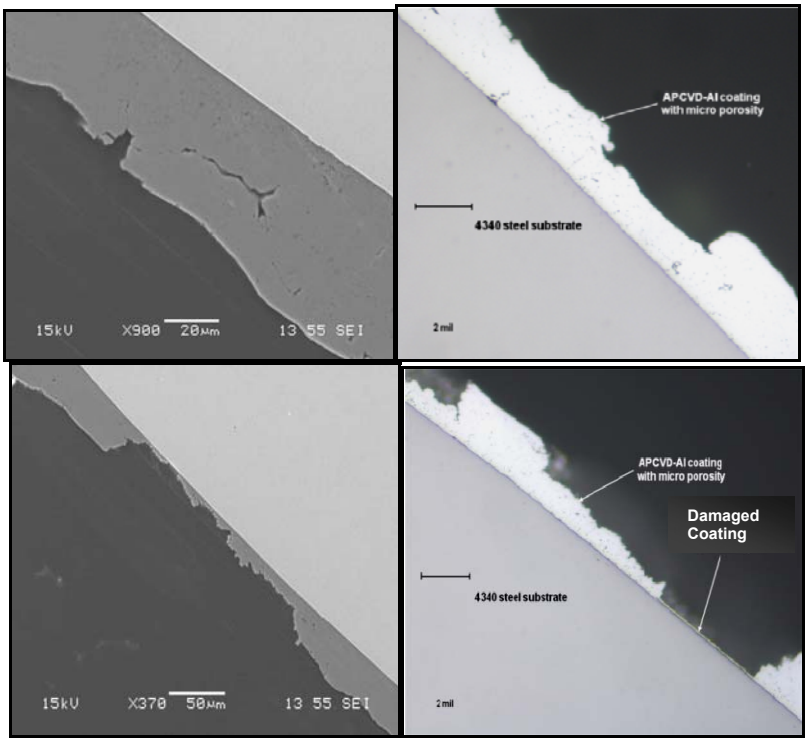

Figure 4-14. Cross-sections of APCVD Al Coatings Showing Areas of Damage, Poor Coverage and Closed Porosity

[22] Anon. "*The Properties and Benefits of the AlumiPlate™ Electrodeposited Aluminum Coating*", AlumiPlate, Inc., company web site: http://www.alumiplate.com/html/body_properties.html.

4.1.4.2 Electrochemical Impedance Spectroscopy

Electrochemical impedance spectra - expressed as Bode plots – showed a greater impedance (Z_{lf}) at a low frequency (0.01 Hz), which confirmed that the APCVD Al coatings on AISI 4130 steel coupons had an equivalent or better corrosion resistance than the IVD Al benchmark. The low frequency impedance values of both types of Al coatings, measured over an immersion time of 10 days in a standard salt solution, are plotted in Figure 4-15 with those for an Al foil and uncoated AISI 4130 steel.

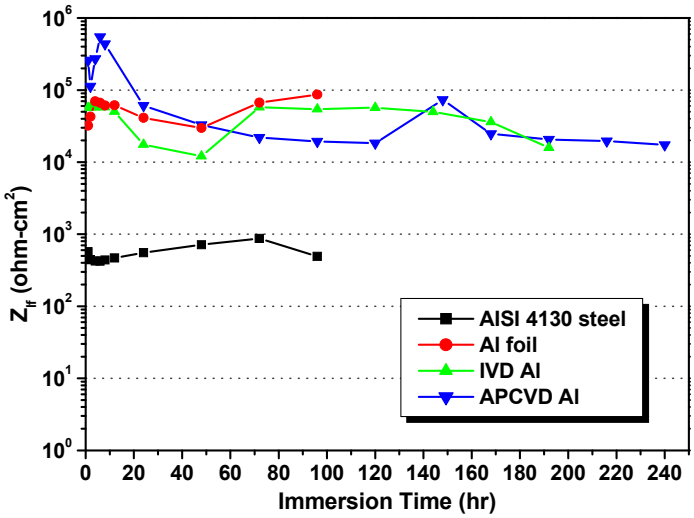

Figure 4-15. Low Frequency Impedance of APCVD Al and IVD Al Coatings on AISI 4130 Steel Obtained from EIS as a Function of Immersion Time

The surface morphology of the APCVD Al and IVD Al coatings was investigated after the EIS measurements and the images obtained are shown in Figure 4-16. Enlargement of open pores that were present originally in the coatings (compare Figure 4-6) was observed due to the galvanic action between the Al coatings and the steel substrate (see also Section 4.1.6 for a discussion of changes in coating surface composition and morphology on AISI 4340 steel).

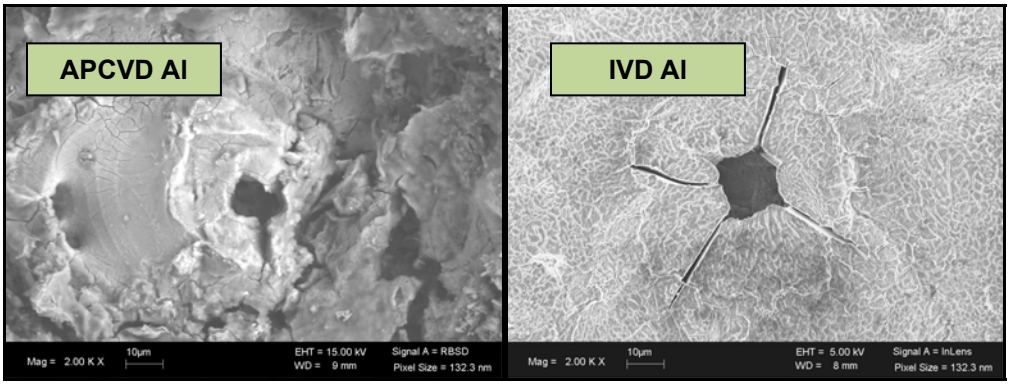

Figure 4-16. SEM Images of APCVD Al and IVD Al Coatings after EIS Measurements

However, no red rust was observed during the immersion time. Overall, these results indicated that both the APCVD and IVD Al coatings provide good sacrificial protection for steel substrates.

4.1.5 Chemical Composition

Besides the early analyses to determine the purity (Al content) of the APCVD coatings, other analytical methods were used to identify the concentrations of the impurities present, and how these concentrations were affected by deposition conditions. The results are presented and discussed in the following subsections.

4.1.5.1 Energy Dispersive Analysis with X-rays

Elemental analyses using SEM/EDAX were conducted on the top of an Al-coated nut and bolt (Figure 4-17 (a) and (b), respectively) using TEAL as a precursor at 300°C, revealed that the ~16-25μm thick coatings consisted of mostly aluminum with some oxygen (O) and iron (Fe) indicated. However, the Fe signal detected by EDAX analysis indicated that either the coating was incomplete or that area of the film was less than 4 μm thick.

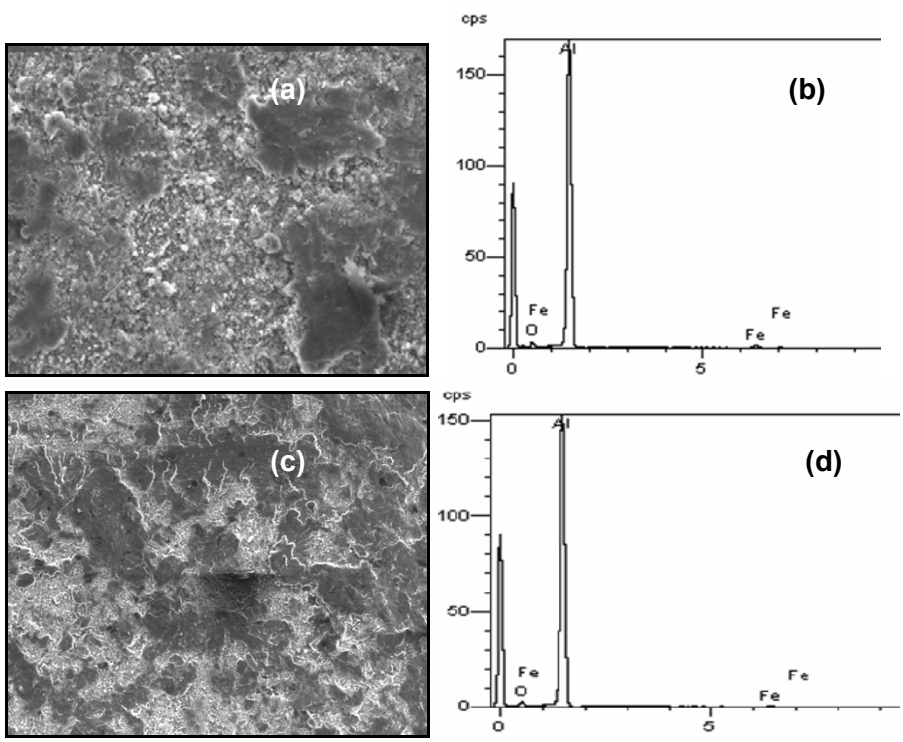

Figure 4-17. SEM Images of the Al Coating (a) on Top of Nut with (b) EDAX Analysis and (c) on Top of Bolt with (d) EDAX Analysis

Figure 4-18 shows cross-sections through a bolt and a coupon with an APCVD Al coating using a TIBAL precursor at 300°C, and the corresponding EDAX results using an Al Kα1 beam. The Al distribution is uniform throughout the coating, as was expected. Unfortunately, EDAX is not

able to detect lighter elements, such as carbon and hydrogen, which as reaction byproducts can be incorporated into the APCVD Al coatings.

4.1.5.2 Auger Electron Spectroscopy

Three different areas on two APCVD Al-coated steel coupons were examined using AES to obtain comprehensive information about composition as a function of depth. Figure 4-19 (a) represents a typical Auger spectrum of an Al coating before Ar sputter etching. It reveals that carbon and oxygen are present as impurities on the surface.

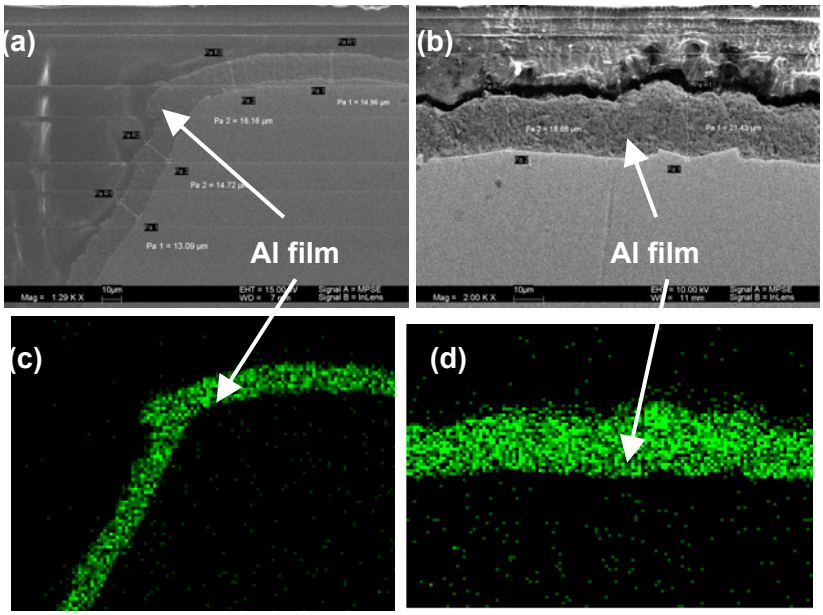

Figure 4-18. FE-SEM Images of Cross-sections of APCVD Al-Coated Bolt (a) and Coupon (b) and Corresponding EDAX Images

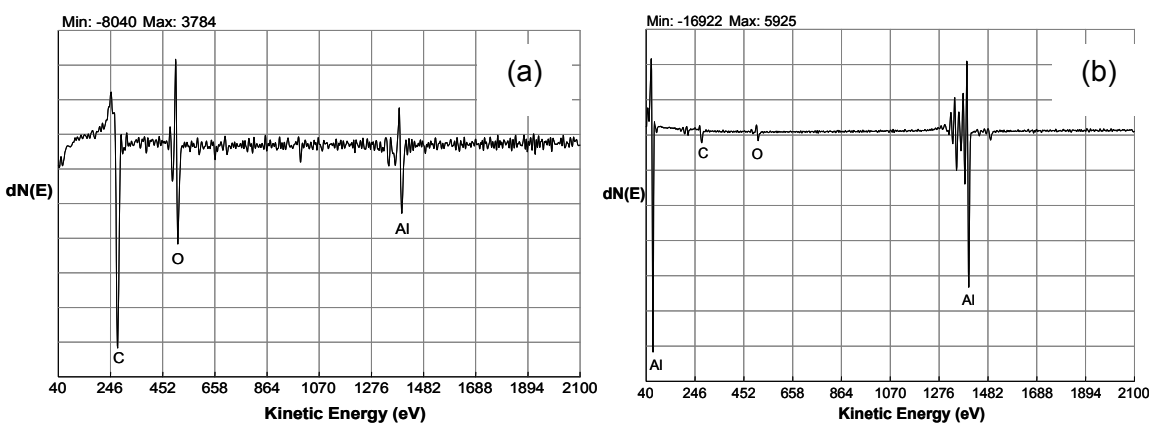

Figure 4-19. AES Spectrum of the Al-coated Steel (a) before and (b) after Eight Minutes Sputter Etching

However, after an eight minute (min) sputter etching treatment, a significant reduction in the peak intensities of carbon and oxygen was observed [Figure 4-19 (b)]. The symmetrical shape

of the Al peak between 1,276 and 1,482 eV in Figure 4-19 (a) is indicative of an oxide species, while the asymmetrical peak in the Auger spectrum in Figure 4-19 (b) is typical for elemental Al.

Figure 4-20 illustrates the compositional depth profile of the detected elements in the coatings, indicating that the concentration of Al increases with depth from the surface. The carbon and oxygen concentrations in the non-optimized, TIBAL derived Al coatings after 15 min sputter etching were found to be 3.0 and 2.0 at.%, respectively, and the Al concentration constitutes the balance (~95 at.%). The inhomogeneous and rough surface topography of the Al coatings caused difficulty in removing surface contaminants during sputter etching and profiling, so it might be assumed that the carbon present in the coatings - even after sputter etching - appears to be due to carbon contamination, and not a function of the coating process. Furthermore, it has been reported that TIBAL pyrolysis on Al (100) at a temperature below 327°C resulted in carbon-free Al deposition[23]. Considering the APCVD Al deposition temperature used (300°C) it was assumed that the carbon detected in the Al mostly originated from carbon contamination, not from the reaction of TIBAL pyrolysis during deposition.

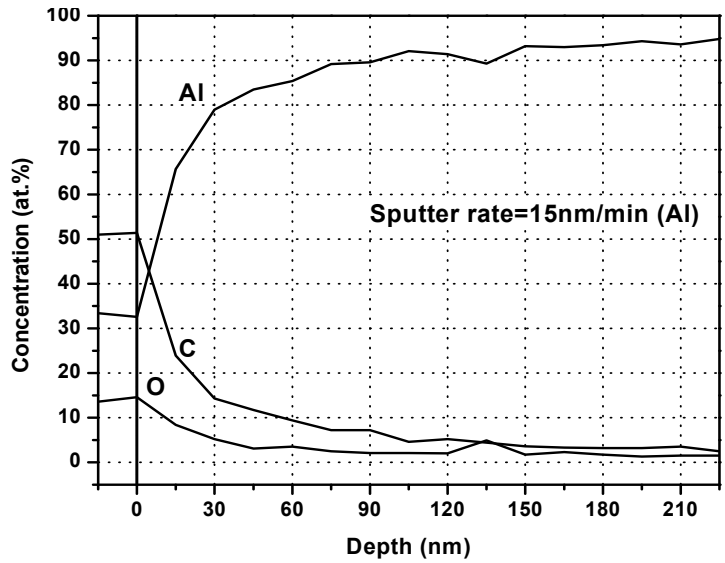

Figure 4-20. AES Composition Depth Profile of APCVD Al Coating on Steel

The effect of deposition temperature and precursor was studied later using pure TIBAL and deposition temperatures of 275°C and 300°C, and PB1 deposited at 300°C. Figure 4-21 confirms that carbon and oxygen are present as impurities, and that the concentration of Al increases with depth from the surface.

The atomic concentration of carbon and oxygen detected in depth was found to be 1.8 and 5.6 at.%, respectively in the Al coating (pure TIBAL, 275°C); 0.7 and 2.2 at.% (pure TIBAL, 300°C); and 0.2 and 11.0 at.% (PB1, 300°C: *note* the different depth scale). Consequently, the Al concentration for each deposition condition is the balance (92.6, 97.1, and 88.8 at.%). It must be pointed out that, due to the inhomogeneous and rough surface of the Al coatings, Ar etching used for depth profiling was not able to completely remove the coatings (evenly) layer by layer. For this reason, it was assumed that the oxygen detected in the deep region (bulk) could be attributed mostly to a native aluminum oxide that was present on the coating surface.

[23] B.E. Bent, R.G. Nuzzo, and L. H. Dubois, "*Surface Organometallic Chemistry in the Chemical Vapor Deposition of Aluminum Films Using Triisobutylaluminum: β-Alkyl Elimination Reactions of Surface Alkyl Intermediates*", J. Am. Chem. Soc. **111**, 1634 (1989).

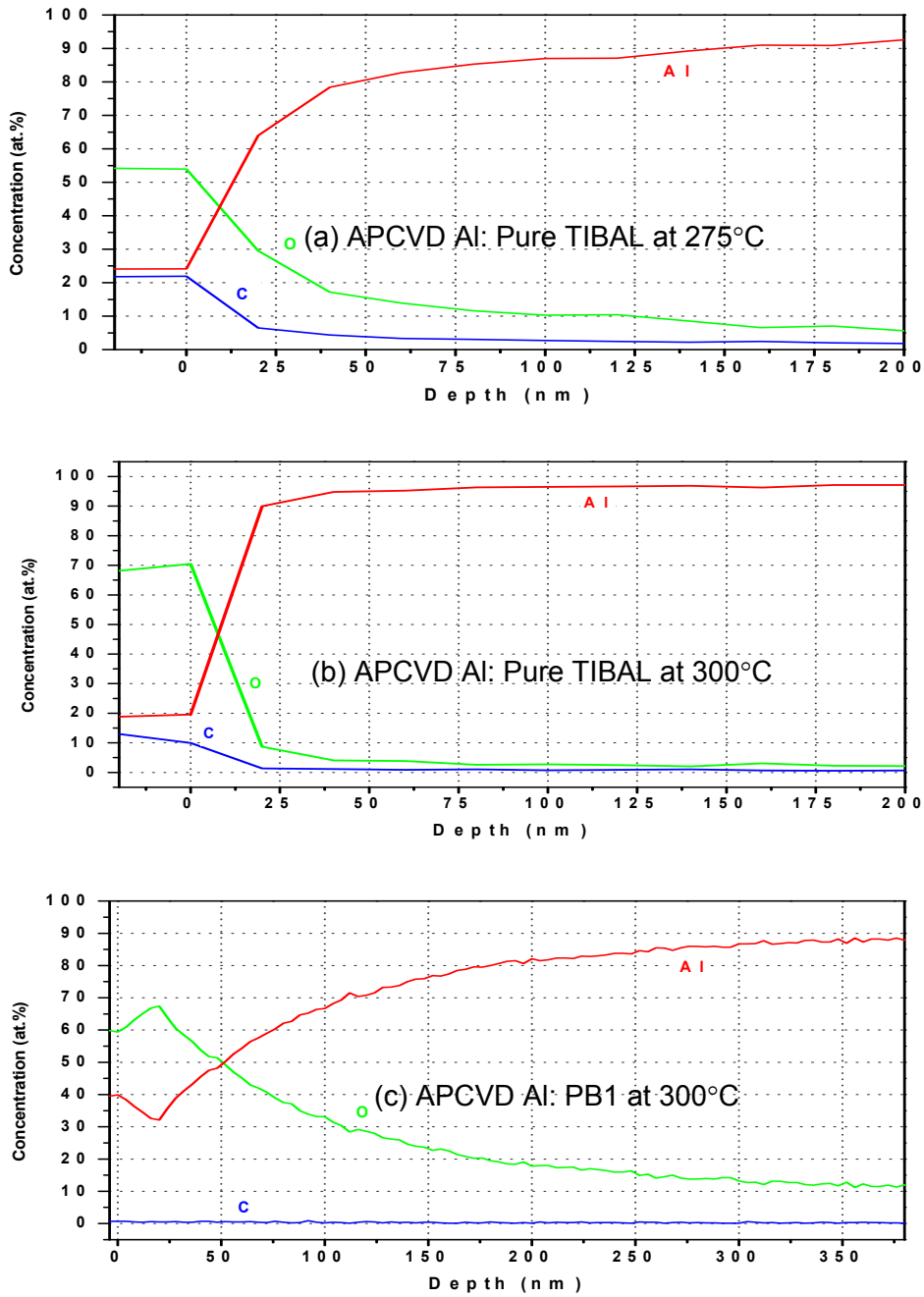

Figure 4-21. AES Depth Profiles of APCVD Aluminum Coatings Produced with Different Deposition Conditions

The depth profile of the carbon impurity for each deposition condition is shown in Figure 4-22. The Al coatings prepared with pure TIBAL exhibit a decrease in carbon concentration with an increase in deposition temperature from 275°C to 300°C. In addition, the carbon concentration in the Al coating with PB1 was found to be lower than that in the coating with pure TIBAL. Both of the coatings deposited at 300°C using pure TIBAL and PB1 showed a significantly lower

carbon concentration (<1.0 at.%).

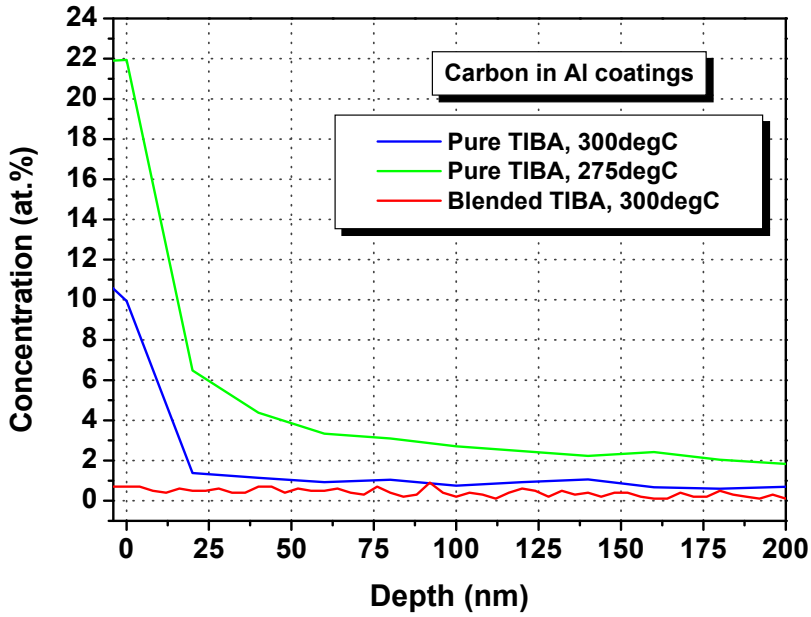

Figure 4-22. AES Depth Profile of Carbon Impurity Present in the Al Coatings Produced with Different Deposition Conditions

The depth profile for oxygen in each deposition condition is shown in Figure 4-23 with the same depth scale for each coating. The effect of the PB1 precursor on increasing the coating oxygen content for a fixed temperature (300°C) is more apparent in this chart.

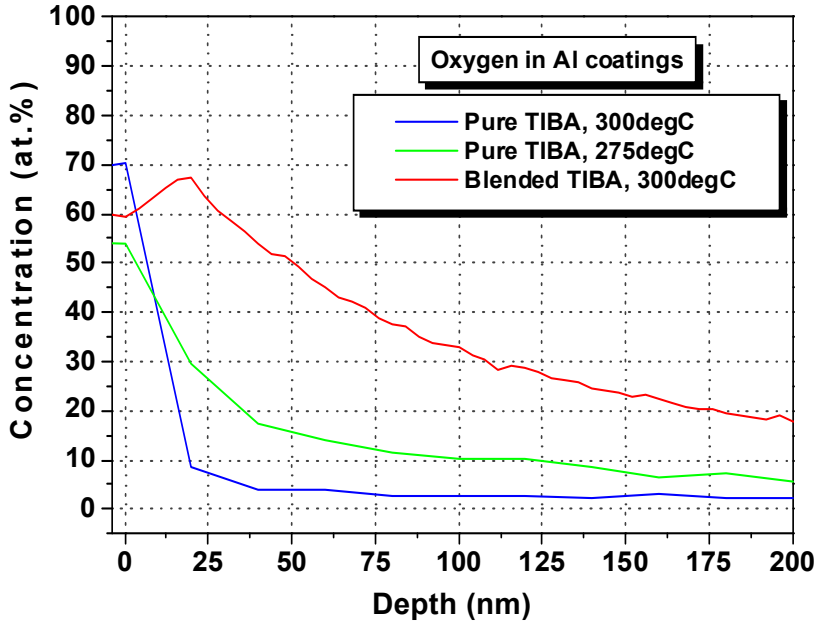

Figure 4-23. AES Depth Profile of Oxygen Impurity Present in the Al Coatings Produced with Different Deposition Conditions

4.1.5.3 Nuclear Reaction Analysis

The hydrogen incorporation in the Al coatings on steel rivets and coupons was evaluated by NRA with ^{15}N ion beam energies of 7.0, 7.2, and 7.4 MeV for probing different depths. The results are summarized below in Table 4-9, where the hydrogen concentrations (with units of ratio and atomic %) from 0.57 to 0.95 μm depth are averaged and shown in red. The average hydrogen concentrations for all measurements in the bulk region are shown in blue.

Table 4-9. Summary of NRA Analysis of Hydrogen in APCVD Aluminum Coatings

Depth(μm)	Pure TIBAL (275°C)		Pure TIBAL (300°C)		PB1 TIBAL Blend (300°C)	
	H/Al ratio	H/Al (at.%)	H/Al ratio	H/Al (at.%)	H/Al ratio	H/Al (at.%)
0.38	0.0111	1.11	0.0154	1.54	0.0064	0.64
0.57	0.0088	0.88	0.0130	1.30	0.0054	0.54
0.76	0.0071	0.71	0.0090	0.90	0.0068	0.68
0.95	**0.0044**	**0.44**	**0.0060**	**0.60**	**0.0054**	**0.54**
0.38*	0.0088	0.88	0.0093	0.93	0.0065	0.65
AVERAGE	**0.0068**	**0.68**	**0.0093**	**0.93**	**0.0059**	**0.59**

* A significant drop was measured from the beginning of the first run at 7 MeV (Row 1) and end of the final run at 7 MeV. This effect was smaller (or absent) on the larger planar samples, such as the coating deposited on steel coupons at 300°C using the PB1 blend, which indicates that that there is an unstable component of the hydrogen in the Al coatings deposited on the rivet substrates at 275°C and 300°C using pure TIBAL.

The average atomic ratio of hydrogen to aluminum was found to be lower for coatings deposited at the lower temperature, and for the blend compared to the pure precursor at the same deposition temperature. The average concentration followed the same trend. Figure 4-24 shows – in graphical form - the concentrations of hydrogen incorporated in the Al coatings on hollow steel rivets versus the coating depth.

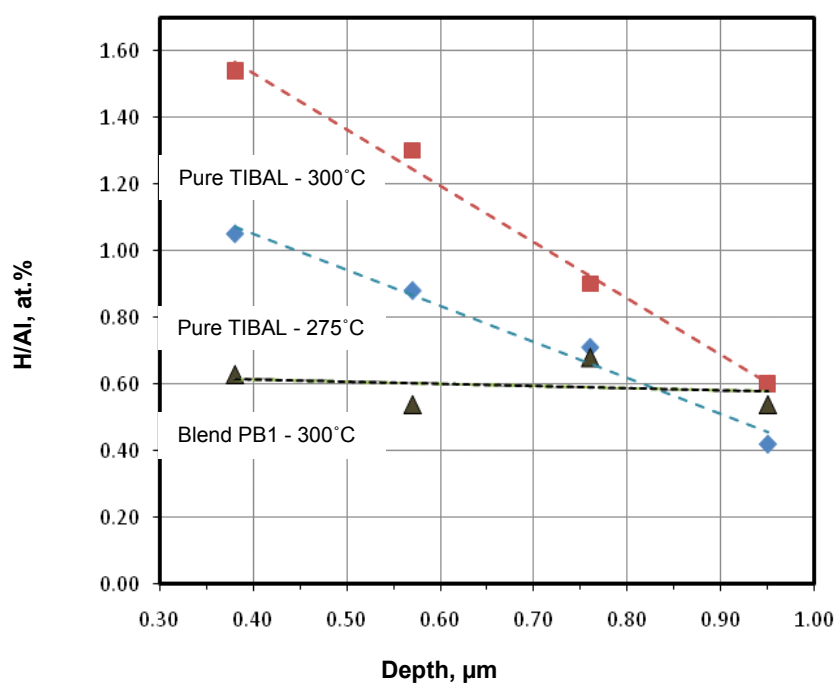

Figure 4-24. NRA Depth Profile of Hydrogen Present in the Aluminum Coatings

4.1.5.4 X-ray Photoelectron Spectroscopy

In order to evaluate the composition of the Al coatings, XPS analysis was conducted on two TIBAL derived, Al-coated steel coupons. Figure 4-25 represents a typical XPS survey spectrum showing all peaks for oxygen, carbon, and aluminum consistent with the AES analysis. The XPS spectra of Al 1p, O 1s, and C 1s are plotted as a function of argon sputter/etching level in Figure 4-25 without correction for binding energy shift due to surface charging[24].

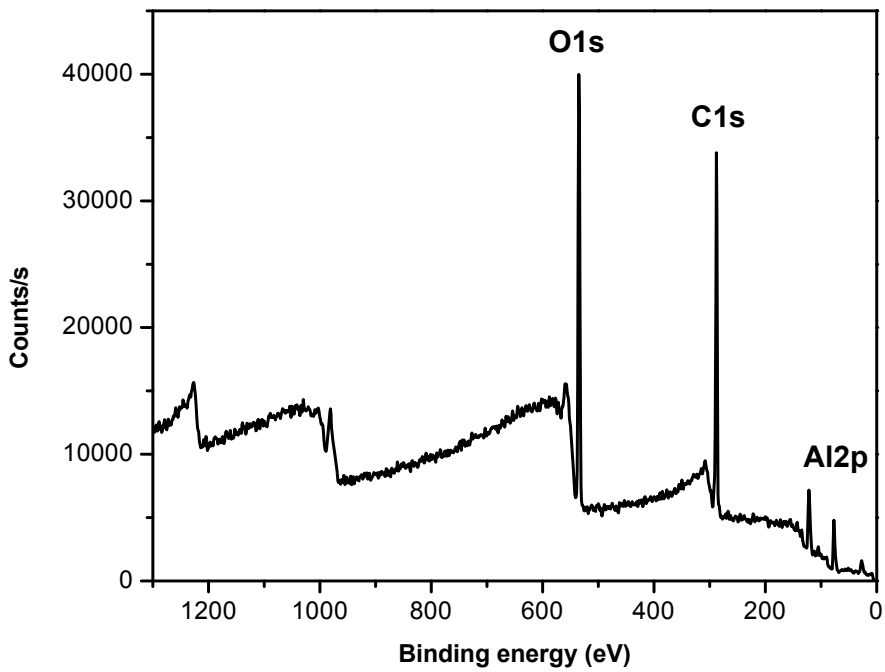

Figure 4-25. XPS Spectrum of the APCVD Al Surface Showing Aluminum, Oxygen, and Carbon Peaks Present in the Coatings

The convention for determining chemical composition in XPS data analysis is to reference the measured peak energy to the energy of the C 1s line for elemental carbon, typically having a binding energy of 285 eV. The peak of C 1s for the Al coating surface was seen at 287.4 eV [Figure 4-26, bottom]. Therefore, this was used to compensate for peak shifts due to the surface charging, which caused all peaks to shift up in binding energy by approximately 2.4 eV. This binding energy shift also is seen in the Al 2p line [Figure 4-26, top]. The reference XPS data base from NIST gives a range of binding energies for Al_2O_3 from 74.2 - 74.9 eV. The average of these values (~74.5 eV) was used for charge adjustments in the Al coatings, as long as there was enough oxygen to ensure that an oxide existed.

As the sputter etching time increased, the appearance of Al 2p peak representative of elemental Al was clearly seen [Figure 4-26, top], indicating that the coatings were mostly pure Al in the bulk region. The peaks for carbon and oxygen, in contrast, decreased with etching time (depth).

[24] The surface of the Al coatings was charged slightly because of the protective oxide film naturally formed on the APCVD Al coatings.

Note that the maximum etching level represents a final depth into the coating of approximately 120 nm.

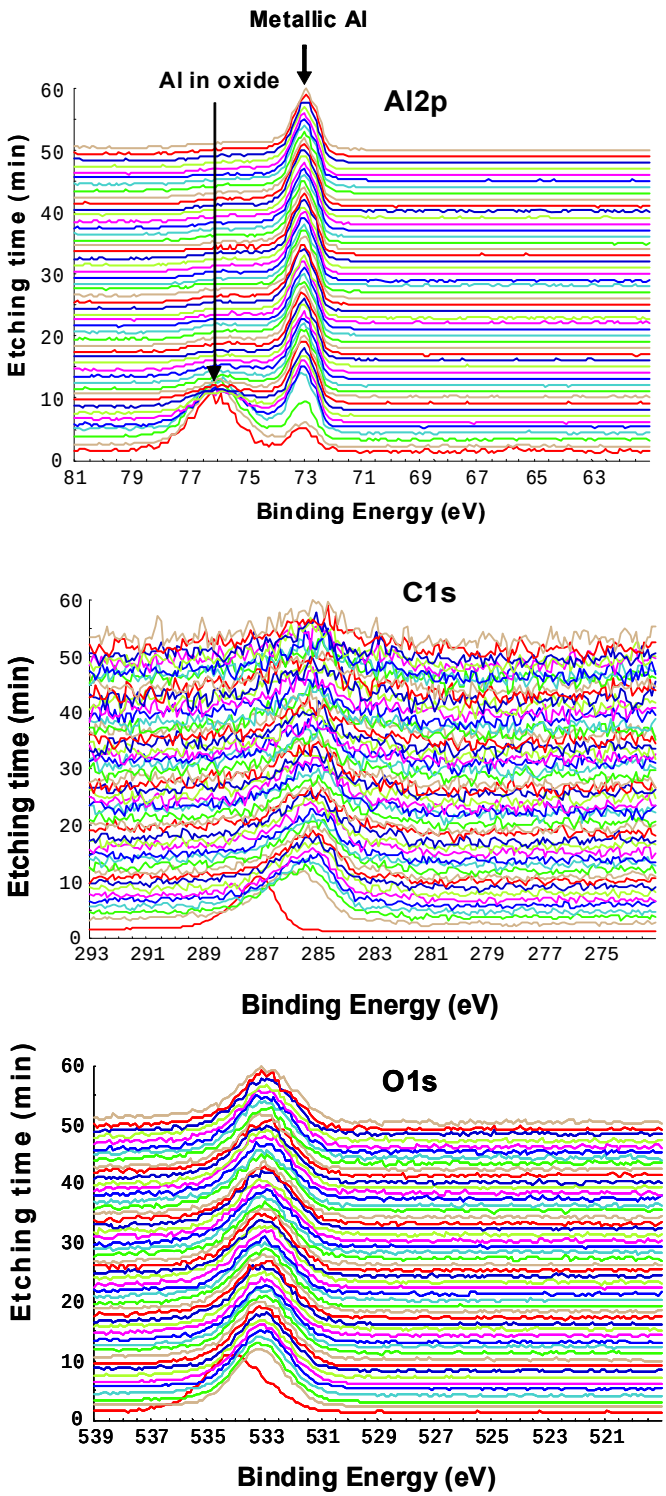

Figure 4-26. XPS Al 2p, O 1s, and C 1s Spectra as a Function of Sputter Time for the APCVD Al Coatings

4.1.5.5 Glow Discharge Optical Emission Spectroscopy

The GD-OES analysis revealed that the APCVD Al coatings deposited at 275°C and 300°C had an Al content of 99.25 and 98.70 wt.%, respectively (Figure 4-27). These data also showed a minor presence of nitrogen (N) and oxygen (O) contamination within the bulk region of coatings (Figure 4-27, *note* the difference in scale for carbon and nitrogen). No presence of carbon was observed for both deposition temperature conditions.

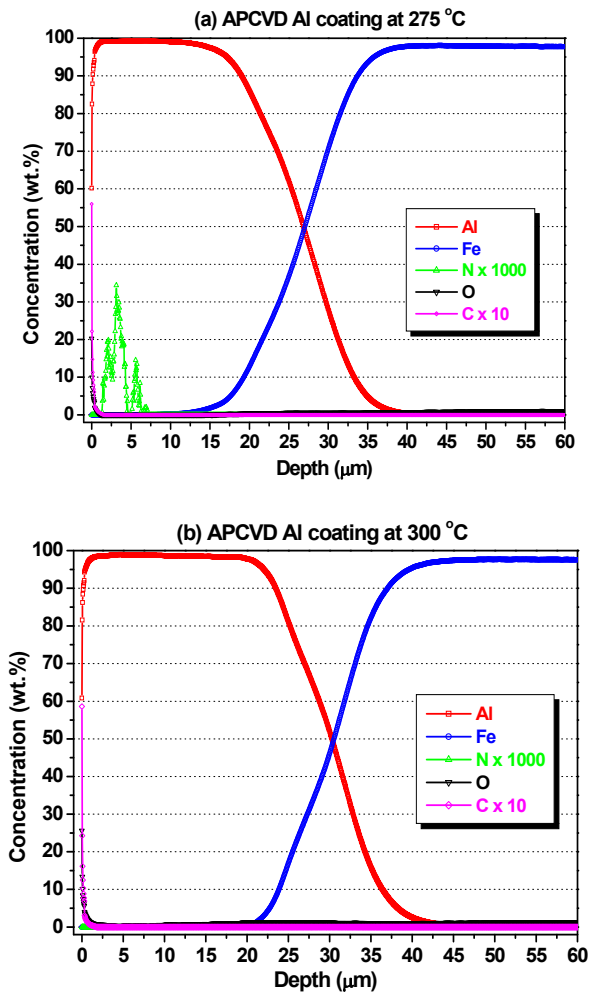

Figure 4-27. GD-OES Depth Profiles of APCVD Al Coatings Deposited at (a) 275°C and (b) 300°C Using Precursor PB1

4.1.5.6 Electron Probe Microanalysis

To obtain information on bulk concentration of components present in the Al coatings, EPMA was used with a sampling depth of ~3 μm, which is at least 10 times greater than that in AES depth profile. The average concentrations of carbon and oxygen detected were 6.79 ±1.07 and 1.62 ±0.29 at. %, respectively, and Al comprised the balance.

4.1.6 Electrochemical and Corrosion Properties

4.1.6.1 Open Circuit (Galvanic) Potential and Polarization Behavior

The open circuit (corrosion) potentials (E_{corr}) of APCVD and IVD Al coatings in a 3.5% salt (NaCl) solution stayed well below that of uncoated AISI 4130 steel, as shown in Figure 4-28. The corrosion potentials of both an APCVD Al and IVD Al coating were similar and leveled off after about three days. They remained about 200mV more negative than that of an AISI 4130 steel substrate even after 10 days. No red rust, due to corrosion of the steel substrate, was observed during the immersion time. The values for the Al foil reference material were more erratic.

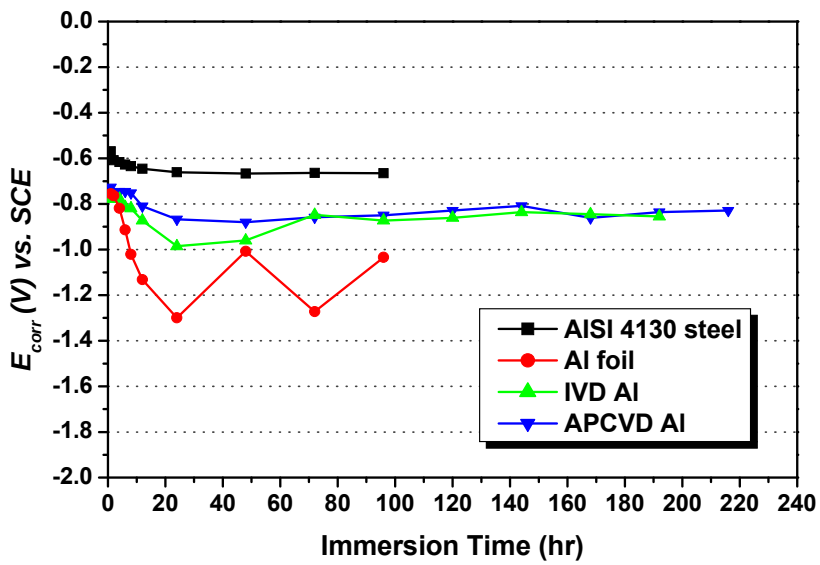

Figure 4-28. Corrosion Potentials of APCVD and IVD Al Coatings on AISI 4130 Steel as a Function of Immersion Time

SEM analysis after the EIS measurements discussed earlier (Section 4.1.4.2) showed localized exposure of the steel substrate resulting from active dissolution of Al coating due to sacrificial protection (Figure 4-29). This corroborates the observation that no red rust was seen after relatively brief exposures to salt solution.

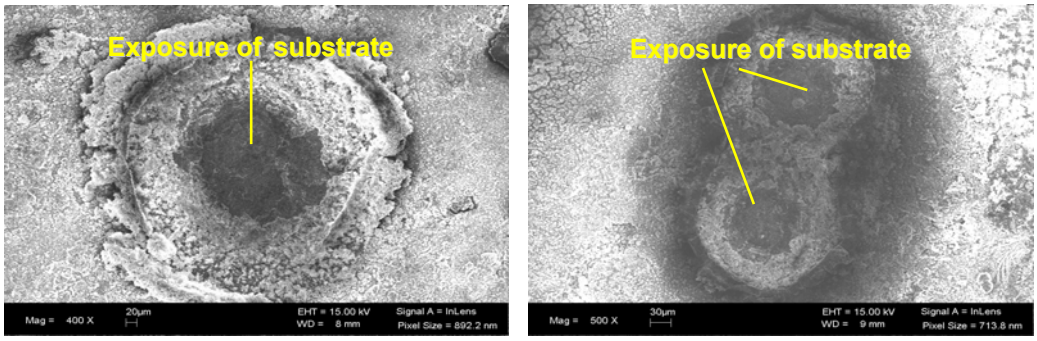

Figure 4-29. Photomicrographs of APCVD Al Coatings Demonstrating Sacrificial Protection of the Steel Substrates

The open circuit potentials obtained later for three bare and APCVD Al-coated notched bar specimens made from AISI 4340 steel are shown in Figure 4-30. The duration of this test was only 12 hours, compared to the 10 days for the tests on coated AISI 4130 steel panels, reported in Section 4.1.4.2. However, the changes for the bare and coated steel specimens were similar during the 12 hour exposure in a 3.5% salt solution, as can be seen by comparing Figure 4-28 with Figure 4-30.

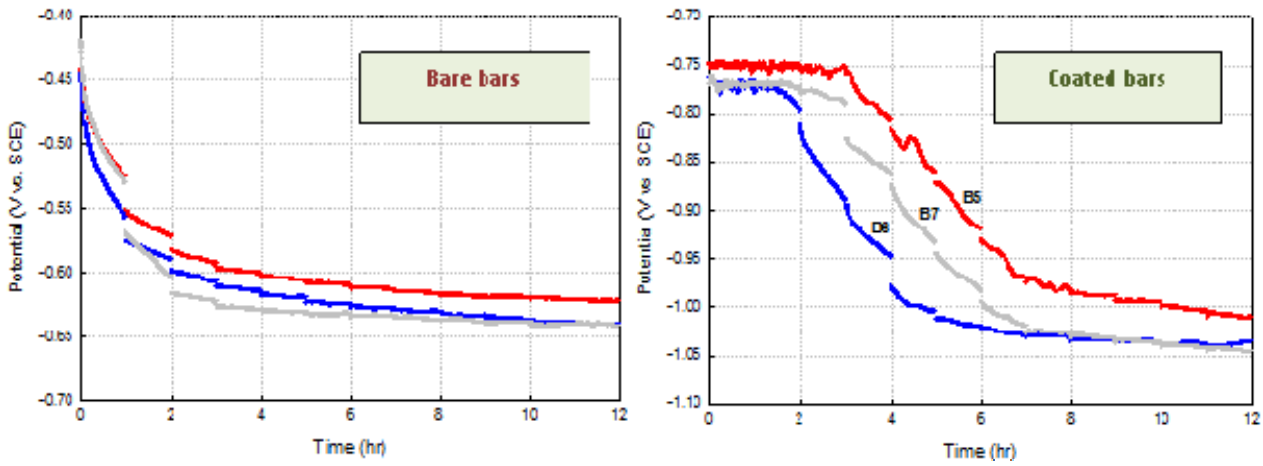

Figure 4-30. Corrosion Potentials of APCVD Al Coatings on AISI 4340 Steel as a Function of Immersion Time

The impedance spectra of the three bare steel bar specimens are shown in Figure 4-31. The polarization resistances decreased with increasing immersion time from 296.6 to 185.8 Ω and the value of P - an exponent in constant phase element (CPE) of the equivalent circuit (EC) model (ZView™, Scriber Associate, Inc.) shown in Figure 4-33 - decreased from 0.82 to 0.71. Figure 4-32 presents the Nyquist and Bode Plot values predicted by the model compared with the measured values for Specimen B3 in the 3.5 wt% NaCl solution after a three hour immersion time.

The bare steel bar exhibited behavior similar to a Randle's circuit, which has a solution resistance, a double layer capacitance, and a charge transfer (or polarization) resistance. The Nyquist plots in Figures 4-31 and 4-32 show a depressed semicircle. The CPE in the model is given by:

$$Z_{CPE} = 1/[T\cdot(j\omega)^P]$$

where T is an amplitude [$\Omega^{-1}\cdot s^{1-P}$]; j is the current; ω is the frequency; and P is an exponent that varies from -1 to 1. With P=0 and T=1/R, the CPE models a *resistor*. With P=1 and T=C, the CPE models an ideal *capacitor*. With P=-1 and T=1/L, the CPE models an ideal *inductor*. With P=1/2 and T=1/($2^{1/2}$W), the CPE models the infinite *Warburg element*. All four of the above elements have different phase angles of: 0° (resistor), -90° (capacitor), $+90^o$ (inductor), and -45° (Warburg impedance). In Figure 4-33, the value of P is 0.79, which indicates that this CPE behaved like a capacitor. The corresponding Bode plot shows that solution resistance was 1.84 Ω at the high frequency, and the polarization resistance was 232.6 Ω at the low frequency listed in Figure 4-32.

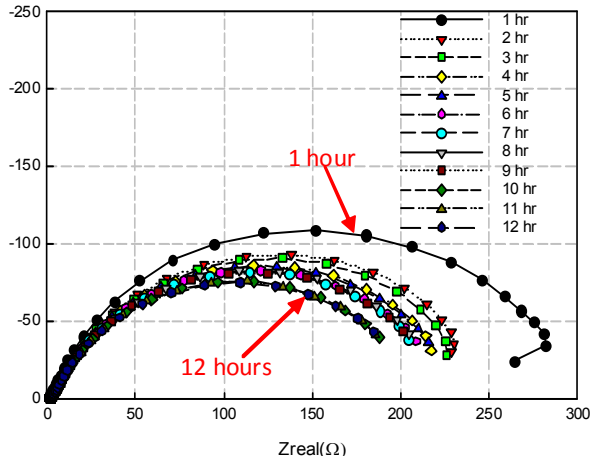

(a) Bare steel bar (B1)

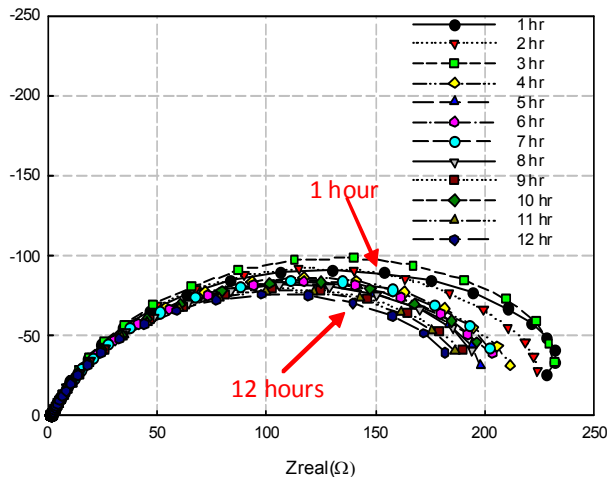

(b) Bare steel bar (B2)

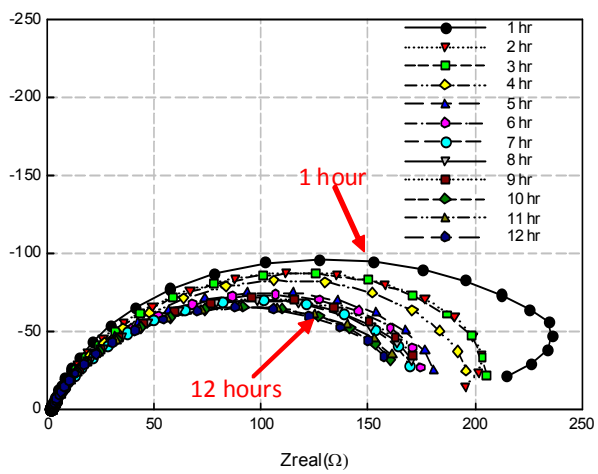

(c) Bare steel bar (B3)

Figure 4-31. Nyquist Plots for Bare AISI 4340 Steel Bars in 3.5 wt% NaCl Solution During 12 Hours Immersion

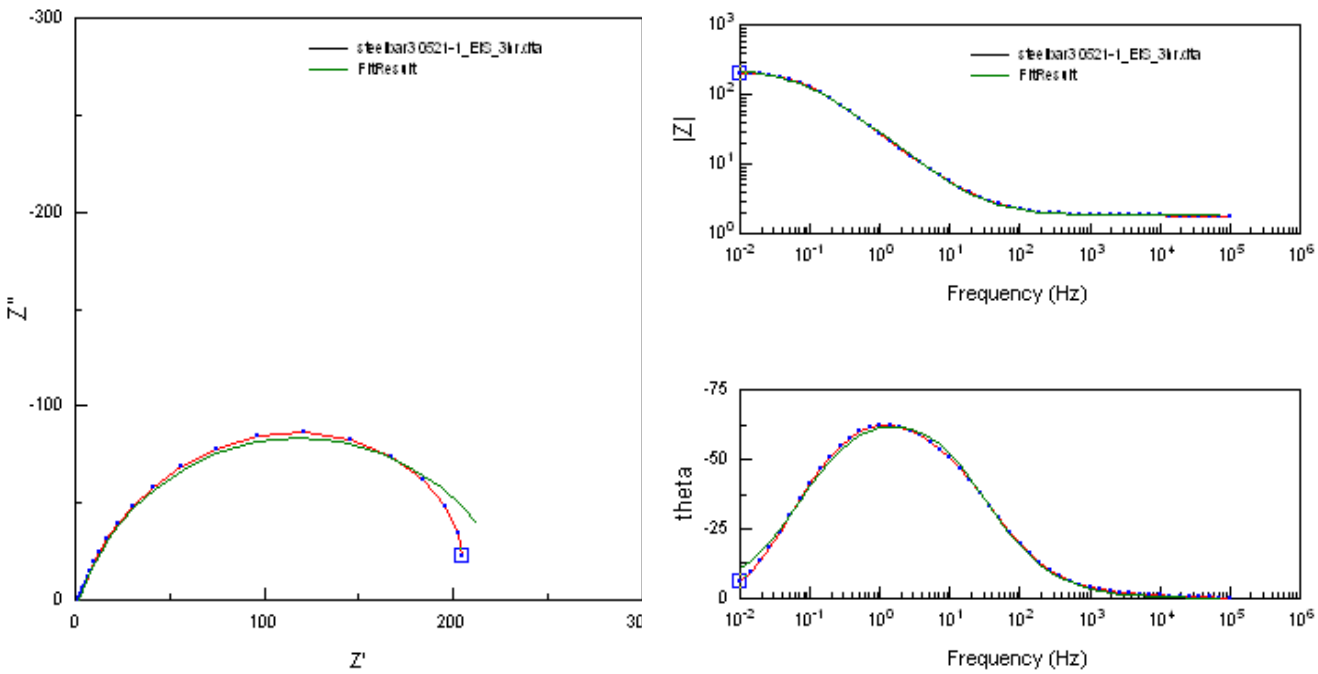

Nyquist plot, left and Bode plot, right
[Note: the green line indicates the fitting data and red/dots the real data]

Figure 4-32. Predicted and Actual Impedance Data for Bare AISI 4340 Steel Bars in 3.5 wt% NaCl Solution During 12 Hours Immersion

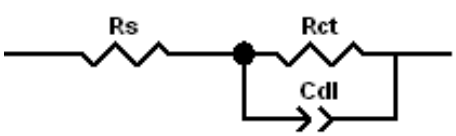

Element	Freedom	Value	Error	Error%
Rs	Free(+)	1.84	0.0082179	0.44663
Rct	Free(+)	232.6	2.3403	1.0061
Cdl-T	Free(+)	0.0080733	6.173E-5	0.76462
Cdl-P	Free(+)	0.79165	0.0022921	0.28953

Figure 4-33. Equivalent Circuit Model and Element Values for Bare AISI 4340 Steel Bars in 3.5 wt% NaCl Solution During 12 Hours Immersion

Figures 4-34 and 4-35 show the impedance spectra of the APCVD Al-coated coated steel bar (B7) in 3.5 wt% NaCl solution immersed for 12 hours, while Figure 4-36 shows the equivalent circuit model and component values. In this EC model, the Warburg impedance was added to represent the diffusion processes at the metal surface-solution interface. In Figure 4-36, the value of P is 0.62, which indicates that this coated steel bar exhibited less capacitance like behavior than the bare steel bar. The Bode plot in Figure 4-35 reveals that the solution resistance was 4.94 Ω at the high frequency, and the coating polarization resistance was

347.2 Ω at the intermediate frequency. The Warburg impedance was 501.8 Ω.

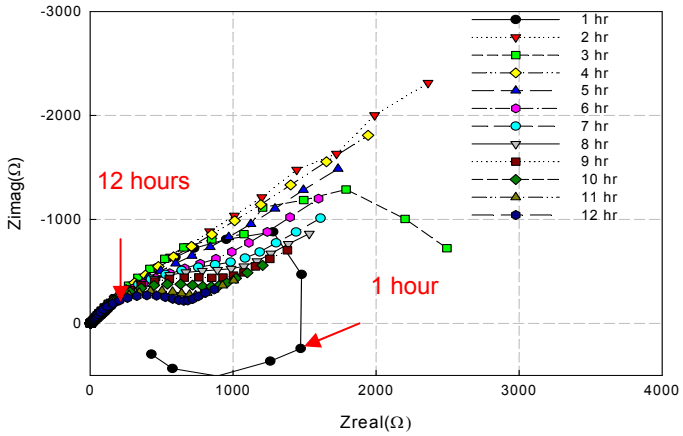

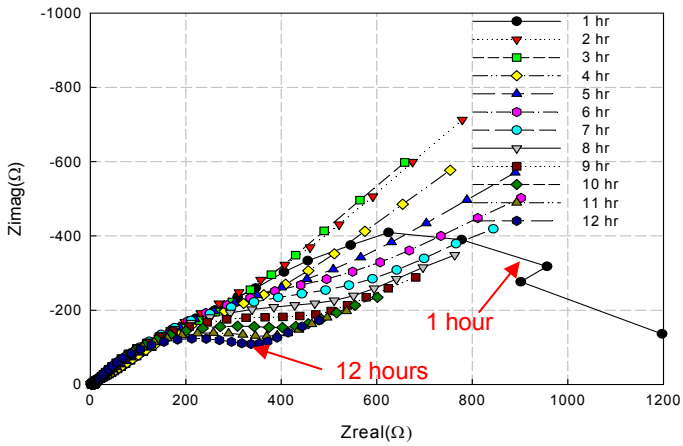

(b) APCVD Al-coated steel bar (B6)

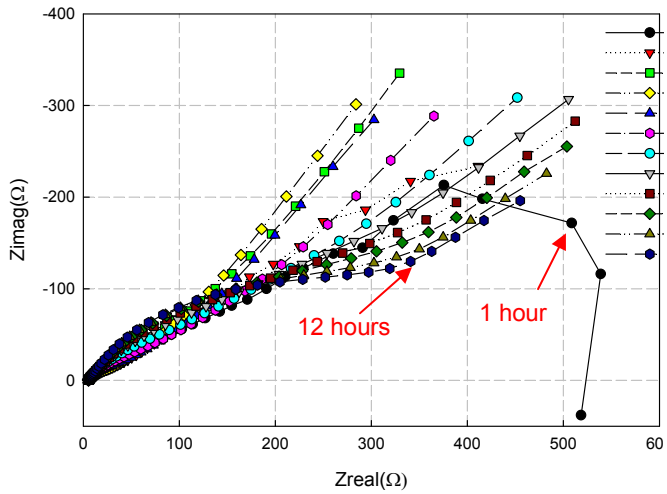

(c) APCVD Al-coated steel bar (B7)

Figure 4-34. Nyquist Plots for APCVD Al-Coated Steel Bars in 3.5 wt% NaCl Solution During 12 Hours Immersion

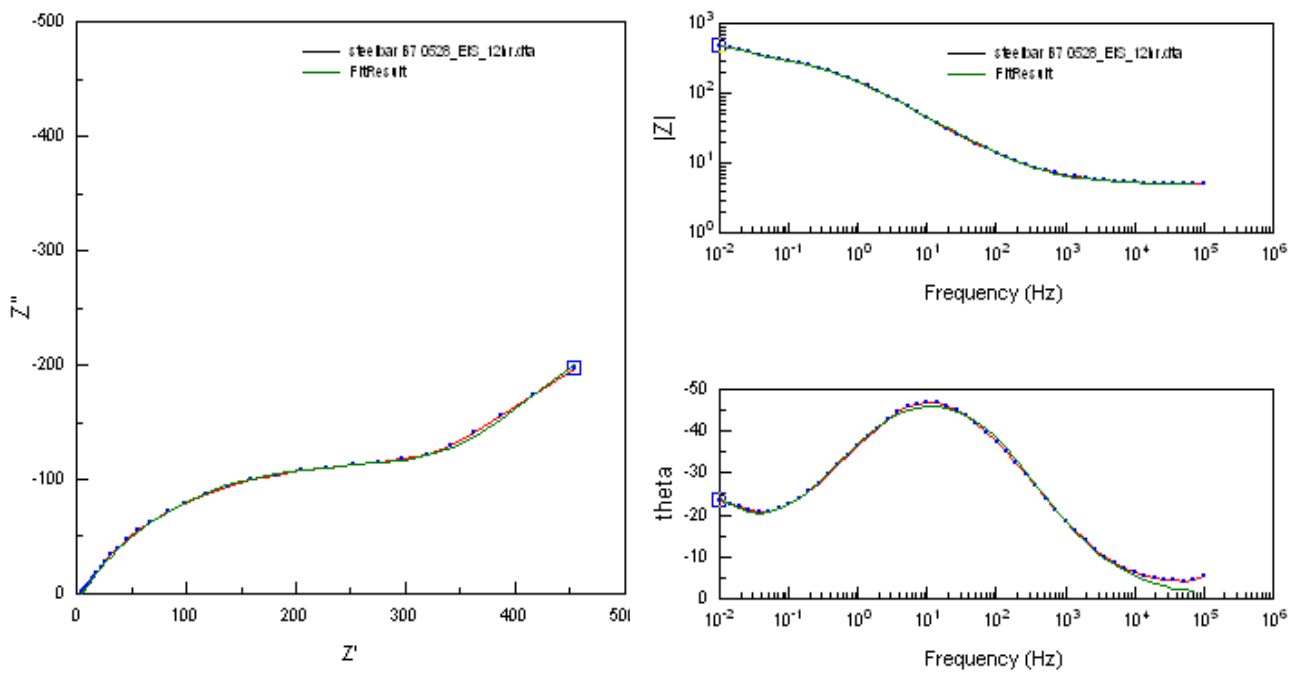

Nyquist plot, left and Bode plot, right
[Note: the green line indicates the fitting data and red/dots the real data]

Figure 4-35. Predicted and Actual Impedance Data for APCVD Al-Coated AISI 4340 Steel Bars in 3.5 wt% NaCl Solution During 12 Hours Immersion

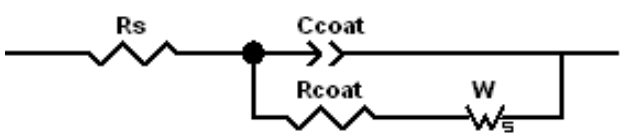

Element	Freedom	Value	Error	Error%
Rs	± Free(?	4.942	0.019131	0.38711
Ccoat-T	± Free(?	0.0016088	1.8084E-5	1.1241
Ccoat-P	± Free(?	0.62845	0.002013	0.32031
Rcoat	± Free(?	347.2	6.8928	1.9853
W-R	+ Free(+)	501.8	50.052	9.9745
W-T	± Free(?	71.92	12.787	17.779
W-P	± Free(?	0.50842	0.016223	3.1909

Figure 4-36. Equivalent Circuit Model and Element Values for APCVD Al-Coated AISI 4340 Steel Bars in 3.5 wt% NaCl Solution During 12 Hours Immersion

The values of P (ranging from 0.429 to 0.676) were smaller than those for bare steel bars, and close to the value of the Warburg impedance. The polarization resistances of the APCVD Al-coated specimens were higher than the polarization resistances observed for the bare steel

bars. In addition, the APCVD Al-coated steel bars exhibited inductive behavior up to three hours immersion time. After the inductance behavior, the diffusion behavior was observed, and continued to increase over time. The initial inductive behavior is reflected by the positive values for its real and imaginary components in the Nyquist plot, and indicated the participation of adsorbed species on the specimens, primarily the formation of an amorphous aluminum hydroxide film ($Al(OH)_3$).

The increase in the diffusion behavior of this aluminum hydroxide film is observed approximately four hours after immersion (Figure 4-34), and is accompanied by a simultaneous decrease in the polarization resistance, as can be seen in Figure 4-37, where the values of the polarization resistance for each bar were averaged from three replications (with standard deviation).

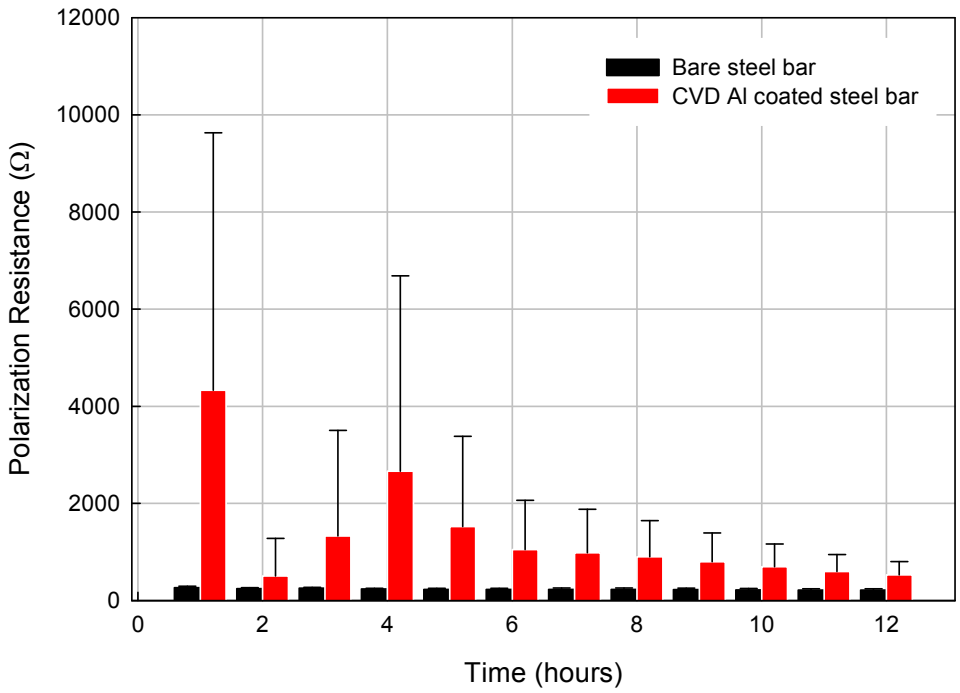

Figure 4-37.Polarization Resistance of Bare and APCVD Al-Coated Bars as a Function of Immersion Time in a 3.5% Salt Solution

Because the $Al(OH)_3$ film is porous and anodic to the underlying cathodic steel substrate, the establishment of a galvanic couple at the bare steel/APCVD Al coating interface will result in the generation and absorption of hydrogen into the steel, and subsequent embrittlement can occur, as will be shown and discussed later in Section 4.1.7.

Finally, Figure 4-38 is a photographic record of the condition of the test bars after 12 hours immersion in the 3.5% NaCl test solution. These specimens were rinsed then air dried. As indicated in Figure 3-10, only the lower portions of the specimens were immersed for the measurement, which explains why corrosion attack (red rust) was seen only on the bottom halves of the bare steel, notched round bars. In contrast, and as expected, the APCVD Al coatings exhibited no signs of red rust after this relatively short exposure time.

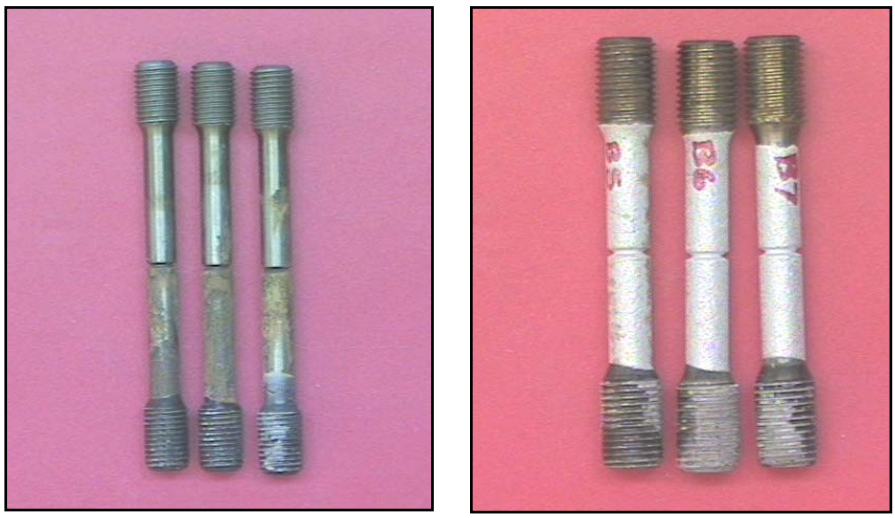

(a) Bare AISI 4340 Steel (b) APCVD Al-Coated Steel

Figure 4-38. Visual Appearance of EIS Specimens after 12 Hours Exposure to Salt Solution

4.1.6.2 Salt Fog Exposure Corrosion Resistance

In some tests conducted during in this project, salt fog corrosion resistance and the effect of a TCP treatment were evaluated on AISI 4130 steel coupons, coated with APCVD Al using pure TIBAL at 300°C. The specification calls for no visible attack after 96 hours. The corrosion resistance of painted, APCVD Al-coated coupons also was investigated. Figure 4-39 shows the results from the ASTM B 117 salt fog exposure testing with APCVD Al coatings on scribed and unscribed steel panels after 24 hours exposure.

(Specimens on left received a commercial Cr(III) post-treatment)

Figure 4-39. APCVD Al Coatings on Steel Panels after 24 hr Salt Fog Exposure

The results after 96 hours exposure are shown in Figure 4-40. Considerable general corrosion attack occurred on the specimens not receiving the TCP post-treatment, but the coatings appeared to be providing galvanic protection to the steel substrate material. At these relatively short exposure times, the benefit of applying additional corrosion protection (i.e., TCP) is obvious from these photographs.

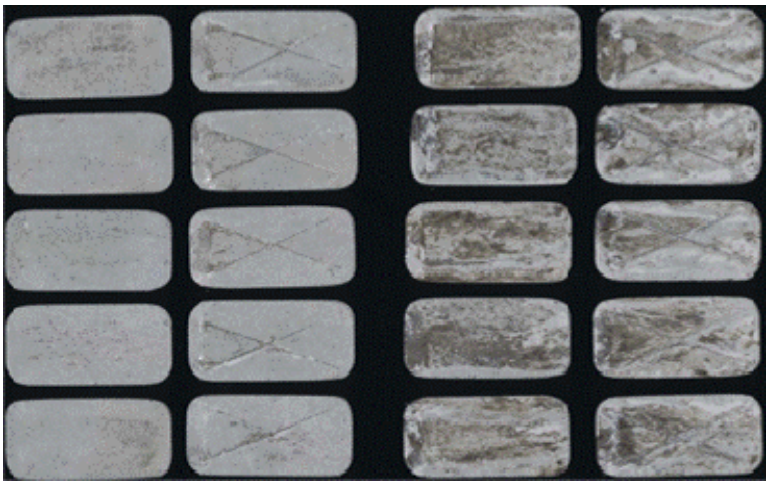

(Specimens on left received a commercial Cr(III) post-treatment)

Figure 4-40. APCVD Al Coatings on Steel Panels after 96 hr Salt Fog Exposure

In a separate experiment, four APCVD Al-coated coupons were used for *bare corrosion testing*: one as deposited; one as deposited and scribed; one as deposited and post treated with TCP - (five minute immersion with 50 % dilution); and one as deposited with TCP and scribed. These coupons were then subjected to ASTM B 117 Salt Fog testing. Figure 4-41 illustrates the APCVD Al-coated coupons 17 days after exposure in the salt fog cabinet, and shows the formation of a white corrosion product with no red rust. The white corrosion product was caused by corrosion of the Al coatings. Red rust from the substrate was observed only after a 27 day-exposure, at which time the test was discontinued.

As deposited | Scribed as deposited | With TCP | Scribed with TCP

Figure 4-41. APCVD Al-coated Coupons after 17 Days in ASTM B 117 Salt Fog Test

These results indicated that the APCVD Al coating could meet the minimum requirement in the specification for Cd coatings (and any alternatives). Post treatment with TCP did not improve the corrosion resistance of the APCVD Al-coated coupons in this test, indicating that it had no beneficial effect. For painted corrosion testing, two APCVD Al-coated coupons were painted with a MIL-PRF-23377C primer and a MIL-PRF-85285 topcoat. A two-week cure time was allowed for the paint prior to initiating the ASTM B 117 salt fog testing. Figure 4-42 illustrates the condition of the painted, APCVD Al-coated coupons 17 days of salt fog exposure. Neither blistering of the paint nor red rust formation was observed during this time.

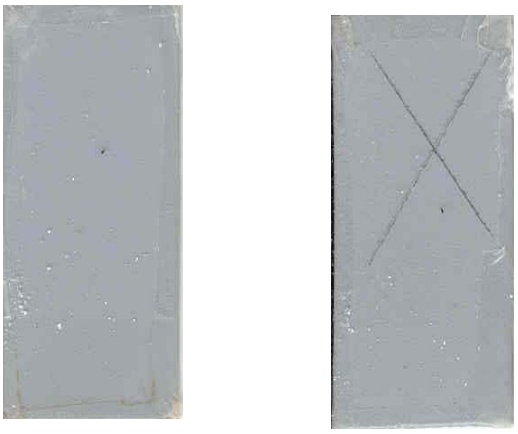

Unscribed Scribed

Figure 4-42. Painted APCVD Al-coated Coupons after 17 Days in ASTM B 117 Salt Fog Test

In addition to the painting corrosion testing, a paint adhesion test based on ASTM D 3359 Method A was performed on four APCVD Al-coated coupons after a two-week cure time for the paint. DI water was used for wet test coupons. Figure 4-43 illustrates APCVD Al-coated coupons with paint in painting adhesion testing. ASTM D 3359 calls for a rating system of 0 to 5, where 5 is the highest rating and 0 indicates a complete removal of the paint. The ratings for these coupons all were 5, indicating that the Al coatings provide excellent paint adhesion.

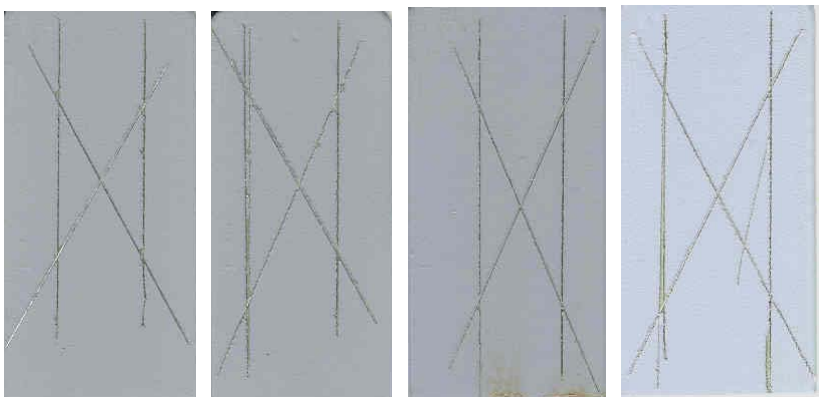

Dry 1day-wet, RT 4 day-wet, 120°F 7 day-wet, 150°F

Figure 4-43. Painted APCVD Al Coatings after Paint Adhesion Testing

4.1.6.3 Alternating Immersion Corrosion Resistance

Cyclic exposure (GM 9450P) testing was performed on unscribed and scribed APCVD Al-coated, mild steel coupons. The coupons were tested both with (Figure 4-44, top) and without a commercial TCP chemical conversion coating (Figure 4-44, bottom).

Figure 4-44. As Received APCVD Al-Coated Panels With and Without a Commercial Trivalent Chromium Treatment

The arbitrary acceptance criteria were 80 cycles with no visible red rust for unscribed specimens, and 40 cycles for scribed specimens.

The panels were removed after 2, 10, 20, 30, 50, 60, 110 and 165 cycles for scanning on a flat bed scanner to provide an electronic record of the appearance of each. In each scan, the top five panels had received the TCP treatment, while the bottom panels had no post-treatment. The test was halted after 165 cycles, well beyond the acceptance criterion value mentioned above.

After only two cycles the beneficial effect of the post-treatment could be seen (Figure 4-45). The APCVD Al-coated panels without the TCP treatment exhibited more corrosion and mottling on their surfaces. Similar mottling appeared on the post-treated panels after 10 cycles, as indicated in Figure 4-46.

Red rust (corrosion of the underlying steel) appeared visible on some of the scribed panels after 20 cycles, although the post-treated panels only showed red rust on one panel. However, this did not seem to progressively corrode much more until after 50-60 cycles of testing, as shown in Figure 4-47.

By 110 cycles all the scribed panels had significant substrate corrosion, but the unscribed panels did not show red rust until 165 cycles (Figure 4-48). At 165 cycles it is still apparent that the post-treatment is providing significant additional corrosion protection.

Figure 4-45. APCVD Al-Coated Panels after 2 Cycles in GM 9540P Test

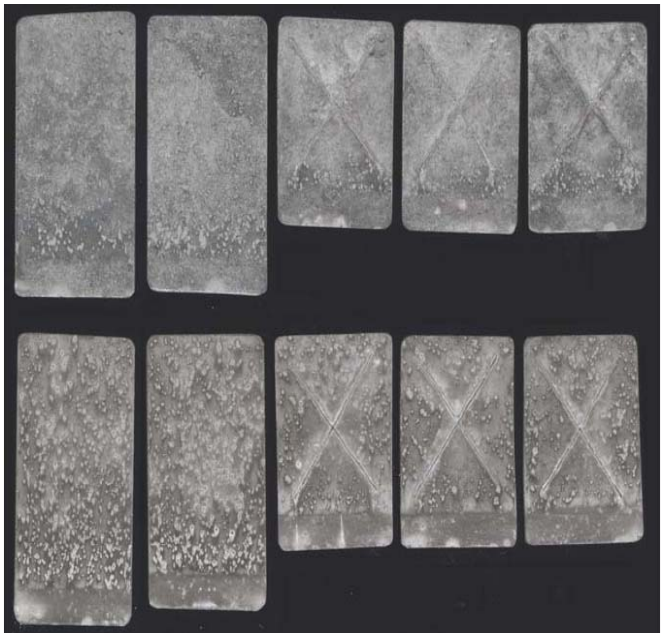

Figure 4-46. APCVD Al-Coated Panels after 10 Cycles in GM 9540P Test

Figure 4-47. APCVD Al-Coated Panels after 60 Cycles in GM 9540P Test

Figure 4-48. APCVD Al-Coated Panels after 165 Cycles in GM 9540P Test

4.1.6.4 Exposure to Aircraft Maintenance Fluids

The change in mass (ΔM, measured in gm**)** was almost negligible across all the TCP-treated samples with the exception of the samples exposed to the peroxide based paint remover, which

experienced a large growth in mass.

The samples immersed in sea water showed a net loss of mass, while all other samples experienced a net gain in mass. The gains in mass on the samples that were not TCP treated were either the same as the TCP treated samples (like those exposed to Turco 6813E) or higher than their TCP treated counterparts. The TCP post-treated samples exposed to reagent water experienced a gain in mass three times greater than the ones that were TCP treated. The samples exposed to sea water went from having no change in mass on those that were not TCP treated to a loss in mass on those that were TCP treated. The untreated samples that were exposed to the hydraulic fluid experienced twice the gain in mass than the TCP treated samples. All the results are documented in Table 4-10.

The ratings after exposure seen in Table 4-11 are given on a scale from 0 to 4, with 0 meaning no visible corrosion, going up to 4 where either pitting has occurred, or the sample experienced discoloration and/or corrosion over 25% of its surface area.

Table 4-10. Mass Changes for APCVD Al-Coated Specimens Exposed to Maintenance Fluids

Fluid	No Cr(III) Treatment				Average ΔM	With Cr(III) Treatment				Average ΔM
	Sample	M_{init}	M_{final}	ΔM		Sample	M_{init}	M_{final}	ΔM	
Reagent Water	1A 1B	8.11 8.09	8.13 8.10	0.02 0.01	0.015	6A 6B	8.19 8.20	8.19 8.21	0.00 0.01	0.005
Sea Water	2A 2B	8.16 8.05	8.16 8.05	0.00 0.00	0.000	7A 7B	7.97 8.09	7.96 8.09	- 0.01 0.00	- 0.005
Turco 6813	3A 3B	8.16 8.29	8.16 8.30	0.00 0.01	0.005	8A 8B	8.10 8.09	8.11 8.09	0.01 0.00	0.005
CEM 483	4A 4B	8.20 8.02	8.28 8.08	0.08 0.06	0.070	9A 9B	8.07 8.14	8.13 8.21	0.06 0.07	0.065
Hydraulic Fluid	5A 5B	8.08 8.07	8.09 8.08	0.01 0.01	0.010	10A 10B	8.16 8.09	8.17 8.09	0.01 0.00	0.005

Table 4-11. Corrosion Ratings of APCVD Al-Coated Specimens Exposed to Maintenance Fluids

Fluid	No Cr(III) Treatment			With Cr(III) Treatment*		
	Sample	Rating	Average	Sample	Rating	Average
Reagent Water	1A 1B	4 4	**4.0**	6A 6B	1 1	**1.0**
Sea Water	2A 2B	4 4	**4.0**	7A 7B	1 2	**1.5**
Turco 6813	3A 3B	3 3	**3.0**	8A 8B	1 1	**1.0**
CEM 483	4A 4B	4 4	**4.0**	9A 9B	4 4	**4.0**
Hydraulic Fluid	5A 5B	0 0	**0.0**	10A 10B	0 0	**0.0**

* Commercial TCP chemical conversion coating.

Figures 4-49 and 4-50 are photo-montages that record the visual appearance of each sample after desiccated storage. The top row of samples in each figure had received a TCP treatment, and the samples in the bottom row were APCVD Al-coated without any TCP treatment.

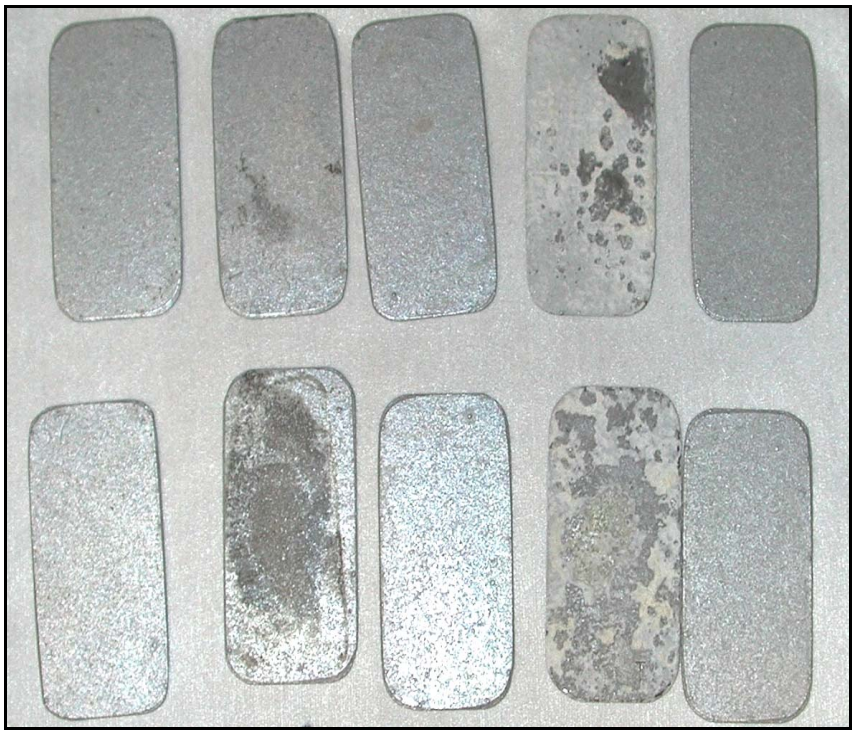

Figure 4-49. Appearance of Post-treated Samples after Immersion
(L to R: Reagent Water, Sea Water, Turco 6813E, CEM48, Hydraulic Fluid)

Figure 4-50. Appearance of Non-post-treated Samples after Immersion
(L to R: Reagent Water, Sea Water, Turco 6813E, CEM48, Hydraulic Fluid)

In general the TCP treated samples fared much better than the untreated samples with respect to visible corrosion. As can be seen in Figure 4-49, there was very little corrosion on the samples. There was slight discoloration on the samples exposed to reagent water and Turco 6813, while there was more widespread discoloration on the samples exposed to sea water.

The TCP treated and untreated samples exposed to the peroxide-based CEM483 came out with a thick layer of crystals, as shown in Figure 4-51. After rinsing and cleaning, there was still a thick white layer on much of the panel, and the areas not coated with the hard white shell revealed that the entire Al layer had been lost.

(a) Top View (b) Side View

Figure 4-51. Whisker (Crystal) Formation on Samples Exposed to CEM483

The untreated samples did not fare as well as their TCP treated equivalents. The samples exposed to reagent water and sea water took on a bronze hue during immersion, and exhibited areas of corrosion across their surfaces. The samples exposed to Turco 6813E did not show any signs of corrosion, but were affected by a color change across much of the exposed surface. Those samples immersed in the hydraulic fluid again showed no detrimental effects.

The fluids and their containers were visually inspected for any signs of dissolved metals that had been leached during the immersion process. No fluid showed any signs of dissolved metals. However, the glass jars that had contained the CEM483 did have a white residue in the positions occupied by the samples. This residue was later determined to be a hydrated aluminum oxide (compare with the product produced during the EIS measurements, and discussed in Section 4.1.6.1).

4.1.6.5 Stress-Corrosion Resistance

Environmentally assisted cracking (SCC) was assessed using the ASTM F 1624 test method on APCVD Al coatings deposited on notched Charpy CV2 bars. Deposition was accomplished using PB1 at 300°C. The AISI 4340 steel used to prepare the test specimens had a Rockwell C hardness of about 52. Some of the coated bars received a standard, hydrogen relief bake post treatment. Table 4-12 summarizes the results from this test.

Table 4-12. Results of Stress-corrosion Cracking Testing

Sample	Hardness RC	Orientation	Sample Coating	Load (lb)	K_{ISCC} (ksi/√in upper bound)	H_2 Relief Bake
E33182	51.6	LT	Bare	51.79	15.97	None
E33183	52.6	LT	Bare	51.54	17.14	None
E33206	52.6	LT	Bare	50.82	18.10	None
E33210	47.9	LT	APCVD Al	56.28	21.61	After Precracking
E33212	49.4	LT	APCVD Al	54.99	22.07	After Precracking

Applying an APCVD Al coating, and post treating it with a hydrogen relief bake, had no adverse effect on cracking behavior in the 3.5% salt solution used in this test. Some softening of the substrate material occurred (~7%: from about 52.3 to 48.7 HRC) but this was offset by a higher K_{ISCC} value (from about 17 to 21.8 ksi/√in) that improved the resistance to SCC[25].

4.1.7 Mechanical Properties

4.1.7.1 Adhesion

Knife Adhesion Test

This test was used solely as a quick, qualitative gage for determining if the coating was adherent to the substrate surface during APCVD Al coating optimization trials. No quantitative data were collected on this project.

Mandrel Bend Adhesion Test

As part of the screening testing, a mandrel bend test (ASTM D 522) was completed to check the adhesion of APCVD Al coatings (~22.7µm thick) on AISI 1010 steel panels. After deposition, the panels were given a hydrogen relief bake (190°C for 22 hr) but no chemical conversion coating. The coated panels were bent 180° around a 47mm (0.185 in) mandrel. No cracking was observed (Figure 4-52), which indicated good coating ductility and adhesion to the substrate material.

Pull Off Test

An APCVD Al coating deposited at 300°C using a pure TIBAL precursor exhibited a "pull" strength of 703 ±85 kg/cm^2. The corresponding value for a coating deposited using PB1 as precursor was 684 ±30 kg/cm^2. In both cases the failure was in the adhesive, not in the coating. It was concluded that there was no significant difference in adhesion between the two types of coating.

[25] The softer substrate was tougher and this led to offsetting the K_{ISCC} value.

Figure 4-52. Photograph of an APCVD Al Coating on Steel after Bending around a Mandrel

4.1.7.2 Hardness

Hardness was measured as a reference for comparison with other types of Al coatings. The average value obtained using a nano-indenter device was ~550 MPa (550.7 ±231.3 MPa). For comparison purposes, two Al single crystals with an (100) orientation were used as reference samples. They exhibited a greater average hardness of 836.5 ±215.4 MPa.

4.1.7.3 Young's Modulus

From the nano-indentation test, the average Young's Modulus of the Al coatings was found to be 36.3 ±14.9 GPa. For comparison purposes, the two Al single crystals with an (100) orientation exhibited an average Young's Modulus of 40.7 ±3.6 GPa.

4.1.7.4 Coefficient of Friction

Figure 4-53 depicts the initial changes in coefficient of friction as a function distance traveled by the "pin" on each disc. The traces for the Cd control show less oscillations than those seen on the APCVD Al coating, indicating that the Cd surface is more lubricious and "sticking" is less of a problem. However, it must be pointed out that differences in coating surface roughness was not taken into account. Overall, the coefficient of friction for Cd was about 0.4 before some corrosion was induced on the surface, after which it was about 0.25. In contrast, similar values for APCVD Al were about 1.0 and 0.5, respectively.

Mean coefficient of friction measurements at a distance of only 6 meters (~20 ft) also were plotted as a function of ASTM B 117 salt fog exposure for unsealed and unlubricated, Cd-plated, mild steel and APCVD Al-coated, 4340 steel substrates. The results are compared in Figure 4-54, while Figure 4-55 depicts the appearance of the surfaces of the: (a) Cd-plated steel, and (b) CVD Al-coated steel coupons after the 75 hours in an ASTM B 117 Salt Fog chamber.

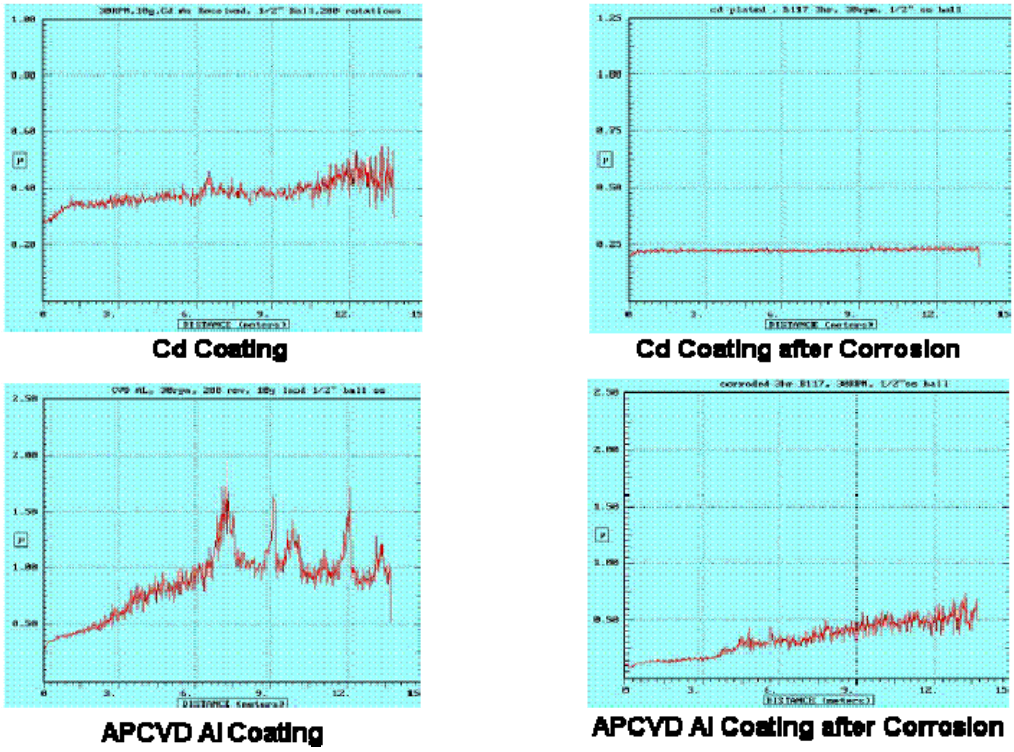

Figure 4-53. Results of the Coefficient of Friction of Cadmium and APCVD Al-Coated Steel Samples as a Function of Wear Track Distance

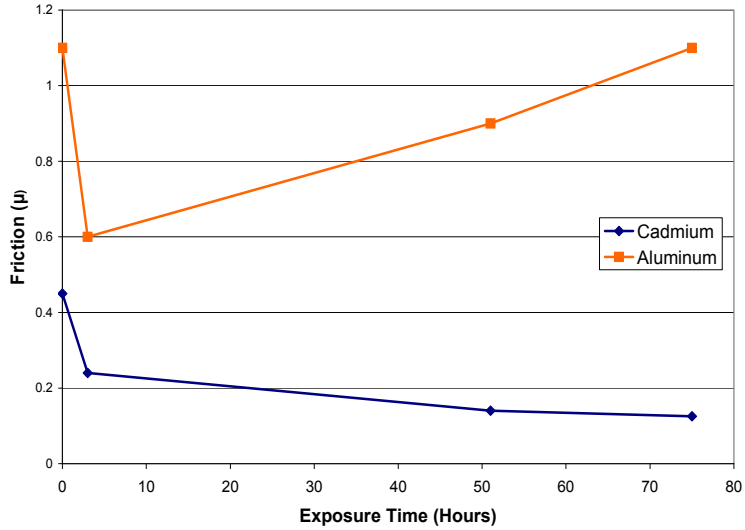

Figure 4-54. Mean Coefficient of Friction of Cadmium and APCVD Al-Coated Steel Substrates as a Function of B 117 Exposure Time

As before, the Cd coating exhibited a lower coefficient of friction, and maintained a low coefficient of friction even after significant exposure to corrosive conditions. The APCVD Al-coated samples also showed an initial reduction in the measured coefficient after a few hours of

exposure, but these returned to the initial levels after the 75 hours of exposure.

(a) Cd-coated steel (b) APCVD Al-coated steel

Figure 4-55. Samples Tested for 75 Hours in an ASTM B 117 Salt Fog Chamber

It is well known that Al coatings (such as IVD Al and AlumiPlate Al) have greater coefficients of friction than a Cd coating, which is a very lubricious. Thus there is a need for an appropriate anti-seize or dry film lubricant for use with any Al coating. The above results should be considered as preliminary baselines. Additional testing is needed after a lubricant is applied to the test samples.

4.1.7.5 Tensile and Notch Fracture Strength

According to the factory specification, the notch fracture strength (NFS) of the AISI 4340 steel bars used for the hydrogen embrittlement and fatigue testing was 400.7 ksi (average of 10 bars) with a minimum value of 395.1 ksi and a maximum of 405.2 ksi. To confirm this, tensile testing on four uncoated (bare) bars was performed at NAVAIR, resulting in an average NFS of 407.3 ksi and a higher standard deviation than the vendor value (Table 4-13). Instead of using the factory value, the average NFS of 407.3ksi from our measurements was adopted as the reference value for this project.

Table 4-13. Notch Fracture Strength of Uncoated AISI 4340 Steel Bars

Lot AU Uncoated Bars					
Specimen Number	**Percentage**	**NFS (Test, ksi)**	**Mean (ksi)**	**NFS (Vendor, ksi)**	**Difference (ksi)**
AU4225	103.3	413.9	407.3	400.7	**+ 6.6**
AU4245	103.3	413.9			
AU4354	96.7	387.4			
AU4492	103.3	413.9			

The NAVAIR results of 1,000 lb/min, tensile testing on Al-coated (at 300°C) bars with, or without baking at 191°C (375°F) for 23 hr, are given in Tables 4-14 and 4-15. The notch fracture strength of the APCVD Al-coated bars after baking is slightly greater than that of the Al-

coated bars without baking.

As discussed in Section 4.1.7.6, the coated bars without baking experienced HE failures (i.e., a difference in tensile strength between the APCVD Al-coated bars with and without baking). Regardless of baking, the coated bars underwent a loss of 4.6-15.3 % in the NFS compared to the bare bars.

Table 4-14. Results of Tensile Testing of APCVD Al-coated Notched Round Bars before Hydrogen Relief Baking

Lot AU CVD Al-Coated Bars Without Baking					
Specimen Number	**Percentage**	**NFS (ksi)**	**Mean (ksi)**	**NFS Uncoated Bars (ksi)**	**Difference (ksi)**
AU4212	90.4	362.3	360.4	407.3	**- 46.9**
AU4007	82.5	380.6			
AU4046	89.7	359.3			
AU4011	84.7	339.2			

Table 4-15. Results of Tensile Testing of APCVD Al-coated Notched Round Bars after Hydrogen Relief Baking

Lot AU CVD Al-Coated Bars With Baking					
Specimen Number	**Percentage**	**NFS (ksi)**	**Mean (ksi)**	**NFS Uncoated Bars (ksi)**	**Difference (ksi)**
AU4057	95.4	382.3	373.2	407.3	**- 34.1**
AU4265	93.5	374.5			
AU4365	92.3	369.7			
AU4292	91.4	366.3			

The weakening of these bars appears to be attributed to the deposition temperature (~300°C) used in the APCVD process. The effect of deposition temperature on the tensile strength of notched round bars was evaluated through measurements on bare (uncoated), heat treated bars. The temperatures used for the heat treatments were 250°, 275°, and 305°C, and the heat treating time was 20 minutes to simulate the typical APCVD Al coating deposition time. The loss in NFS over this temperature range was approximately linear (~0.35 ksi per °C). Heat treatment also was conducted on a sample at 275°C for 45 minutes to evaluate the effect of a longer heat treating time. The results given in Table 4-16 reveal that the loss in tensile strength is highly dependent on temperature, while no significant difference in tensile strength is seen with exposure time at a given temperature.

The effect of the pre-cleaning procedure, including HCl etching, that might introduce some hydrogen into the substrate (steel), also was evaluated through tensile testing. As shown in Table 4-17, the results indicate that there was no lowering of tensile strength or hydrogen embrittlement.

Table 4-16. Results of Tensile Testing of Notched Round Bars as a Function of Temperature and Time

Lot AU Heat Only Bars Tensile Test, 250°C with Exposure of 20 Minutes					
Specimen Number	**Percentage**	**NFS (ksi)**	**Mean (ksi)**	**NFS Uncoated Bars (ksi)**	**Difference (ksi)**
AU4148	95.5	382.6	383.5	407.3	**- 23.8**
AU4379	94.0	376.5			
AU4475	95.9	384.2			
AU4217	97.4	390.5			
Lot AU Heat Only Bars Tensile Test, 275°C with Exposure of 20 Minutes					
AU4332	94.3	377.8	373.2	407.3	**- 34.1**
AU4022	93.2	373.6			
AU4049*	NA	NA			
Lot AU Heat Only Bars Tensile Test, 275°C with Exposure of 45 Minutes					
AU4066	94.1	377.2	374.2	407.3	**- 33.1**
AU4138	90.4	367.2			
AU4013	94.4	378.2			
AU4262	93.4	374.3			
Lot AU Heat Only Bars Tensile Test, 305°C with Exposure of 20 Minutes					
AU4142	91.4	366.1	365.4	407.3	**- 41.9**
AU4099	91.0	364.8			
AU4374	90.4	362.3			
AU4226	91.9	368.2			

* Note round bar AU4049 was tested but a software error occurred during testing giving a false result that is not listed.

Table 4-17. Results of Tensile Testing of Notched Round Bars Cleaned with HCl

Lot AU Clean Only Bars (4 min 12 % HCl)		
Specimen Number	**Environment**	**Result**
AU4437	Air	**Passed** - fractured at 103.6%
AU4458	Air	**Passed** - fractured at 103.7%

4.1.7.6 Hydrogen Embrittlement and Re-embrittlement Resistance

The results of the preliminary HE testing - performed at the AFRL - for Al coatings on AISI 4340 steel specimens are summarized in Tables 4-18 and 4-19. The Cd coating controls shown in Table 4-18, after the specified hydrogen relief bake, passed the test criterion, as expected, when exposed to both air and a standard salt solution. In contrast, the APCVD Al-coated specimens - as deposited at 275°C - and tested in air failed this test.

The results of the preliminary HE testing for Al coatings on AISI 4340 steel specimens given the hydrogen relief bake heat treatment also are shown in Table 4-18. The specimens coated at 300°C, and then given the post heat treatment before being tested in air, passed this HE test. Even though most specimens coated at 275°C that had received the hydrogen relief bake did last for 200 hr without cracking, some did fail, and according to the test pass/fail criterion were

classified as failures. APCVD Al-coated specimens exposed to a salt solution failed.

Table 4-18. Results of Preliminary Hydrogen Embrittlement Testing for Cd Controls and APCVD Al-Coated AISI 4340 Steel Specimens

Coating	Material	Heat Treat	Specimen No.	Avg. Notch Tensile Strength (lbf)	Environment	Test % NFS	Total Hours	Spec. Fail?	Step Load?	Step Load Fail?	Process Embrittling?
Cd Electroplated & Baked											
Cd Control (QQ-P-416, Type I, Class 1)	4340 Steel	375F / 23hr	A-5	9,553	Lab Air	75	200	No	N/A	N/A	**No**
			A-6				200	No	N/A	N/A	
			A-7				200	No	N/A	N/A	
			A-8				200	No	N/A	N/A	
Cd Control (QQ-P-416, Type I, Class 1)	4340 Steel	375F / 23hr	A-9	9,553	3.5% Salt Soln	45	200+	No	N/A	N/A	**No**
			A-10				200+	No	N/A	N/A	
			A-11				200+	No	N/A	N/A	
			A-12				200+	No	N/A	N/A	
APCVD Al at 275C/527F As Coated											
Al CVD, 527F	4340 Steel	None	C-5	8,805	Lab Air	75	0.3	Yes	-	-	**Yes**
			C-6				0.5	Yes	-	-	
			C-7				2.8	Yes	-	-	
			C-8				1.7	Yes	-	-	
APCVD Al at 275C/527F & Baked											
Al CVD, 527F	4340 Steel	375F / 23hr	D-9	9,054	Lab Air	75	48.4	Yes	Req'd.	-	Yes
			D-10				200	No	Yes	Yes, 85%, 30 min	
			D-11				200	No	Yes	Yes, 85%, 32 min	
			D-12				200	No	Yes	Yes, 90%, 0 min	
Al CVD, 527F	4340 Steel	375F / 23hr	D-1	9,054	3.5% Salt Soln	45	31	Yes	-	-	Yes
			D-2				30.9	Yes	-	-	
			D-3				31	Yes	-	-	
			D-4				31	Yes	-	-	
APCVD Al at 300C/572F & Baked											
Al CVD, 572F	4340 Steel	375F / 23hr	B-5	8,744	Lab Air	75	200	No	N/A	N/A	**No**
			B-6				200	No	N/A	N/A	
			B-7				200	No	N/A	N/A	
			B-8				200	No	N/A	N/A	

Table 4-19. Results of Additional Hydrogen Embrittlement Testing for Heat Treated APCVD Al-Coated AISI 4340 Steel Specimens

Coating	Specimen Substrate Material	Heat Treat (Bake Out)	Spec. No.	Avg. Notch Tensile Strength (lbf)	Test Environment	Test % NFS	Total Hours	Spec. Fail?	Step Load?	Fail during Step Load?	Process/ Environment Embrittling?
APCVD at 275C/527F & Baked											
Al	4340 Steel	375F/23hr	AU-4385	9,054	Lab Air	75	200	No	N/A	N/A	**No**
			AU-4401				200	No	N/A	N/A	
			AU-4424				200	No	N/A	N/A	
			AU-4488				200	No	N/A	N/A	
Al	4340 Steel	375F/23hr	AU-4039	9,054	3.5% Salt Soln	45	0.3	Yes	-	-	**Yes**
			AU-4090				17.1	Yes	-	-	
			AU-4151				0.1	Yes	-	-	
			AU-4218				0.1	Yes	-	-	
Al	4340 Steel	375F/23hr	AU-4291	9,054	Deionized Water	45	0.6	Yes	-	-	**Yes**
			AU-4318				13.7	Yes	-	-	
			AU-4337				0.4	Yes	-	-	
			AU-4384				0.1	Yes	-	-	
APCVD at 300C/572F & Baked											
Al	4340 Steel	375F/23hr	AU-4127	8,744	Lab Air	75	200	No	Yes	No	**No**
			AU-4145				200	No	Yes	No	
			AU-4279				200	No	Yes	No	
			AU-4333				61.7	Yes	Req'd	-	
Al	4340 Steel	375F/23hr	AU-4395	8,744	3.5% Salt Soln	75	0.2	Yes	-	-	**Yes**
			AU-4409				2.8	Yes	-	-	
			AU-4448				0.3	Yes	-	-	
			AU-4457				1.1	Yes	-	-	

Table 4-19 summarizes the results for the additional tests in laboratory air and the 3.5% salt solution that were repeated for the specimens coated with APCVD Al at 275°C and 300°C and given a hydrogen relief bake, as well as for the specimens coated at 275°C and tested in deionized water. In these tests, the specimens coated at 275°C and tested in air after being heat treated passed the 200-hour test criterion. In contrast, the specimens tested in the salt solution failed this test. The specimens tested in deionized water also failed. The specimen coated at 300°C and heat treated, then tested in the salt solution environment, failed the 200-hour test criterion.

Table 4-20 summarizes the results of the preliminary HE testing for Al coatings on AerMet 100 specimens.

Table 4-20. Results of Preliminary Hydrogen Embrittlement Testing for APCVD Al-Coated AerMet 100 Specimens

Coating	Specimen Substrate Material	Heat Treat (Bake Out)	Spec. No.	Avg. Notch Tensile Strength (lbf)	Test Environment	Test % NFS	Total Hours	Spec. Fail?	Step Load?	Fail during Step Load?	Process/ Environment Embrittling?
Cd Plated & Baked											
Cd Control (QQ-P-416, Type I, Class 1)	AerMet 100	375F/23hr	Z-1 Z-2 Z-3 Z-4	10,600	Lab Air	75	200 200 200 200	No No No No	N/A N/A N/A N/A	N/A N/A N/A N/A	**No**
Cd Control (QQ-P-416, Type I, Class 1)	AerMet 100	375F/23hr	Z-5 Z-6 Z-7 Z-8	10,600	3.5% Salt Soln	45	21.4 12.9 22.7 29.2	Yes Yes Yes Yes	- - - -	- - - -	**Yes**
Cd Control (QQ-P-416, Type I, Class 1)	AerMet 100	375F/23hr	Z-9 Z-10 Z-11 Z-12	10,600	Deionized Water	45	200 200 200 58.2	No No No Yes	Yes Yes Yes Req'd	Yes, 66 hr @ 75% No Yes, 24.8 hr @ 75% -	**Yes**
APCVD at 300C/572F & Baked											
Al	AerMet 100	375F/23hr	AD AE AF AG	10,545	Lab Air	75	200 200 200 200	No No No No	N/A N/A N/A N/A	N/A N/A N/A N/A	**No**
Al	AerMet 100	375F/23hr	AH AI AJ AK	10,545	3.5% Salt Soln	45	22 13 3.8 1.9	Yes Yes Yes Yes	- - - -	- - - -	**Yes**
Al	AerMet 100	375F/23hr	AL AM AN AO	10,545	Deionized Water	45	1.7 20.8 20.5 0.1	Yes Yes Yes Yes	- - - -	- - - -	**Yes**

In summary, in a liquid environment the coated AISI 4340 steel and AerMet 100 specimens were susceptible to hydrogen embrittlement. Specimens D4 (tested in 3.5% salt solution) and D9 and D11 (tested in air for comparison, see Table 4-18) were selected for failure analysis at NJIT in order to try to determine the reason(s) for failure.

The fracture surfaces were examined in a field emission, scanning electron microscope with a backscattered electron detector. The following observations were made: (a) the coatings were uniform in thickness and polycrystalline (not columnar) with no sign of rupture, indicating good adhesion; (b) the fracture surface of the specimen (D9) that failed the 200-hour test in air exhibited a typical ductile failure in the center, but at the edges a small amount of ductile failure and some intergranular brittle failure was seen, as well as a shear lip seen (Figure 4-56); (c) all of the fracture surface of the specimen (D11) that passed the 200-hour test in air, but failed in

the rising step load test, exhibited a structure characteristic of ductile failure due to overloading (Figure 4-57); (d) the fracture surface of the specimen (D4) that failed the 200-hour test in salt solution exhibited a typical ductile failure in the center, but some intergranular brittle fracture and a shear lip at the edges (Figure 4-58).

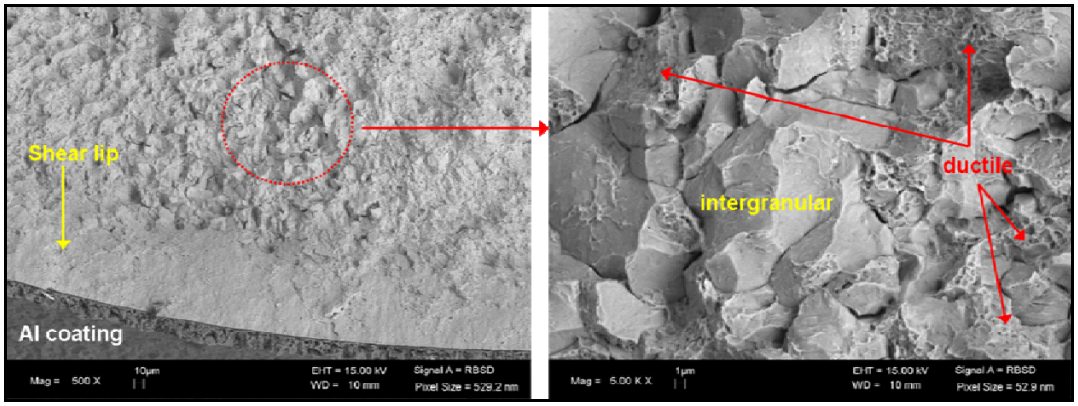

Figure 4-56. Photomicrographs of the Fracture Surface of the Specimen D9

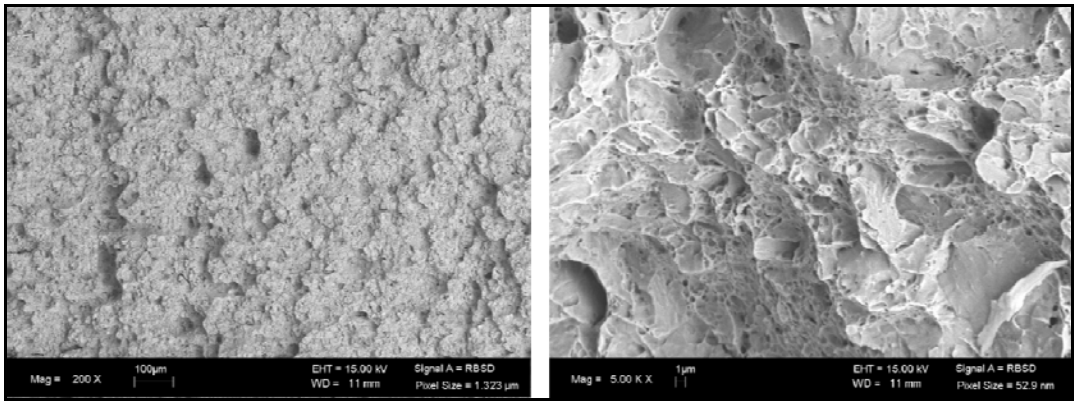

Figure 4-57. Photomicrographs of the Fracture Surface of the Specimen D11

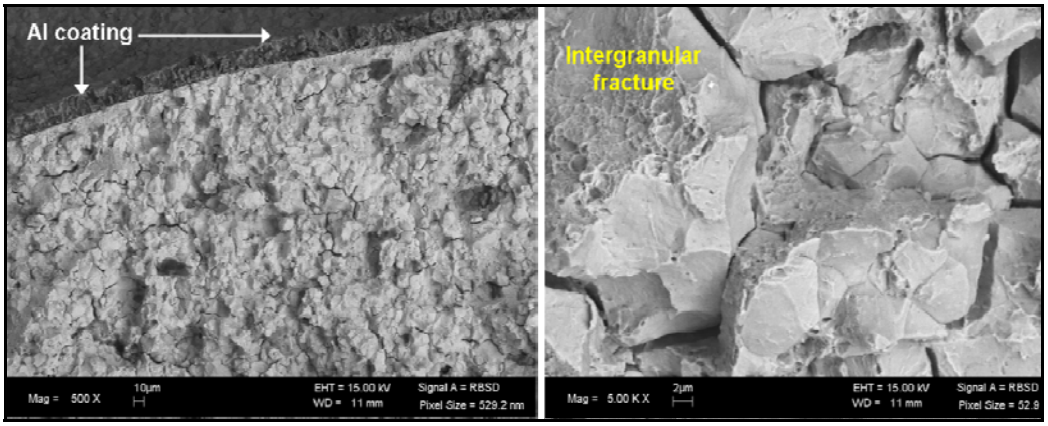

Figure 4-58. Photomicrographs of the Fracture Surface of the Specimen D4

These observations for the specimens tested in air were consistent with a much earlier analysis of fractured, AISI 4340 notched round bars, as machined and cleaned, after a hydrogen relief bake, and after an APCVD Al coating had been applied.[26] The findings in that report were that the fracture surfaces of the bare and the coated specimens exhibited "*a region of 45° shear failure (shear lip) around the periphery of the fracture, surrounding a relatively flat interior*", and that on the APCVD Al-coated specimen "*the shear lip was larger and more irregular in general. with some lobes*". The fracture surface of the bare specimen "*consisted entirely of ductile dimple rupture" "typical of well-behaved metal overload*". The coated specimen fracture showed ductile failure in the center region, but "*all around the periphery*" the appearance was consistent with brittle, "*intergranular failure*". Both brittle and ductile failure characteristics could be seen in a transition region. Figure 4-59 from the NAVAIR Report is a SEM image of part of the fracture surface from a coated specimen showing three features indicative of hydrogen embrittlement; namely; "*intercrystalline subsidiary cracks (yawning grain boundaries)* [1]*, ductile hair lines* [2]*, and microporosity* [3] *at the grain boundaries*". These features also may be seen in Figure 4-56.

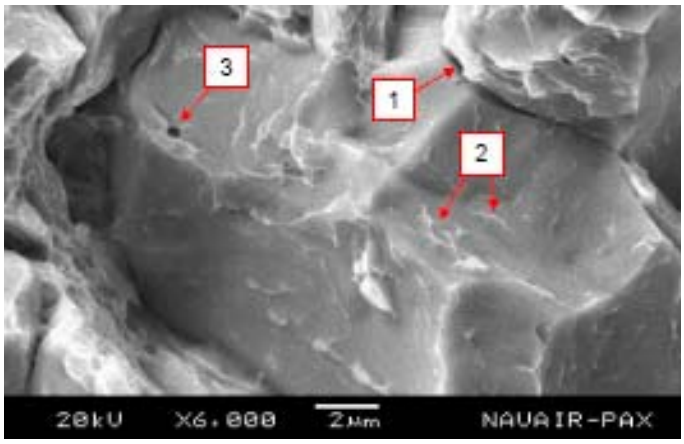

Figure 4-59. SEM Image of Part of the Fracture Surface of an APCVD Al-Coated Specimen after HE Testing

One explanation considered for the brittle failures was that the Al coatings might be porous, or damaged during the tumbling action of the round bars (with sharp edges) during deposition in the bench top, small rotary reactor (see examples in Figure 4-14). This damage would allow ingress of a corrosive environment. Additional metallographic examination of cross-sections of similar test and control specimens did indicate some closed micro-porosity and some surface damage to the coatings, with areas where the coating had been nearly completely removed. EIS measurements on the coatings indicated that pathways for the liquid environments to penetrate to the substrate could be present (see Section 4.1.6). Further investigations are needed to explain the test results and observations.

4.1.7.7 Fatigue Resistance

Constant amplitude, axial fatigue testing - according to ASTM E 466 Method - was conducted on Cd control specimens and APCVD Al-coated specimens (Pure TIBAL at 275°C and 300°C) on 4340 steel and AerMet 100 smooth round bars, without and with a hydrogen relief bake post

[26] B. A. Pregger, "*Microstructural Analysis Laboratory Report*", Report No. MA-1681, Aerospace Materials Division, Air Vehicle Department, Naval Air Warfare Center, Patuxent River, MD (28 August, 2006).

treatment. Uncoated 4340 steel smooth, round bars were used as a baseline.

Figure 4-60 shows Cd-plated and APCVD Al coatings on AerMet 100 specimens after some preliminary testing. The Cd coatings spalled off the substrate material on some specimens during the test, with a stress level of 140 ksi and R = -1, but this had only a small effect on depressing the fatigue (S/N) curve. None of the APCVD Al coatings exhibited any spalling when tested at 80 ksi and R = -1.

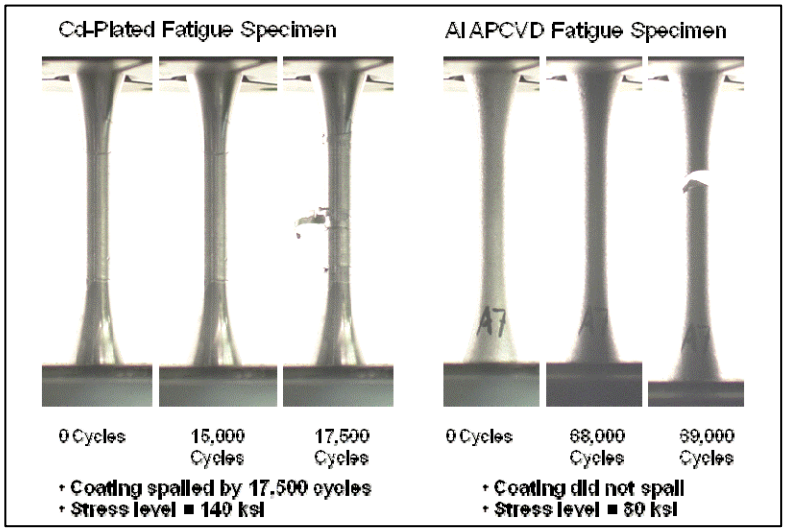

Figure 4-60. Cadmium and APCVD Al-Coated AerMet 100 Specimens after Fatigue Testing

Figure 4-61 shows the fatigue (S/N) data obtained for additional Cd-plated, APCVD Al-coated, and uncoated AerMet 100 smooth round bars for the conditions listed in the figure. A greater fatigue debit was measured for the APCVD Al-coated than for the Cd- plated specimens.

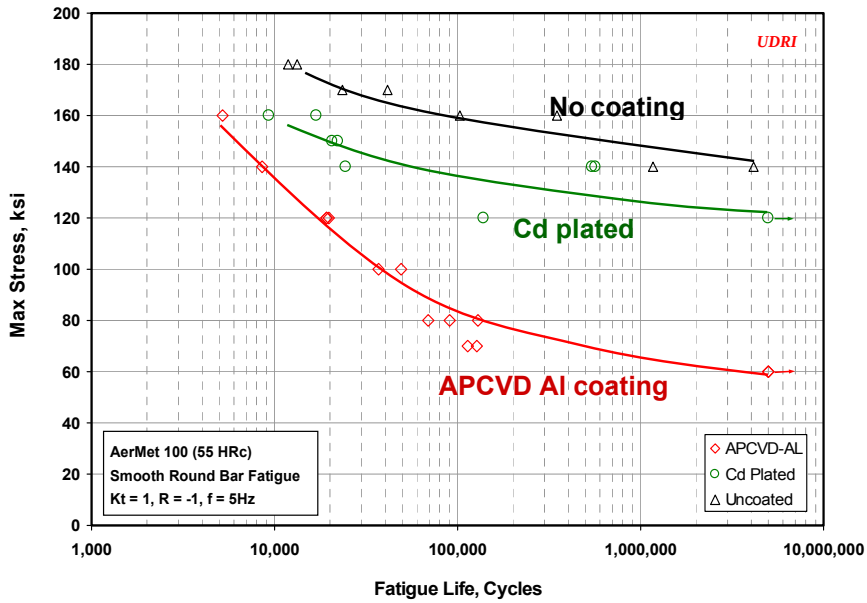

Figure 4-61. Fatigue Curves for Cadmium-Plated, APCVD Al-Coated,

and Uncoated AerMet 100 Specimens

At ~10,000,000 cycles, the debit for the Cd-plated coating was about 14%, but for the APCVD Al coating it was about 56%. Two possible reasons suggested for this observation are:

1. The greater debit may have been caused by surface damage to the substrate during tumbling of the specimens with their sharp edges and threaded sections in the rotary reactor - see Section 4.1.4.1 and Figure 4-14: additional tests with stationary specimens should be performed, and the possibility of coated surfaces sticking to one and another, then being forced apart should be investigated.

2. The small size and low heat capacity of the smooth, round bar specimens may have been a problem for the relatively high temperature (275° to 300°C) and duration (~15 to 30 minutes) of the coating process. Loss of fatigue strength may not be as much of a problem with parts having a much greater thermal mass/heat capacity, such as landing gear and actuator components. However, this cannot explain the results for the AerMet 100 specimens, because this alloy is more heat resistant than the AISI 4340 steel.

4.1.8 Electrical Properties

4.1.8.1 Contact Resistance

The ECR test results are shown in Table 4-21. All samples passed the initial electrical contact resistance test criterion by measuring less than 5 milli-ohms per square inch. After the APCVD Al coatings (with chromate conversion coatings) were removed from the salt fog chamber, rinsed, and dried, they were subjected to electrical contact resistance measurement. The results were a little higher than those measured before salt fog exposure. However, all coatings met the test criteria by measuring less than 10 milli-ohms per square inch.

Table 4-21. Electrical Contact Resistance of APCVD Al Coatings

Sample	Condition	ECR (milli-ohms/in^2)			
		Before Salt Fog Testing		After Salt Fog Testing	
APCVD Al at 275°C	As deposited	1.76	Average **1.66**	1.79	Average **1.75**
		1.56		1.70	
APCVD Al at 300°C	As deposited	1.70	Average **1.71**	2.78	Average **2.54**
		1.71		2.29	
APCVD Al at 310 – 320°C	Glass bead peened (burnished) and with chromate conversion coating	1.83	Average **1.84**	1.80	Average **1.90**
		1.78		1.89	
		1.87		2.16	
		1.96		1.79	
		2.00		1.88	
		1.60		1.90	

4.1.8.2 Electrical Resistivity

A non-optimized, APCVD Al coating - approximately 79.4 μm (3 mil) thick - was deposited on a Si_3N_4-coated steel. The electrical resistivity was measured to be 11.9 μΩ-cm, which is greater than that of bulk Al (2.7 μΩ-cm), although the compositional analysis showed that the APCVD Al

coating was relatively pure. The high value of electrical resistivity obtained appears to be mostly attributable to the porous, nodular surface morphology of the coating used in this measurement (Figure 4-62).

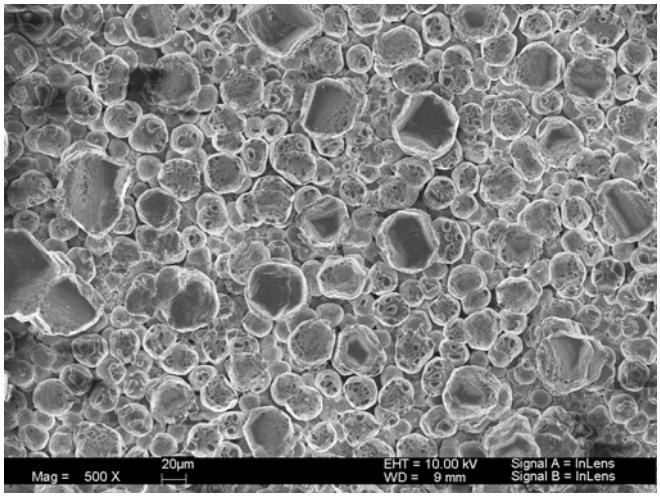

Figure 4-62. SEM Image of an APCVD Al Coating Deposited on a Si_3N_4-Coated Steel Substrate

The value of electrical resistivity of later, thinner - 13 to 26 µm (0.0005 to 0.001 in) - APCVD Al coatings deposited directly on steel substrates was found to be 3.5 ±0.1µohm.cm, which is close to that of bulk Al (2.7 µohm.cm). This result indicates that the APCVD Al coatings with an improved morphology exhibit good electrical conductivity.

4.2 Accomplishments

In this section, the major accomplishments of this research and development project are summarized. The discussion of the accomplishments is presented in three parts. First, what was accomplished in *adapting the APCVD technology* for depositing Al coatings at temperatures in the range of 300 ±25°C (Section 4.2.1). Second, what was accomplished with respect to the *properties* of the Al coatings (Section 4.2.2). And finally, what was accomplished with respect to the *performance* of the Al coatings Section 4.2.3). This discussion concludes with the *property* and *performance* findings from the latest effort to deposit APCVD Al coatings at ≤ 250°C, which was the goal established by the SERDP Office for a practical alternative for parts and components fabricated from low *and* high-strength steel substrates (Sections 4.2.4 and 4.2.5, respectively).

4.2.1 APCVD Process for Depositing Aluminum Coatings

It was established that the APCVD process could be used to successfully deposit Al coatings on substrate materials of interest by using the right combination of equipment design, substrate preparation, precursor chemicals, and carrier gases, and operating parameters, such as temperature and deposition time. The effects of precursor composition and deposition temperature on important coating properties and performance have been investigated.

It also was demonstrated that the process could be scaled up from using a laboratory scale reactor, to a small, bench top reactor, to a full size commercial unit for applying Al coatings to discrete, small parts, such as fasteners.

By analogy with other commercial uses of the processing chemicals, especially the precursors, worker and equipment safety and environmental issues are considered to pose a low risk to technology insertion.

Deposition rates depended on processing temperature and other process variables, but typical values for the required (MIL-SPEC defined) 8.5 - 25.4 µm (0.3 - 1.0 mil) thick coatings are given in Table 4-22.

Table 4-22. Typical APCVD Aluminum Deposition Rates and Times

Deposition Temperature, ºC	Precursor	Deposition Rate, µm/min	Deposition Time, min*	
			8.5 µm	25 µm
230	Proprietary Blend 2	≈ 0.30	~25.3	~75.9
246	Proprietary Blend 2	≈ 0.50	~16.7	~50.1
250	Proprietary Blend 2	≈ 0.65	~13.3	~39.9
275	Proprietary Blend 1	≈ 1.10	~7.3	~21.9
300	Proprietary Blend 1	≈ 2.00	~4.7	~14.1

* Approximate time for required thickness shown.

In addition, techniques are being developed for recovering and recycling process chemicals (see Figure 3-7) to satisfy environmental compliance issues, as well as to lower coating cost.

4.2.2 Properties of APCVD Aluminum Coatings Deposited at 275-300ºC

Coatings with **high aluminum content** (average ~96.9 at.%; ~98.3 wt.%) were obtained with pure TIBAL, as shown in Table 4.23. The actual amount in each coating varied according to the deposition temperature and the accuracy of the methods that were used for analysis. Consequently, the average concentrations listed for the constituents shown do not add up to 100%. With optimization of the processing parameters, it was possible to obtain Al contents greater than 99%.

Small amounts of oxygen, carbon, and hydrogen were incorporated into the coatings during deposition at 300ºC, but only in the surface regions (≤25 nm). Of these, the presence of hydrogen is the greatest concern with high-strength steels, but it can be removed by the conventional heat treatment (low temperature “bake”) that is specified for Cd coatings to prevent hydrogen embrittlement. Use of PB1 blend as the precursor resulted in a greater concentration of oxygen in the coatings, as expected, and a lower concentration of carbon.

Coatings obtained at 275ºC exhibited similar behavior to those deposited at 300ºC, with concentrations of oxygen and carbon lying between those found in the coatings deposited at the higher temperature with either pure TIBAL or PB1. It is worth mentioning that the penetration depth examined in the XPS and AES analyses was much smaller (approximately one tenth) than the Al coating thickness, which means that the impurities such as carbon and oxygen are attributed to surface contamination, not the intrinsic deposition process. Therefore, the purity of the Al coatings is thought to be greater than that measured by XPS and AES.

Table 4-23. Summary of the Composition of APCVD Aluminum Coatings Deposited at 275ºC and 300ºC

TIBAL Precursor	Deposit. Temp., ºC	Analysis Method	Carbon, at.%		Hydrogen, at.%		Oxygen, at.%		Aluminum, at.%		Al wt.%
			Actual	Ave.	Actual	Ave.	Actual	Ave.	Actual	Ave.	Ave.
Pure	275	AES	1.8		NM*		5.6		~92.6		
Pure	275	GD-OES	Trace**	**~0.9**	NM	**≤0.5**	0.3	**≤3.0**	<99.3	**<97.1**	**~98.4**
Pure	275	NRA	NM		0.5		NM		<99.5		
Pure	300	AES	0.7		NM		2.2		~97.1		
Pure	300	XPS	Present**		NM		Present		- -		
Pure	300	EDAX	NM	**≤3.7**	NM	**≤0.6**	Present	**~1.4**	- -	**~96.7**	**~98.3**
Pure	300	GD-OES	Trace		NM		~0.3		~98.7		
Pure	300	EPMA	6.8		NM		1.6		~91.6		
Pure	300	NRA	NM		0.6		NM		<99.4		
Blend PB1	300	AES	0.2	**≤0.2**	NM	**≤0.4**	11.0	**≤11.0**	<88.8	**<94.2**	**<96.5**
Blend PB1	300	NRA	NM		0.4		NM		<99.6		

* Not detected/not measured. ** Detected but not quantitatively analyzed.

For comparison, coatings deposited by the Instituto Nacional de Técnica Aeroespacial (INTA) in Spain in their MOCVD pilot plant equipment - at temperatures in the range of 280º to 350ºC using pure TIBAL - produced coatings containing ~93.1 at.% (94.9 wt.%) aluminum, ≤1.53 at.% carbon, ~0.001 at.% hydrogen, and ~5.33 at.% oxygen. Their results are very similar to those produced by the APCVD process used in this project.

Coatings with a **thickness** in the range of 12.5 - 25 µm (0.5 - 1.0 mil) are easily deposited by the APCVD process in reasonable times because of the relatively high deposition rates (Table 4-21). The throwing power and conformal coverage were excellent, and in this thickness range the coverage was uniform and the surfaces were relatively smooth (≤1,000 nm, rms).

The **crystalline structure** of the APCVD Al coatings was not columnar but equi-axed, which is desirable for providing good properties and satisfactory performance in service. The coatings had a face-centered cubic crystalline structure with an (111) preferred orientation, comparable to that obtained for pure, bulk Al metal. This structure was found to be independent of the deposition conditions for the ranges of pretreatment, deposition, and post treatment parameters used.

The overall APCVD Al **coating integrity** was very good. The as-deposited coatings were denser and exhibited fewer defects than the benchmark IVD Al coating. However, in a few instances, small pits were detected in the APCVD Al coatings in some of the electrochemical and corrosion tests. Such pits also were found in IVD Al coatings. The density measured for the APCVD Al coatings (~2.6 ±0.04 gm/cm^3) was similar to that reported for the benchmark electroplated Al coating (see Table 7-14: note that a typical value in the literature for bulk Al metal is 2.70 gm/cm^3). The appearance of glass bead burnished APCVD Al coatings was very similar to that observed for an IVD Al coating receiving the same treatment in the same equipment.

No problems with coating **adhesion** were observed in either the pull off test or the mandrel bend adhesion test. Cracking of the coatings did not occur.

Hardness is not considered to be a critical parameter for Air Force and most other applications. Nano-hardness measurements yielded an average value of approximately 550 MPa for the APCVD Al coatings, compared to an average of about 835 MPa for an Al single crystal used as a reference material. The calculated **Young's Modulus** was between 21.4 and 51.2 GPa, compared to 70 GPa for bulk Al metal and IVD Al coatings (see Table 7-14).

A low **coefficient of friction** is desirable for threaded fasteners, and torque tension behavior is an important parameter for such an application. However, the COF was measured for APCVD Al coatings as an indicator for possible sliding or abrasive wear performance in service. As expected, the value obtained (~1.1) was higher than that for Cd (~0.4) and, although some surface oxidation/corrosion of the APCVD Al lowered the COF to ~0.6, after a few days exposure to salt fog, the COF rose back to its original value. This higher value is similar to that for IVD Al coatings, for which post-treatments are used to attain the desired friction behavior. Thus, it is expected that there will not be a problem if APCVD Al is used as a replacement for IVD Al, which is a qualified alternative to Cd coatings.

APCVD Al coatings deposited at 275º to 300ºC passed the **contact resistance** requirement of 10 milli-ohms per square inch, even after being exposed to a salt fog environment for 168 hours. The same was true for APCVD Al coatings deposited at 310º to 320ºC, glass bead burnished, and then subjected to a chromium-containing, chemical conversion coating.

The **electrical resistivity** of an APCVD Al coating 12-25 µm (0.5-1.0 mil) thick was found to be 3.5 ±0.1 µohm.cm, which is similar to, but a little higher than that for bulk Al metal.

4.2.3 Performance of APCVD Aluminum Coatings Deposited at 275-300ºC

It was demonstrated that APCVD Al coatings can provide the required **galvanic (sacrificial) protection** to high-strength and other steels. As an example, the **corrosion potential** (E_{corr}) of the coatings was about 200mV more anodic than that observed for AISI 4130 steel, and remained constant (and similar to that measured for IVD Al coatings) even after 10 days exposure to salt fog. The E_{corr} difference was found to be 300-400 mV for AISI 4340 steel. At the sites of any pits present in the APCVD Al coatings, SEM analysis showed that the exposed substrate material remained free of corrosion products (red rust) and the adjacent Al coating had dissolved to provide protection.

In the ASTM B 117 test, the APCVD Al coatings, either as deposited or painted, provided **corrosion protection** that met the modest requirement set for pass or failure. However, coating optimization will be necessary to demonstrate that this type of Al coating can perform well in a salt fog environment for at least 1,000 hr, as has been demonstrated for electro-deposited Al coatings (see Table 7-14). In addition, during the electrochemical corrosion reaction that occurs aluminum hydroxide is formed and some hydrogen is generated that can lead to hydrogen re-embrittlement in service. This latter obstacle must be overcome before technology insertion can occur.

In the GM 9540P **accelerated corrosion** tests, the APCVD Al coatings, as deposited at 300ºC, provided corrosion protection that also met the requirement set for pass or failure. Coatings that had received a commercial, trivalent chromium chemical **conversion coating** performed better than the as deposited coatings with no post-treatment.

In the ASTM F 1624 test, the APCVD Al coatings, as deposited at 300ºC demonstrated that they had no adverse effect on **stress-corrosion cracking**, provided that they had received a standard hydrogen relief bake.

Fluid compatibility tests were conducted with five common liquids used in aircraft maintenance, repair, and overhaul (MRO) operations. In general, the results were similar to those for the corrosion tests mentioned above; namely, the samples that had received the standard hydrogen relief bake fared much better than those that had not, and those with the commercial, TCP chemical conversion coating performed better than the as deposited coatings with none. The average corrosion rating for the latter was about 1, on a scale of 0 to 4, where 0 corresponds to no corrosion seen, to 4 where either pitting attack has occurred, or there was discoloration or corrosion over 25% of the surface. The one exception was with a hydrogen peroxide-based paint stripper (CEM 483) where (corrosion) attack was significant, and whisker like crystals had grown all over the surface. However, peroxide-based strippers are rarely used in DoD MRO operations, and this should not be a barrier to implementing the APCVD process.

The deposition temperatures used in the first part of this project (usually 275º to 300ºC) had a negative impact on the high-strength steel substrate materials, reducing their **tensile strength**, in some cases to unacceptable levels that would not meet design specifications for strength. This, in turn, had a negative effect on fatigue resistance, yielding an unacceptable **fatigue debit**. The standard hydrogen relief bake applied to the APCVD Al-coated notched test bars had a positive effect in so far as there was less loss in tensile strength of this substrate material, but it was not sufficient to alleviate the problem. In the constant amplitude, axial fatigue tests the Cd-plated AerMet 100 specimens exhibited some flaking of the coatings whereas the APCVD Al-coated specimens did not. The latter failed after just under 69,000 cycles, but the former failed after only 20,500 cycles. In other fatigue tests with Cd-plated, APCVD Al-coated, and bare AerMet 100 specimens, S/N curves (with Kt = 1, R = -1, and f = 5Hz) were generated over 5,000,000 cycles. However, the fatigue debit was about three times greater for the APCVD Al-coated specimens than the Cd-plated specimens.

The **hydrogen embrittlement** test results with both the coated AISI 4340 steel and AerMet 100 alloy were mixed. Specimens receiving the standard hydrogen relief bake treatment passed the test criterion for the experiments done in air, but failed when the tests were done in deionized water or a 3.5% salt solution. In contrast, the Cd-plated AISI 4340 steel control specimens passed when tested in air and the salt solution, but the Cd-plated AerMet 100 control specimens failed when tested in both deionized water and the salt solution. Thus, to some degree, the APCVD Al-coated specimens performed as well as the Cd-plated control specimens. Further investigation is needed to explain the results that were obtained.

4.2.4 Properties of APCVD Aluminum Coatings Deposited at 230-245ºC

The measurements obtained for APCVD Al coatings deposited at lower temperatures were composition, thickness, structure/morphology, coverage, conformity, and roughness. Unless otherwise stated, the substrates were either AISI 4130 steel coupons, or hollow rivet sleeves - with a step present on the inside as shown in Figure 4-63 - for evaluating the step (conformal) coverage of APCVD Al coatings. APCVD Al deposition was conducted at 230º and 246ºC using PB2. All of the Al-coated samples were baked at 191ºC for 23 hr after deposition. Some of the 32μm thick Al coatings that were deposited at 246ºC underwent the glass-bead burnishing (shot peening) treatment specified for IVD Al coatings, to evaluate the effect of the burnishing process on the corrosion resistance of the Al coating. The coating sample matrix is listed in Table 4-24.

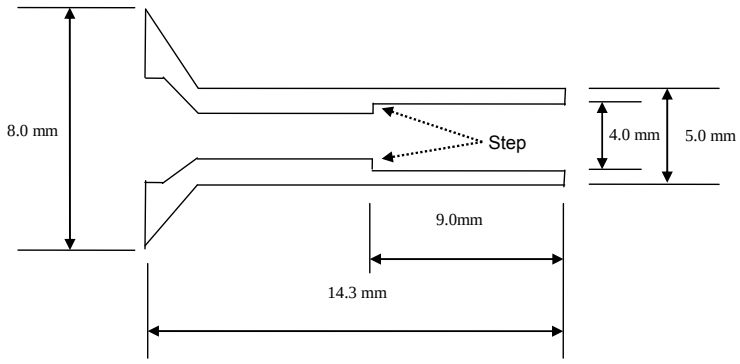

Figure 4-63. Diagram of Hollow Rivet Sleeve Showing Dimensions

Table 4-24. APCVD Al Lower Temperature Deposition Coating Matrix

Run ID	Substrate	Deposition Temp. (°C)	Coating Thickness (µm)
PP-482	AISI 4130 coupon	230	18
	Hollow rivet sleeve	230	12
PP-481	AISI 4130 coupon	246	32
PP-483	AISI 4130 coupon	246	13
	Hollow rivet sleeve	246	14

Coating structure was determined using X-ray diffraction analysis. The coupons used for this analysis included those with Al coatings deposited at 230ºC to a **thickness of 18 µm**; and at 246ºC with a **thickness of either 13 µm or 32 µm**. The XRD patterns of the Al coatings shown in Figure 4-64 were compared to those of an Al powder reference spectrum. The details of the XRD spectra - including miller indices, relative intensity, and FWHM - are listed in Table 4-25.

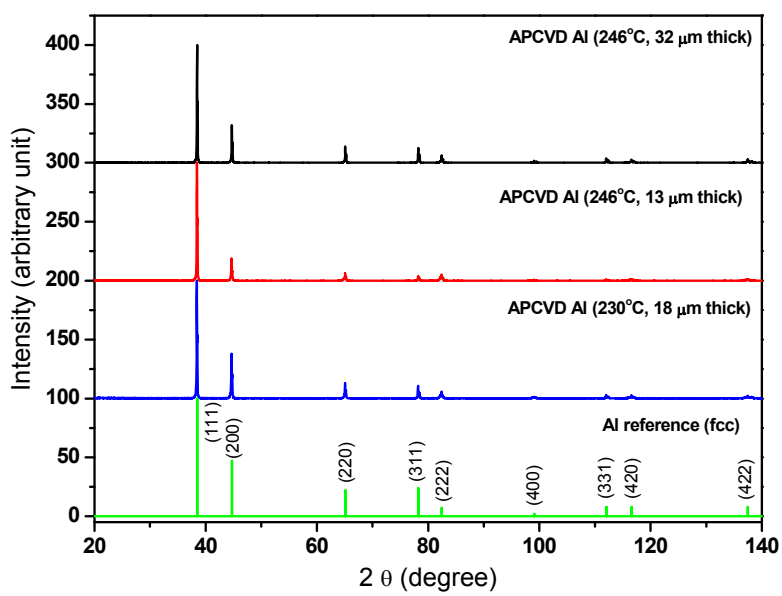

Figure 4-64. XRD Patterns of APCVD Al Coatings

Deposited at 230°C and 246°C

Table 4-25. XRD Results for Coatings Deposited at 230°C and 246°C

2θ (deg)	Miller Indices (hkl)	APCVD Al coatings						Al Reference
		230°C, 18µm thick		246°C, 13µm thick		246°C, 32µm thick		
		FWHM (deg)	Rel. Int. (%)	FWHM (deg)	Rel. Int. (%)	FWHM (deg)	Rel. Int. (%)	Rel. Int. (%)
38.47	(111)	0.072	100.0	0.072	100.0	0.072	100.0	100.0
44.74	(200)	0.096	39.1	0.096	19.0	0.072	32.1	47.0
65.14	(220)	0.096	13.4	0.072	6.4	0.096	14.1	22.0
78.23	(311)	0.144	10.3	0.120	3.9	0.120	10.8	24.0
82.44	(222)	0.120	5.5	0.096	5.2	0.096	5.8	7.0
99.08	(400)	0.384	1.2	0.768	0.5	0.192	1.4	2.0
112.05	(331)	0.192	2.6	0.192	1.0	0.120	3.6	8.0
116.57	(420)	0.192	2.3	0.960	0.6	0.168	2.5	8.0
137.46	(422)	0.192	2.1	0.288	0.8	0.192	2.6	8.0

These results reveal that the XRD peak patterns of these coatings also are very similar to those of the Al reference (i.e., face-centered cubic structure). Apparently, all APCVD Al coatings, independent of deposition temperature in the range studied (230º to 300ºC - see Tables 4-2 and 4-3 for the latter), exhibit a **crystalline fcc structure**, and the FWHM values (generally used for determining crystallinity) indicate that there is no significant influence of deposition temperature and coating thickness on the crystallinity of APCVD Al coatings.

The **surface roughness** of APCVD Al coatings deposited on non polished steel coupons was measured using the profilometry method described in Section 3.3.2. For these measurements, the coatings were not glass bead burnished. Three points on each side of the coatings were randomly selected, and the measured arithmetic roughness (R_a) was determined as shown in Table 4-26.

Table 4-26. Surface Roughness of APCVD Al Coatings Deposited at 230°C and 246°C

Deposition Temp. (°C)	Coating Thickness (µm)	Ra (µm)
230	18	4.2 ±1.0
246	13	5.1 ±2.0
	32	6.9 ±2.5

Figures 4-65 and 4-66 illustrate the surface morphology of these coatings, showing uneven coverage, and regions of surface damage and delamination (defects) that lead to inadequate coating coverage. The **coating integrity** of these coatings, which were not optimized, is not as good as that for the coatings deposited at the higher temperatures for which considerable development work was undertaken in the first two years of this project.

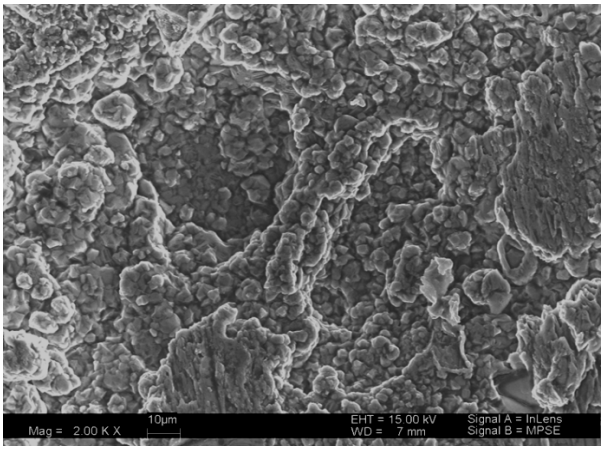

Figure 4-65. Surface SEM Image of 18µm Thick APCVD Al Coating Deposited at 230°C

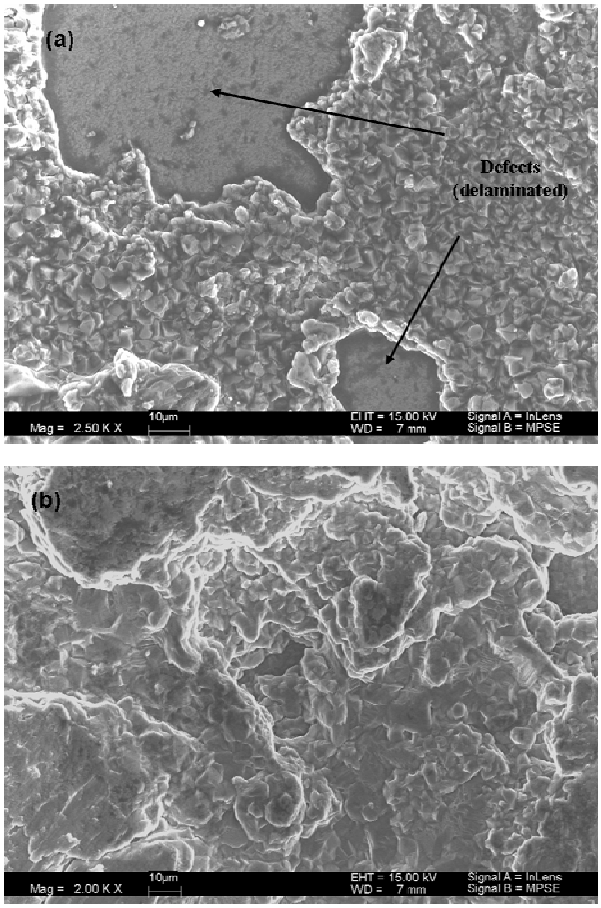

Figure 4-66. Surface SEM Images of APCVD Al Coatings of Different Thickness Deposited at 246°C
(Coating thickness of (a) 13 µm and (b) 32 µm)

The coating uniformity and **conformal (step) coverage** of the Al coatings were investigated by using a field emission SEM to determine thickness distributions on the inside and outside surfaces of small, hollow rivets (shown in Figure 4-63) that had a step on the inside. After depositing APCVD Al coating using the PB2 precursor, the specimens were cross-sectioned lengthwise, followed by mounting and polishing procedures described earlier. Figures 4-67 and 4-68 are FE-SEM photomicrographs of selected surfaces.

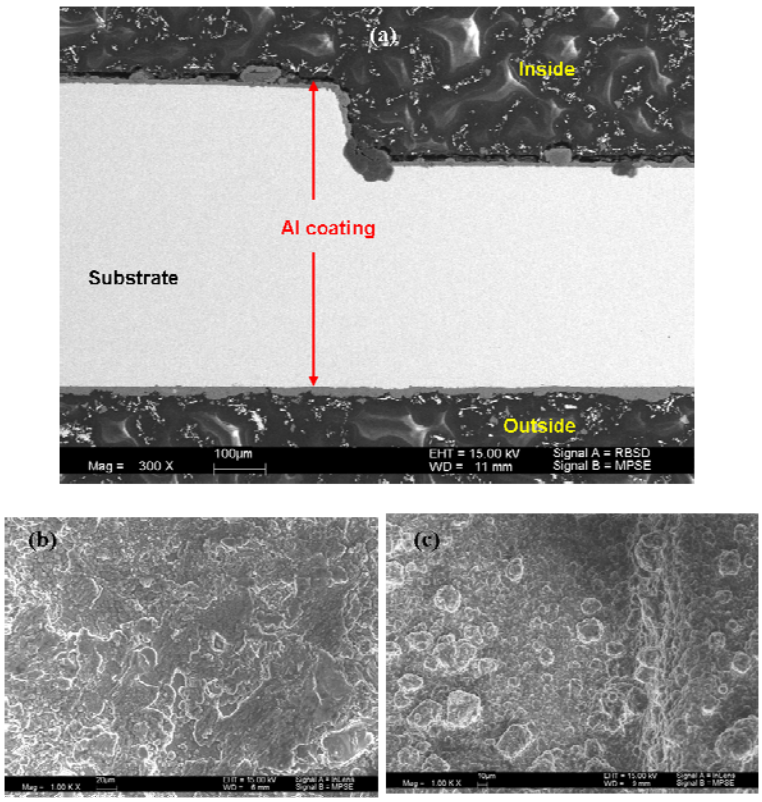

Figure 4-67. SEM Images of APCVD Al Coating Deposited on Hollow Rivet Sleeve at 230°C

(Cross sectional image (a) and surface morphology of outside (b) and inside (c) at the step)

The **coating uniformity** outside appears to be relatively poor compared to that on the inside surfaces, especially for the APCVD Al coating deposited at 246ºC, and the morphology (extent of nodularity) appears to be different from that inside. Nodular deposits are observed more on the inner surfaces of coatings deposited at 230ºC than in case of those deposited at 246ºC. A SEM image of a cross-section of a hollow rivet sleeve coated at 246ºC is shown in Figure 4-69 with the dimensions d_1 and d_2 shown, which are used to calculate the step coverage ratio - d_2/d_1 - a measure of throwing power for parts with complex geometries.

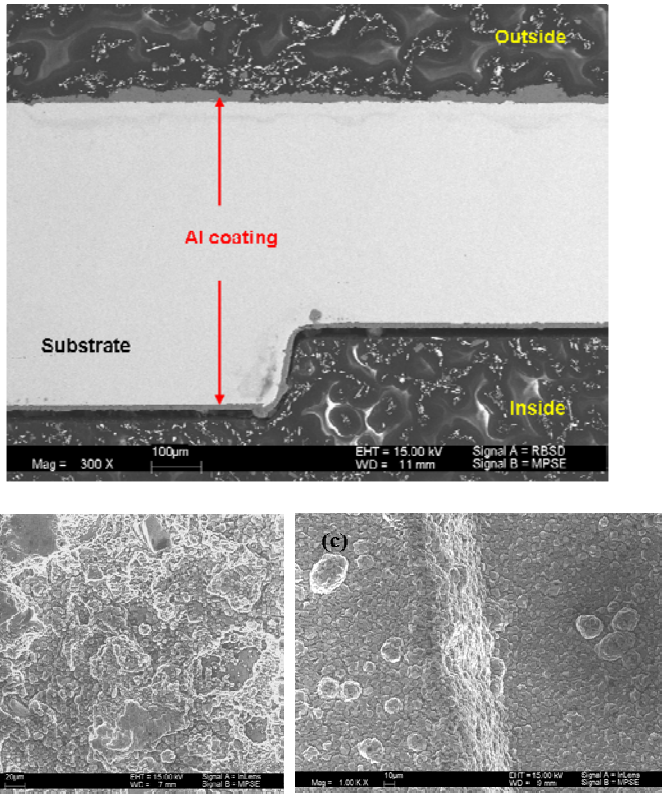

Figure 4-68. SEM Images of APCVD Al Coating Deposited on Hollow Rivet Sleeve at 246°C

(Cross sectional image (a) and surface morphology of outside (b) and inside (c) at the step)

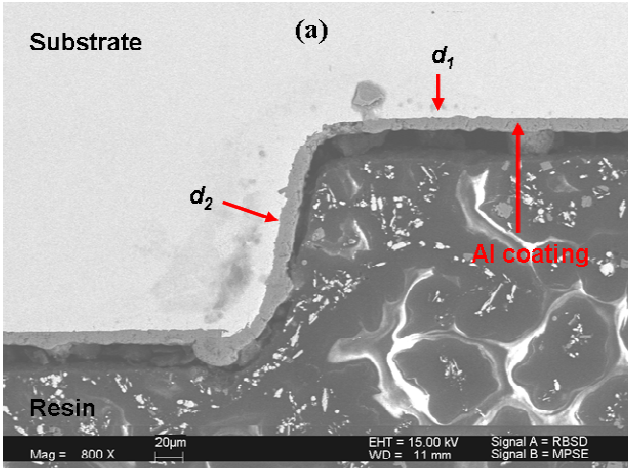

Figure 4-69. SEM Image of APCVD Al Coating at 246°C Used to Calculate the Step Coverage Ratio

The average step coverage ratio for APCVD Al coatings deposited at 230º and 246ºC was found to be as close to 1.0 as was the case of coatings deposited at a temperature of 300ºC, indicating that the APCVD Al process using a lower deposition temperature can exhibit **excellent conformal step coverage** on small diameter internal and external design elements, as was found for deposition done at higher temperatures (Figure 4-13).

The **chemical composition** depth profile analysis on as deposited APCVD Al coatings was conducted by GD-OES for comparison with the depth profiles obtained for coatings deposited at 275º to 300ºC. The Al coatings were deposited on polished steel coupons at 230º and 246ºC using the PB2 precursor. The coating thickness was 13 µm for coatings deposited at 230ºC and 32 µm for 246ºC. The concentration (wt. %) of elements detected in the Al coatings is plotted as a function of depth in Figure 4-70 (compare with Figure 4-27 for coatings deposited at 275º to 300ºC).

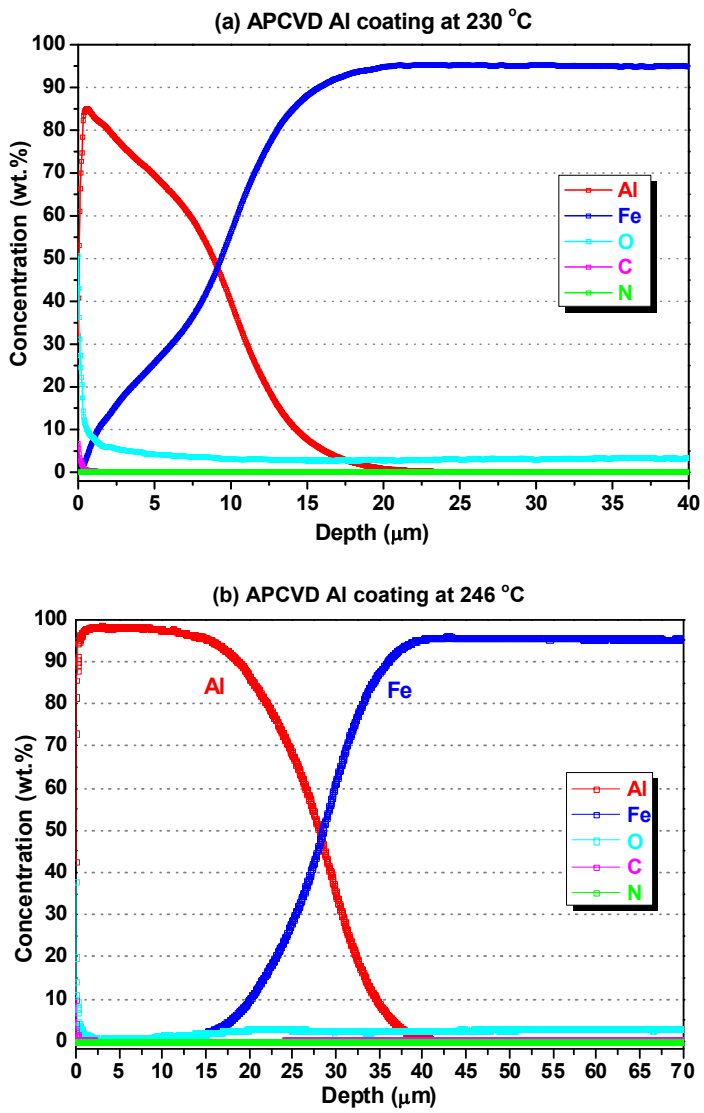

Figure 4-70. GD-OES Depth Profiles of APCVD Al Coatings

Deposited at (a) 230°C and (b) 246°C using Precursor PB2

The results indicate that the maximum **Al concentration** (wt.%) in the coating deposited at 230ºC occurred at the depth of 0.6 µm, and the other elements detected were as follows:

- Al = 85%: and O = 10.0%, Fe = 3.6%, and C = 0.5% for the 230ºC coating.

The maximum **Al** concentration in the coating deposited at 246ºC occurred at the depth of ~2.56 µm, and the other elements detected were as follows:

- Al = 98.3%: and O = 0.8%, Fe = 0.5%, and C = 0.05% for the 246ºC coating.

No nitrogen was detected in either coating. The aluminum concentration for the coating deposited at 246ºC is comparable to that obtained for the coatings deposited at the higher temperatures (Table 4-23). If there were no defects in the coating deposited at 230ºC (i.e., no Fe detected; see Figure 4-66) or the coating was thicker, the concentration of Al would be higher (~89%) and more in line with the coatings deposited at 275º to 300ºC.

The **carbon content** and the **oxygen content** was slightly higher than measured for the coatings deposited at the higher temperatures. Carbon and oxygen concentrations plotted as a function of depth are shown in Figure 4-71. (Similar curves for the coatings deposited at the higher temperatures are shown in Figure 4-27.)

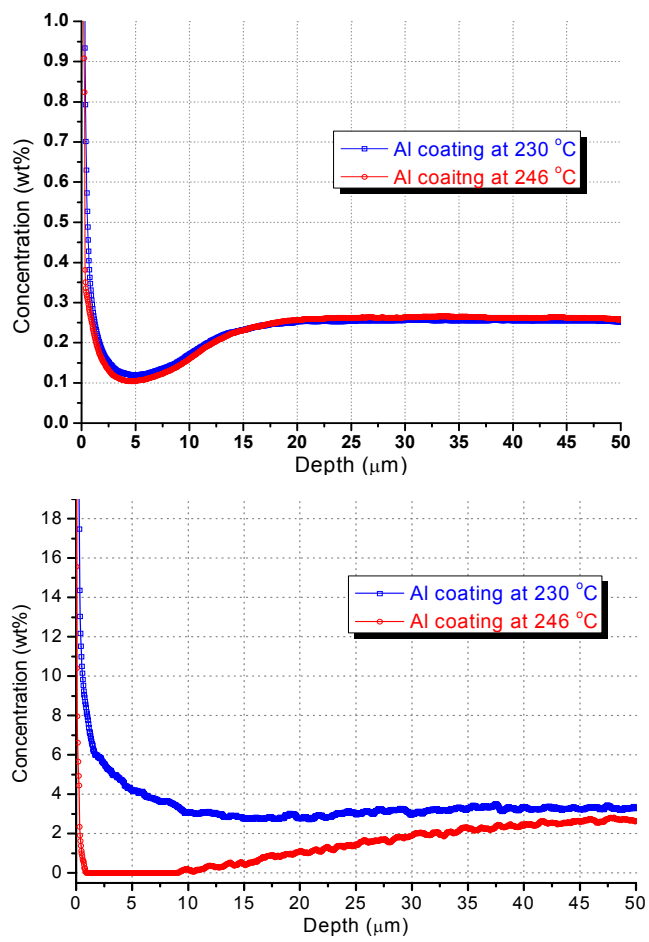

Figure 4-71. GD-OES Depth Profiles of Carbon and Oxygen

Present in APCVD Al Coatings Deposited at 230°C and 246°C

The high concentration of carbon observed at the surface was due to contamination. Any carbon incorporated in Al coating during deposition process is a concern; however, it is worth while noting that the carbon concentration for both coatings in the bulk region is below 0.25 wt.%, the value that is observed at the surface of the steel substrate itself.

4.2.5 Performance of APCVD Aluminum Coatings Deposited at 230-245ºC

The measurements obtained for APCVD Al coatings deposited at lower temperatures were galvanic protection/corrosion resistance, corrosion potential, notch tensile strength, hydrogen embrittlement in air, and hydrogen embrittlement in salt solution.

In order to evaluate the **corrosion resistance** of APCVD Al coatings deposited at a lower temperature (246ºC) and the effect of shot-peening as a post treatment on corrosion resistance, corrosion experiments were performed in a 3.5 wt.% NaCl solution saturated with oxygen at room temperature. Electrochemical impedance spectroscopy measurements were made for different immersion times up to six days. Six samples of APCVD Al coatings were deposited on non polished, AISI 4130 steel coupons at 246ºC. The coating thickness as deposited was 32 µm. Three of these coupons were glass-bead burnished, as is done with IVD Al coatings.

At first, one APCVD Al-coated coupon in each set of three samples was randomly selected for the EIS measurements (see Section 3.3.6). All electrochemical tests were carried out with an exposed area of 1 cm^2. EIS data were collected at the coating corrosion potential (E_{corr}) with sinusoidal voltage perturbation of 10 mV (rms) over the frequency range of 10 mHz to 100 kHz with 10 points per decade. The data were analyzed to obtain the value of polarization resistance (R_p), which can be interpreted as corrosion resistance. The EIS data for an Al foil (reference - 99.999% purity) and an uncoated AISI 4130 steel coupon (control) from previous corrosion experiments were used as baselines for comparison purposes. **Corrosion potential** (E_{corr}) and **polarization resistance** (R_p) values of the APCVD Al coatings - with and without shot-peening - are plotted in Figures 4-72 and 4-73, along with the baseline data.

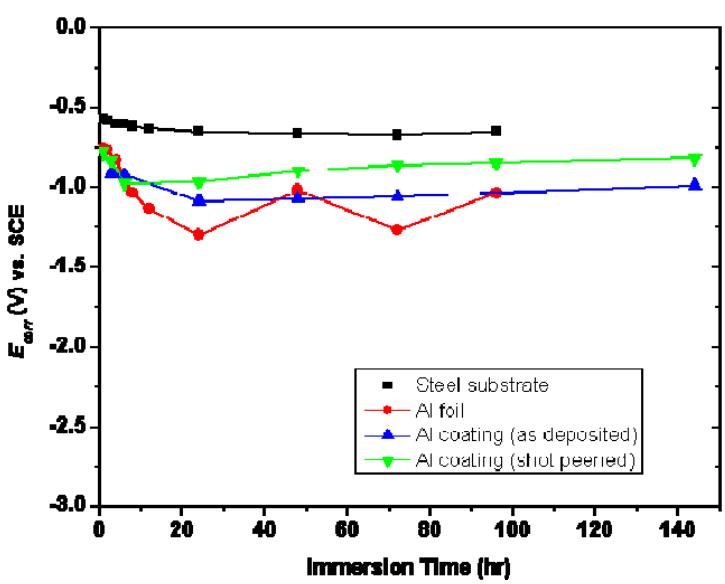

Figure 4-72. Corrosion Potential of APCVD Al Coatings Deposited at 246°C

as a Function of Immersion Time in a Salt Solution saturated with Oxygen

Data for the coatings deposited at the higher temperatures, for comparison, are given in Figure 4-28.

The corrosion potential of the as deposited Al coating was observed to be lower (~ 200 mV more negative) than that of the shot-peened coating. The latter may have experienced some additional surface oxidation during handling and this additional post-deposition treatment. However, the corrosion potential values of both coatings stayed below that of uncoated steel substrate during the immersion time, so both can provide **galvanic (sacrificial) protection**.

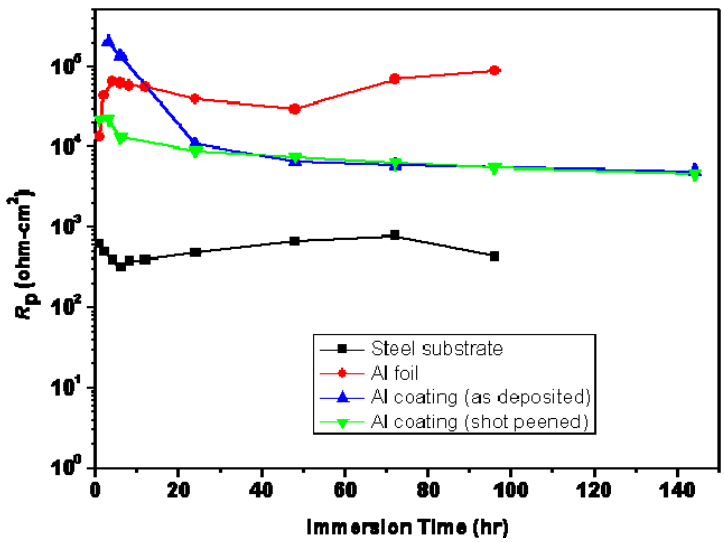

Figure 4-73. Polarization Resistance of APCVD Al Coatings Deposited at 246°C as a Function of Immersion Time in a Salt Solution Saturated with Oxygen

In addition, the data in Figure 4-73 show that shot-peening the coating did not provide any enhancement of R_p (corrosion resistance) in these experiments, once a near equilibrium state had been reached. Further testing is required to confirm this result.

Visual examination of the coatings after EIS measurements indicated that the coatings underwent localized corrosion, which occurred through thin areas and porous sites in the coatings.

The effect of the lower deposition temperature and other variables on the **notch fracture strength** of the AISI 4340 steel and AerMet 100 substrate materials was investigated and the results are summarized in Tables 4-27 and 4-28. These results may be compared with the results from previous test data discussed in Section 4.1.7.5.

The AISI 4340 steel specimens were more sensitive to the temperature-time parameters used to deposit the APCVD Al coatings than the AerMet 100 specimens according to the data presented in the two tables. The “as received”, (i.e., uncoated) samples when heated at the temperature used for the standard hydrogen relief bake, essentially showed no difference in the NFS compared to the measured baseline value, as was expected, but deposition temperatures in the range of 230º to 300ºC caused a loss in NFS.

Table 4-27. Effect of Lower Deposition Temperature, Burnishing and Cr(VI) CCC Post-Treatment on Notch Fracture Strength of AISI 4340 Steel

		Load			Notch Fracture Strength (NFS)			
Notch Dia.	**Notch Area**	**Max (lbf)**	**Min (lbf)**	**Avg (lbf)**	**Max (ksi)**	**Min (ksi)**	**Avg (ksi)**	**Delta (ksi)**
Dirats Lab Specification (1st lot "as delivered" specimens)							Baseline	
0.175	0.02405			**9,639**	405.2	395.1	**400.7**	N/A
AFRL Results (4 Cd plated specimens from 1st lot)								
0.175	0.02405			**9,553**			**397.2**	**-3.5**
AFRL Results (4 coated at **300**C specimens from 1st lot)								
0.175	0.02405			**8,744**			**365.5**	**-37.2**
SMI Specification (2nd lot "as delivered" specimens)							Baseline	
0.175	0.02405			**9,054**			**376.4**	N/A
AFRL Results (4 uncoated "as received" specimens from 2nd lot)								
0.175	0.02405	9,150	8,980	**9,055**	380.4	373.3	**376.5**	**0.0**
AFRL Results (4 uncoated, baked at **191**C specimens from 2nd lot)								
0.175	0.02405	9,208	8,885	**9,060**	382.8	369.4	**376.7**	**0.2**
AFRL Results (4 coated at **246**C specimens from 2nd lot)								
0.175	0.02405	8,707	8,332	**8,462**	362.0	346.4	**351.8**	**-24.7**
AFRL Results (4 coated at **246**C, peened, and Cr(VI) CCC from 2nd lot)								
0.175	0.02405	8,711	8,476	**8,570**	362.2	352.4	**356.3**	**-20.2**
AFRL Results (4 coated at **230**C, peened, and Cr(VI) CCC from 2nd lot)								
0.175	0.02405	8,748	8,620	**8,693**	363.7	358.4	**361.4**	**-15.1**

The data for specimens coated at 246ºC in Table 4-27 also indicate that using a burnishing and Cr(VI)-based CCC post-treatment often given to IVD Al coatings decreases the loss in NFS by nearly 20%. Depositing the Al coating at 230ºC and using the same post-treatments provides less of a loss in NFS, and brings the result much closer to the ±10 ksi deviation allowed by the design guidelines. Especially in view of the fact that depositing Cd as a control can lead to a 3.5 ksi loss in NFS. Also of note, is that the loss of about 15 ksi in NFS at 230ºC corresponds to the value extrapolated from the results from the first lot of AISI 4340 specimens tested (Table 4-16).

Table 4-28. Effect of Lower Deposition Temperature and Burnishing Post-Treatment on Notch Fracture Strength of AerMet 100

		Load			Notch Fracture Strength (NFS)			
Notch Dia.	**Notch Area**	**Max (lbf)**	**Min (lbf)**	**Avg (lbf)**	**Max (ksi)**	**Min (ksi)**	**Avg (ksi)**	**Delta (ksi)**
AFRL Results (4 Cd plated control specimens)							Baseline	
0.175	0.02405			**10,600**			**440.7**	**-18.6**
AFRL Results (4 uncoated "as received" specimens)							Baseline	
0.175	0.02405	10,890	11,227	**11,047**	452.8	466.8	**459.3**	N/A
AFRL Results (4 uncoated "as received", baked at **191**C specimens)								
0.175	0.02405	11,186	11,074	**11,143**	465.1	460.4	**463.3**	**4.0**
AFRL Results (4 coated at **300**C specimens)								
0.175	0.02405			**10,545**			**438.4**	**-20.9**
AFRL Results (4 coated at **246**C, glass bead peened specimens)								
0.175	0.02405	10,886	10,766	**10,827**	452.6	447.6	**450.1**	**-9.1**

With respect to the results for the AerMet 100 specimens, a similar trend in decreasing loss in NFS is found as the deposition temperature is lowered, as was expected. Table 4-28 shows that the hydrogen relief bake has negligible effect on the NFS. Of note, is that the Cd-plated control exhibited a loss of about 19 ksi. Lowering the APCVD Al deposition temperature to 246ºC, combined with a standard glass bead burnishing (see Figure 4-74) as done on IVD Al coatings, lowered the loss in NFS to about 9 ksi. This value falls in the acceptable range of ±10 ksi variation in NFS during processing, prior to the coated part being put in service. Deposition at 230ºC should provide an even better result.

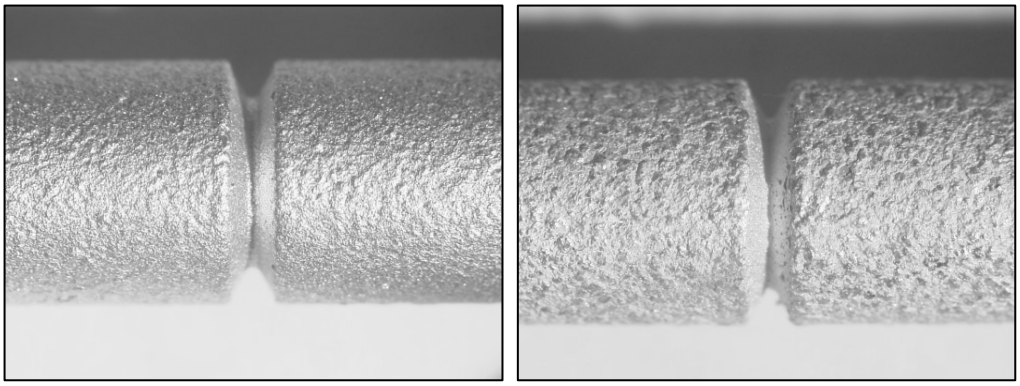

(a) AerMet 100 (b) AISI 4340

Figure 4-74. Examples of Glass Bead Burnished APCVD Al Coatings Deposited at 246°C onAerMet 100 and AISI 4340 Specimens

The results of the **hydrogen embrittlement testing** in air and in salt solution for AISI 4340 steel and AerMet 100 specimens coated with APCVD Al deposited at the lower temperatures are summarized in Tables 4-29 and 4-30, respectively

The coatings deposited on AISI 4340 steel specimens at the lower temperatures of 230º and 246ºC behaved similarly to the coatings deposited at 275º and 300ºC (Figures 4-17 and 4-18); namely, the coating exhibited no signs of HE when tested in air, but failed when tested in a 3.5 % salt solution. The same behavior was observed with the coatings deposited on AerMet 100 specimens at 246ºC, which is consistent with the results shown in Figure 4-19, where both the APCVD Al coating deposited at 300ºC and the Cd-plated control passed the test done in air, but failed when tested in the salt solution.

In summary, the results obtained with the coatings deposited at the lower temperatures are promising, in so far as better performance was observed, but it is obvious that, to meet all the specified test criteria, a better understanding of the benefits of post-treatments (e.g., if glass bead burnishing is effective in modifying the properties in the coated notched areas on test specimens), and further optimization of the deposition parameters are needed to determine the optimum deposition temperatures and post-treatments for each high-strength alloy of interest.

Table 4-29. Results of Additional Hydrogen Embrittlement Testing for APCVD Al-Coated AISI 4340 Specimens

Coating	Substrate Material	Heat Treat (Hydrogen Relief)	Spec. No.	Avg. Notch Tensile Strength (lbf)	Test Environment	Test Load % NTS	Total Hours	Spec. Fail?	Step Load?	Fail during Step Load?	Process Embrittling?
APCVD at 246C (475F) + Baked											
Aluminum Coated	4340 Steel	191C / 23hr	Y-5	8,462	Lab Air	75	200	No	N/A	N/A	No
			Y-6				200	No	N/A	N/A	
			Y-7				200	No	N/A	N/A	
			Y-8				200	No	N/A	N/A	
Aluminum Coated	4340 Steel	191C / 23hr	Y-9	8,462	3.5% Salt Soln	45	2.0	Yes	-	-	Yes
			Y-10				1.3	Yes	-	-	
			Y-11				3.0	Yes	-	-	
			Y-12				0.1	Yes	-	-	
APCVD at 246C (475F) + Baked + Glass Bead Peened + Chromate Conversion Coat											
Aluminum Coated	4340 Steel	191C / 23hr	W-9	8,570	Lab Air	75	200	No	N/A	N/A	No
			W-10				200	No	N/A	N/A	
			W-11				200	No	N/A	N/A	
			W-12				200	No	N/A	N/A	
Aluminum Coated	4340 Steel	191C / 23hr	W-13	8,570	3.5% Salt Soln	45	6.1	Yes	-	-	Yes
			W-14				7.6	Yes	-	-	
			W-15				0.3	Yes	-	-	
			W-16				1.2	Yes	-	-	
APCVD at 230C (446F) + Baked + Glass Bead Peened + Chromate Conversion Coat											
Aluminum Coated	4340 Steel	191C / 23hr	Z-5	8,693	Lab Air	75	46.2	Yes	-	-	Yes
			Z-6				200	No	-	-	
			Z-7				200	No	-	-	
			Z-8				79.7	Yes	-	-	

Table 4-30. Results of Additional Hydrogen Embrittlement Testing for APCVD Al-Coated AerMet 100 Specimens

Coating	Substrate Material	Heat Treat (Hydrogen Relief)	Spec. No.	Avg. Notch Tensile Strength (lbf)	Test Environment	Test Load % NTS	Total Hours	Spec. Fail?	Step Load?	Fail during Step Load?	Process Embrittling?
APCVD at 246C (475F) + Baked + Glass Bead Peened											
Aluminum Coated	AerMet 100	191C / 23hr	X-9	10,827	Lab Air	75	200	No	N/A	N/A	No
			X-10				200	No	N/A	N/A	
			X-11				200	No	N/A	N/A	
			X-12				200	No	N/A	N/A	
Aluminum Coated	AerMet 100	191C / 23hr	X-13	10,827	3.5% Salt Soln	45	0.3	Yes	-	-	Yes
			X-14				0.4	Yes	-	-	
			X-15				0.7	Yes	-	-	
			Z-16				0.6	Yes	-	-	

5.0 Technology Transfer

Successful technology transfer and implementation will depend on many factors, two of which are: (1) the compatibility of the APCVD Al coating process with the materials commonly used on aircraft that currently require a Cd coating; and (2) the robustness of the process and its demonstrated ability to coat discrete small parts and other components. This section discusses these two important technology transfer issues.

5.1 Suitable Substrate Materials and Applications

The main concern with using an APCVD Al process - as originally configured - was the need to apply the coating at an elevated temperature, typically about 300°C (572°F). Section 7.1.8 summarizes the findings from the survey of the effect of tempering temperature on mechanical properties of many high-strength steels and alloys, which were of interest as substrate materials that could be coated with APCVD Al for a range of applications. Based on the survey results, if a deposition temperature of 300°C is used as the guideline, it will soften the highest strength steels too much (below performance requirements). However, there are other high-strength steels that could be used. The best possible applications for APCVD Al (if deposition temperature cannot be lowered from ~300°C) are for steels that can be tempered above 400°C. For example, components could be made from:

- AISI 4130 steel at 160-180 ksi UTS for brackets and fasteners
- AF1410 alloy at 220-250 ksi UTS for landing gear parts
- 300M steel at 260-280 ksi UTS for landing gear parts
- AerMet 100 alloy at 280-300 ksi UTS for landing gear parts.

The selection of the best candidates was based on the assumption that the maximum deposition temperature would not exceed 191ºC (375ºF) because most aerospace engineers define the allowable maximum temperature for shot peened, high-strength steels as the hydrogen relief (or bake) temperature of 191ºC, held for 23 hours, and for Cd-plated steels, the maximum allowable temperature is 207ºC (405ºF) to prevent liquid metal embrittlement[27].

However, as Tables 5-1 and 5-2 show, the accepted government design allowables in the "Metallic Materials Properties Development and Standardization" (MMPDS)[28] document and military specification MIL-S-13165 (now AMS 2430N[29]), indicate that for many alloys of interest in this Project, and the anticipated deposition times, the allowable temperature is as high as 246ºC (475ºF).

The upper temperature limit defined in MMPDS is about 56ºC (100ºF) below the tempering temperature to achieve the designated strength for a specific alloy. The allowable length of time at the temperature limit is ~1 hour per 2.54 cm (1 inch) of thickness, or ~0.5 hour for 1.27 cm (0.5 inch) of thickness or less, without a reduction in strength occurring. Specification MIL-S-13165/AMS 2430N permits the temperature limits shown in Table 5-1 for shot peened, high-strength steels, but as mentioned above, it is usually arbitrarily set as the hydrogen relief temperature of 191ºC (375ºF). Table 5-2 includes the allowable temperatures for materials other than high-strength steels referenced in MIL-S-13165/AMS 2430N.

---

[27] K. Legg, Rowan Technology Group, personal communication to E. Berman (9 May, 2008).
[28] MMPDS-03, Federal Aviation Administration (October, 2006).
[29] Aerospace Material Specification AMS 2430N, "*Shot Peening, Automatic*", (June, 2008).

Table 5-1. Allowable Temperatures for Some High-strength Aerospace Alloys

Alloy	Strength (ksi)	Shot Peened	Temp. Limit °C	Temp. Limit °F	Notes and Data Sources
AISI 4340	260-280	Yes	246 191 177	475 375 350	MIL-S-13165/AMS 2430N Hydrogen bake 375°F, 23hr AMS 2448 for HVOF on HSS
		No	177	350	MMPDS 03 Table 2.3.0.3 MIL-H-6875 heat treat 425-500°F
AISI 4340	180-200	Yes	246	475	MIL-S-13165/AMS 2430N
		No	427	800	MMPDS 03 Table 2.3.0.3
300M	270-280	Yes	246 191 177	475 375 350	MIL-S-13165/AMS 2430N Hydrogen bake 375°F, 23hr AMS 2448 for HVOF on HSS
		No	245	475	MMPDS 03 Table 2.3.0.3
AerMet 100	260-280	Yes	246 191 177	475 375 350	MIL-S-13165/AMS 2430N Hydrogen bake 375°F, 23hr AMS 2448 for HVOF on HSS
		No	416	780	100°F below tempering temperature
15-5PH,17-4PH	H900, 190	Yes	246	475	MIL-S-13165/AMS 2430N
		No	427	800	MMPDS
Al alloys		Yes	93	200	MIL-S-13165/AMS 2430N

Table 5-2. Allowable Temperatures for Some Shot Peened Aerospace Alloys

Part Materials	Maximum Temperature* °C	Maximum Temperature* °F
Aluminum-based Alloys	93	200
Cobalt-based Alloys	538	1,000
Magnesium-based Alloys	93	200
Nickel-based Alloys	538	1,000
Corrosion Resistant Steel Alloys**	245-399	475-750
Steel Alloys***	149-246	300-475
Titanium-based Alloys	246	475

* Per MIL-S-13165.
** 246°C/475°F for PH steels and cold worked 300 series stainless steels.
*** 149°C/300°F for steel parts that are tempered below the recommended 475°F maximum after a quench hardening operation.

Table 5-3 summarizes the data from Section 7.1.8 that discusses the effects of temperature on the strength of many materials used in the aerospace industry, and shows the approximate difference (loss in tensile strength) in depositing the coatings at 300ºC as opposed to 246ºC.

Table 5-3. Approximate Loss in Design Allowable Tensile Strength at 246°C and 300°C for Selected Materials

Material	Approximate Ultimate Tensile Strength (ksi)				
	Room Temp.	246°C (475°F)	Ave. Loss Δ(RT-246)	300°C (572°F)	Ave. Loss Δ(RT-300)
AISI 4130*	255	245	4.9%	232	9.4%
AISI 4340	290	274	5.7%	260	10.2%
300M	340	302	8.6%	292	14.1%
15-5PH	190	163	14,2%	160	15.8%
AerMet 100	295	253	14.2%	247	16.3%

* Water quenched.

Based on the data given in Section 7.1.8 and Table 5-3, the following materials may be suitable candidates benefitting from the application of an APCVD Al coating to replace a Cd coating if the deposition temperature is lowered from 300ºC to 250ºC or lower:

- AISI 4130 steel
- AISI 4340 steel
- AF1410 alloy
- 300M steel
- AerMet 100 alloy.

However, AF 1410 is rarely used on newer aircraft, and currently only the U.S. Navy uses AerMet 100 (e.g., on the F/A-18 aircraft). If the deposition temperature could be lowered further, as the additional experiments with the new precursor have shown, then this list of suitable substrates might be expanded.

Ogden Air Logistics Center at Hill AFB, UT is responsible for the MRO operations on aircraft landing gear. They were contacted to provide guidance for the processing capabilities of the third generation APCVD Al deposition equipment. The information provided by knowledgeable personnel indicates that typical components are tubular and measure between 50 mm and 150 mm (2 in and 6 in) in diameter and from 650 mm to 915 mm (12 in to 36 in) long. Currently, the largest part handled has an od of ~75 mm (3 in) with an id of ~50 mm (2 in), and is ~1,300 mm (24 in) long. These parts require a Cd or approved alternative coating, typically 7.6 µm to 15.2 µm thick (0.3 mil to 0.6 mil), which must have passed hydrogen embrittlement, hydrogen re-embrittlement (ASTM F 519), and fatigue debit testing (ASTM E 466) requirements. A fixed, tubular reactor and special fixturing would be needed to coat such components.

The open literature, however, contains a reference[17] to a fixed, pilot scale, tubular reactor for the deposition of Al coatings using the MOCVD process, so designing a fixed APCVD process should not be difficult. The MOCVD system was designed and built at the Instituto Nacional de Técnica Aeroespacial. Dense and uniform MOCVD Al coatings (Figure 5-1) - about 12.5 µm (0.5 mil) thick - have been obtained after grinding and cleaning by vapor degreasing, then exposing the substrates to pure TIBAL at 300ºC at 1 mbar. These coatings are similar to those obtained on this project at the same temperature by the APCVD process in a rotating barrel reactor. The INTA MOCVD, as deposited coatings exhibited no corrosion after 100 hours exposure to salt fog.

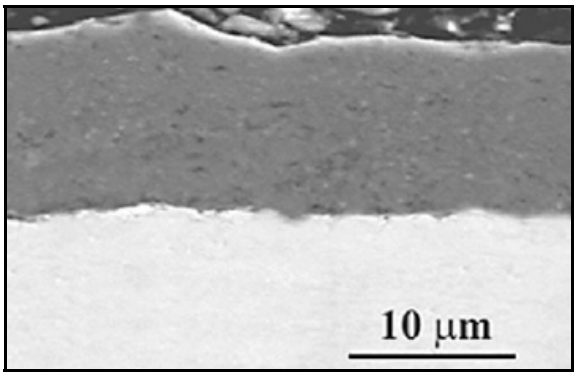

Figure 5-1. SEM Photomicrograph of an Aluminum Coating Deposited in the INTA MOCVD Process Pilot Plant

Figure 5-2 is a photograph of the MOCVD small pilot scale deposition system. It is comprised of: (a) an evaporator for the TIBAL precursor, and (b) a 500 mm tall, 180 mm diameter, vertical deposition chamber heated by a three zone furnace in order to achieve a uniform temperature in the deposition zone. This unit has a pumping system that allows working pressures in the range of 0.1–100 mbar. Stated important advantages of this particular process are: (i) the possibility of recovering the un-reacted precursor; as well as (ii) the byproduct isobutylene produced in the process by means of (c) a condenser, and (d) a cryogenic trap, respectively. The system can be manually or automatically controlled, and can be easily modified to deposit other materials. Notice the similarity with the small AkzoNobel, bench-scale APCVD system (Figure 3-8) used in this project.

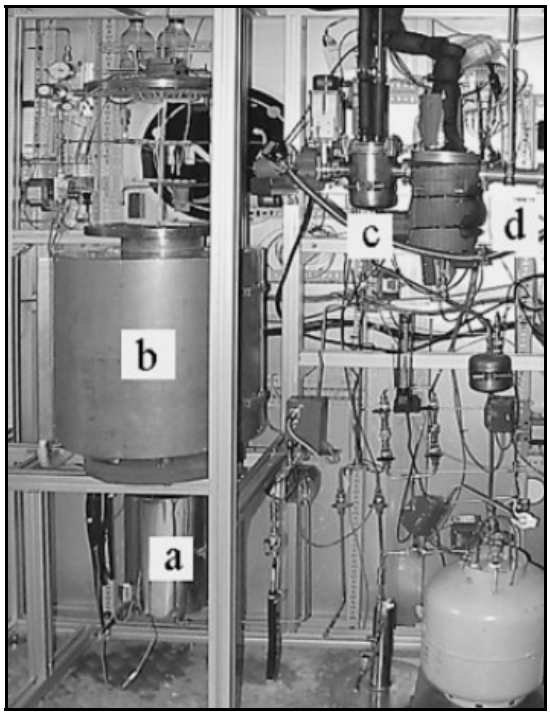

Figure 5-2. MOCVD Pilot Plant with a Fixed,

Vertical Reactor for Depositing Al-based Coatings

As with any other type of CVD process, coatings can be deposited on complex geometry components, such as in the cooling passages of turbine blades, and on the inner surfaces of heat exchanger tubes. Three potential industrial applications of these coatings have been explored by INTA, namely: (1) the protection of Ni- and Co-based super-alloys in gas turbine engines; (2) the protection of ferritic-martensitic steels for steam turbine components; and (3) the replacement of Cd coatings used for corrosion protection.

INTA currently is attempting to lower deposition temperatures, and have found they obtain better results at reduced pressure using a primary pump[30]. Also, INTA has investigated the possible hazard of using TIBAL, and concluded that, because this chemical is a Ziegler Natta co-catalyst widely used in plastic manufacturing, handling it is "pretty much under control"[30], and states that TIBAL is easier to work with than hydrogen (often used as the fuel on HVOF processes) because leaks are easily detected and dealt with. With respect to coating cost, INTA found that truck (tanker) loads of TIBAL are available at "very low prices".

A note of caution is warranted when considering the implementation of an APCVD Al process for MRO and other operations. Ogden ALC personnel have stated[31] that in the past they have used IVD Al coatings on some high-strength steel parts to provide corrosion resistance "with disastrous results". In "wet" areas the Al coating dissolved too fast, causing a buildup of hydrogen in the substrate, and subsequent hydrogen embrittlement. Consequently, they use IVD Al coatings only in dry areas, and still use a Cd-plated coating for wet areas. This would suggest that - by analogy - the corrosion rate of APCVD Al coatings must be controlled (by composition or post-treatments) if they are to be used in wet areas.

Finally, it should be remembered that the primary focus of this project was on coating high-strength steels and alloy substrates used in the DoD and aerospace industry, but the process is considered to be a dual use technology. The APCVD Al process already can be used on a wide range of other substrates, including lower strength steels, corrosion resistant steels, Co-based alloys, and Ni-based alloys (see Table 5-2, for example), and is being used to coat steel fasteners and other small components for a variety of markets and applications (e.g., automotive, general transportation, industrial machinery).

5.2 Status of APCVD Process Commercialization

The APCVD Al deposition is robust enough that a commercial coating unit is available, operating at a deposition temperature of 300 ±10ºC, from the Project's commercialization partner AkzoNobel Chemicals (see Section 3.2.3). Commercial units have been operated as low as 240 ±10ºC, but at lower temperatures the coating rate decreases and coating adhesion can be adversely affected.

Also, to date, the commercial/production units have employed a rotating, cylindrical reactor. A fixed reactor chamber is possible, and with suitable fixturing, longer, cylindrical parts could be coated. However, the scale up of this type of deposition equipment would require additional development work, and would require some assurance of an adequate market to justify expending the funds to accomplish this.

[30] A. Agüero, Instituto Nacional de Técnica Aeroespacial, Spain, personal communication to E. Brooman (February, 2006).
[31] T. Layne, 309 CMXG/ENL, Hill AFB, UT, personal communication to J. Kleek (August, 2007).

The first production scale unit for coating fasteners and other comparable small components has been installed at the production site of one of AkzoNobel's strategic development partners in the United States. AkzoNobel expects to make the production unit available for commercial operation and/or contract work towards mid-2009 as part of their commercialization and market development strategy. In addition, pending the success of this production unit, engineering solutions for greater capacity plants and/or larger substrate capability will be considered. However, the design and manufacture of alternative deposition equipment will require additional technical development work, and - as stated above - would require a business model with some assurance of sufficient market interest to justify the investment.

6.0 Conclusions and Recommendations

The overall objective of this SERDP funded program is to investigate the use of APCVD to produce high quality Al coatings to protect high-strength steels from corrosion. In the first Annual Report [19], it was reported that Al coatings produced using a TIBAL precursor exhibited better properties than a TEAL precursor. In the second Annual Report, it was reported that further work was carried out on Al coatings deposited on high-strength steels using pure TIBAL at 275º and 300ºC, and using a proprietary TIBAL blend, PB1 at 300ºC. Additionally, corrosion, throwing power, tensile strength, and preliminary electrical conductivity, hydrogen embrittlement, and lubricity tests were performed on the APCVD Al coatings. The results were encouraging, and the third year effort was continued. In the third Annual Report, it was reported that:

1. A post deposition hydrogen relief bake (as used with Cd-plated coatings) is needed to provide acceptable properties (e.g., no adverse substrate effects on lowering resistance to environmentally enhanced cracking, such as hydrogen embrittlement)
2. APCVD Al coatings are not as lubricious as Cd-plated coatings, but a small amount of exposure to operating environments (e.g., surface corrosion) can reduce the coefficient of friction into an acceptable range
3. APCVD Al coatings can meet the requirement for a Type I, Class 1 Cd coating in neutral salt fog testing
4. Painted APCVD Al coatings exhibit no loss of adhesion for the exposure time used in neutral salt fog testing
5. APCVD Al coatings exhibit better corrosion resistance in the cyclic corrosion test if treated with a commercial Cr(III)-based (TCP) treatment
6. The effect of coating deposition parameters on introducing a fatigue debit for high-strength steel substrates has been investigated, with deposition temperature being an important process parameter in softening some of the substrate materials
7. A prototype, commercial APCVD reactor has been built and is being commissioned for providing Al coatings on small discrete parts for the automotive and other industry sectors: this development indicates that the basic deposition technology is maturing, which will facilitate technology transitioning to the aerospace industry sector.

The findings from the added subtasks to investigate the feasibility of lowering the deposition temperature to 250ºC, or less, expanded the knowledge base about the utility of the APCVD Al deposition technology. These findings are included in the overall project conclusions, given in Section 6.1.

In addition, there are recommendations in Section 6.2 for additional, follow on work that could have the greatest impact on technology acceptance and insertion, as well as the range of applications for which APCVD Al coatings can offer significant benefits as a replacement for cadmium coatings.

6.1 Conclusions

The conclusions from this project - based on all the results obtained for the APCVD Al coatings - may be summarized as follows:

1. Overall, the APCVD Al coating process and coatings exhibit comparable or better performance and properties than IVD Al and electroplated Al coatings, and meet most of the property and performance required of Cd-plated coatings.

2. APCVD Al coatings are dense, with a roughness on a nano-scale when deposited at 275º to 300ºC. For the non-optimized coatings deposited at 230º to 246ºC, the coatings are sometimes nodular, and similar to those observed with Cd-plated and IVD Al coatings.
3. The thickness of the APCVD Al coatings can be controlled to conform to the range in SAE AMS QQ-P-416, which is the specification governing Cd plating. Thinner or thicker coatings may be deposited, but properties and performance may be affected.
4. APCVD Al coatings exhibit excellent throwing power and conformal coverage, with uniform thickness distribution on complex shapes, and inside and outside diameters of cylindrical parts and holes of all sizes.
5. APCVD Al coatings exhibit an XRD pattern identical to that for an Al powder reference material (fcc polycrystalline structure). The grains are equi-axed and not columnar, as found with IVD Al, sputtered Al, and Cd-plated coatings.
6. APCVD Al coatings are oxidized on the surface (thin film) and relatively pure within the bulk (>250 nm); concentrations of C, H and O in the surface layers (0-25 nm) seem to be independent of the deposition temperatures. Coatings deposited from blended TIBAL precursors, tend to have a higher oxygen contamination.
7. APCVD Al coatings exhibit good adhesion to the steel substrates used and provide a good surface to accept primers and top coats, if required.
8. Nano-hardness was measured, although it is not considered to be a critical parameter for applications of interest to this project. Measurements yielded an average value of ~550 MPa for the APCVD Al coatings, compared to an average of about 835 MPa for an Al single crystal used as a reference material. The calculated Young's Modulus was between 21.4 and 51.2 GPa, compared to 70 GPa for bulk Al metal and IVD Al coatings.
9. The electrical resistivity of the APCVD Al coatings is acceptable for the anticipated Air Force applications.
10. A post deposition, hydrogen relief bake (as specified for Cd-plated coatings) is needed to provide no adverse effects on the substrate with respect to their resistance to environmentally enhanced cracking (e.g., hydrogen embrittlement) or fatigue debit.
11. APCVD Al coatings are not as lubricious as Cd-plated coatings, but similar to IVD Al coatings. A short exposure to operating environments (e.g., surface oxidation/corrosion) can reduce the coefficient of friction from about 1.0 to 0.6; however, further testing is required to confirm this observation.
12. APCVD Al coatings can meet the requirements for a Type I, Class 1 Cd-plated coating in neutral salt fog testing. However, coating optimization will be necessary to demonstrate that this type of Al coating can perform well in a salt fog environment for at least 1,000 hours, as has been demonstrated for electroplated Al coatings.
13. Painted APCVD Al coatings exhibited no loss of adhesion for the exposure times used in neutral salt fog testing.
14. APCVD Al coatings provide good sacrificial (galvanic) protection to the high-strength alloys studied. Glass bead burnishing does not seem to provide any benefit with respect to the corrosion potential in a 3.5% salt solution, or to the polarization resistance.
15. Results from the fluid compatibility testing were positive: the APCVD Al coupons that had received the standard hydrogen relief bake fared much better than those that had not, and those with the TCP commercial Cr(III) CCC conversion coating performed better than the as deposited coatings with none. The exception was with a hydrogen peroxide-based paint stripper, where corrosion attack of the Al was significant, and whisker like crystals grew all over the exposed surfaces. However, peroxide-based strippers are not used much in DoD MRO operations, so this does not constitute a barrier to implementing the APCVD process.

16. APCVD Al coatings exhibit good corrosion resistance in the accelerated (cyclic) corrosion test, especially if treated with a TCP after deposition.
17. APCVD Al coatings on AISI 4340 steel and AerMet 100 specimens provide good resistance to substrate hydrogen embrittlement when tested in air, but not in deionized water or a salt solution - however, some of the Cd-plated controls also failed in this performance test. Initial data for coatings deposited at 230º to 246ºC exhibited a similar performance to those deposited at the higher temperatures. Any benefits from glass bead burnishing need to be investigated further.
18. APCVD Al coatings deposited at 300ºC had no adverse effect on substrate susceptibility to stress-corrosion cracking if they had received a standard hydrogen relief bake.
19. The effect of APCVD Al coating deposition parameters on introducing a fatigue debit for high-strength steel substrates also has to be investigated further. Initial data for coatings deposited at 275º to 300ºC showed they introduce a significant fatigue debit on high-strength steels, but coatings deposited at 230º to 250ºC gave more promising results, and optimized coatings may meet the acceptance criterion for this property.
20. A prototype, commercial APCVD reactor has been built and is being commissioned for providing Al coatings on small discrete parts for (but not limited to) the automotive industry sector: this development indicates that the basic deposition technology is maturing and robust, which will facilitate technology transitioning to the aerospace industry sector.

6.2 Recommendations for Future Work

Overall, the property and performance test results obtained for coatings deposited over a range of temperatures - and summarized in Table 6-1 - indicate that the APCVD process and APCVD Al coatings have demonstrated sufficient promise that further optimization and demonstration and validation activities should be conducted for one or more selected end use applications. Suggestions for follow on efforts are listed below.

1. Explore further the use of precursor blends to deposit coatings at, or below 250ºC and optimize the *properties* of such coatings. Emphasis should be placed on: (a) coating integrity, especially eliminating porosity and other defects that can lead to problems with corrosion attack, and excessive nodular growth; (b) coating purity, especially lowering surface contaminants and the uptake of hydrogen from the processing steps that can cause hydrogen embrittlement; and (c) controlling surface composition – with or without post-treatments – to provide a low coefficient of friction.
2. Explore further the use of precursor blends to deposit coatings at, or below 250ºC and optimize the *performance* of such coatings. Emphasis should be placed on: (a) minimizing any adverse effects on the (ultimate tensile and notch fracture) strength of steels heat treated to 200 ksi, or higher that could cause an unacceptable fatigue debit, or increase the susceptibility to hydrogen embrittlement; (b) the potential for hydrogen re-embrittlement for the best coatings obtained; and (c) improving the corrosion resistance, especially extending the life to 1,000 hr or more in the ASTM B 117 salt fog test.
3. In parallel with the above, work should continue - with the cooperation of this Project's commercialization partner - to explore different reactor designs to facilitate the coating of larger and heavier parts, and to monitor progress with the commercial APCVD Al coating unit on site at a facility in the Chicago area.

Table 6-1. Summary of the Ability of APCVD Al Coatings to meet Property and Performance Requirements for High-strength Steel Substrates

Property/Performance Requirement	Status	Comments
Thickness	Acceptable	Easily controlled by adjusting deposition time
Throwing Power	Acceptable	Excellent; good conformal coverage
Surface Roughness	Some improvement needed	For coating thickness in range of interest, excellent for deposition temperatures of 275-300ºC: coatings deposited at 230-246ºC need to be optimized
Structure	Acceptable	Not columnar
Porosity/Defects	Some improvement needed	Similar to Cd-plated and IVD Al coatings; coatings need to be optimized to reduce possible sites for corrosion attack: post-treatments can be beneficial
Composition	Some improvement needed	Some surface contamination; primarily carbon and oxygen, but some hydrogen also detected: concentrations depend on precursor and deposition temperature
Adhesion	Acceptable	
Coefficient of Friction	Acceptable	Comparable to IVD Al, but higher than plated Cd
Electrical Resistivity	Acceptable	If needed for contacts or bonding
Tensile/Notch Fracture Strength/ Fatigue Strength	Mixed results: some improvement needed	Some high-strength steels are softened too much when coatings deposited at 275-300ºC, leading to an excessive fatigue debit: data for coatings deposited at 230-246ºC show promise to meet deficit guidelines: additional testing and coating optimization required
Hydrogen Embrittlement	Mixed results: some improvement needed	Coatings pass when tested in air, irrespective of deposition temperature, but fail when tested in deionized water or a salt solution; however, some Cd-plated controls also failed in these tests
Galvanic Protection	Acceptable	Comparable to plated Cd, IVD Al and electroplated Al
Electrochemical/Corrosion Properties	Acceptable	Comparable to plated Cd, IVD Al and electroplated Al
Compatibility with MRO Fluids	Acceptable	Only problem found in this study was with a peroxide-based paint stripper, which is not often used in MRO operations
Salt Fog Resistance	Some improvement needed	Passed the test criteria, but test duration needs to be extended to 1,000 hr or more to match electroplated Al
Cyclic Corrosion Resistance	Acceptable	Better than electroplated Al in this study
Stress-corrosion Cracking	Acceptable	No adverse effects of coating observed for 300ºC deposition temperature studied

7.0 Appendices

This section contains supporting information - including test data, published related materials property data, charts, plots, and graphics - that have not been included in the main body of text, but are necessary to support some of the observations, conclusions, and recommendations that are made in this Final Report.

7.1 Effect of Temperature on High-strength Alloy Substrate Properties

A survey was conducted on the tempering temperature and the effect service temperature on the mechanical properties of certain high-strength steels (AISI 4130, AISI 4340, and 300 M, H11 Modified), LESCALLOY® AF1410, AerMet® 100, and AerMet® 310) that are used for parts in aircraft. This knowledge provides guidance for selecting substrates suitable for the APCVD Al process with respect to current process deposition temperatures. Data for mechanical properties at various tempering temperatures for AISI 4130, AISI 4340, 300 M, and H11 Modified are well established, and are presented in this survey. As for AF 1410, AerMet 100, and AerMet 310, the published data available are limited, but some mechanical properties are presented here.

Structural steels with very high strength levels are often referred to as ultrahigh-strength steels. The commercial structural steels that are capable of a minimum yield strength of 1,380 MPa (200 ksi) are commonly called high-strength steels[32, 33]. AISI 4130, AISI 4340, and 300M are classified as medium-carbon, low alloy, ultrahigh-strength steels. 300 M steel is a modification of AISI 4340 (i.e., greater silicon content). Table 7-1 gives the compositions of these steels.

Table 7-1. Compositions of the Medium-carbon, Low-alloy, Ultra-high-strength Steels

Steels	Composition, wt %									Ref.
	C	Mn	Si	Cr	Ni	Mo	V	P	S	
AISI 4130	0.28 -0.33	0.40 -0.60	0.20 -0.35	0.80 -1.10	-	0.15 -0.25	-	≤0.035	≤0.040	30
	0.28 -0.33	0.40 -0.60	0.15 -0.35	0.80 -0.11	-	0.15 -0.25	-	≤0.035	≤0.040	31
AISI 4340	0.38 -0.43	0.60 -0.80	0.20 -0.35	0.70 -0.90	1.65 -2.00	0.20 -0.30	-	≤0.035	≤0.040	30
	0.37 -0.43	0.70	0.23	0.70 -0.90	1.83	0.20 -0.30	-	≤0.035	≤0.040	31
300M	0.40 -0.46	0.65 -0.90	1.45 -1.80	0.70 -0.95	1.65 -2.00	0.30 -0.45	≥0.05	≤0.035	≤0.040	30
	0.40 -0.46	0.65 -0.90	1.45 -1.80	0.70 -0.95	1.65 -2.00	0.30 -0.45	≥0.05	≤0.035	≤0.04	31

H11 Modified (H11 Mod) alloy is a modification of the martensitic, hot work die steel AISI H11, the significant difference being a slightly higher carbon content. AF1410 alloy was developed specifically to have high strength, excellent fracture toughness, and excellent weldability when heat treated to 235 to 255 ksi ultimate tensile strength. AerMet 100 is a higher strength derivative of AF1410. AerMet 310 alloy possesses higher hardness and strength than AerMet 100 alloy, while maintaining exceptional ductility and toughness.

[32] T. V. Philip, "*Ultrahigh-Strength Steels*", Metals Handbook, 9th Edition, Volume 1: Properties and Selection: Irons, Steels, and High-Performance Alloys, ASM International, Materials Park, OH (1978).
[33] Company web site, http://www.aerospacemetals.com/steelalloys.html, Aerospace Specification Metals, Inc. (2007).

Alloys with maximum service temperatures to 400ºC (750ºF) include AF 1410/high carbon AF1410, AerMet 100, AerMet 310, and MP35N alloy. The compositions of H11, AF1410, AerMet 100, and AerMet 310 are listed in Table 7-2 below[34, 35].

Table 7-2. Compositions of the Ultra-high-strength Steels

Steels	Composition, wt %													Ref.
	C	Mn	Si	Cr	Ni	Mo	V	P	S	Cu	Co	Ti	Al	
H11 Mod	0.38-0.43	0.20-0.40	0.80-1.00	4.75-5.25	≤0.25	1.20-1.40	0.40-0.60	≤0.02	≤0.02	≤0.35	-	-	-	32
AF1410[a]	0.13-0.17	≤0.10	≤0.10	-	9.50-10.50	0.90-1.10	-	≤0.008	≤0.005	1.80-2.20	13.50-14.50	≤0.015	≤0.015	32
AerMet 100	0.23	-	-	3.10	11.10	1.20	-	-	-	-	13.40	-	-	33
AerMet 310	0.25	-	-	2.40	11.00	1.40	-	-	-	-	15.00	-	-	33

(a) O = 0.0015 %; N = 0.0015 %.

A brief description of the properties of the high-strength steels of interest in this project follows.

7.1.1 AISI 4130 Steel

This heat-treatable low-alloy steel has relatively low hardenability; nevertheless, it is one of the most popular alloy steels because of its good formability and weldability, along with an excellent combination of mechanical properties. It is recommended for use at temperatures up to 357ºC (700ºF) because its strength decreases markedly with increasing temperatures above this level. This steel is not subject to temper embrittlement, and can be nitrided. Table 7-3 summarizes some typical mechanical properties of AISI 4130 steel bars (25 mm diameter) het treated at various tempering temperatures[32].

The mechanical properties of various diameters of rods with tempering temperatures[31] are listed in Table 7-4.

The standard heat treatments applying to AISI 4130 are as follows [32, 34]:

- **Normalize**: heat to 870-925ºC and hold for a time that depends on section thickness; air cool (tempering at 480ºC or above is often done after normalizing to increase yield strength)
- **Anneal**: heat to 830-860ºC and hold for a time that depends on section thickness or furnace load; furnace cool
- **Harden**: Heat to 845-870ºC and hold, then water quench; or heat to 860-885ºC and hold, then oil quench (holding time depends on section thickness)
- **Temper**: heat at least 0.5hr at 200-700ºC; air cool or water quench (temperature and time at temperature depend mainly on desired hardness or strength level).

[34] Aerospace Structural Metals Handbook (1991 Edition), Code 1201 for AISI 4130 steel, Code 1206 for AISI 4340 steel, Code 1217 for 300 M, Metals and Ceramics Information Center, Columbus, OH (1991).
[35] Company web site; http://www.cartech.com/products/wr_products_aero_100.html, Carpenter Technology Corp., 2 Meridian Blvd., Wyomissing, PA (2007).

Table 7-3. Typical Mechanical Properties and Tempering Temperatures for AISI 4130

Tempering Temperature		Tensile Strength		Yield Tensile Strength		Elongation in 50 mm	Reduction in area	Brinnell Hardness
°C	°F	MPa	ksi	MPa	ksi	%	%	HB
Water Quenched and Tempered [(a)]								
205	400	1,765	256	1,520	220	10.0	33.0	475
260	500	1,670	242	1,430	208	11.5	37.0	455
315	600	1,570	228	1,340	195	13.0	41.0	425
370	700	1,475	214	1,250	182	15.0	45.0	400
425	800	1,380	200	1,170	170	16.5	49.0	375
540	1,000	1,170	170	1,000	145	20.0	56.0	325
650	1,200	965	140	830	120	22.0	63.0	270
Oil Quenched and Tempered [(b)]								
205	400	1,550	225	1,340	195	11.0	38.0	450
260	500	1,500	218	1,275	185	11.5	40.0	440
315	600	1,420	206	1,210	175	12.5	43.0	418
370	700	1,320	192	1,120	162	14.5	48.0	385
425	800	1,230	178	1,030	150	16.5	54.0	360
540	1,000	1,030	150	840	122	20.0	60.0	305
650	1,200	830	120	670	97	24.0	67.0	250

(a) 25 mm diameter round bars quenched from 845 to 870°C (1,550 to 1,600°F).
(b) 25 mm diameter round bars quenched from 860°C (1,575°F).

Table 7-4. Mechanical Properties and Tempering Temperature for AISI 4130 Steel Water Quenched at 855°C

Tempering Temperature		Rod Diam.	Notch Fracture Strength		Yield Tensile Strength		Elongation in 50 mm	Reduction in Area	Hardness	
°C	°F	mm (in)	MPa	Ksi	MPa	ksi	%	%	HB	HRC
480	900	13 (0.5)	1,145	166	1,110	161	16.4	61	331	36
		25 (1.0)	1,110	161	951	138	14.7	54.5	321	35
		50 (2.0)	917	133	758	110	19.0	63.0	269	27
		100 (4.0)	841	122	655	95	20.5	63.6	241	22
540	1,000	13 (0.5)	1,040	151	979	142	18.1	63.9	302	32
		25 (1.0)	993	144	896	130	18.5	61.8	293	31
		50 (2.0)	841	122	685	99.4	21.2	66.3	241	22
		100 (4.0)	800	116	635	92.1	21.5	63.5	235	21
595	1,100	13 (0.5)	917	133	841	122	20.7	69.0	269	27
		25 (1.0)	883	128	779	113	21.2	67.5	262	26
		50 (2.0)	786	114	635	92.1	21.7	67.7	229	19
		100 (4.0)	703	102	540	78.3	24.5	69.2	197	13

Typical applications of 4130 steel are automotive connecting rods, engine mounting lugs, shafts, fittings, bushings, gears, bolts, axles, gas cylinders, airframe components, hydraulic lines, and nitrided machinery parts.

7.1.2 AISI 4340 Steel

AISI 4340 steel is considered to be the standard to which other ultrahigh-strength steels are compared. It is immune to temper embrittlement, and does not soften readily at elevated

temperatures; i.e., it exhibits good retention of strength. Hydrogen embrittlement is a problem for 4340 steel heat treated to tensile strengths greater than about 1,240 MPa (180 ksi). Parts exposed to hydrogen - such as during pickling and plating - should be subsequently hydrogen relief baked. 4340 steel exhibits extremely poor resistance to stress-corrosion cracking when tempered to tensile strengths of 1,500 to 1,950 MPa (220 to 280 ksi). The steel can be readily nitrided, which often improves fatigue life. Mechanical properties of AISI 4340 with tempering temperatures[32] are given in Table 7-5. The mechanical properties of various diameters of rods with tempering temperatures[33] are listed in Table 7-6.

Table 7-5. Typical Mechanical Properties and Tempering Temperatures for AISI 4340

Tempering Temperature*		Tensile Strength		Yield Tensile Strength		Elongation in 50 mm	Reduction in Area	Hardness	
°C	°F	MPa	ksi	MPa	ksi	%	%	HB	HRC
205	400	1,980	287	1,860	270	11	39	520	53
315	600	1,760	255	1,620	235	12	44	490	49.5
425	800	1,500	217	1,365	198	14	48	440	46
540	1,000	1,240	180	1,160	168	17	53	360	39
650	1,200	1,020	148	860	125	20	60	290	31
705	1,300	860	125	740	108	23	63	250	24

* Oil quenched from 845°C (1,550°F) and tempered at various temperatures.

Table 7-6. Mechanical Properties and Tempering Temperatures for AISI 4340 Steel

Tempering Temperature		Rod Diam.	Tensile Strength		Yield Tensile Strength		Elong. 50 mm	Redn. in Area	Hardness	
°C	°F	mm (in)	MPa	ksi	MPa	ksi	%	%	HB*	HRC*
Oil quenched 855°C (1,570°F), tested at -255°C (-430°F)										
230(4hr)	450 (4hr)	N.A.	2,290	332	-	-	0.6	0.2	851 Knoop	818 Vickers
Oil quenched 855°C (1,570 °F), tested at -195°C (-320°F)										
230	450	N.A.	2,200	319	1,915	278	10	24	666 Knoop	639 Vickers
Oil quenched 855°C (1,570°F), tested at -78°C (-108°F)										
230	450	N.A.	2,020	293	1,935	281	12	40	572 Knoop	548 Vickers
Oil quenched 855°C (1,570°F), tested at 26°C (79°F)										
230	450	N.A.	1,855	269	1,550	225	12	40	555 Knoop	531 Vickers
Oil quenched 845°C (1,553°F), tested at 25°C (77°F)										
425	800	N.A.	1,595	231	1,475	214	12	46	-	-
650	1,200	N.A.	1,005	146	938	136	20	60	-	-
Oil quenched 800°C (1,470°F)										
540	1,000	13 (0.5)	1,255	182	1,165	169	13.7	45	363	40
		25 (1.0)	1,207	175	1,145	166	14.2	45.9	352	39
		50 (2.0)	1,172	170	1,103	160	16	54.8	341	37
		100 (4.0)	1,138	165	1,000	145	15.5	53.4	331	36
595	1,100	13 (0.5)	1,145	166	1,117	162	17.1	57	331	36
		25 (1.0)	1,138	165	1,096	159	16.5	54.1	331	36
		50 (2.0)	1,014	147	958	139	19	60.4	293	31
		100 (4.0)	924	134	786	114	19.7	60.7	269	27
650	1,200	13 (0.5)	1,000	145	938	136	20	59.3	285	30
		25 (1.0)	958	139	883	128	20	59.7	277	28
		50 (2.0)	931	135	834	121	20.5	62.5	269	294
		100 (4.0)	855	124	731	106	21.7	63	255	25

* Unless otherwise indicated.

The standard heat treatments for AISI 4340 steel are as follows[32, 34]:

- **Normalize**: heat to 845-900ºC (1,550-1,650ºF) and hold for a time period that depends on section thickness; air cool
- **Anneal**: heat to 830-860ºC (1,525-1,575ºF) and hold for a time period that depends on section thickness or furnace load; furnace cool
- **Harden**: heat to 800-845ºC (1,475-1,550ºF) and hold 15 minutes for each 25 mm of thickness (15 minutes are minimum); oil quench to below 65°C (150°F), or quench in fused salt at 200-210ºC (390-410ºF) and hold 10 minutes, then air cool to below 65ºC
- **Temper**: heat at least 0.5 hour at 200-650ºC (400-1,200ºF); air cool (temperature and time at temperature depend mainly on desired final hardness)
- **Bake**: to avoid hydrogen embrittlement, plated parts must be baked at least eight hours (preferably 23 hours) at 190-204ºC (375-400ºF) as soon after plating as possible.

Typical applications of 4340 steel include bolts, screws, and other fasteners; gears, pinions, shafts and similar machinery components; crankshafts and piston rods for engines; and landing gear and other critical structural members for aircraft.

7.1.3 300 M Steel

Alloy 300 M is a 4340 high-strength, low-alloy steel that has a silicon content of 1.6 %, and has slightly higher carbon and molybdenum contents, with some vanadium. This steel exhibits deep hardenability, and has ductility and toughness at tensile strengths of 1,860 to 2,070 MPa (270 to 300 ksi). The modifications provide resistance to softening during tempering, and they increase the tempering temperature range for tempered-martensite embrittlement (also known as “500ºF embrittlement”) to above 300ºC (600ºF). Consequently, 300 M generally is used after it has been oil quenched and then tempered at approximately 300ºC, which provides tensile strengths in the range of 270 - 300 ksi and good toughness. Because of the high silicon and molybdenum contents, 300M is particularly prone to decarburization.

During thermal processing, care should be taken to avoid decarburization, or the decarburized layer should be removed after processing. When heat treated to strength levels higher than 1,240 MPa (180 ksi), 300M is susceptible to hydrogen embrittlement. If the steel is properly baked after plating, the resulting improvement in properties is better than for 4340 steel of equal strength. The mechanical properties of 300 M with tempering temperatures[30] are listed below in Table 7-7.

Table 7-7. Typical Mechanical Properties and Tempering Temperatures for 300M Steel

Tempering Temperature*		Tensile Strength		Yield Tensile Strength		Elongation in 50 mm	Reduction in Area	Hardness
°C	°F	MPa	ksi	MPa	ksi	%	%	HRC
90	200	2,340	340	1,240	180	6.0	10.0	56.0
205	400	2,140	310	1,650	240	7.0	27.0	54.5
260	500	2,050	297	1,670	242	8.0	32.0	54.0
315	600	1,990	289	1,690	245	9.5	34.0	53.0
370	700	1,930	280	1,620	235	9.0	32.0	51.0
425	800	1,790	260	1,480	215	8.5	23.0	45.5

* 25 mm diameter round bars oil quenched from 860°C (1,575°F).

The standard heat treatments for 300M steel are as follows[32, 34]:

- **Normalize**: heat to 900-940ºC (1,650-1,725ºF) and hold for a time that depends on section thickness; air cool (if normalizing to enhance machinability, load into a tempering furnace at 650-675ºC (1,200-1,250ºF) before the steel reaches room temperature).
- **Harden**: traditionally the alloy has been hardened by austenitizing at 857-885ºC (1,575-1,625ºF) and oil quenching to below 71ºC (160ºF) or quenching in salt at 200-210ºC and holding for 10 minutes, then air cooling to 70ºC, or below.
- **Temper after Hardening**: heat for a minimum of two hours at 273-329ºC (525-625ºF), air cool; double tempering is recommended. (Tempering within this range provides the optimum combination of high strength and toughness; consequently, tempering at other temperatures is not normally recommended. This tempering procedure produces the best combination of high yield strength and high impact properties. Tempering outside the temperature range given above results in severe deterioration of properties. Like other heat-treatable low-alloy steels, tensile strength and hardness continuously decrease with increasing tempering temperatures up to about 650ºC (1,200ºF), while corresponding increases take place in ductility, except in the tempered-martensite-embrittlement range, which is about 357-468ºC (700-900ºF) for 300 M.

300 M is available as bar, sheet, plate, wire, tubing, forgings, and castings. Typical applications are aircraft landing gear, airframe parts, fasteners, and pressure vessels.

7.1.4 H11 Modified Steel

This steel is a modification of the martensitic, hot work die steel AISI H11, the significant difference being a slightly higher carbon content. H11 Mod can be heat treated to strengths exceeding 2,070 MPa (300 ksi). It is air hardening, which results in minimal residual stress after hardening. H11 Mod is a secondary hardening steel, and thus develops optimum properties when tempered at temperatures above 510ºC (950ºF). The high tempering temperatures used for this steel provide substantial stress relief and stabilization of properties, so that the material can be used advantageously at elevated temperatures.

Typical applications include aircraft landing gear components, airframe components, internal parts for steam and gas turbines, fasteners, springs, and hot work dies.

Parts to be used at elevated temperatures are commonly protected by nickel-cadmium plating. If this is done, baking to avoid hydrogen induced cracking (embrittlement) is usually specified. Alternatively, part surfaces may be protected from oxidation by hot dipping in Al, or by applying a heat resistant paint.

The following standard heat treatments for H11 Mod steel are:

- **Normalize**: this generally is not necessary; for effective homogenization, heat to about 1,065ºC (1,950ºF), soak one hour for each 25 mm of thickness; air cool and anneal immediately after the part reaches room temperature.
- **Anneal**: heat to 845-885ºC (1,550-1,625ºF) and hold to equalize temperature; cool very slowly in the furnace to about 480ºC (900ºF), then more rapidly to room temperature.
- **Harden**: preheat to 760-815ºC (1,400-1,500ºF), then raise the temperature to 995-1,025ºC (1,825-1,875ºF) and hold for 20 minutes plus five minutes for each 25 mm of thickness; air cool, which produces less distortion than oil quenching.

- **Temper**: heat at the secondary hardening temperature of about 510ºC (950ºF) for maximum hardness and strength, or above the secondary hardening peak to temper back to a lower hardness or strength. A minimum of one hour at temperature should be allowed, but preferably parts should be double tempered (two hours at temperature, cool to room temperature, then two hours more at temperature. A triple tempering is more desirable, especially for critical parts). For high temperature application, parts should be tempered at a temperature above the maximum service temperature to guard against unwanted changes in properties during service.
- **Stress Relief**: heat to 650-675ºC (1,200-1,250ºF); cool slowly to room temperature. This treatment often is used to achieve greater dimensional accuracy in heat treated parts by stress relieving rough machined parts, then finish machining, and finally heat treating to the desired hardness.
- **Nitride**: Finish machined and heat treated parts should be gas or liquid nitrided at a temperature of about 525ºC (980ºF). The depth of the nitrided case is a function of time.
- **Bake**: after plating in an acid bath, or after other processing that might introduce hydrogen into the metal, parts should be baked for 23 hours or longer at 191ºC (375ºF).

Variations in typical room temperature, longitudinal mechanical properties with tempering temperatures[32] are shown in Table 7-8.

Table 7-8. Typical Longitudinal Mechanical Properties of H11 Mod Steel

Tempering Temperature*		Tensile Strength		Yield Tensile Strength		Elongation in 50 mm	Reduction in Area	Hardness
°C	°F	MPa	ksi	MPa	ksi	%	%	HRC
510	950	2,120	308	1,710	248	5.9	29.5	56.6
540	1,000	2,010	291	1,675	243	9.6	30.6	56.0
565	1,050	1,850	269	1,565	227	11.0	34.5	52.0
595	1,100	1,540	223	1,320	192	13.1	39.3	45.0
650	1,200	1,060	154	850	124	14.1	14.2	33.0
705	1,300	940	136	700	101	16.4	42.2	29.0

* Air cooled from 1,010°C (1,850°F); double tempered, 2 + 2 hr at indicated temperature.

Because of secondary hardening characteristics, H11 Mod has good temper resistance, resulting in high temperature property retention, as seen in Table 7-9.

Table 7-9. Longitudinal Room Temperature Tensile Properties of H11 Mod Steel after Exposure at Elevated Temperatures for 10 or 100 Hours

Exposure Temperature		Exposure Time	Tensile Strength		Yield Tensile Strength		Elongation in 50 mm	Reduction in Area
°C	°F	hr	MPa	ksi	MPa	ksi	%	%
510[(a)]	950[(a)]	100	1,790	260	1,760	255	11.5	42.8
540[(b)]	1,000[(b)]	10	1,650	239	1,410	204	12.4	49.9
		100	1,450	210	1,300	188	13.7	52.9
540[(c)]	1,000[(c)]	10	1,385	201	1,190	173	14.1	52.4
		100	1,300	189	1,100	160	15.2	58.2

(a) Tempered 2 + 2 hr at 540°C (1,000°F); (b) tempered 2 + 2 hr at 565°C (1,050°F); (c) tempered 2 + 2 hr at 595°C (1,100°F).

7.1.5 AF1410 Steel

LESCALLOY® AF1410 alloy was developed specifically to have high strength, excellent fracture toughness, and excellent weldability when heat treated to about 1,620-1,750 MPa (235-255 ksi) ultimate tensile strength. AF1410 has good weldability and does not require preheating prior to welding. The alloy maintains good toughness at cryogenic temperatures, and high strength and stability at temperatures up to 412ºC (800ºF). This alloy is available in a wide variety of sizes and forms, including billet, bar, plate, and die forgings, and is produced by vacuum induction melting followed by vacuum remelting. However, this alloy is available only in the United States for DoD approved/funded projects.

The heat treatment for this alloy consists of heating to ~885ºC (1,650 ±25ºF) for one hour, forced-air cooling to room temperature, reheating to ~815ºC (1,525 ±25ºF) for one hour, forced-air cooling to room temperature, cooling to ~-55ºC (-100 ±5°F), holding at temperature for one hour, warming to room temperature, and aging at ~495ºC (950 ±10ºF) for five hours, and air cooling. A forced-air cool from austenitizing temperatures should be used for section thicknesses up to ~5 cm (two inches). For sections of greater thickness, an oil quench should be utilized. A single austenitizing treatment ~885ºC (1,525 ±25ºF) can be used to minimize heat treating distortion with a resulting slight decrease in fracture toughness[36].

AF1410 has a general corrosion resistance similar to the maraging steels. It should not be used in the unprotected condition. This alloy is highly resistant to stress-corrosion cracking compared to other high-strength steels[36].

7.1.6 AerMet 100 Alloy

AerMet 100 is a higher strength derivative of AF1410, and this Ni-Co-Fe alloy can be heat treated to 280-310 ksi tensile strength while exhibiting excellent fracture toughness and high resistance to stress-corrosion cracking. AerMet 100 has good weldability and does not require preheating prior to welding. AerMet 100 is available in a wide variety of sizes and forms including billet, bar, sheet, strip, plate, wire, and die forgings. The alloy also is produced by vacuum induction melting followed by vacuum-arc remelting[36].

AerMet 100 may be considered for use up to about 427ºC (800ºF). This alloy is not subject to the same restrictions as AF1410, thus may be considered a better substitute[35]. The main applications of AerMet 100 alloy include armor, fasteners, landing gear, actuators, jet engine shafts, ballistic tolerant components, and structural tubing.

The heat treatments applied to AerMet 100 are:

- **Decarburize**: like other carbon bearing, high strength alloys, AerMet 100 alloy is subject to decarburization during hardening: heat treatment should take place in a neutral atmosphere furnace, salt bath, or vacuum, and decarburization should be determined by comparing the surface and internal hardness of a small test cube for proper response (metallographic determination of decarburization is not recommended for this alloy).

[36] Metallic Materials and Elements for Aerospace Vehicle Structures, MIL-HDBK-5H (December, 1998).

- **Normalize**: heat to 899ºC (1,650ºF) holding for one hour and air cooling to room temperature: optimum softening for machining is obtained by following this with a 16-hour 677ºC (1,250ºF) “over-age” anneal.

- **Anneal**: heat at 677ºC (1,250ºF) for 16 hours: the optimum annealed hardness of 40 HRC maximum is obtained following this over-age anneal.
- **Solution Treat**: heat in the treatment temperature range of 885 +/-14ºC (1,625 +/-25ºF) for one hour (temperature must be monitored by a thermocouple attached to the load).
- **Quench:** the proper quenching practice is essential for AerMet 100 alloy and water quenching is not recommended - the alloy should be cooled from the solution treatment temperature to 66ºC (150ºF) in one to two hours to develop optimum properties, and individual sections larger than ~5 cm (two inches) diameter or 2.54 cm (one inch) thick (plate) must be quenched with oil in order to obtain this temperature in this time frame (the cooling rate of the furnace load must be monitored by a thermocouple attached to the hottest spot in the load).
- **Cold Treatment**: following cooling to room temperature, to obtain the full toughness capability, the AerMet 100 alloy should be cooled to -73ºC (-100ºF) and held for one hour: the parts can then be air warmed.
- **Age**: the standard aging treatment for AerMet 100 alloy is 482 +/-6ºC (900 +/-10ºF) for five hours: parts made from this alloy should never be aged at a temperature below 468ºC (875ºF).

Typical mechanical properties of AerMet 100 (heat treated 885ºC (1,625ºF) - 1 hour, air cooled, -73ºC (-100ºF) - 1 hour, aged 482ºC (900ºF) - 5 hours) are given in Table 7-10[37].

Table 7-10. Typical Mechanical Properties of AerMet 100 Alloy

Tensile Strength		Yield Tensile Strength		Elongation in 50 mm	Reduction in Area	Charpy V Notch		Fracture Toughness	
MPa	ksi	MPa	ksi	%	%	J	ft-lb	MPa √m	Ksi√in
Longitudinal Direction									
1,965	285	1,724	250	14	65	41	30	126	115
Transverse Direction									
1,965	285	1,724	250	13	55	34	25	110	100

7.1.7 AerMet 310 Alloy

An AerMet 310 alloy possesses more cobalt and less chromium, and higher hardness and strength than an AerMet 100 alloy, while maintaining exceptional ductility and toughness. At a 310 ksi (2,137 MPa) ultimate tensile strength, AerMet 310 alloy exhibits toughness values equivalent to alloys 20 ksi (138 MPa) lower in strength.

The alloy should be considered as a candidate for use in components requiring high strength, high fracture toughness, and exceptional resistance to stress corrosion cracking and fatigue[37]. Examples are armor, landing gear, actuators, ordnance, structural tubing, ballistic tolerant components, jet engine shafts, structural members, and drive shafts.

Typical mechanical properties of AerMet 310[35] are given in Table 7-11 and typical longitudinal mechanical properties at room temperature and elevated temperature are listed in Table 7-12.

[37] Anon., "*AerMet® 100*", Alloy Data Sheet, Carpenter Technology Corporation (September, 1995).

Table 7-11. Typical Mechanical Properties of AerMet 310 Alloy

Tensile Strength*		Yield Tensile Strength		Elongation	Reduction in Area
MPa	ksi	MPa	ksi	%	%
Longitudinal Orientation					
2,172	315	1,896	275	14.5	63
Transverse Orientation					
2,172	315	1,896	275	13.0	53

* Heat treatment: 913 ± 14°C (1,675 ± 25°F) 1 hr; air cool; -73°C (-100°F) 1 hr; 482 ± 6°C (900 ± 10°F) 6 hr; air cool.

Table 7-12. Typical Longitudinal Mechanical Properties at Room Temperature and Elevated Temperatures of AerMet 310 Alloy

Test Temperature		Tensile Strength*		Yield Tensile Strength*		Elongation*	Reduction in Area*
°C	°F	MPa	ksi	MPa	ksi	%	%
Room Temperature		2,145	311	1,852	269	15.2	66.4
204	**400**	1,948	283	1,737	252	16.0	66.2

* Heat treatment: 913°C (1,675°F) 1 hr; air cool, -73°C (-100°F) 1 hr; air warm; 482°C (900°F) 5 hr, air cool.

The heat treatments applied to AerMet 310 alloy are:

- **Decarburize**: like other carbon bearing, high-strength alloys, AerMet 100 alloy is subject to decarburization during hardening. Heat treatment should take place in a neutral atmosphere furnace, salt bath or vacuum, and decarburization should be determined by comparing the surface and internal hardness of a small test cube for proper response (metallographic determination of decarburization is not recommended for this alloy).
- **Normalize**: heat to 968ºC (1,775ºF), holding for one hour and air cooling to room temperature. Optimum softening for machining is obtained by following this with a 16-hour, 677ºC (1,250ºF) "over-age" anneal.
- **Anneal**: soften by using a 677ºC (1,250ºF) over-age anneal for 16 hours to obtain the optimum annealed hardness of 40 HRC.
- **Solution Treat**: heat for one hour in the solution treatment temperature range of 913 +/-14ºC (1,675 +/-25ºF): the temperature must be monitored by a thermocouple attached to the load.
- **Quench**: the proper quenching practice is essential for AerMet 100 alloy, and water quenching is not recommended. The alloy should be cooled from the solution treatment temperature to 66ºC (150ºF) in one to two hours to develop optimum properties. Individual sections larger than ~5 cm (two inches) diameter or 2.54 cm (one inch) thick (plate) must be quenched with oil in order to obtain this temperature in this time frame. The cooling rate of the furnace load must be monitored by a thermocouple attached to the hottest spot in the load.
- **Cold Treat**: following cooling to room temperature, to obtain the full toughness capability, the AerMet 100 alloy should be cooled to -73ºC (-100ºF) and held for one hour; the parts can then be air warmed.
- **Age**: the standard aging treatment for AerMet 310 alloy is 482 +/-6ºC (900 +/-10ºF) for three to eight hours. Parts made from this alloy should never be aged at a temperature below 468ºC (875ºF).

7.1.8 Best Substrate Choices for Using APCVD Aluminum Coatings

In order to determine the most suitable substrates for implementing the APCVD Al coating, it is necessary to know how they might be affected by the time at temperature during the deposition. The following information was extracted from several data sources. Figure 7-1 summarizes the results for the effects of tempering temperature on the ultimate tensile and yield strengths of AISI 4130, AISI 4340, 300M, and H11 Modified Steels, from the literature survey.

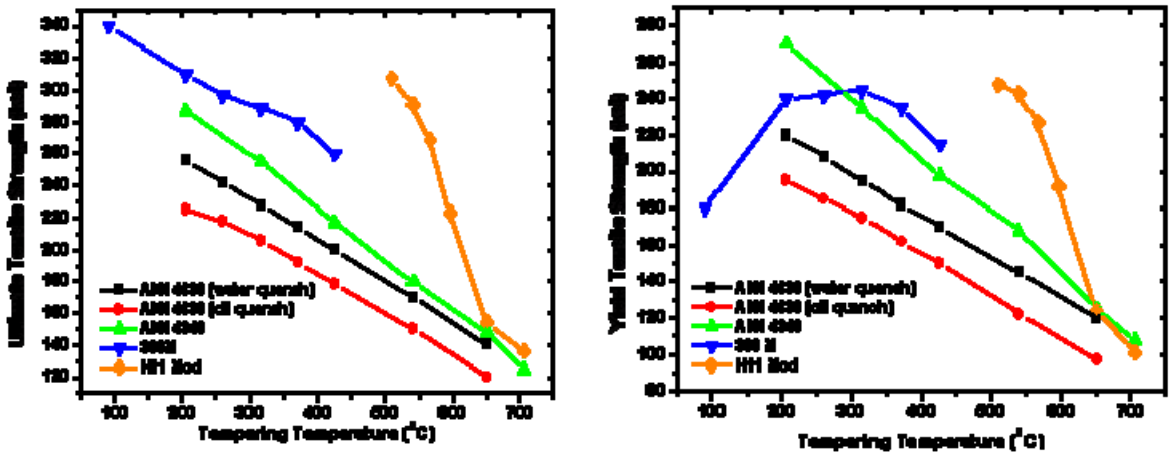

Figure 7-1. Ultimate Tensile Strengths and Yield Tensile Strengths vs. Tempering Temperatures of High-strength Steels

Based on the survey results given above, and the data in Figure 7-1, if a 300ºC (572ºF) deposition temperature is used as the guideline, it will soften the highest strength steels to below performance requirements. However, there are other high-strength steels that could be used. The best possible applications for APCVD Al if the deposition temperature cannot be lowered from 300ºC are on steels that can be tempered above 400ºC. For example, components could be made from:

- AISI 4130 steel at 160-180 ksi UTS for brackets and fasteners
- AF1410 alloy at 220-250 ksi UTS for landing gear parts
- 300M steel at 260-280 ksi UTS for landing gear parts
- AerMet 100 alloy at 280-300 ksi UTS for landing gear parts.

However, if the APCVD process temperature could be lowered to the MMPDS-03 and MIL-S-16135/AMS 2430N recommended design limits, such as 246ºC (475ºF) shown in Tables 5-1 and 5-2, respectively, in Section 5.1, other substrate materials may become candidates for receiving APCVD Al coatings to replace Cd coatings.

7.2 Comparison of APCVD Al with Other Candidate Replacement Coatings

A survey was conducted to obtain property and performance data for some of the other alternative Al coatings in use or being considered as replacements for Cd in military applications. The amount of published data is limited, and there is a problem with making comparisons

because not all the references provided information on the details of the deposition process, the coating itself, or details of the testing conditions.

In addition, it was not always clear if the substrates had received any special treatments, nor if the coatings had received any post-treatments, such as chemical conversion coatings and/or sealers. Notwithstanding these caveats, the data found in the open literature are summarized in Table 7-13. Additional information about some of the properties of these alternative coatings is given below.

7.2.1 IVD Aluminum

IVD Al has been selected as a replacement for Cd-plated coatings for corrosion protection of ferrous alloy parts at Air Force Logistic Center MRO facilities. A wide variety of parts are coated, including trunnions, cylinders, retainers, caps, retainer rings, spacers, strikers, springs, bolts, brackets, standoffs, links, flap tracks, rings, outboard actuators, strut terminals, blower impellers, stops, screw assembly ball nuts, plates, housing leg bolts, fasteners, covers, and housings [38, 39]. In addition, IVD Al is used for aircraft structural steel parts and the external steel surface of missiles to prevent corrosion during storage. As noted in MIL-DTL-83488, IVD Al can be applied to copper, titanium, and stainless steel alloys to provide corrosion compatibility with Al structures. It is assumed that the uses for APCVD Al coatings, as a minimum, are the same as for IVD Al coatings. Other applications may be possible because, unlike the IVD process, the APCVD process is *not* a line-of-sight limited technology.

For comparison with an APCVD Al coating, an IVD Al coating (25 µm, 1 mil thick) was deposited on steel panels (AISI 4130) by Team member Boeing-St. Louis. The IVD Al coating was subjected to a typical post-treatment of glass bead burnishing (shot-peening) followed by the application of a Type II (chromate) conversion coating. As discussed in Sections 4.1.1, 4.1.2, and 4.1.4, some properties were determined during the testing of the APCVD Al coatings. These included morphology, surface roughness, and structure. In addition, corrosion potential and electrochemical impedance spectroscopy parameters were determined as a function of immersion time (up to 4 days). The testing solution was oxygen saturated 3.5 wt.% NaCl.

The IVD Al coating showed conformal coverage and was dimpled. Also, as expected, coating defects such as pores or pin-holes could be seen using a SEM at high magnification (see Figure 7-2). The average surface roughness (R_a) of this coating was ~2 µm.

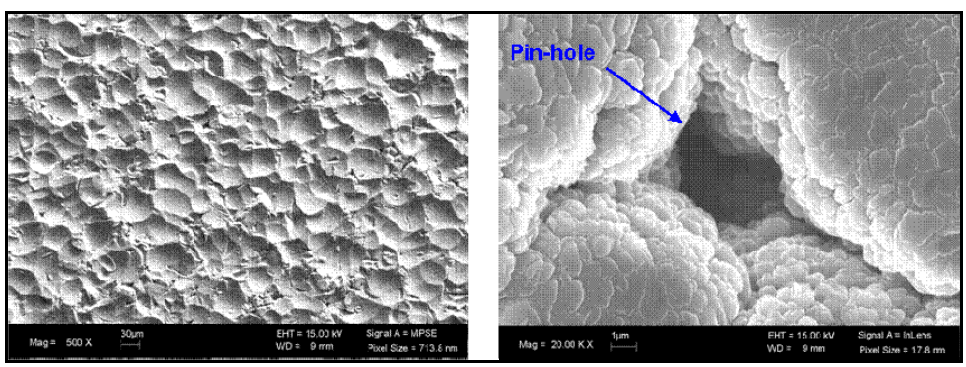

Figure 7-2. Typical Surface Morphology of an IVD Aluminum Coating

[38] V. L. Holmes and J. J. Reilly, "*Ion Vapor Deposition Aluminum Qualification Tests*", Pollution Prevention Project PRJY 921609, Environmental Management Directorate, McClellan AFB, CA 95652 (June, 1995).
[39] V. L. Holmes, "*Expanded Ion Vapor Deposition (IVD) Aluminum Program*", Pollution Prevention Project PRJY 961610, Environmental Management Directorate, McClellan AFB, CA 95652 (September, 1998).

Table 7-13. Comparison of Properties for Aluminum Coatings Deposited by Different Methods

Property	Units	APCVD	IVD	MS PVD	ED	Comments
Deposition Rate	µm/hr	≤ 120*	10-12	- -	25?	* APCVD not optimized for lower emperatures
Composition: Al	wt %	≥ 99.0*	≥ 99.0	≥ 99.0	≥ 99.9	* APCVD not optimized (range = 97.1 - 99.3%); higher values obtained by GDOES
Density	g/cm^3	≥ 2.60*	≤ 2.71*	< than Cd	2.64*	* All are porous or micro-cracked to some degree; APCVD has fewer defects than IVD: Al = 2.70
Porosity	%	TBD*	> than Cd	> than Cd	Negligible	* Less than IVD
Morphology	N/A	Polycrystalline*	Columnar*	Columnar*	Polycrystalline*	* All are porous or micro-cracked to some degree; APCVD has fewer defects overall
Roughness	µm rms	≤ 1.0	≤ 2.0	- -	12-30*	* Thicker coatings are more nodular (rougher)
Adhesion (Pull Test)	$kg.cm^{-2}$	Pass*	Pass*+	Pass	Pass	* Adhesive failed; + failed bend test
Hardness	KHN MPa	TBD 550*	60 N/A	70-90 - -	- -* - -	* 19-25 Vickers hardness * 835 for Al single crystal
Young's Modulus (E)	GPa	~25	~ 70*	- -	- -	* Pure Al = 70
Ductility/Elongation	%	TBD	≥ 12*	- -	- -	* Al 1100 alloy
Coefficient of Friction	-	> Cd, ≤ 1.0*	> Cd	> Cd	> Cd	* Coating formed in service can lower value to ~0.5
Torque/Tension	ft-lb	TBD	Pass*	- -	- -	* IVD Al within ~10% of Cd value with post-treatments (e.g., CCCs, lubricants)
Contact Resistance	$m\Omega.in^{-2}$	1.68*	≤ 5*	- -	2.5*	* After 168 hr salt fog exposure
Corrosion Resistance						
• B117 Neutral Salt Fog	• hr to white/ red rust	• ≥ 648	• 500-1,000*	• ≤ 240*	• ≥ 1.020; 1,500**; 6,000***	* Scribed ** Class 2, Type IA chromate *** Class III chromate (3,000 when scribed)
• G 85 Acid Salt Fog	• Ditto	• - -	• ≥ than Cd	• - -	• - -	
• GM 9540P	• Ditto	• >100+	• - -	• - -	• Fail+ - -	+ 80 cycles = pass criterion
• Outdoor Exposure	• cycles	• - -	• > than Cd	• - -	• - -	
• Electrochemical Polarization	• mV vs. SCE	• 200-300	• - -	• - -	• ≤ 500****	**** Class III chromate on 6061 alloy
• Open Circuit Potential	• mV vs. SCE	• ~ -800++	• ~ -750	• - -	• - -	++ Cd = -800
Hydrogen Embrittlement	N/A	Passes after H_2 relief bake*	None	Passes after H_2 relief bake*	Passes*	* Requires baking after stripping and before replating
Fatigue Debit	%	• > than Cd (with no CCC)	None*	- -	None**	* With CCCC ** Uniaxial, low cycle; no Ni flash; notched bars

The composition of the IVD coatings is usually about 99.9% Al, which is supported by the XRD curves obtained and reproduced here in Figure 7-3 for the coatings tested on this project.

The cross-sections of an IVD Al coating-shown in Figure 7-4 - indicate that even after shot peening some pores/pin-holes penetrate to the surface of the substrate. The region within the red box on one of the photomicrographs is a location where corrosion attack of the substrate could be expected in service. In addition, closed pores are present in the coatings.

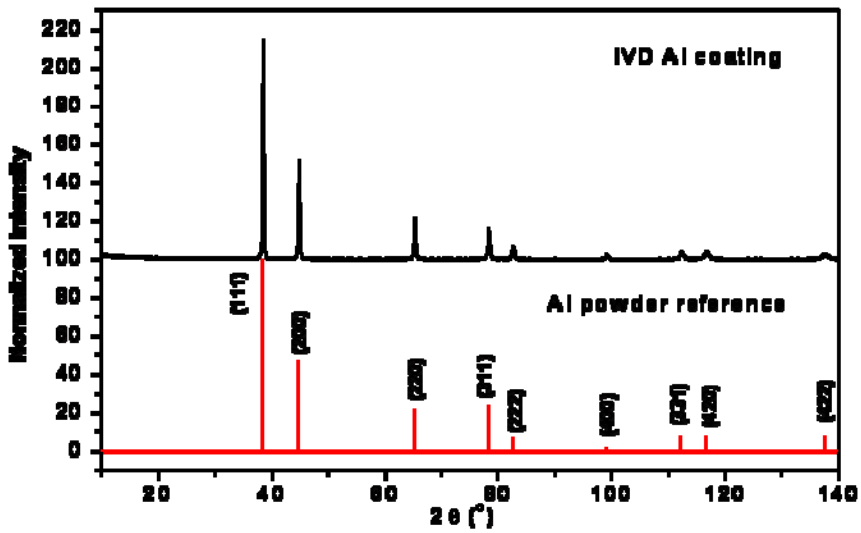

Figure 7-3. Composition of an IVD Aluminum Coating Compared to a Reference Material

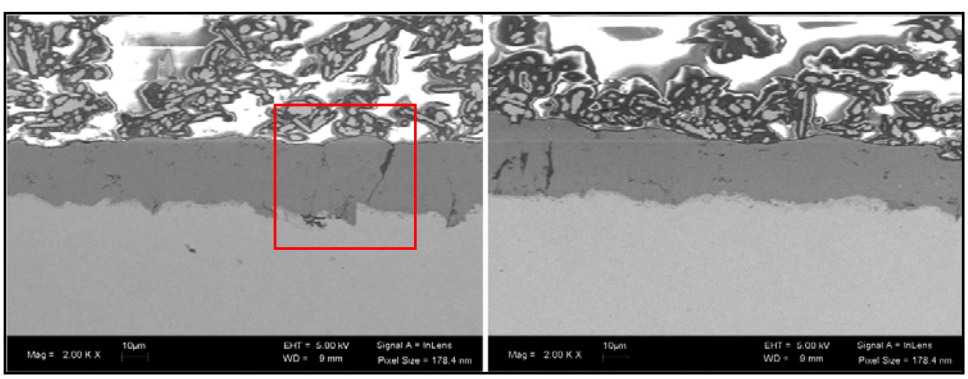

Figure 7-4. Cross-sections of an IVD Aluminum Coating Showing Porosity

The presence of "micro-cracks" in IVD Al coatings can cause hydrogen re-embrittlement (HRE) under the right conditions. Unlike hydrogen embrittlement (HE) that results from hydrogen introduced during the surface preparation and/or deposition process, HRE results from hydrogen generated through a corrosion reaction at the substrate surface as the Al dissolves in cracks (or other defects) in the coating that are filled with a corrosive medium from the operating environment. While the sacrificial protection from the Al is beneficial in preventing localized corrosion of the substrate, unfortunately the byproduct is hydrogen that enters the substrate

material and embrittles it, often leading to catastrophic failure. An example of this is the delayed failure of PH13-8Mo steel coated with IVD Al[40]. Fortunately, it has been determined that by controlling the carbon and aluminum contents in this steel, HRE can be mitigated. In addition, no HRE failure has ever occurred on an aircraft in service with IVD Al-coated components because these typically are painted (not applied to notched, high-strength steel parts sitting in a salt solution, as is done during performance testing).

7.2.2 Sputtered Aluminum

Attempts have been made to adapt (inverted), cylindrical, magnetron sputtering technology to coat inside and outside surfaces of landing gear components with limited success. Marshall Laboratories, working with the Boeing Company and Hill AFB personnel, developed a process during 2002-2004 for depositing Al coatings inside hollow, cylindrical landing gear components for the C-17 aircraft to provide corrosion protection[41]. The coatings had a very columnar structure, prone to corrosion attack, as shown in Figure 7-5. Consequently, they received a chromated, chemical conversion coating (CCC) before being placed in service (Figure 7-6).

Figure 7-5. Cross-section of a Magnetron Sputtered Al Coating

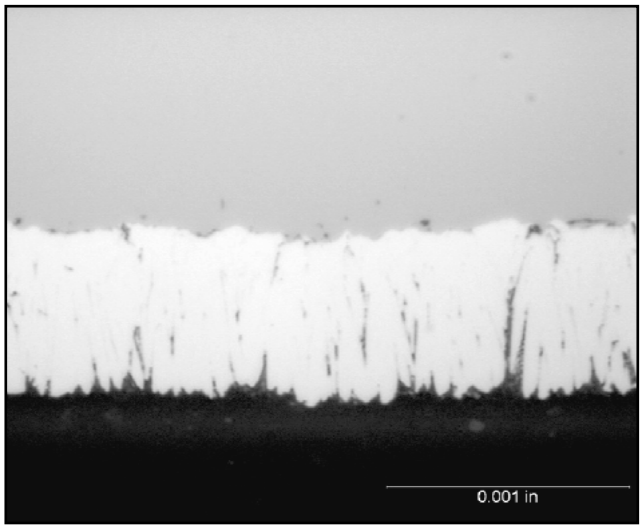

The post-treated, sputtered coating on C-17 axles met or exceeded the military specification MIL-DTL-83488 requirements for thickness, adhesion, salt fog corrosion, and paint adhesion for a Class 2, Type II cadmium coating. However, the sputtered Al required a coat of epoxy primer to pass the sustained load, hydrogen re-embrittlement test in distilled water, and an epoxy primer and polyurethane top coat to pass this test in a 0.5% NaCl corrosive medium[41].

[40] Y. Asayama, M. Ibaragi, and Y. Kawase, "*Delayed Failure of PH13-8Mo Steel Plated With Al IVD*", Metallurgical and Materials Trans. A, **22**, No. 12, pp. 2935-2945 (1991).
[41] S. Gaydos, "*Cadmium Alternative Studies for C-17 P2 Projects*", JCAT Meeting, Greensboro, NC (March, 2005).

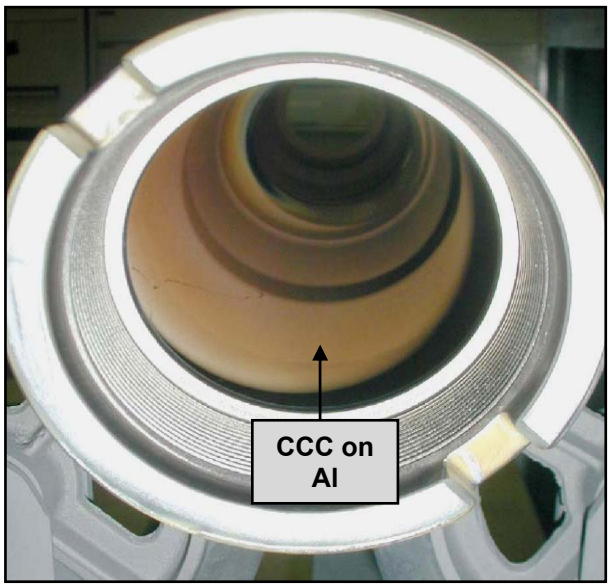

Figure 7-6. Magnetron Sputtered Al Coating with Conversion Coating

Later, on a project funded by the ESTCP, using a JTP, it was found[42] that this type of Al coating could pass the ASTM F 519 HE test, but with a substantial decrease in tensile strength (83.1%) compared with IVD Al (98.4%), electroplated Al (95.3%), and the Cd-plated control (91.8%). In addition, the notch fracture strength measured was outside the 10 ksi difference allowed, and the magnetron sputtered Al-coated specimens were considered to have failed this test, because these small test specimens were overheated during the deposition process. Overheating does not occur during the sputter coating of large landing gear components at Ogden ALC. In HRE testing - when using deionized or sea water as the corrosive medium - the sputtered Al-coated specimens failed, as do the APCVD Al and IVD Al-coated test specimens. Only the electroplated Al-coated specimens passed this HRE test.

7.2.3 Electroplated Aluminum

The substrates for AlumiPlate Al coatings include Al alloys (2024, 5052, 6061, 7075, A-35x/380), pure beryllium and alloys (AlBeMet™162), stainless steels (303, 304, 304L, 17-7 PH), high-strength steels (4130, 4340, 300M, AerMet 100), copper and its alloys (brass, bronze, Be-Cu), Fe-Ni alloys (Haynes 242™, Inconel™), and titanium[43]. APCVD Al can be applied to all of the above materials if they are stable and do not lose their desirable properties at or below the process deposition temperatures.

In general, the properties and performance of electroplated Al coatings compare very favorably with those for Cd-plated coatings, especially with respect to fatigue resistance and HE/HRE resistance[44]. However, in some independent testing done under this project, the performance in

[42] E. Beck, "*Phase I Test Results: Joint Test Protocol for Cadmium Alternatives for high Strength Steel*", JCAT Meeting, San Diego, CA (January, 2006).
[43] D. Deeken, "*An Alternative to Cadmium Plating in Aerospace Applications*" JCAT Meeting, Greensboro, NC (March, 2005).
[44] Anon., "*AlumiPlate® Aluminum Stands up to Cadmium to Meet Aerospace Specifications*", company web site: http://www.alumiplate.com/html/body_aerospace.html (2007).

the GM 9540P cyclic exposure test was surprisingly unacceptable. This test was performed on unscribed AlumiPlate Al-coated "C-ring" specimens for comparison with APCVD Al, with and without a commercial hexavalent chromium chemical conversion coating. After 29 cycles, no red rust was observed on the outer surfaces of the AlumiPlate Al-coated C-rings (Figure 7-7).

Figure 7-7. AlumiPlate Al Coating on C-ring Specimens after 29 Cycles in GM 9540P Test - Outside Diameter

In contrast, the inner surfaces of the C-rings were corroded and red rust was visible (Figure 7-8). The reasons for this difference need to be investigated. However, it is known that, pitting and corrosion attack of the electroplated Al coating can occur after extended exposure to salt fog, and a nickel strike under the coating, originally used to promote adhesion, has been shown to be a physical barrier against localized corrosion[45], as seen in Figure 7-9.

Figure 7-8. AlumiPlate Al Coating on C-ring Specimens after 29 Cycles in GM 9540P Test - Inside Diameter

[45] K. Legg and J. Sauer, "*AlumiPlate® as a Cadmium Alternative*", Report to Joint Strike Fighter ESOH Working Group (August, 2004).

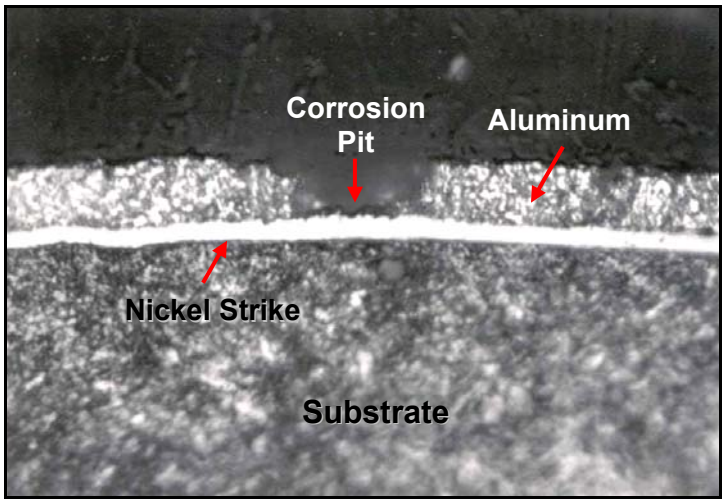

Figure 7-9. AlumiPlate Al Coating on a Grade 8 Bolt after 3,420 Hour Salt Fog Exposure

8.0 Technical Publications

The following is a list of technical presentations and publications prepared as part of the outreach and communication efforts considered to be an important aspect of sharing information on an important topic and soliciting feedback and comments.

8.1 Technical Papers and Articles

1. E. W. Brooman and T. A. Allmann, "New AFRL Project for Cadmium Replacement Using Novel Chemical Vapor Deposition Technology", Monitor, **8**, No. 11 (2004) p.16.
2. S. Maeng, S. Gu, R. Levy et alii, "Synthesis and Characterization of Chemical Vapor Deposited Aluminum", Proc. Materials Science & Technology Conference, Session MATL-05, Detroit, MI (16-20 September, 2007).
3. E. S. Berman and E. W. Brooman, "Evaluation of APCVD Al Coatings as an Environmentally Acceptable Alternative to Electroplated Cd Coatings", Metal Finishing, **107**, No. 2 (2009) p. 35.
4. S. Gu, S. Maeng, R. Levy, et alii, "Investigation of Atmospheric Pressure Chemically Deposited Aluminum Coating for Corrosion Protection", submitted to J. Surface & Coatings Technology, (January, 2009).

8.2 Technical Reports

No technical reports, including SERDP Annual Reports, were prepared for external distribution except this Final Report. The following Annual Reports were prepared for internal distribution only:

1. T. A. Allmann and E. W. Brooman, First Annual Report, SERDP Project PP-1405 (12 December, 2005).
2. E. S. Berman and E. W. Brooman, Second Annual Report, SERDP Project WP-1405 (22 December, 2005).
3. E. S. Berman and E. W. Brooman, Third Annual Report, SERDP Project WP-1405 (14 December, 2005).

8.3 Conference/Symposium Presentations and Proceedings

1. E. W. Brooman, "Atmospheric Pressure CVD of Aluminum Coatings", 2nd Joint Services Plating Meeting, Hill AFB, UT (10-13 January, 2005).
2. E. W. Brooman and T. A. Allmann, "Chemical Vapor Deposited Aluminum as a Replacement Coating for Cadmium", Joint Cadmium Alternatives Team Meeting, San Diego, CA (25-26 January, 2006).
3. E. S. Berman, E. W. Brooman, et alii, "Investigation of Chemical Vapor Deposited Aluminum as a Replacement for Cadmium", Joint Cadmium Alternatives Team Meeting, New Orleans, LA (23-25 January, 2007).
4. E. S. Berman, E. W. Brooman, et alii, "Year 2 Update: Investigation of Chemical Vapor Deposited Aluminum as a Replacement for Cadmium", Aerospace Chromate and Cadmium Elimination Team Meeting, Colorado Springs, CO (9-10 May, 2007).
5. S. Maeng, S. Gu , R. A. Levy et alii, "Synthesis and Characterization of Chemical Vapor Deposited Aluminum", Materials Science & Technology Conference, Session MATL-05, Detroit, MI (16-20 September, 2007).

6. E. S. Berman, "Update: Investigation of Chemical Vapor Deposited Aluminum as a Replacement for Cadmium", Joint Cadmium Alternatives Team Meeting, San Diego, CA (25-26 January, 2008).
7. E. S. Berman, "Year 3 Update: Investigation of Chemical Vapor Deposited Aluminum as a Replacement for Cadmium", Aerospace Chromate and Cadmium Elimination Team Meeting, Wichita, KS (13-14 May, 2008).
8. E. S. Berman, E. W. Brooman, et alii, "Properties of APCVD Aluminum Coatings - an Environmentally Acceptable Replacement for Electroplated Cadmium Coatings", Proc. Airline/Aerospace Symposium, SUR/FIN 2008, Indianapolis, IN (16-18 June, 2008).

8.4 Published Technical Abstracts

1. E. W. Brooman, T. A. Allmann, et alii, "APCVD Aluminum as a Replacement Coating for Cadmium - I", poster presentation at the Partners in Environmental Technology Symposium & Workshop, Washington, DC (29 November - 1 December, 2005).
2. E. W. Brooman, E. S. Berman, et alii, "APCVD Aluminum as a Replacement Coating for Cadmium - II", poster presentation at the Partners in Environmental Technology Symposium & Workshop, Washington, DC (27-30 November, 2006).
3. E. S. Berman, E. W. Brooman, et alii, "APCVD Aluminum as a Replacement Coating for Cadmium - III", poster presentation at the Partners in Environmental Technology Symposium & Workshop, Washington, DC (4-6 December, 2007).
4. E. S. Berman, E. W. Brooman, et alii, "APCVD Aluminum as a Replacement Coating for Cadmium -IV", poster presentation at the Partners in Environmental Technology Symposium & Workshop, Washington, DC (2-4 December, 2008).

8.5 Text Books and Book Chapters

No text books, nor chapters, sections, or addenda to books, were prepared for publication.

REPORT DOCUMENTATION PAGE

Form Approved
OMB No. 0704-0188

The public reporting burden for this collection of information is estimated to average 1 hour per response, including the time for reviewing instructions, searching existing data sources, gathering and maintaining the data needed, and completing and reviewing the collection of information. Send comments regarding this burden estimate or any other aspect of this collection of information, including suggestions for reducing the burden, to Department of Defense, Washington Headquarters Services, Directorate for Information Operations and Reports (0704-0188), 1215 Jefferson Davis Highway, Suite 1204, Arlington, VA 22202-4302. Respondents should be aware that notwithstanding any other provision of law, no person shall be subject to any penalty for failing to comply with a collection of information if it does not display a currently valid OMB control number.
PLEASE DO NOT RETURN YOUR FORM TO THE ABOVE ADDRESS.

1. REPORT DATE *(DD-MM-YYYY)*	2. REPORT TYPE	3. DATES COVERED *(From - To)*
01-02-2009	FINAL REPORT	OCT 2004 - FEB 2009

4. TITLE AND SUBTITLE
Investigation of Chemical Vapor Deposited Aluminum as a Replacement Coating for Cadmium

5a. CONTRACT NUMBER

5b. GRANT NUMBER

5c. PROGRAM ELEMENT NUMBER

6. AUTHOR(S)
Dr. Elizabeth S. Berman & Dr. Eric W. Brooman
AFRL/RXSC
2179 12th Street - Building 652, Room 122
WPAFB, OH 45431

5d. PROJECT NUMBER
WP-1405

5e. TASK NUMBER

5f. WORK UNIT NUMBER

7. PERFORMING ORGANIZATION NAME(S) AND ADDRESS(ES)
Materials & Manufacturing Directorate, Air Force Research Laboratory, WPAFB OH
Army Research Laboratory (ARL), Aberdeen Proving Ground MD
Naval Air Systems Command (NAVAIR), Patuxent River MD
New Jersey Institute of Technology, Newark NJ

8. PERFORMING ORGANIZATION REPORT NUMBER

9. SPONSORING/MONITORING AGENCY NAME(S) AND ADDRESS(ES)
Strategic Environmental Research & Development Program
901 North Stuart Street, Suite 303
Arlington VA 22203

10. SPONSOR/MONITOR'S ACRONYM(S)
SERDP

11. SPONSOR/MONITOR'S REPORT NUMBER(S)

12. DISTRIBUTION/AVAILABILITY STATEMENT
APPROVED FOR PUBLIC RELEASE, DISTRIBUTION UNLIMITED

13. SUPPLEMENTARY NOTES

14. ABSTRACT

The overall objective of this effort was to evaluate the use of atmospheric pressure, chemical vapor deposition (APCVD) to produce uniform and conformal aluminum (Al) coatings with desirable properties, primarily on high-strength steel substrates. This process offers an environmentally benign alternative to cadmium plated coatings, as well as promises to provide high production through-put, low cost, and coatings with the performance necessary to meet a wide range of end use requirements. The findings are summarized as follows: (1) APCVD Al coatings exhibit excellent throwing power and conformal coverage, with uniform thickness distribution on complex shapes, and inside and outside diameters of cylindrical parts of all sizes; (2) the coatings exhibit a fcc polycrystalline, equi-axed structure, unlike IVD Al coatings; (3) the coatings are oxidized on the surface and relatively pure within the bulk - there is some contamination with oxygen and carbon, which depends in part on the composition of the precursor and the deposition temperature; (4) the coatings exhibit good adhesion to the steel substrates used and provide a good surface to accept primers and top coats; (5) the electrical resistivity is satisfactory for the anticipated applications; (6) a post deposition, hydrogen

15. SUBJECT TERMS
Atmospheric pressure chemical vapor deposition, aluminum coatings, high-strength steels and alloys, adhesion, density, porosity, morphology, structure, throwing power, conformal coverage, chemical composition, contact resistance, porosity, corrosion resistance, sacrificial protection, coefficient of friction, notch fracture strength, fatigue strength, hydrogen embrittlement, technology

16. SECURITY CLASSIFICATION OF:			17. LIMITATION OF ABSTRACT	18. NUMBER OF PAGES	19a. NAME OF RESPONSIBLE PERSON
a. REPORT	b. ABSTRACT	c. THIS PAGE			Elizabeth Berman
Unclassified	Unclassified	Unclassified	Unclassified	133	19b. TELEPHONE NUMBER *(Include area code)* 937-656-5700

Reset

Standard Form 298 (Rev. 8/98)
Prescribed by ANSI Std. Z39.18

INSTRUCTIONS FOR COMPLETING SF 298

1. REPORT DATE. Full publication date, including day, month, if available. Must cite at least the year and be Year 2000 compliant, e.g. 30-06-1998; xx-06-1998; xx-xx-1998.

2. REPORT TYPE. State the type of report, such as final, technical, interim, memorandum, master's thesis, progress, quarterly, research, special, group study, etc.

3. DATES COVERED. Indicate the time during which the work was performed and the report was written, e.g., Jun 1997 - Jun 1998; 1-10 Jun 1996; May - Nov 1998; Nov 1998.

4. TITLE. Enter title and subtitle with volume number and part number, if applicable. On classified documents, enter the title classification in parentheses.

5a. CONTRACT NUMBER. Enter all contract numbers as they appear in the report, e.g. F33615-86-C-5169.

5b. GRANT NUMBER. Enter all grant numbers as they appear in the report, e.g. AFOSR-82-1234.

5c. PROGRAM ELEMENT NUMBER. Enter all program element numbers as they appear in the report, e.g. 61101A.

5d. PROJECT NUMBER. Enter all project numbers as they appear in the report, e.g. 1F665702D1257; ILIR.

5e. TASK NUMBER. Enter all task numbers as they appear in the report, e.g. 05; RF0330201; T4112.

5f. WORK UNIT NUMBER. Enter all work unit numbers as they appear in the report, e.g. 001; AFAPL30480105.

6. AUTHOR(S). Enter name(s) of person(s) responsible for writing the report, performing the research, or credited with the content of the report. The form of entry is the last name, first name, middle initial, and additional qualifiers separated by commas, e.g. Smith, Richard, J, Jr.

7. PERFORMING ORGANIZATION NAME(S) AND ADDRESS(ES). Self-explanatory.

8. PERFORMING ORGANIZATION REPORT NUMBER. Enter all unique alphanumeric report numbers assigned by the performing organization, e.g. BRL-1234; AFWL-TR-85-4017-Vol-21-PT-2.

9. SPONSORING/MONITORING AGENCY NAME(S) AND ADDRESS(ES). Enter the name and address of the organization(s) financially responsible for and monitoring the work.

10. SPONSOR/MONITOR'S ACRONYM(S). Enter, if available, e.g. BRL, ARDEC, NADC.

11. SPONSOR/MONITOR'S REPORT NUMBER(S). Enter report number as assigned by the sponsoring/ monitoring agency, if available, e.g. BRL-TR-829; -215.

12. DISTRIBUTION/AVAILABILITY STATEMENT. Use agency-mandated availability statements to indicate the public availability or distribution limitations of the report. If additional limitations/ restrictions or special markings are indicated, follow agency authorization procedures, e.g. RD/FRD, PROPIN, ITAR, etc. Include copyright information.

13. SUPPLEMENTARY NOTES. Enter information not included elsewhere such as: prepared in cooperation with; translation of; report supersedes; old edition number, etc.

14. ABSTRACT. A brief (approximately 200 words) factual summary of the most significant information.

15. SUBJECT TERMS. Key words or phrases identifying major concepts in the report.

16. SECURITY CLASSIFICATION. Enter security classification in accordance with security classification regulations, e.g. U, C, S, etc. If this form contains classified information, stamp classification level on the top and bottom of this page.

17. LIMITATION OF ABSTRACT. This block must be completed to assign a distribution limitation to the abstract. Enter UU (Unclassified Unlimited) or SAR (Same as Report). An entry in this block is necessary if the abstract is to be limited.